Novel Processing Methods and Mechanisms to Control the Cast Microstructure in Al Based Alloys - *390 and Wrought Alloys*

by

Deepak Saha

A Dissertation

Submitted to the Faculty

of the

WORCESTER POLYTECHNIC INSTITUTE

in partial fulfillment of the requirements for the

Degree of Doctor of Philosophy

in

Materials Science and Engineering

May 2005

APPROVED:

_____

Professor Diran Apelian, Materials Science and Engineering, Advisor

_____

Professor Richard D. Sisson Jr., Materials Science and Engineering, Program Head

_____

Professor Makhlouf M. Makhlouf, Materials Science and Engineering

_____

Dr. Rathindra DasGupta, SPX Contech

_____

Dr. Ray Donahue, Mercury Marine Corp.

_____

Mr. John Jorstad, JLJ Technologies

ABSTRACT

The enactement of the Energy Policy and Conservation Act of 1975, led to a paradigm shift in material selection and design in the automotive industry. The net effect was an increased focus by the automotive industry toward the use of light metals leading for the reduction of weight and hence, the dependence of imported oil. Increasing use of aluminum was a transition in that direction. However, raw aluminum on an average is 1.5 – 2 times as expensive as steel. Near net shape manufacturing processes (Die casting, Thixo-forging, etc) provided the much needed competitive advantage vis-à-vis steel / iron parts by permitting the manufacturing of Al components.

Semi solid processing involves the net shape manufacturing of alloys in a two phase region (liquid + solid). The reduced turbulence (during casting), less entrapped gases and lower operating temperatures (processes below the liquidus) make semi solid processing ideal for the manufacturing of high integrity Al parts. Traditionally, semi solid processing involved the heating of billets to a two phase region (called Thixocasting). Rheocasting is a new semi solid processing technique wherein the alloy is cooled from a liquid state (a combination of controlled heat / nucleation and growth phenomena) to yield structures similar to the Thixocasting process. Rheocasting or Slurry-On-Demand is in its early stages of development (the first industrial prototype of rheocasting was invented in the late 1990's) and forms the central point of interest in this work. Much research is underway around the globe to understand the controlling mechanism as well as the structure – property relationships in rheocast parts, primarily limited to the hypoeutectic Al-Si alloys (less than 12.6% Si). This work is dedicated in the development of novel methods for the rheocasting of hypereutectic Al-Si alloys (greater than 12.6% Si) and Al based wrought alloys (alloys with Cu, Zn, Mg and Si as alloying elements).

The thesis presents the problems associated with microstructure control of hypereutectic Al-Si (primary Si coarsening and accelerated growth) and Al based wrought alloys (dendritic structures and hot tearing) with currently available technologies. Novel processing techniques are presented for the casting of hypereutectic Al-Si alloys and Al based wrought alloys with a combination of industrial trials and a through analysis of the underlying mechanisms.

ACKNOWLEDGEMENT

I would like to thank Prof. Diran Apelian for providing me the opportunity to conduct research at WPI. It has been an honor to be associated with someone who has imbibed in me certain principles and positive traits, things I lacked when I first started working with him as a graduate student. It has been a long transformation for me, from being able to plan, conduct, and analyze research independently. I look forward in taking my future career with this sense of independence and confidence which was he has fostered and taught. He always preached that "the God lies in the details", and it shall be a guiding principle.

It was a pleasure working with Prof. Makhlouf, without him 50% of my thesis would not have been complete. I clearly remember the exam he pulled out of his closet for the PhD qualifier (Phase transformation), his toughness preaches the principle of humbleness and hard work in an individual.

However, none of this work would be possible without the support of SPX Corporation. I am thankful to SPX Contech, which provided me the financial support and more importantly, identifying the potential in me, and encouraging me. It has been a pleasure working with Dr. Rathindra Dasgupta for his civility and his knack to listen, not many people in this world listen. I would like to thank John Jorstad, for his involvement in the project and giving me a lot of useful tips during the course of my research. After-all, he is called "the father of 390" in the industrial circles, and I hope I have lived upto his expectations. I would like to thank Dr. Sumanth Shankar, who played a very important role in the design of experiments, and the analysis of the results in the wrought alloys work. I am sure the work on wrought alloys would have been incomplete without his infectious enthusiasm.

I would like to thank my wife Payel, for putting up with all the mood-swings and the roller coaster ride of success and failures that I experienced during the last months of my thesis. I would like to thank my parents for supporting me through the tough times we went through. It was overwhelming to see my parents having withstood the tough winter of 2002 near death experience and come out strong. I am dedicating this thesis to their strength and courage and all they ever did to make me what I am. Even a lifetime is short to repay the debt.

TABLE OF CONTENT

Chapter 1. Introduction

During the last decade we have witnessed major advances in the use of aluminum for a variety of societal applications. Specifically, in the automotive industry, we have seen increased use of aluminum in power train and structural applications. For example, the Aluminum industry is a 40 billion dollar industry in the US comprising of products and exports. This figure was significantly smaller, less than 10 billion two decade ago. **Figure 1** shows the breakdown of the aluminum industry (2003 Aluminum Association report).

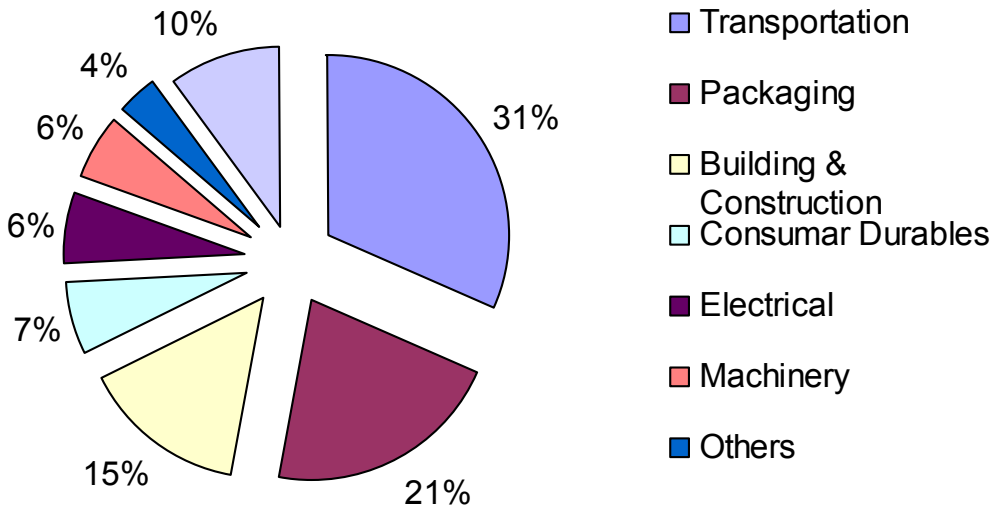

Figure 1: Sector-wise breakdown of Aluminum consumption.

It is evident from **Figure 1** that, the automotive industry accounts for nearly a third of all aluminum products consumed in the USA. The increased consumption of aluminum in the automotive industry has been largely dictated by oil crises in the US during the 1970's. In response to the then-restricted world supply of oil, Congress enacted the Energy Policy and Conservation Act of 1975, which was intended to induce automobile manufacturers to improve fuel efficiency. Congress established a CAFE standard for passenger cars that required the building of fuel efficient cars with fuel standards that have progressively increased several times and now is at 27.5 miles per

gallon for model years 1985 and beyond. The automotive industry was under pressure from the US government to introduce fuel efficient cars and reduce the consumption of imported oil. The net effect was an increased focus by the automotive industry toward the use of light metals and complete overhaul of traditional material selection and design. Aluminum offers many opportunities for the replacement of components traditionally manufactured utilizing iron based alloys. It is generally accepted that Aluminum offers certain advantages over similar steel / iron parts; for example:

Fuel savings: A 6 to 8 percent fuel savings for every 10 percent weight reduction.

Emissions: Each pound of aluminum that replaces 2 pounds of steel can save a net 20 pounds of carbon dioxide equivalents over the lifetime of a vehicle.

Recycling: Nearly 90 percent of the aluminum used in the automotive industry is recovered and recycled

The above mentioned advantages have propelled an investment in the research and development by both industry and the government, for process development, structure – property relationship, of aluminum and its alloys as a direct or indirect replacement of heavier iron based parts. One important impact of the rise of the Aluminum revolution is the emphasis towards near net shape manufacturing. Near net shape manufacturing provided the much needed competitive advantage vis-à-vis steel / iron parts, as raw aluminum on average is 1.5 – 2 times as expensive as steel. Die casting is a near net shape manufacturing process, which is a 7 – 8 billion dollar industry - see **Figure 2** (Aluminum Association 2003 report). Die cast components constitute a major portion of aluminum products that are used in the automobile industry.

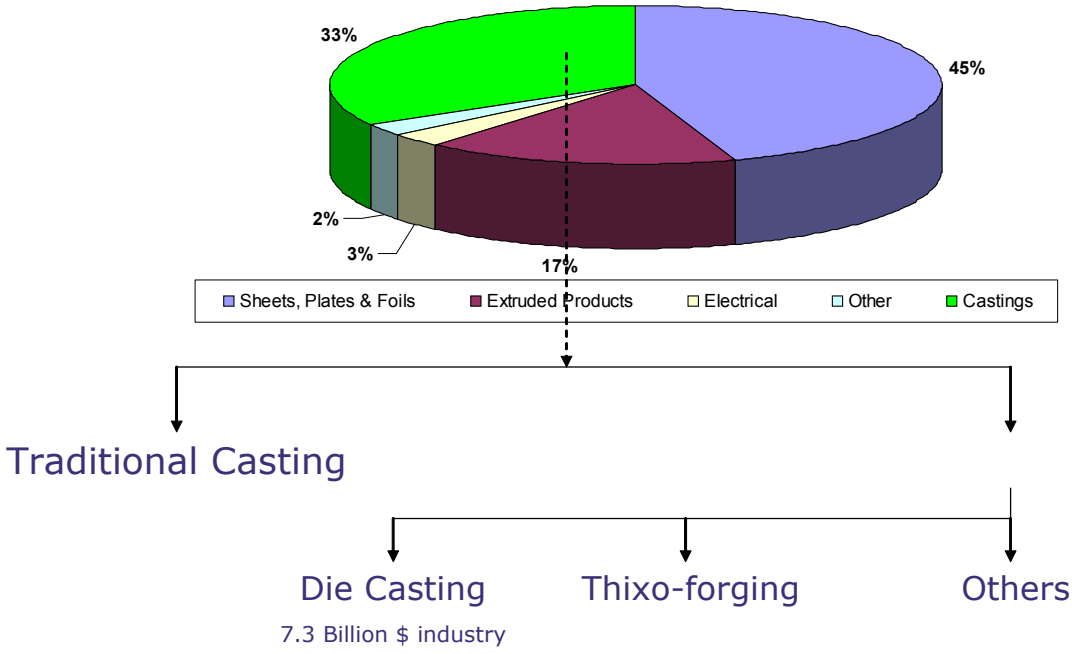

Figure 2: Typical processing routes of Aluminum[1].

The rise of the near net shape manufacturing of aluminum based alloys, led to an explosion in the number of available techniques for the net shape manufacturing of these alloys. Die casting is a successful near net shape manufacturing route; however, with the automotive industry demanding products with high strength – high ductility regimes at the same cost / weight ratio, there has been a renewed interest in emerging technologies to produce high integrity parts via net shape manufacturing. Some critical issues with traditional die casting process are:

- Liquid metal is introduced into die cavities at extremely high velocities. The resultant turbulent flow leads to a non-stable liquid front, leading to entrapped gases and oxide entrapment.
- The entrapped gases do not allow for the cast parts to be heat treated. Heat treatment can lead to enhanced mechanical properties, which cannot be fully exploited.

[1] From the Aluminum Association 2003 Report

- The turbulent flow and entrapped gases lead to decreased mechanical properties due to formation of free surfaces which oxidize etc.

The advent of semi solid processing has opened many avenues for the processing of Aluminum alloys for the production of high integrity net shaped components. Semi solid processing involves the net shape manufacturing of alloys in a two phase region (liquid + solid). Reduced turbulence “during casting”, less entrapped gases and lower operating temperatures (processes below the liquidus) make semi solid processing ideal for the manufacturing of high integrity Al parts. Traditionally, semi solid processing involved the heating of billets to a two phase region (called Thixocasting). Rheocasting is a new semi solid processing technique wherein the alloy is cooled from a liquid state (a combination of controlled heat flow and enhanced nucleation) to yield structures similar to the thixocasting process. Rheocasting or Slurry-On-Demand is in its early stages of development (the first industrial prototype of rheocasting was invented in the late 1990’s) and forms the central point of interest in this work. Much research is underway around the world to understand the controlling mechanism as well as the structure – property relationships in rheocast parts, primarily limited to the hypoeutectic Al-Si alloys. This work is dedicated in understanding the problems and possible novel routes for the rheocasting of hypereutectic Al-Si alloys as well as Al based wrought alloys. Novel techniques are presented for the casting of hypereutectic Al-Si alloys and Al based wrought alloys and substantiated with industrial trials and through analyses of the underlying mechanisms.

During the investigation, we were fortunate to have the opportunity to publish results in various Transactions and Journals. Accordingly, the thesis is organized such that chapters 5 through 11 contain the published and submitted manuscripts. Chapter 4 is an executive summary of the key results and underscores the significance of the results for hypereutectic and wrought Al based alloys. Chapter 3 elucidates the problem statement and the motivation of this work. Chapter 2, provides a background on semi solid processing techniques.

Chapter 2. Semi solid processing

Metallic alloys freeze over a temperature range, as they are cooled below their liquidus. **Figure 3** shows traditional casting and semi solid casting, as a metal alloy of composition X is cooled below the liquidus. Traditional casting involves the cooling of a metal from above its liquidus into a final shape. The imposed cooling rate and grain refining determines the final structure of the net shaped component. Semi solid processing, is the processing of the alloy when it is in the two phase region.

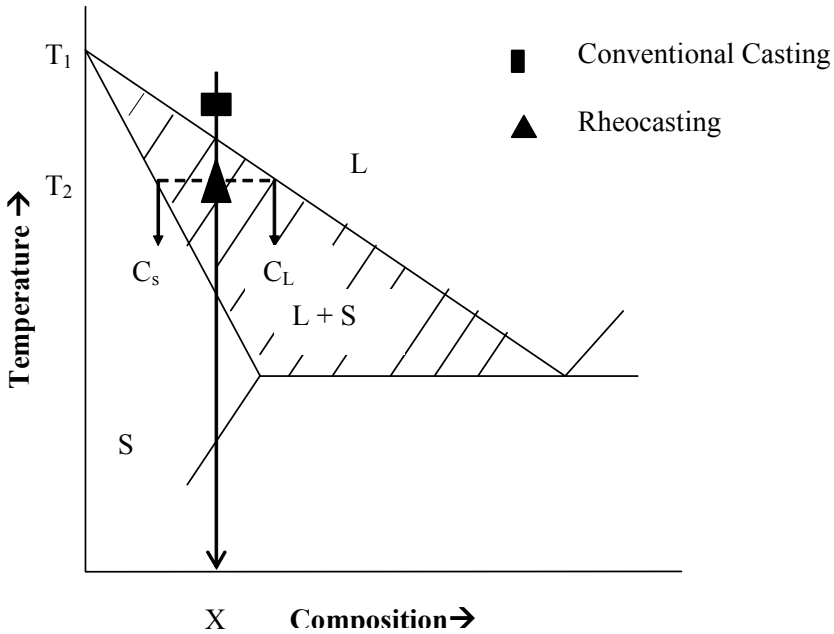

Conventional casting at temperature T_1

Rheocasting: alloy X is cooled to T_2 and isothermally agitated. The solid-liqiud mixtures consists of liquid phase of composition C_L of an amount f_L and solid phase of composition C_s and amount f_s, such that $f_sC_s + f_LC_L = X$

Figure 3: Thermal history during the semi solid processing versus conventional casting.

Some of the advantages of processing a metal in the two-phase range are:

- As the alloy is partially cooled (in the Liquid + Solid region), the casting process occurs at a lower temperature. Low casting temperatures have a direct benefit with respect to die life, reduced erosion, etc
- The alloy is in the two phase region, leading to a non – turbulent flow. Laminar flow of viscous liquid and solid mixture causes little or no turbulence or entrapment of air and oxides; and mechanical properties are improved by SSM processing.
- Rapid die fill makes thin cast sections feasible and lower processing temperatures extend tool life.

Semi solid processing can be broadly classified into two categories as described below:

2.1 Thixocasting

The idea of processing materials in the two phase region was first discovered at MIT by D. B. Spencer [1]. He discovered that by breaking up the dendrites (by shearing them in a Couette type viscometer), the viscosity of the metal while partially frozen decreased significantly. Close examination of the microstructure, revealed a non-dendritic microstructure. It was assumed during the early development and as late as mid 1990's, that the process for the formation of globular microstructure was due to the shearing of the dendrites, which led to the fragmentation of the dendritic arms. **Figure 4** illustrates the generally accepted theory for the formation of a globular microstructure.

The "concept" that shearing force was necessary for the formation of a globular primary phase, led to the development of Thixocasting. Billets containing grain refiners were cast and stirred under the influence of electromagnetic forces to produce a globular structure. **Figure 5** is a schematic showing the Thixocasting process. The cast billets are then reheated to the two-phase region and the final part is then manufactured.

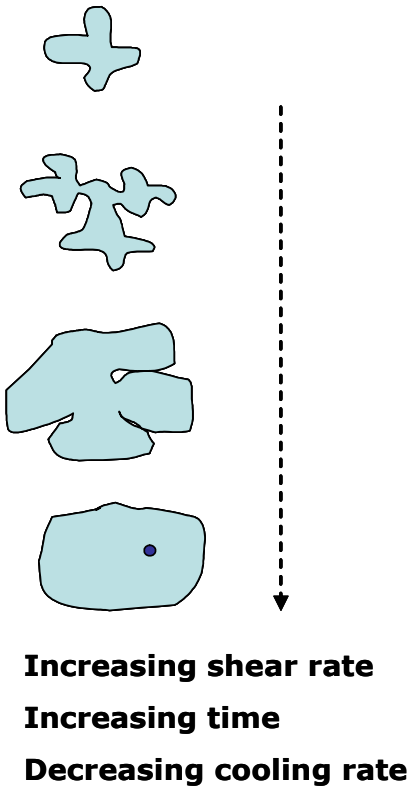

Figure 4: Breakdown of dendritic arms by shearing was accepted theory for the formation of globular primary phase [1, 21].

Thixocasting was a positive change towards net shape manufacturing of Aluminum based alloys for the production of high quality, high integrity parts. There was an explosion in the amount of research conducted around the world, assessing and developing Thixocasting and extending it as a mainstay in the manufacturing of high integrity near net shape parts. Research was extended to not just Aluminum alloys, but to magnesium, aluminum wrought alloys, steel and recently to titanium based alloys [4–12]. However, reheating billets and costly scrap led to a new emerging technology called, Rheocasting.

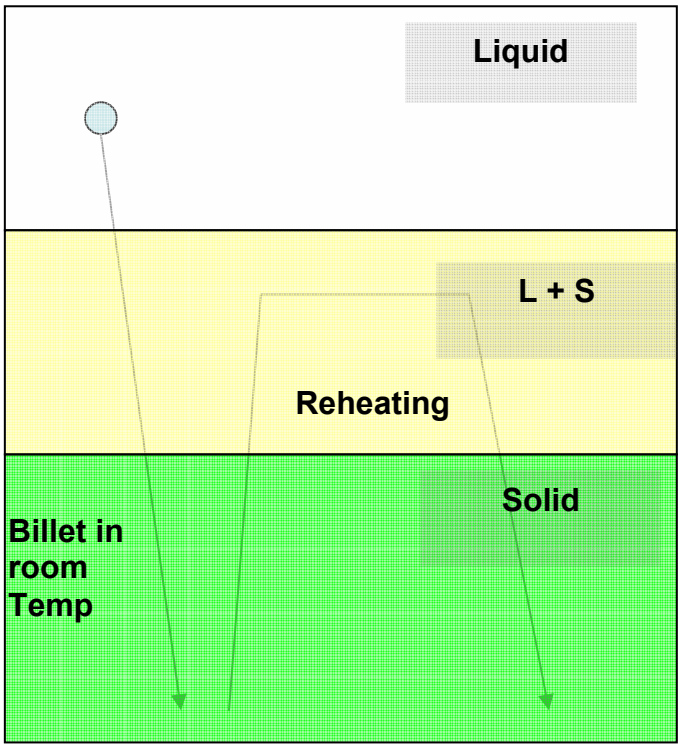

Figure 5: Schematic of a Thixocasting process. Billets are cast utilizing grain refiners or electromagnetic forces and then reheated to the two phase region and subsequently the part is manufactured.

2.2 Rheocasting

In the recent past, it has been discovered that one may obtain a refined SSM structure without breaking up the dendritic structure[3], but rather by creating an environment where copious nucleation can occur near the liquidus temperature of the alloy[13,14], and with limited growth of the formed nuclei [15]. Essentially, SSM structures develop by controlling the nucleation and growth processes during the early stages of freezing. The first industrial prototype for the rheocasting of aluminum component was patented by UBE [16] in 1996.

Figure 6 is a schematic diagram of the UBE NRC process and the steps involved during SSM processing. The UBE NRC process was a boost to the rheocasting industry, as it provided direct evidence that shearing of dendritic arms is not a

necessary condition for the formation of globular microstructures. This was a paradigm shift for the industry. Rheocasting not only provided the advantages of near net shape manufacturing and the inherent quality advantages of semi solid processing, but reduced the cost of billet reheating associated with Thixocasting.

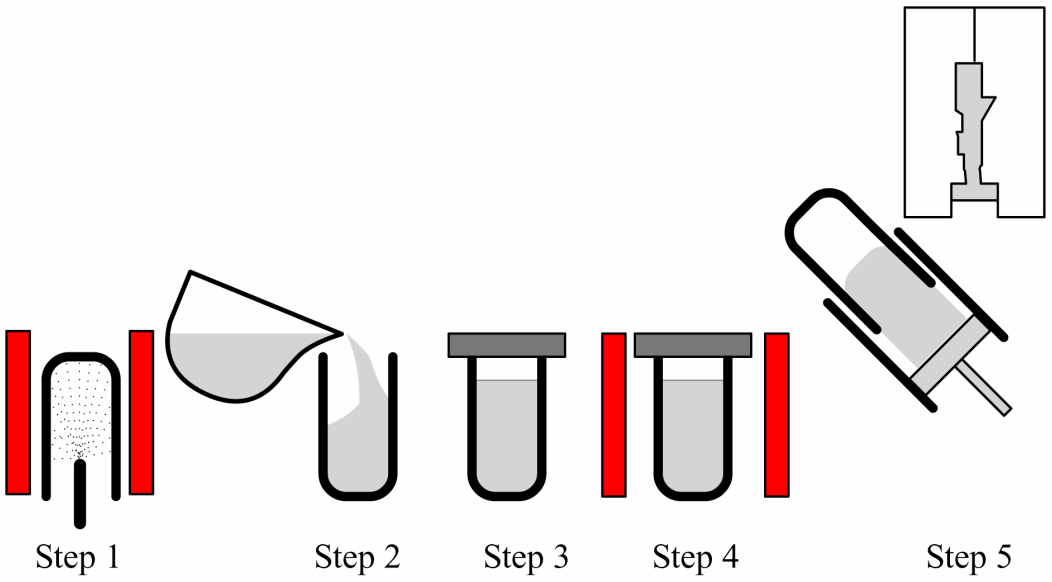

Figure 6: The UBE process. The first industrial rheocasting process consisted of five steps; Step 1 – Carousel cleaning, Step 2 – Liquid metal pouring, Step 3 – Isothermal holding, Step 4 – Thermal balance, Step 5 – Casting.

Recent research [17] has shown that the formation of globular microstructure is a result of convection and diffusion, which is a departure from the earlier view that shearing was a necessary requirement for globular microstructure. The nucleation of the primary phases as the liquid is poured into a steel crucible [18], and the natural convection leads to the formation of globules. **Figure 7** clearly shows the effect of convection for the formation of SSM microstructures.

The understanding of the fundamentals for the formation of globular microstructures has led to new processes and inventions. Some of the new processes that have sprung and have utilized the concept of nucleation, convection and growth are:

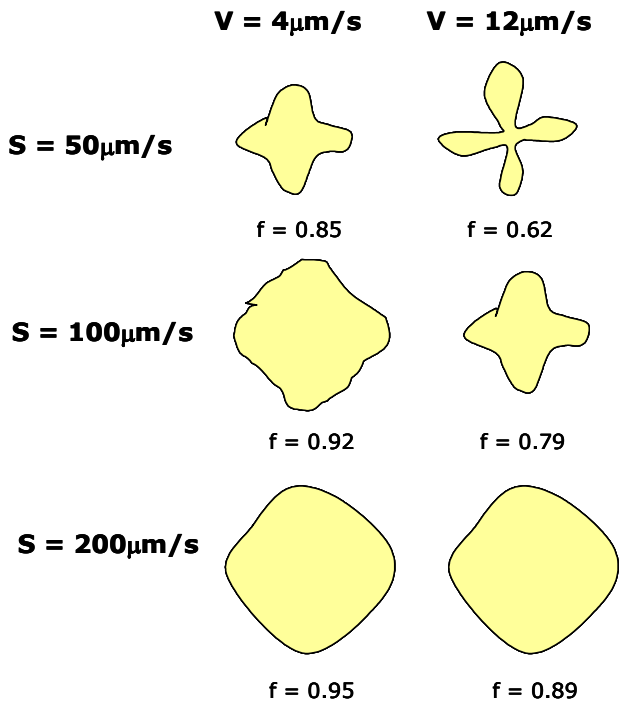

Figure 7: Effect of growth rate (R) and convection speed (S) on the shape factor (f) after nucleation of the primary phase [17]. Cleary, convection and nucleation play a very important role in the formation of SSM structures. It is a departure from the earlier view that shearing is necessary for the formation of globular structures.

- Mechanical Stirring of the liquid metal (SSR process, or new MIT process) [13] where the liquid metal is stirred mechanically during the initial solidification region, leading to the nucleation of the primary phase and the dispersion of nuclei across the melt.
- CRP^{TM} (Continuous Rheocasting Process) developed by the ACRC-MPI team wherein liquid from two different reservoirs is fed into a reactor to produce a slurry. The reactor aids in the formation of the nuclei, and dispersing them throughout the bulk [19]
- Sub Liquidus Casting [20], which utilizes pouring molten metal at low superheats into a cavity giving semi solid structures.
- AEMP process [21], which utilizes electromagnetic stirring to supposedly, break up the dendrite arms and create a semi solid slurry.

Rheocasting provides the advantages of semi solid processing with cost advantages over Thixocasting. It is a technology that is at its infancy stage (less than 10 years old) and has the potential to replace conventional die casting process for the production of high integrity near net shaped parts. The central theme of this Thesis is to explore the possibilities of utilizing rheocasting for the casting of hypereutectic Al-Si alloys and Al based wrought alloys. The next chapter presents the challenges and opportunities and a need for the rheocasting of hypereutectic Al-Si alloys as well as Al based wrought alloys.

References

1. D.B. Spencer, R. Mehrabian, and M.C. Flemings, "*Rheological behavior of Sn-15 Pct Pb in the crystallization range",* Metallurgical Transactions A (Physical Metallurgy and Materials Science), 1972, Vol. 3(7), p. 1925-1932.
2. M.C. Flemings, Materials and Metallurgical Transactions A, Vol. 22. 1991
3. D.H. Kirkwood, "*Semisolid metal processing",* International Materials Reviews, 1994. Vol. 39(5), p. 173-189.
4. H. Iwasaki et al., "*Shear deformation behavior of Al-5% Mg in a semi solid state",* Acta Materialia, 1998, Vol. 46(18), p. 6351-6360.
5. E.J. Zoqui and M.H. Robert, "*Structural modifications in rheocast Al-Cu alloys by heat treatment and implications on mechanical properties",* Journal of Materials Processing Technology, 1998, Vol. 78(1-3), p. 198-203.
6. P. Kapranos et al., "*Near net shaping by semi solid metal processing",* Materials & Design, 2000, Vol. 21(4), p. 387-394.
7. A.A. Kazakov, "*Alloy compositions for semisolid forming",* Advanced Materials and Processes, 2000, Vol. 157(3), p. 31-34.
8. M.H. Robert and M. Adamiak, "*Preliminary studies on the suitability of rheocast Al alloys for deep drawing"* Journal of Materials Processing Technology, 2001, Vol. 109(1-2), p. 168-173.
9. L. Sang-Yong, L. Jung-Hwan, and L. Young-Seon, "*Characterization of Al 7075 alloys after cold working and heating in the semi solid temperature range",* Journal of Materials Processing Technology, 2001, Vol. 111(1-3), p. 42-47.

10. A.M. Camacho et al., "*Thermodynamic predictions of wrought alloy compositions amenable to semi solid processing",* Acta Materialia, 2003, Vol. 51(8), p. 2319-2330.
11. J. Dong et al., "*Liquidus semi-continuous casting, reheating and thixoforming of a wrought aluminum alloy 7075",* Materials Science and Engineering A, 2003, Vol. 345(1-2), p. 234-242.
12. D. Liu et al., "*Microstructural evolution and tensile mechanical properties of thixoformed high performance aluminium alloys",* Materials Science and Engineering A, 2003, Vol. 361(1-2), p. 213-224.
13. R. Martinez, A.M. de Figueredo, J. Yurko and M.C. Flemings, "*Efficient Formation Structures Suitable for Semi solid Forming",* Transactions of the 21st International Die Casting Congress and Exposition, Cincinnati, Ohio 2001.
14. P. Wang, G. Lu, and J. Cui, "*Microstructure of nearby liquidus semi-continuous casting aluminum alloy A356",* Acta Metallurgica Sinica, 2002, Vol. 38(4), p. 389-392.
15. Van Boggelen, J.W.K., D.G. Eskin, and L. Katgerman, "*First stages of grain coarsening in semi solid Al-Cu alloys",* Scripta Materialia, 2003, Vol. 49(7), p. 717-722
16. European Patent EP 0 745 694 A1 (1996), By UBE Industries Ltd.
17. Shusen Wu, Xueping Wu and Zehui Xiao, Acta Materialia, 2004, Vol. 52, p. 3519 – 3524.
18. P. J. Ugoowitzer and Helmut Kaufmann, "*Evolution of globular microstructure in new rheocasting and super rheocasting semi solid slurries*", Steel Research Institute, 2003, Vol. 75, No. 8/9, p 525 – 530.
19. A.M. de Figueredo, M. Findon, D. Apelian, and M.M. Makhlouf, "*Melt Mixing Approaches for the Formation of Thixotropic Semi solid Metal Structures*", Proceedings of the Seventh International Conference titled Advanced Semi solid Processing of Alloys and Composites, Tsukuba, Japan, 2003, September 24-28, page 557-562.
20. John L. Jorstad, "*Semi solid metal processing: The high integrity die casting process*", Die Casting Engineer, Vol. 48, No. 1, January, 2004, p. 42-44 & 46-48.

21. Merton Flemings, “Semi solid Processing – The Rheocasting Story”, Test Tube to Factory Floor: Implementing Technical Innovations, In the proceedings of the Spring Symposium May 22, 2002 published by Metal Processing Institute, Worcester Polytechnic Institute, Worcester MA 01609.

Chapter 3. Problem statement and impact

The heart of this thesis is the development of novel processes for the semi solid casting of hypereutectic Al-Si and Al based wrought alloys. In this regard, Chapter 3 is dedicated to highlighting the challenges to processing these alloys via the rheocasting route.

3.1 Hypereutectic Al-Si alloys

Hypereutectic Al-Si alloys have gained enormous significance in the recent past due to superior properties (low coefficient of thermal expansion, high yield strength and high wear resistance). Typical composition of the most commonly used hypereutectic Al-Si alloys is shown is **Table 3-1.**

Table 3-1: Typical composition (wt.%) of a hypereutectic Al-Si alloy (390)

Si	Fe	Cu	Mg	Mn	Zn	Ti	P
16-18	1.0 max	4.0-5.0	0.5-0.65	0.1 max	0.2 max	Traces	0.1 max

The hard primary silicon in a soft matrix of Al-Si eutectic provides the requisite wear resistance. Some of the most common applications are: engine blocks, cylinder heads, clutch input housing, clutch assembly, brake cylinders, oil pump cooler, valve cover, cylinder sleeves, drives sleeves, clutch assemblies, brake cylinder, gears, pump housing, pulley wheels and brake drums. The difficulty in processing hypereutectic Al-Si alloys arise from the fact that, as primary Si nucleates from the liquid, it develops complex shapes depending on the cooling rate imposed on it. Nine different morphologies of primary Si have been observed and reported in the literature [1]. The morphology of the Si depends on the imposed temperature gradient, presence of impurities and the ease of nucleation. A halo of Aluminum are frequently reported around the primary Si particles. Yilmaz and Elliot [2] have attributed these halos of aluminum to growth rate and growth composition effects. The presence of a “halo” is

not desirable in the final microstructure. Traditionally the refinement of primary Si is achieved by the addition of phosphorus to the melt. Researchers [3] have used other refining agents to refine primary Si - i.e.; Germanium, Gallium, Selenium, Tellurium, Lithium, Cadmium, and Lithium Chloride. The final properties in the cast component are dictated by the distribution and size of the primary silicon phase. Sneider et al [4] established that an increase in the volume fraction of primary silicon (or reduced size) increases the resultant mechanical properties. A brief summary of the challenges and solutions for the casting of hypereutectic Al-Si alloys are given below:

3.1.1 Conventional die casting of 390 alloy and challenges

Hypereutectic alloys have been successfully cast (for parts amenable to die casting), by the use of high pressure die casting process (HPDC). It is well known that the cooling rate during solidification plays an important role in the final size of primary silicon. HPDC solves the problem of primary silicon size for small parts, but does not produce a final part with an uniform distribution of primary silicon. **Figure 8** shows a typical microstructure obtained from a part produced via HPDC. One can clearly see the non uniform distribution of primary silicon.

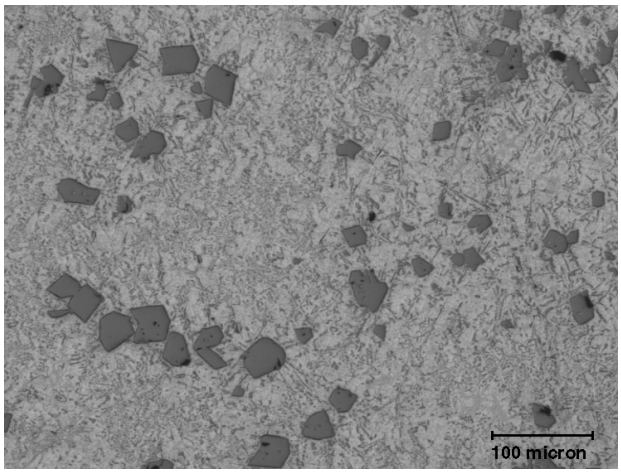

Figure 8: Typical microstructure obtained via the casting of hypereutectic Al-Si alloys via HPDC die casting process. Notice the non uniform distribution of primary Si.

Some of the problems associated with HPDC are:

- Primary silicon segregation or floatation caused by convection currents or low holding temperatures
- Primary silicon size control
- Primary silicon size distribution
- Surface depletion of primary Si by casting in steel dies

Some of the typical parts made via HPDC are power train components, such as compact variable compressor cylinders (CVC).

Squeeze casting is a variation of high pressure die casting, but with a change with respect to the speed of the metal flowing into the die. The melt velocity in squeeze casting is much lower than in HPDC and offers a less turbulent flow of the melt into the die compared to HPDC. The lower metal fill rate leads to distinct advantages over HPDC:

- Reduced turbulence
- Reduced air entrapment
- Reduced shrink porosity
- Better/similar dimensional control similar to that of HPDC
- Heat treatable (T6, T4)

An example of a common part produced by squeeze casting is a crankshaft hub. Squeeze casting has many advantages compared to HPDC, as well as certain disadvantages which are summarized below:

- Longer cycle time compared to HPDC, leading to higher costs
- Higher melt temperatures in squeeze casting, leading to poor dimensional tolerences
- Thicker gates in squeeze casting

In summary, there are inherent disadvantages in HPDC and Squeeze casting processes for the net shape manufacturing of hypereutectic Al-Si alloys. Silicon segregation, silicon depletion on the outer skin of the part, are common problems in convention die casting (HPDC and squeeze casting), as nucleation and solidification occur in the die. High pressures and rapid solidification involve a complex process of turbulent flow coupled with nucleation and growth under meta-stable conditions.

3.1.2 Thixocasting of hypereutectic Al-Si alloys

Thixocasting, [**Section 2.1**] is the preferred route for semi solid processing of hypereutectic Al-Si alloys to attain a fine primary silicon size and distribution. During the Thixocasting of hypereutectic Al-Si alloys, a billet (MHD cast) containing extremely fine primary Si (< 15 microns) particles is re-heated to the SSM temperature, transferred to a shot sleeve and then injected into the die cavity and cast. Casting of hypereutectic alloys via SSM processing is difficult for the following reasons:

- Longer range of solidification (from typically 650 – 577 ^{0}C for 390 alloy)
- Higher enthalpy of fusion as hypereutectic Al-Si alloys, consist of 90% volume fraction eutectic liquid. A typical hypoeutectic alloy (7% Si) consists of 50% eutectic liquid, and hence more heat (the Si in the eutectic) is released in the casting of hypereutectic Al-Si alloy compared to hypoeutectic Al-Si alloys.
- Growth of primary silicon (most primary silicon nucleates early and grows to large size as the alloy cools from 650 – 577 ^{0}C)

Figure 9 is a schematic diagram showing the typical billet size used for Thixocasting of hypereutectic Al-Si alloys. **Figure 10** shows the samples cut from a typical billet for microstructural analysis. Microstructural analysis was performed on each strip and an average of 4-5 pictures were utilized to map the primary Si size across the billet from the side towards the center.

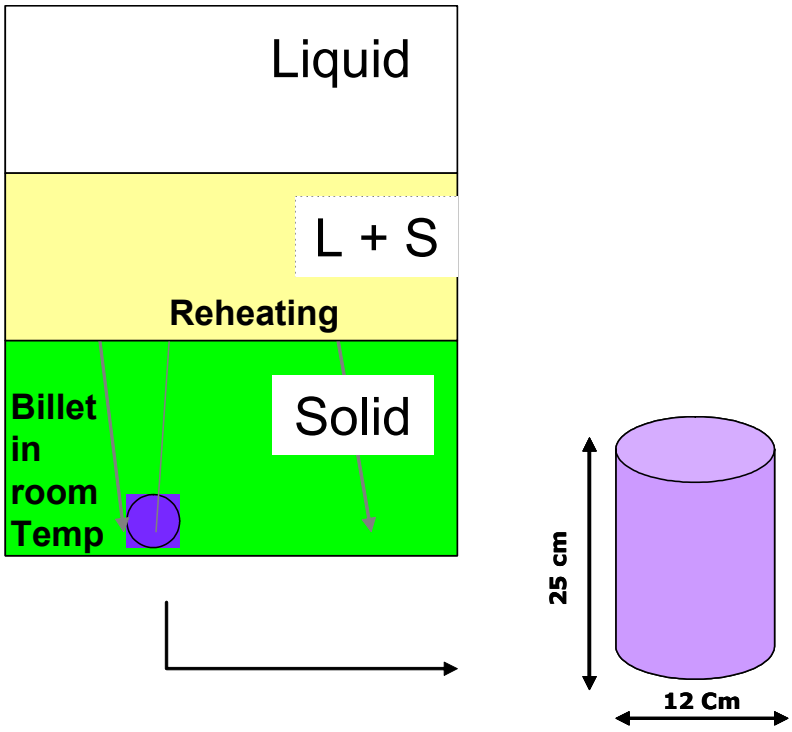

Figure 9: Schematic showing dimensions of the typical billets, which are reheated to the semi solid range.

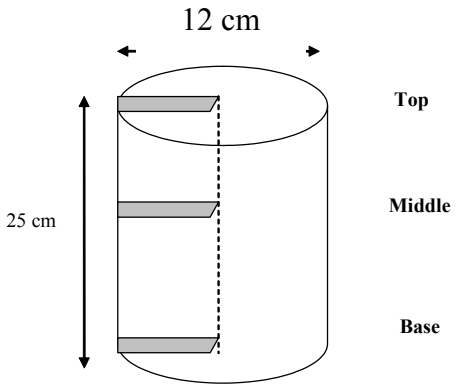

Figure 10: Sections taken from the 390 slugs (EM stirred) for microstructural analysis.

2-D sections of the microstructure were captured and through image analysis, various structural features were analyzed and measured. **Figure 11** shows the typical silicon size from the edge to the center. The values clearly show that the typical primary Si sizes in the billets range between 15 – 25 microns.

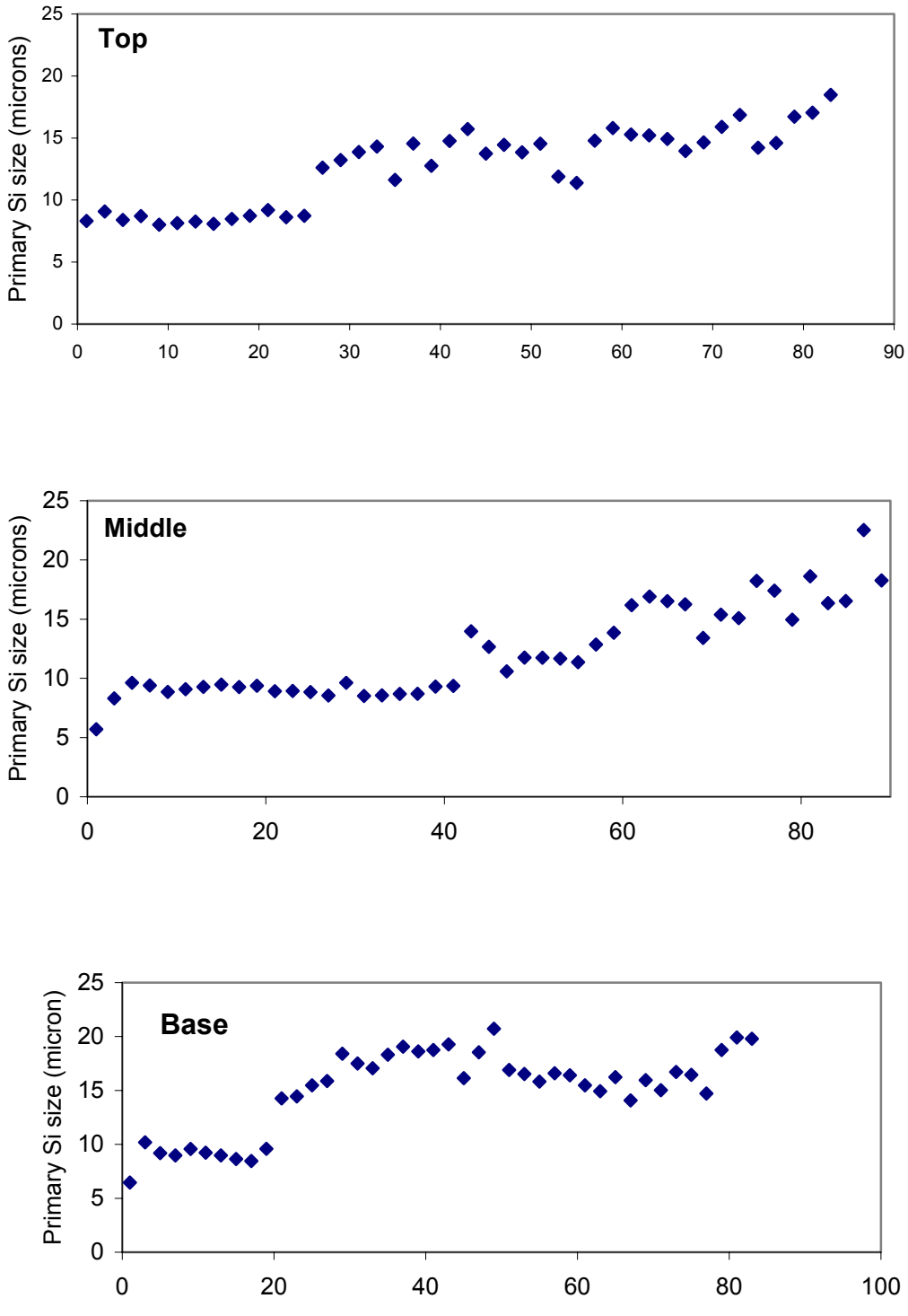

Figure 11: Primary Si size distribution from the edge to the center (x-axis: 10 units = 500 microns). Each point is an average of 4 – 5 micrographs.

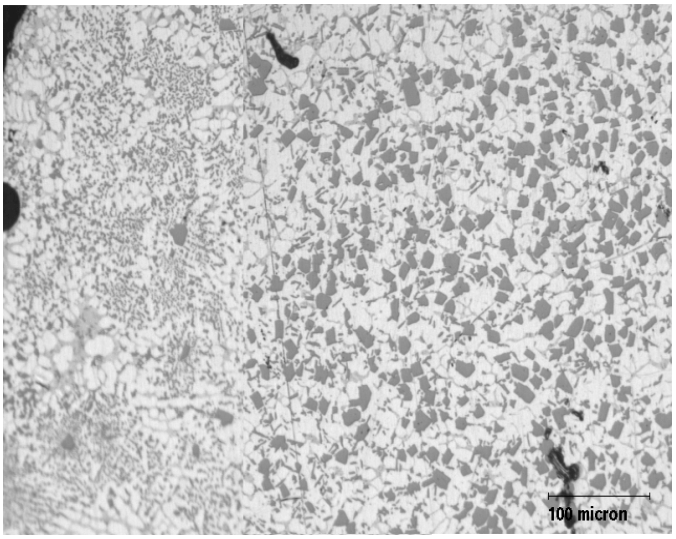

Figure 12: Typical microstructure of a slug (left to right: edge → center). Notice the region at the edge which is devoid of primary Silicon.

Billets of hypereutectic Al-Si alloys are made by continuous casting, the surface of the billets experience high cooling rates, leads the development of a shell around the billet, which is devoid of any primary silicon. This region is essentially a low melting liquid (eutectic or aluminum) as shown in **Figure 12**. As the billet is reheated, improper heating leads to the melting of this thin shell leading to metal losses. Also, hypereutectic alloy is a mixture of low melting eutectic Al-Si and primary Si (does not provide rigidity as α-Al in hypoeutectic Al-Si alloys), which leads to issues that can be summarized as follows:

1. The low melting point eutectic constitutes 80-85% of the total volume in a typical 18-19% Si alloy, indicating that a very close control on the temperature is essential as the slug (cut billet) is reheated to temperatures above the eutectic temperature. The drainage (flow of the liquid from the billet during reheating) is high in hypereutectic alloy.
2. The lower density of primary Si compared to Al, worsens the situation as silicon tends to agglomerate as the slug is improperly reheated. The primary Si tends to cluster near the grain boundaries of the eutectic grains (depending on the amount

of eutectic that has melted). **Figure 13** shows a typical part microstructure showing the distribution of primary silicon.

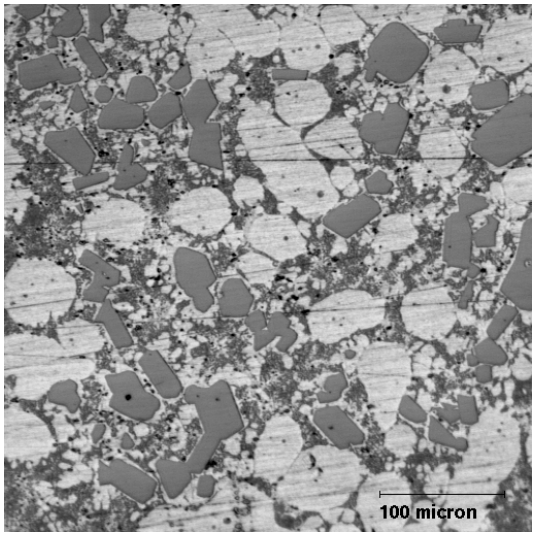

Figure 13: Typical microstructure obtained by the Thixocasting process (after heat treatment) if the heating is not controlled. Notice the clustering of the primary silicon, though there is a very good control on the primary silicon size.

Clearly, Thixocasting provides the advantage of net shape manufacturing of hypereutectic Al-Si alloys; however, certain issues still remain:

- The cost of billets
- There is considerable control on the size of primary silicon, though the distribution of primary silicon is lost during reheating as the primary Si tends to form agglomerated around the eutectic grains if the billet is improperly re-heated to temperatures above the eutectic temperature.
- As the essential ingredients of hypereutectic Al-Si alloys are primary Si and low temperature eutectic, reheating these slugs to a semi solid temperature involves considerable control. The process control window for the processing of hypereutectic Al-Si is therefore reduced.
- Recycling scrap

3.1.3 Hypereutectic Al-Si alloys rheocasting issues

Rheocasting [**Section 2.2**] or Slurry-On-Demand approach offers cost advantages over Thixocasting in terms of alleviating billet premiums, reheating costs, recycling, etc. Rheocasting of hypereutectic Al-Si alloys has been hampered by the growth of the primary Si phase to an unacceptable range (> 100 μm). Ironically, a large solidification range, which is believed to be ideal for SSM processing, in this instance (i.e., 390 alloys) causes accelerated growth of the primary Si phase as the alloy cools from the liquidus to the SSM processing temperature. **Figure 14** shows the primary silicon size and distribution as a 390 alloy is cooled below the liquidus.

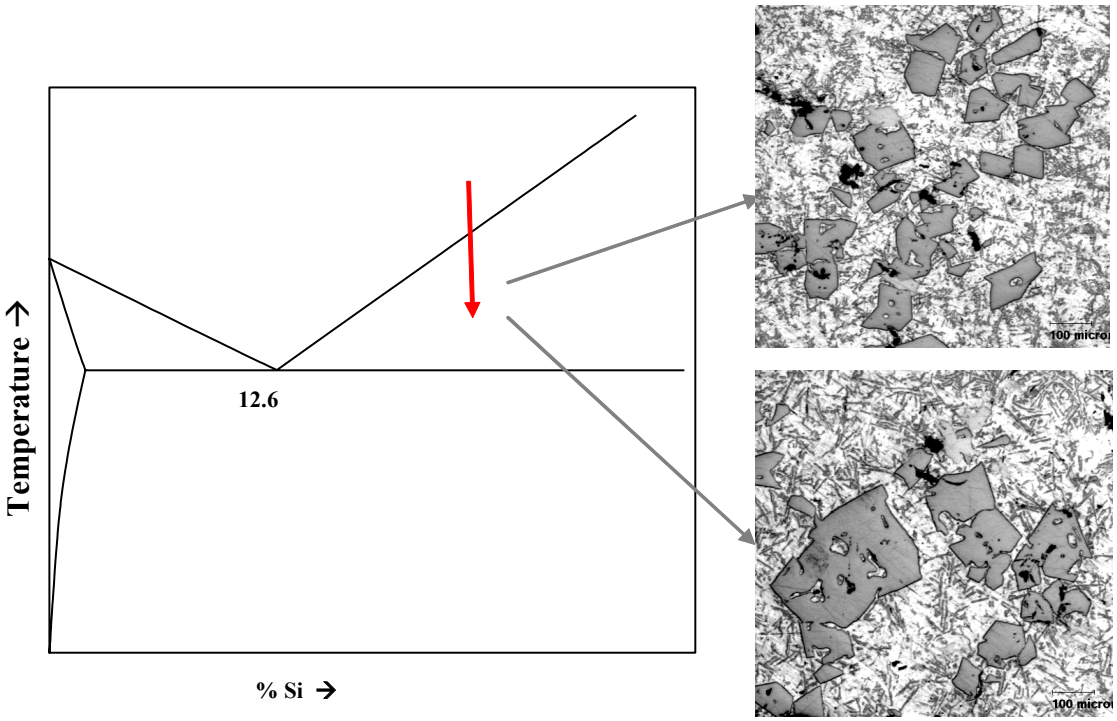

Figure 14: Typical microstructures obtained when a 17 - 18% Al-Si alloy is cooled and cast. Notice the primary Silicon size and distribution. The large primary silicon size and clustering of silicon makes rheocasting of these alloys difficult.

Processing of hypereutectic Al-Si alloys is also a challenge because of the heat associated during the solidification of primary Si. **Figure 15** shows the heats evolved per mole of a hypereutectic Al-Si alloy (A356) and a hypereutectic Al-Si alloy (A390). The

data were obtained by PANDAT software (using non-equilibrium solidification assumptions / Gulliver-Scheil equation). It can be seen from **Figure 15** that the heat associated during the cooling of a hypereutectic alloy is at least 2-3 times that of an equivalent solid fraction of the hypoeutectic alloy. This heat aids the fluidity of these alloys. In traditional castings of hypereutectic alloys, the energy released during solidification is removed by generous use of chills in the castings. The high heat released in hypereutectic Al-Si alloys is attributed to the high entropy of fusion that is released during solidification. Current rheocasting processes involve the cooling of the alloy a very slow rate.

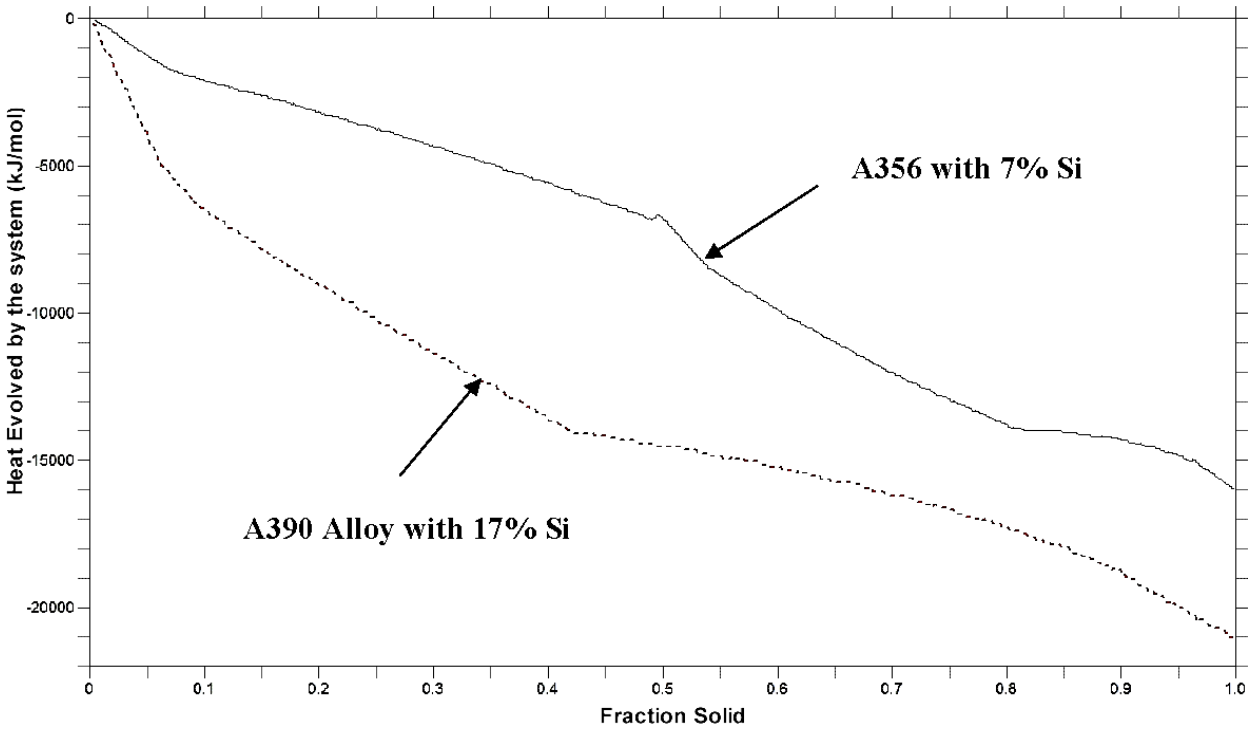

Figure 15: Heat released during the solidification of a hypereutectic Al-Si alloy (dashed) and a hypoeutectic Al-Si (continuous line) with respect to fraction solid. The large difference in the amount of heat released necessitates a new approach for the semi solid casting of hypereutectic Al-Si alloys.

As almost all processes are designed for the rheocasting of hypoeutectic alloys, they do not account for the extra heat during the solidification of hypereutectic alloys. The extra heat is due to amount of eutectic in the alloy. A typical hypoeutectic alloy has

50% liquid fraction (Al-SI eutectic), in contrast a typical hypereutectic Al-Si alloy has 90% liquid, leading to an extra amount of heat released during the solidification of these alloys. Slow heat extraction leads to the rapid growth of primary Si. Another problem associated with casting of hypereutectic Al-Si alloys is the role undercooling plays on the size of the primary Si. The ideal microstructure of hypereutectic Al-Si alloys should consist of primary Si, which is small in size and evenly distributed throughout the matrix. However, it is the nature of primary Si to grown into faceted structure if the undercooling is not high. The required high undercooling is in direct conflict with the concept of semi solid processing. The transition from continuous to faceted growth was analyzed by Wang et al [5], and is shown in **Figure 16**.

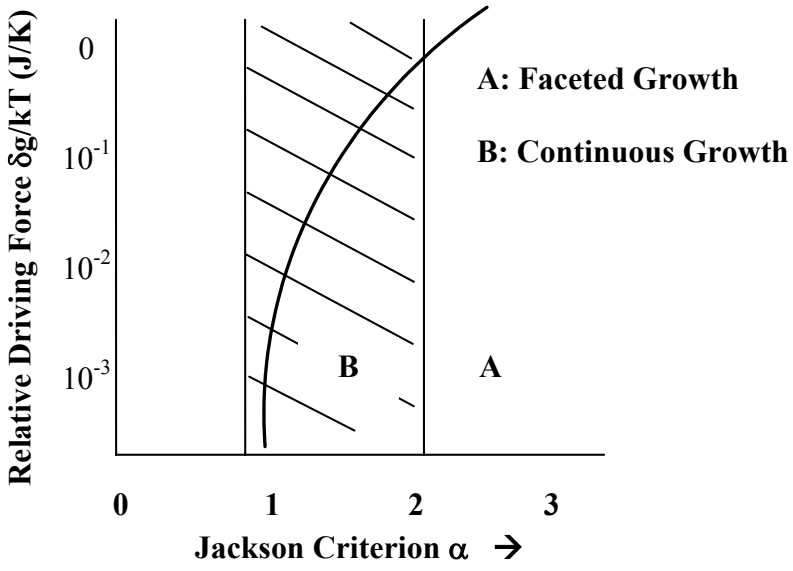

Figure 16: The variation in the driving force of transition from faceted to continuous growth [5]. The shaded region corresponds to the region of desired interest for silicon size. Clearly, higher undercooling is a desired path for the casting of hypereutectic Al-Si alloy to achieve fine primary Si.

The shaded region in **Figure 16** shows the region relevant to a “fine” primary silicon size. It can be seen that the driving force (which is directly proportional to the undercooling) determines the growth mode of primary silicon – i.e., faceted / un-faceted

structures. Traditional castings have employed high undercooling (use of chills, etc.) to precisely prevent the coarsening of the primary silicon (regions marked Region A in **Figure 16**). The regions labeled as the Region B give rise to the most desired primary Si microstructures. The transition from the un-faceted (Region B) to faceted (Region A) is due to the crystal structure of primary Si. Jackson [5] related crystal faceting to the entropy of melting and the crystal structure. **Table 3-2** lists the values and conclusions from his studies.

Table 3-2: Jackson Criterion for the Morphology of Silicon Phase [5].

Plane	Ns / Nv	α	Growth Mode
111	3/4	2.67	Faceted
100	2/4	1.78	Non-Faceted
110	1/4	0.89	Non-Faceted

Where: Ns = No. of atoms on the surface and Nv = No. of atoms in the cell and alpha equals the ratio (Ns/Nv) multiplied by the entropy change divided by the transformation temperature ($\Delta S/T_E$), i.e., alpha = (Ns/Nv) x ($\Delta S/T_E$). These studies lay the foundation for the motivation for the rheocasting of hypereutectic Al-Si alloys. Primary silicon refinement and distribution is a direct function of the undercooling achieved during the solidification of a hypereutectic alloy, which is dramatically different from rheocasting. Whereas previously it has been assumed that in most semi solid processing methods for hypoeutectic Al-Si alloys, the slow cooling aids the coarsening of α-Al as it is cooled below the liquidus.

The challenges of processing 390 alloy with a fine distribution of primary silicon phase have been reviewed. Before investigating the use of rheocasting (semi solid processing route), efforts were directed to controlling the primary silicon size by the use of inoculants. Specifically, selenium, nickel selenide, sulphides of iron and copper. These results were intriguing in that selenium refined both the primary as well as eutectic silicon. However, a major drawback is that the use of selenium is not

commercially viable for environmental reasons and toxic to humans. These results are given in Chapter 10.

3.1.4 Motivation for the rheocasting of hypereutectic Al-Si alloys

The possibilities of refining primary Si via rheocasting are therefore limited to:

a) breaking of primary Si (using external forces), and/or
b) use of growth restrictors, and/or
c) rapid heat extraction within the shot sleeve, without the formation of a chill zone.

As the alloy is cooled to the SSM range, and isothermally held in the two-phase range for a period of time before casting, primary Si grows rapidly and thwarts the very purpose of utilizing hypereutectic alloys. Uneven shape and size distribution of primary Si has been reported to be detrimental to the final mechanical properties and wear characteristics [4]. Lee et al. have used mechanical stirring [6], while others have used ultrasonic treatment [7] to break down the primary Si in the two-phase range. Traditional rheocasting techniques have shown limited success, as the inherent thermal properties of the Si phase require high undercooling to achieve a fine primary Si size and distribution. The unique requirement of high nucleation and arrested growth of primary Si coupled with an inherent slow cooling process of traditional semi solid rheocasting process, provided the much needed motivation for this work. The Thesis was essential to explore “possibilities” in the rheocasting of Al-Si alloys (emphasis on hypereutectic Al-Si), via a paradigm shift from a heat controlled solidification to a mass / diffusion controlled one.

3.2 Aluminum based wrought alloys

Aluminum based wrought alloys combined with differing percentages of other metals such as silicon, copper, magnesium, and manganese form alloys that are used in many domestic, automotive and aerospace applications. Net shape manufacturing of wrought alloys (*via* casting) has been difficult due to the tendency of these alloys to form

“hot tears”. Aluminum wrought alloys are characterized by their inability to be cast into net shaped components using conventional casting methods. This is mainly due to their high tendency to form hot tears and hot cracks [8]. Hot tears are cracks, which develop as an alloy passes through a transition from the liquid to the solid state. Wrought alloys have a very large solidification range [9] necessitating a longer time in the mushy zone (liquid + solid region) during solidification. Eskin et al [10] have classified the solidification into four stages:

- ***Mass feeding*** : where the liquid and solid are free to move
- ***Inter-dentritic feeding***: flow of liquid through the dendritic network
- ***Inter-dentritic separation***: fragmented liquid network, formation of pores and cracks
- ***Solid feeding***: solid network has considerable strength and solid state creep compensates shrinkage and thermal stresses. This is usually at a solid fraction of greater than 90%

Industrial and fundamental studies have shown that the development of cracks or hot tears in a casting / part occurs during the final stages of solidification, when 80-90% of the solid network is organized in a network of grains [10]. There are various studies that have shown that stress, strain rate and cumulative strain accumulation play a vital role in the development of hot tears [10]. There is a group of researchers that believe hindered feeding of the solid phase by the liquid as being the main cause of hot tearing [10]. Most Al based wrought alloys have coherency temperatures that are only a few degrees lower than their liquidus temperatures [9]. presents estimated coherency point for some of these alloys investigated [9]. Note that in each case, the coherency temperature is very close to the liquidus temperature of the alloy. The high coherency temperature coupled with the large solidification range renders these alloys prone to hot tearing.

Table 3-3: Coherency point of some aluminum-based wrought alloys [9].

Alloy	Coherency point		Liquidus (°C)	$\Delta T = T_{Liquidus} - T_{Coherency}$
	Temperature (°C)	Solid Fraction (wt %)		
2014	642 – 643	25	648 - 650	~ 6 - 8
5056	630 – 631	25	635 – 637	~ 5 - 7
7050	622 – 624	25	630 – 631	~ 7 - 9

The high coherency temperatures coupled with an extended freezing range result in inconsistent and inadequate feeding of liquid into the semi solid mushy zone during solidification of these alloys. The inadequate feeding leads to the development of hot tears rendering this class of alloys, not *"castable"*. Accordingly, these alloys are hot forged or hot worked which increase the mechanical properties and offered near net shape manufacturing [11,12]. **Figure 17** shows mechanical properties obtained from Thixoforged Al based wrought alloys [13]. It can be seen that this class of alloys have good mechanical properties and in some cases exceed plain carbon steel (7xxx series in **Figure 17**).

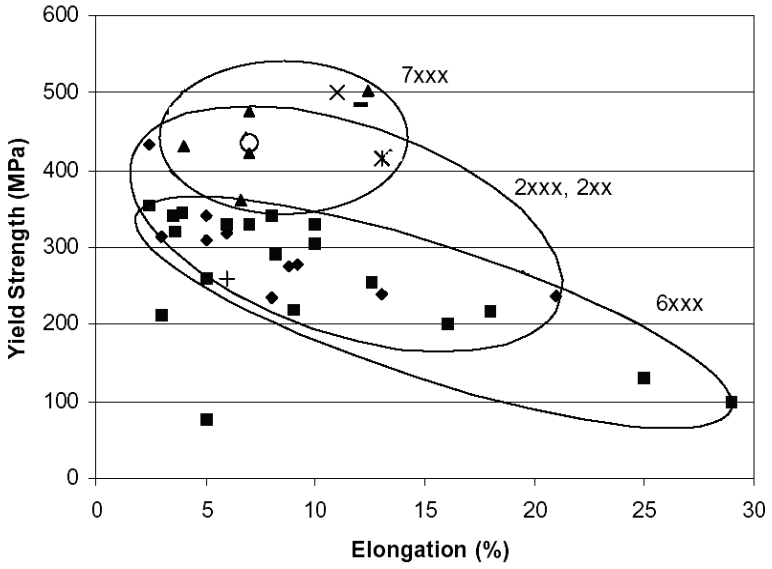

Figure 17: Typical mechanical properties of thixoforged Al based wrought alloys [13].

Even though this class of Al alloy is difficult to cast and process, their superior properties have made them attractive suitors in high integrity aerospace applications.**Figure 18** shows the various steps for the manufacture of components of wrought Al based alloy – via Thixocasting and Rheocasting. It can be clearly seen from **Figure 18** there is a considerable reduction in the number of processing steps if wrought alloys were rheocast. However, a cost advantage in reduced processing steps in rheocasting, cannot replace the superior properties obtained from mechanical worked material (thixoforging etc). In an exhaustive study performed by Eugenio Hose [14], rheocast Al-Cu alloys were made by stirring the liquid metal during solidification, cast and heat

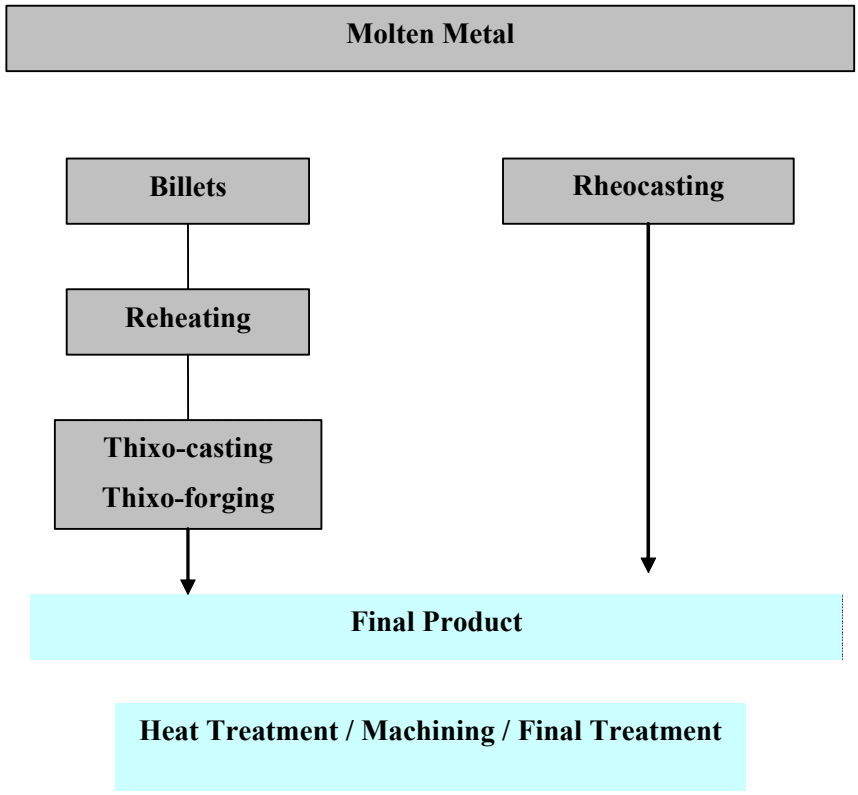

Figure 18: The elimination of processing steps if Al based wrought alloys were rheocast.

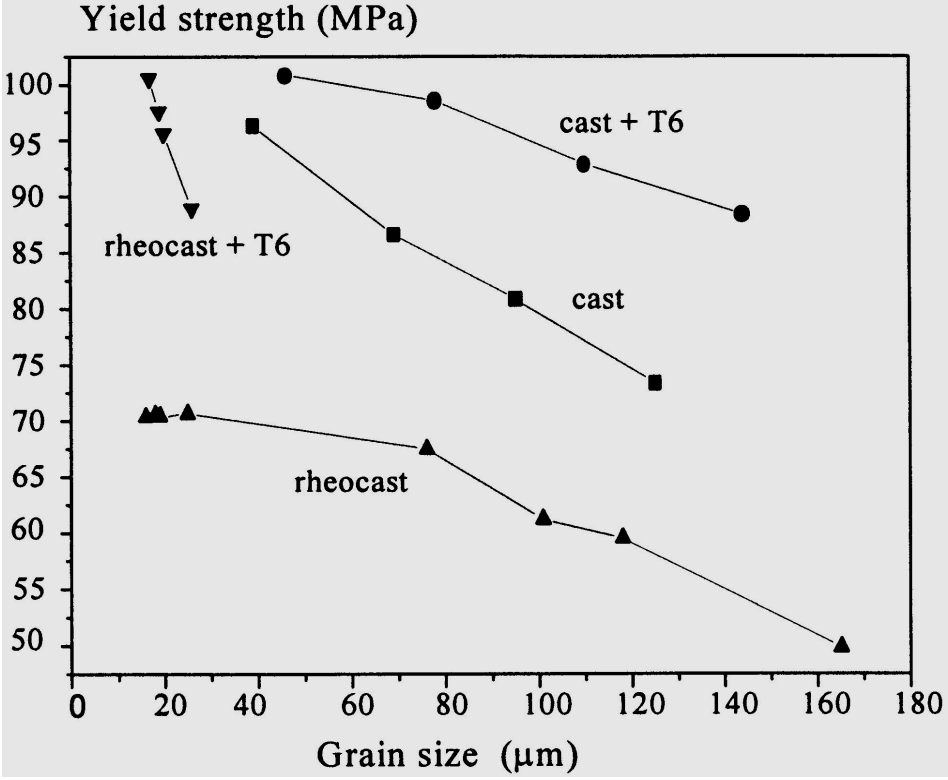

Figure 19: Typical mechanical properties obtained in a Rheocast Al-Cu (2xxx series) compared to a dendritic cast structure with heat treatment (T6) [14]. Success of any future rheocasting process for wrought alloys is dependent on the final grain size.

treated with a T6 condition (rheocast and heat treated). **Figure 19** shows the results obtained from this study.

3.2.1 Motivation for the rheocasting of Al based wrought alloys

It is apparent that rheocasting of wrought Al based alloys, offers opportunities and challenges for the development of alloys and parts with superior strength and ductility. The success of any new rheocasting process for the casting of Al based wrought alloys is however dependent on two variables:

1. Elimination of dendritic microstructures obtained during the casting of Al based wrought alloys. The dendritic structure hinders the ability of the final liquid to flow into the shrinking structure during the final stage of solidification, leading to hot tears

and cracks. A globular microstructure can partially eliminate the problem of inter-dendritic feeding due to the presence of an interconnected liquid surrounding the α-Al.

2. Achieving a globular microstructure with a very fine primary Al is a pre-requisite for enhanced mechanical properties. As rheocasting involves the casting of the slurry (liquid + solid) with 50-70% liquid fraction (commonly practiced), the primary grains are depleted in solute. Heat treatment homogenizes the solute in the matrix, and the finer grains make it amenable for solute strengthening.

In summary, rheocasting of Al based wrought alloys offers unique challenges and opportunities for the near net shape manufacturing of this class of high strength and high ductility alloys. The central challenge in the rheocasting of wrought alloys is to eliminate the dendritic microstructure with a globular primary phase. The next chapter is dedicated to the various processing routes that were pursued for rheocasting of hypereutectic Al-Si and Al based wrought alloys.

References

1. Gruzleski, N. Tenekedjiev, "*Hypereutectic Aluminum-Silicon Casting Alloys - A Review*" Cast Metals, 1990 Volume 3, Number 2, p. 96 - 105.
2. F.Yilmaz and R.Elliot, "*Halo Formation in Al-Si Alloys*", Metals Science, 1994, Volume 18, p. 362 – 366
3. S. Ghosh and W. J. Mott "*Some aspects of Refinement of Hypereutectic Aluminum - Silicon Alloys*", AFS Transactions, 1962, Volume 72, p. 721 - 732.
4. K. Schneider "*Aluminum casting alloys properties – Improvements by grain refinement*", AFS transactions, 1960, Vol. 68, p. 176 – 181.
5. Ru-yao Wang, Wei-hua Lu, L.M Logan, "*Growth morphology of primary Silicon in cast Al-Si alloys and the mechanism of concentric growth*", Journal of Crystal Growth, 1999, Vol. 207, p. 43 -54.
6. J.J.Lee, H.I. Lee and M.I. Kim, "*Formation of Spherical Primary Silicon Crystals During the Semi solid Processing of Hypereutectic Al-15.5 wt% Si Alloy*", Scripta Metallurgica, 1995, Volume 32, No. 12, p. 1945 – 1949.

7. "*Hypereutectic Al-Si Based Alloy with a Thixotropic Microstructure Produced by Ultrasonic Treatment*", Materials and Design, 1997, Volume 18, No 4/6, pages: 323 – 326.
8. W.M. van Haaften, W.H. Kool, and L. Katgerman, "*Hot Tearing Studies in AA5182*," Journal of Materials Engineering and Performance, 2002, Vol. 11(5), p. 537-543.
9. L. Arnberg, G. Chai, and L. Backerud, "*Determination of Dendritic Coherency in Solidifying Melts by Rheological Measurement*" Materials Science and Engineering A, 1993, 173(1-2), p. 101-103.
10. D.G. Eskin, Suyinto, and L. Katgerman, "*Mechincal Properties in the semi solid state and hot tearing of aluminum alloys",* Progress in Materials Science*,* 2004, Volume 49, Issue 5, p. 629-711
11. C.Y. Chen et al., "*Thixoforging of aluminum alloys",* Materials Science and Engineering, 1979, Vol. 40(2), p. 265-272.
12. M.M. Rovira, B.C. Lancini, and M.H. Robert, "*Thixo-forming of Al-Cu alloys",* Journal of Materials Processing Technology, 1999, Vol. 92-93, p. 42-49.
13. D. Liu, H.V. Atkinson, P.K. Kapronas, W. Jirattiticharoen and H. Jones, " *Microstructure evolution and tensile mechanical properties of thixoformed high performance aluminum alloys*", Material Science and Engineering, 2003, Vol. A361, p. 213 – 224.
14. Eugenio Jose Zoqui and Maria Helena Robert, "*Structural modification in rheocast Al-Cu alloys by heat treatment and implications on mechanical properties*", Journal of Materials Processing Technology, 1998, Vol. 78, p. 198 – 203.

Chapter 4. Synopsis and organization of thesis

This chapter is dedicated in presenting the various experiments, results and a brief synopsis of the subsequent chapters.

4.1 Rheocasting of hypereutectic Al-Si alloys

As detailed in Section 3.1.4, the possibilities of refining primary Si via rheocasting are therefore limited to: ***a)*** breaking of primary Si (using external forces), and/or ***b)*** use of growth restrictors, and/or ***c)*** rapid heat extraction within the shot sleeve, without the formation of a chill zone. We addressed the challenge of rheocasting Al-Si alloys by mixing two melts of two different compositions, each held at different temperatures. Specifically, we mixed two Al-Si alloys, one a hypoeutectic melt (6-7% Si, A356), and the other a hypereutectic alloy (25% Si). Chapter presents the first experiments performed by a variation in temperatures of the two alloys mentioned above. The 25% Si alloy was held above its liquidus temperature, whereas the 6-7% Si alloy was held in the semi solid range (two phase range) – see **Figure 20**. The purpose of adding the hypereutectic alloy to the cooler A356 alloy was to rapidly extract thermal energy from the hypereutectic melt, and to lower its temperature to the SSM casting temperature. The weight ratio of the two starting melts is 1:1, and the resultant alloy composition (based on a mass balance) is that of A390. The conceptual framework is to increase diffusion of heat from the hypereutectic alloy by the dissolution of the primary aluminum phase of the hypoeutectic alloy. The thermal / mass imbalance leads to two advantages:

- heat from the higher Si alloy is absorbed by the cooler alloy, and concomitantly
- rapid chilling prevents the growth of primary silicon to unacceptable ranges.

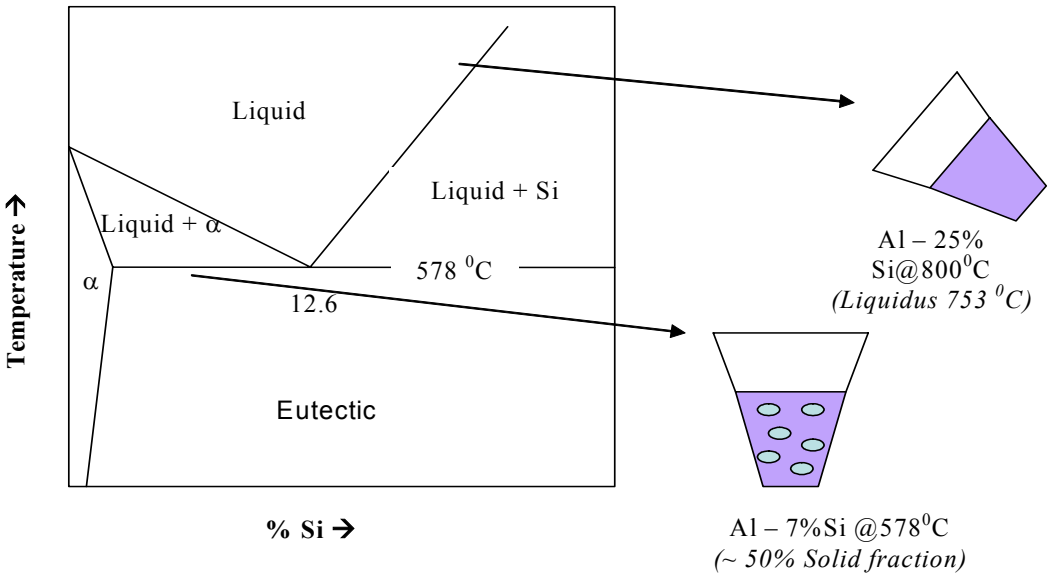

Figure 20: Diffusion Solidification concept of mixing liquid Al-Si at 800 ^{0}C, and hypoeutectic Al-Si alloy (7% Si) at 578 ^{0}C.

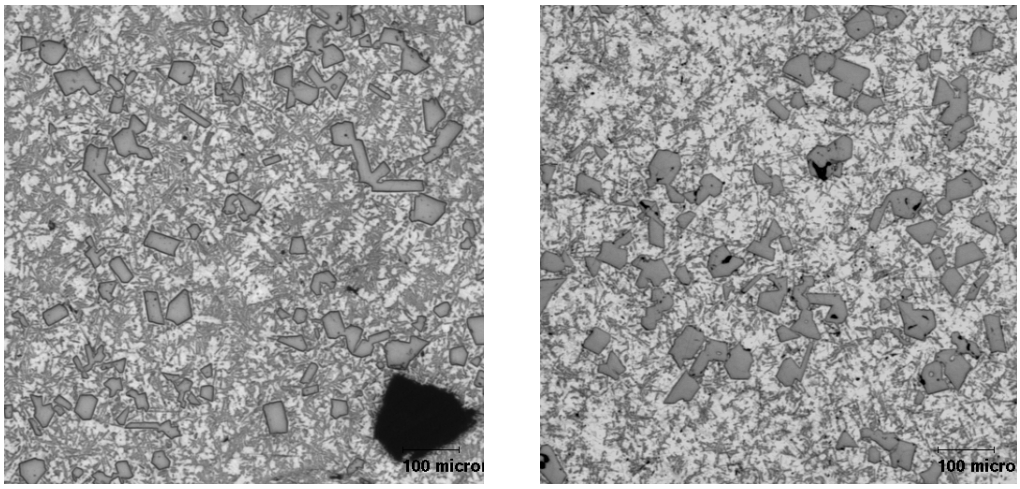

Figure 21: Microstructures obtained from the experiments in Figure 20.

The details of the experimental plan and results are described in Chapter 4. **Figure 21** shows the microstructures obtained by the mixing of a hypereutectic Al-Si alloy with a hypoeutectic Al-Si alloy. The reactions can be broadly classified as follows:

Liquid Hypereutectic Alloy (Al-25%Si): **L → Primary Si and Eutectic (1)**

Semi solid Hypoeutectic Alloy (Al-7%Si): **L + Primary Al → Eutectic (2)**

Another variation of the above discussed diffusion solidification approach was developed. In this process, solid particles/chunks of hypereutectic alloy were added into a liquid melt of hypereutectic Al-Si alloy (the alloy investigated being commercial 390 alloy). The addition of particles was performed to remove the heat from the liquid at a very rapid rate and to initiate nucleation of primary Si. **Figure 22** shows the time temperature curve of the liquid 390 alloy during the addition of chips of 390. The microstructure obtained from the experiment is shown in **Figure 23** ; the microstructure clearly shows the fine primary Si (< 25microns in diameter).

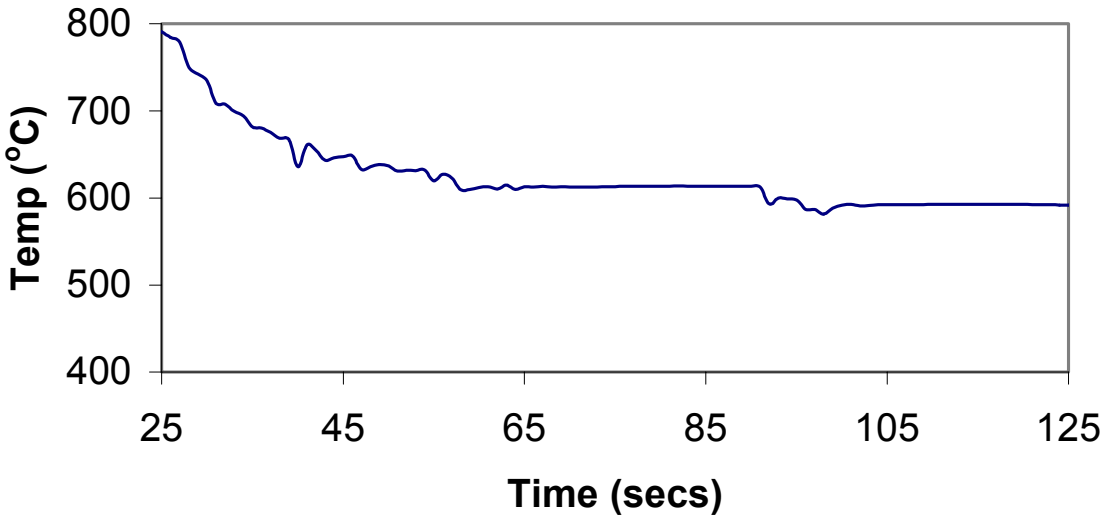

Figure 22: Time- temperature plot of Liquid 390 alloy held at 760 ^{0}C and rapidly cooled to 590 ^{0}C by the addition of 390 chips to the melt.

These encouraging results were utilized in performing industrial trials at SPX Contech. **Figure 24** shows one such experiment performed at SPX contech by mixing 390 alloy solids (10% the total weight of the casting) with 390 liquid in a cold chamber die cast machine.

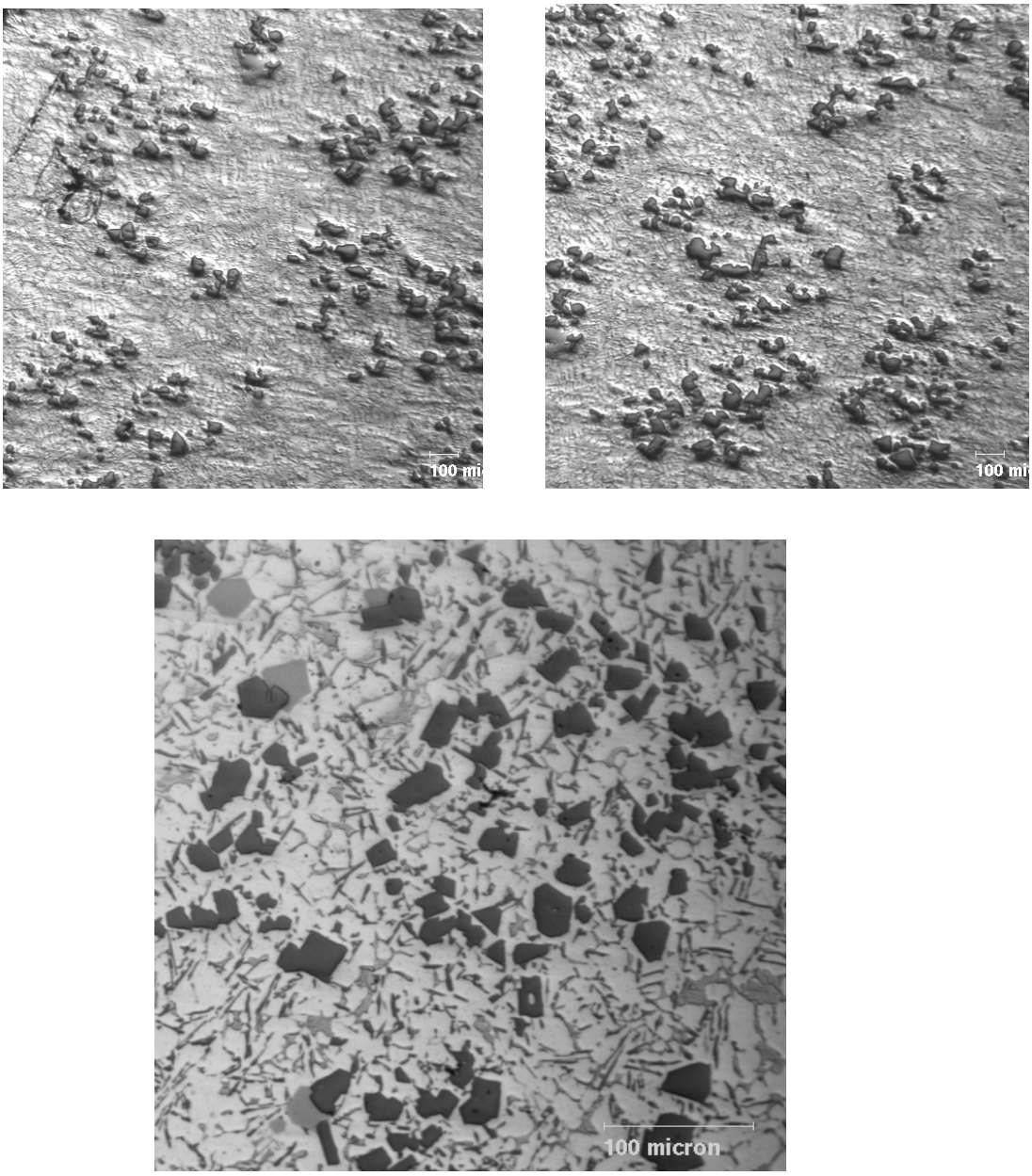

Figure 23: Representative microstructures, at various different magnifications, of 390 Alloy at 760 ^{0}C quenched to 590 ^{0}C by the addition of 390 alloy chips (initially at room temperature).

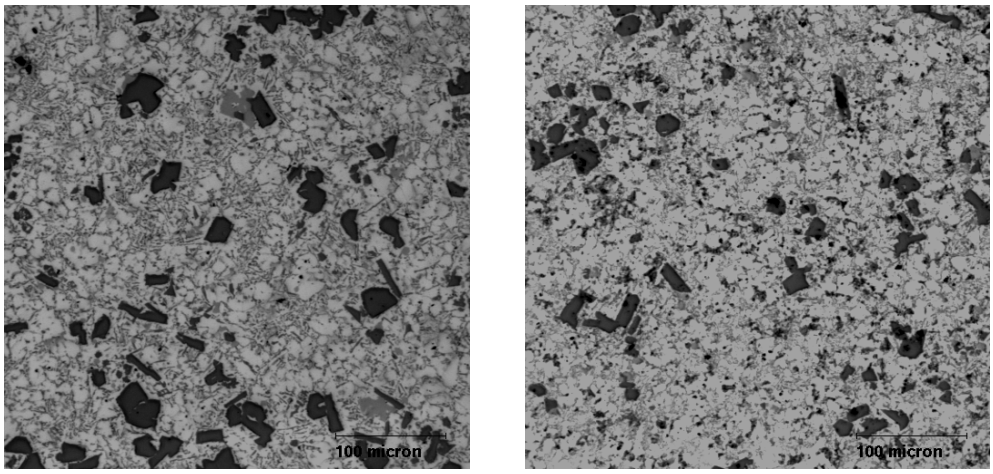

Figure 24: Representative microstructures by mixing solid 390 (10% of the total weight) and liquid 390 in a cold chamber die casting machine; thick section (left) and thin section (right). Details and other experiments are detailed in Chapter 5 and 6.

4.1.1 Mechanism of α-Al dissolution– hypereutectic Al-Si alloys

The mixing of a hypereutectic Al – 25% Si and Al-7%Si involves a complex process of heat and mass transfer, which can be broadly classified as follows:

1. A drop in the temperature of the Al-25% Si below the liquidus leading to the nucleation of primary Si
2. The absorption of the superheat of the Al-25% Si by the Al-7%Si
3. The gradual dissolution of the primary phase (α– Al) and the nucleation of any primary Si from the Al-25%Si

To understand the mechanism of α-Al dissolution (Diffusion controlled or Interfacial controlled), pure Al rods were dipped in Al-Si liquids with varying Si content and the resultant distance dissolved (z) was measured.

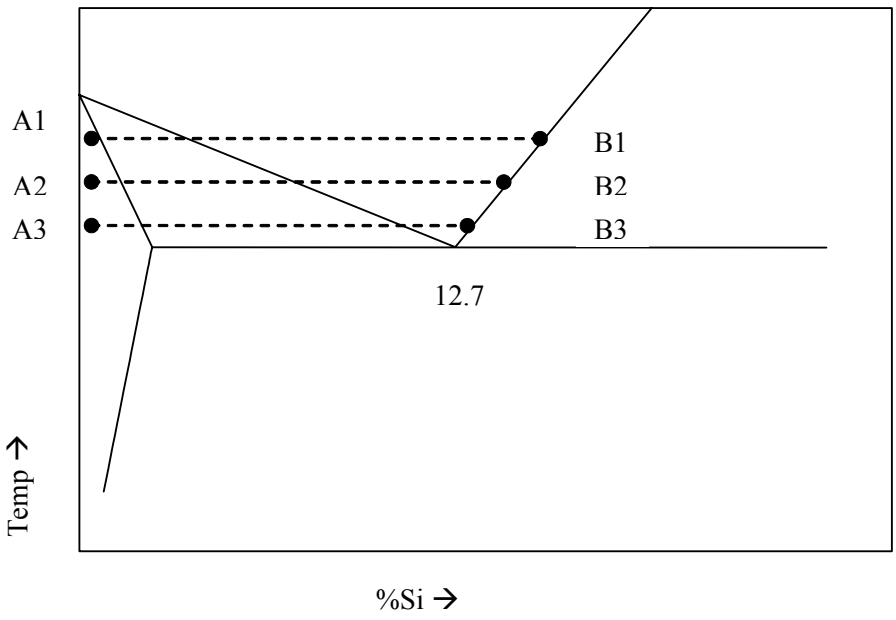

Figure 25: Schematic of the experiments performed to study the dissolution of α-Al in a liquid supersaturated with Si.

Figure 25 shows the experimental conditions utilized to establish the dissolution mode of α-Al in varying concentration of Si in Al-Si liquid. Different temperatures were selected to precisely control the Si content and also simulate the rate of dissolution as a function of temperature. **Figure 26** shows the dissolved Al rods in Al-Si liquid at 640 ^{0}C.

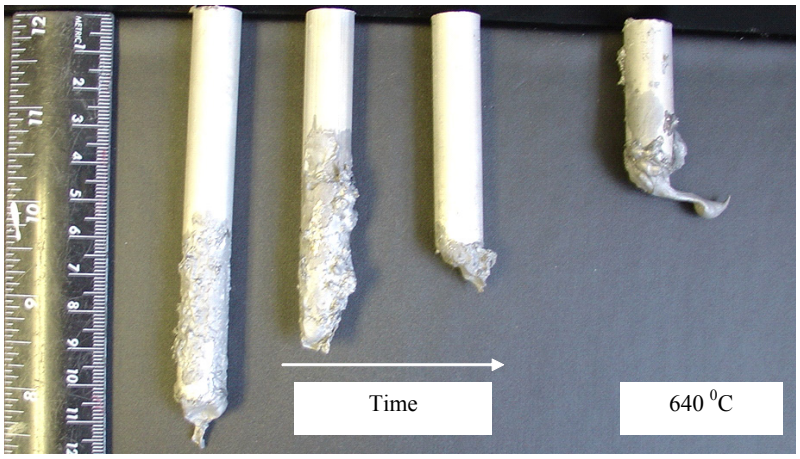

Figure 26: Rods of Pure Al dipped into Al-Si liquid and held for various times at a fixed temperature (A1 – B1 from Figure 25).

Similar experiments were performed at various temperatures to determine the dissolved distance as a function of time. The details of the experimental plan and design are described in Chapter 7. **Figure 27** shows the rate of Al rod dissolution in a Al-Si liquid. $\dot{z}\ (=\frac{dz}{dt})$ at different temperatures were then plotted as a function of $\frac{1}{T}$. **Figure 27** shows the slope, $\dot{z}$ versus $\frac{1}{T}$ for the experiments performed. It was also observed that the dissolution of Al was not diffusion controlled but rather interface controlled. Lommers and Chalmers [1] laid the mathematical foundations for the dissolution of solid into a liquid in a metal system. The details of their mathematical analysis are presented in Appendix I.

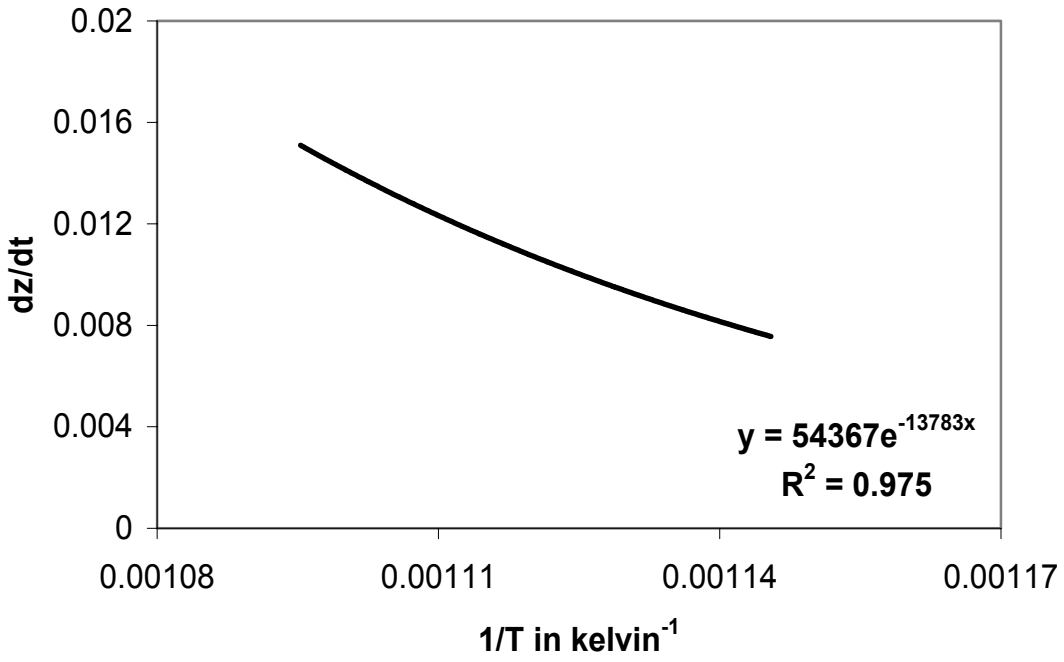

Figure 27: The rate of dissolution of Al in Al-Si liquid. Z is the length of dissolved Al rod dipped into Al-Si liquid.

The data was fitted with an exponential curve to calculate the activation energy. From equation 19, page 8-19;

$$\dot{z} = k[\exp(-\frac{Q_F}{RT})]*[C_L - C_0] \;=\; 54367*[\exp(-\frac{13783}{T})]$$

$$\Rightarrow Q_F = 27.3 kcal/mol.K$$

A similar value of 30 kcalmol^{-1}K^{-1} was obtained by Craighead [from 1] for the Al-Si alloy system.

4.1.2 Al-Si hypereutectic Alloys – synopsis and contribution

Traditional casting technology is based on the premise that one can control the microstructure by "Heat Control", or in the classical equation;

$$q_e\left(\frac{A}{V}\right) = -c\left(\frac{dT}{dt}\right) + \Delta h_f\left(\frac{df_s}{dt}\right)$$

where q = heat absorbed through area (A) and volume (V)

c = Heat capacity of the system at constant pressure; $\left(\frac{dT}{dt}\right)$ = Thermal Gradient,

$\Delta h_f\left(\frac{df_s}{dt}\right)$ = Amount of heat released (Δh_f) as the solid fraction (df_s) changes with time (t). The thermal gradient is actually a product of interface velocity (V) and thermal gradient (G) as shown below:

$$\left(\frac{dT}{dt}\right) = \left(\frac{dT}{dx}\right)\left(\frac{dx}{dt}\right) = G.V$$

The above equation forms the basis for evolution of various microstructure for a host of metallic systems and alloys. In rheocasting, the energy from the system is removed (q) very slowly, to coarsen the primary phase (most rheocasting was directed towards hypoeutectic Al alloys). However, in hypereutectic Al-Si alloys for low solid fractions, the amount of heat evolved is 2.5 – 3 times that of hypoeutectic Al-Si alloys per mole [Refer to **Figure 15**]. Added to the amount of heat released, the growth of primary Si is

faceted and is a strong function of undercooling [**Figure 16**]. In our process of mixing solids or semi solids with a liquid of the same or different composition, we have demonstrated a process of controlling the microstructure via a combination of heat balance and mass balance by diffusion. One such system where a liquid hypereutectic Al-25% Si was mixed with a semi solid Al-7% Si, it was realized that the α-Al in the Al-7% Si dissolved via interfacial reaction. The process of mixing was verified in an industrial setting and successful castings were produced at SPX Contech utilizing the process of mixing liquid metal with solid.

Chapters 5, 6 and 7 present laboratory and industrial rheocasting trials for hypereutectic Al-Si alloys, and Chapter 8 offers the mechanism for the mixing of two different entities to control the final resultant microstructure.

4.2 Globular primary phase in Al based wrought alloys

Controlled Diffusion Solidification (CDS) is a novel casting method wherein two precursor alloys of precisely controlled composition, quantity, and temperature are brought together and then cast to produce a component with a microstructure that is akin to that of semi solid processed parts [2]. **Figure 28** shows a schematic of a typical CDS process. The precursor alloys are selected at temperatures close to their respective liquidus and the mass ratios are fixed to achieve the final alloy. CDS relies on the differences between the surface tensions of two liquids [3], difference in heat and thermal diffusivities [4] and natural convection during mixing to nucleate and grow a non-dendritic primary phase from the liquid phase. In general, when two alloy melts of controlled composition and temperature are brought together, two events occur: (1) thermal equilibration by the redistribution of thermal energy in the resulting alloy *via* conduction and convection, and (2) chemical equilibration by mass diffusion across the liquid interfaces. **Figure 29** illustrates the various routes when liquids with different compositions are brought together [5].

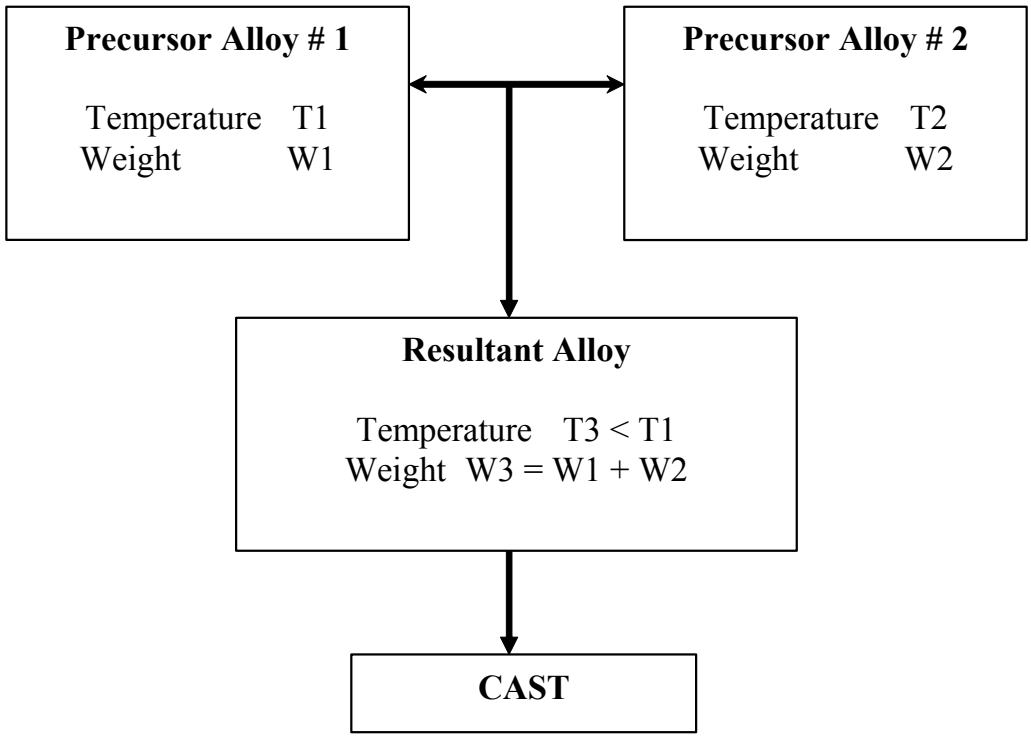

Figure 28: Schematic showing the process of mixing two liquids close to their liquidus to obtain the final resultant alloy.

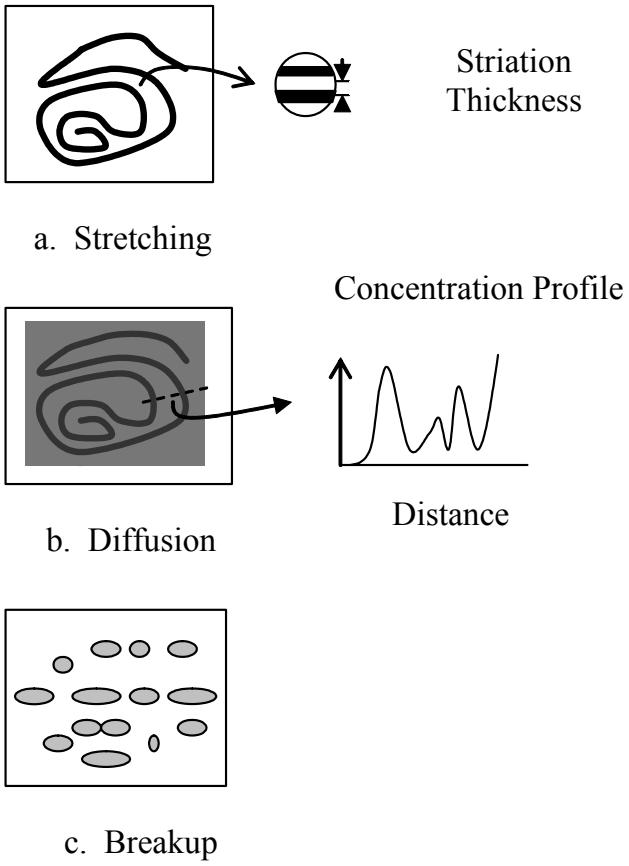

Figure 29: Various phenomena that may occur during mixing of liquids. (a) No surface tension difference and inter-diffusion, (b) diffuse boundary, (c) interfacial tension dominating [5].

Mass diffusivities are many orders of magnitude lower than thermal diffusivities, and mixing of two liquids at different compositions and temperatures lead to the development of pockets of undercooled liquid that favors the nucleation of a primary phase if certain conditions of surface energies are met [6]. Nucleation alone does not ensure a globular microstructure, rather the natural convection during the process of mixing generates the necessary condition for the formation of a globular microstructure [6-7].

Figure 30 shows typical microstructures of cast samples of wrought alloys 2024, 5056, and 7050. The microstructures are typical of dendritic microstructures obtained

during the casting of Al based wrought alloys. **Figure 31** shows typical microstructures obtained, via CDS process developed at WPI. The structures contain non-dendritic/globular primary α-Al phase and an interconnected network of secondary phases.

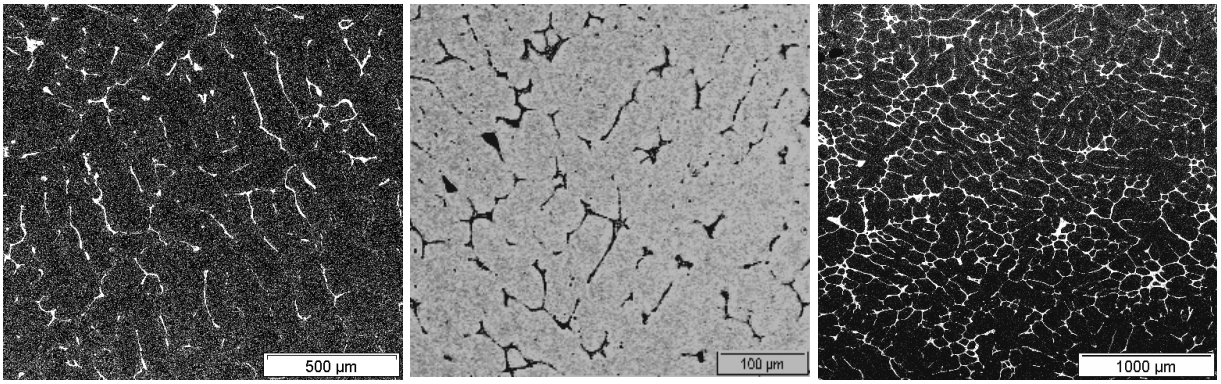

(a) **(b)** **(c)**

Figure 30: Typical microstructures obtained when Al based wrought alloys are solidified in a crucible with a super heat. Notice the dendritic microstructures in a) 2024 b) 5056 and c) 7075 alloy.

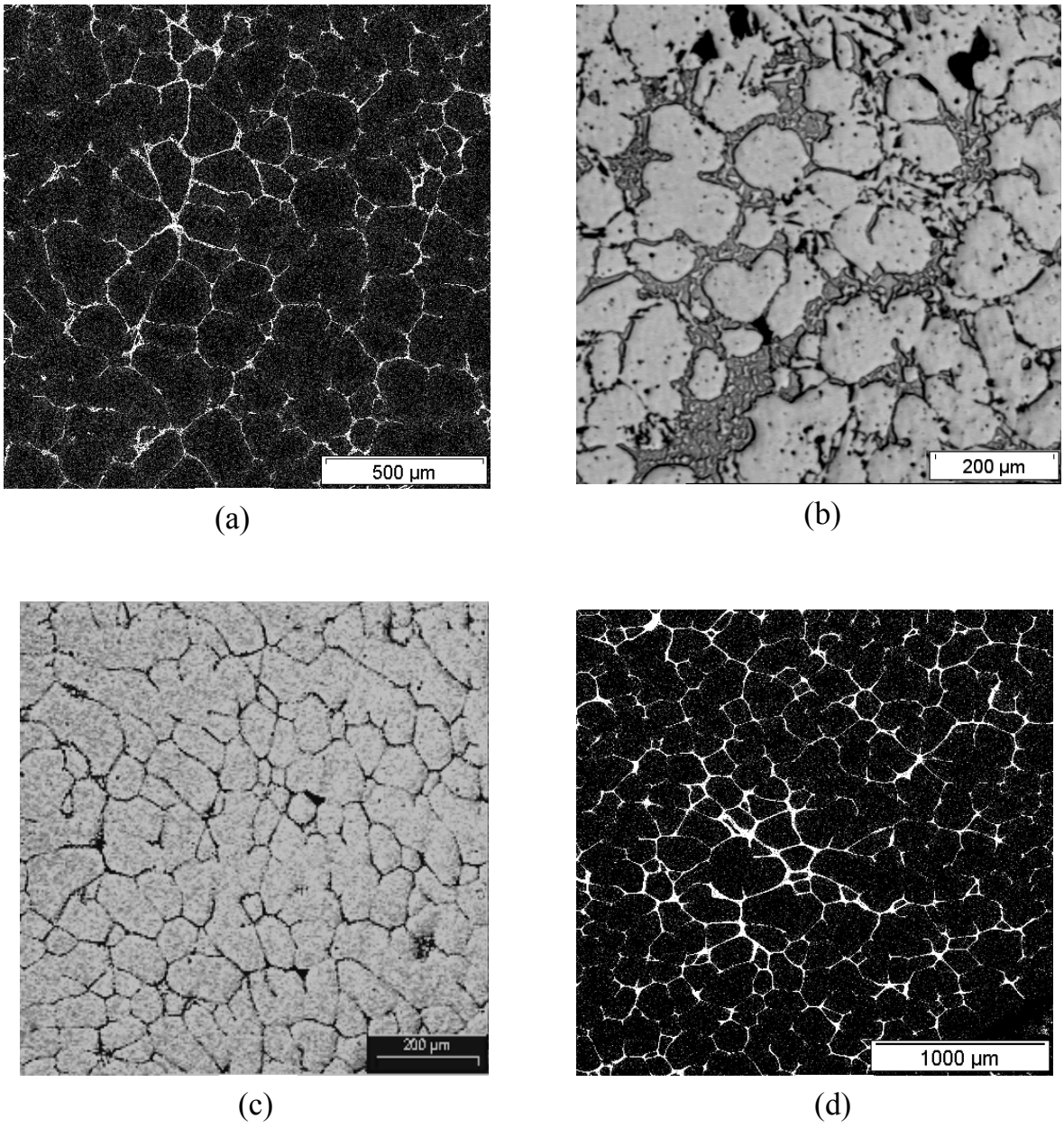

Figure 31: Typical microstructures of wrought alloys cast using CDS. (a) An SEM backscatter electron image of 2024 alloy taken in an SEM, (b) An optical microscope image of 4145 alloy, (c) An optical microscope image of 5056 alloy, and (d) An SEM backscatter electron image of 7050 alloy.

4.2.1 Necessary Conditions for a globular primary phase

When two liquids are brought together and their atoms are allowed to intermix, either one of three processes depicted schematically in **Figure 29** occurs [5]. Moreover, competition between thermal diffusion and mass diffusion occurs in the resultant liquid due to the difference in solute concentration and temperature between the two liquids. Thermal equilibration of the resultant liquid occurs by the transport of heat *via* electronic conduction from the hotter to the relatively colder regions of the liquid (if the liquids are metallic) [4], and equilibration of solute concentration occurs by diffusion of solute atoms across the diffuse interface that forms between the two liquids [9]. The formation of a diffuse interface between liquids has been observed experimentally and its decay rate has been mathematically modeled and shown to be proportional to $1/\sqrt{t}$ [9 - 11]. Typically, when two metallic liquids are brought together their temperatures tend to equilibrate faster than their composition. The result of this difference between thermal and concentration equilibration leads to the formation of pockets in the resultant liquid that are undercooled relative to their local composition. These pockets of undercooled liquid may act as nucleation sites for the solid phase, provided that their surface energy favors the formation of the solid phase.

Cini et al [6] have shown that "suitable concentration fluctuations can provide favored sites for nucleation". According to Cini et al, the energy barrier for nucleation due to a concentration gradient is lower than the classical energy barrier for nucleation if

$$\frac{a}{a+b} < (1+\frac{\sigma^{SL}-\sigma_{Al}^{SL}}{\sigma_{Al}^{SL}})^{\frac{3}{2}} \qquad (3)$$

In Equation (3), $a=\mu_A^{(s)}-\mu_A^l(c_0)$ is the chemical potential difference of component A between its solid phase and its liquid phase that has composition C_0, *i.e.*, X_A^f and X_B^f. Similarly, $b=\mu_A^{(1)}-\mu_A^l(c=1)$ is the chemical potential difference of component B between its solid phase and its liquid phase if the solid phase has formed from pure liquid, *i.e.*, if *C* =1. σ^{Sl} is the solid-liquid interface energy between the solid and liquid of

composition C_0, σ_A^{SL} is the solid-liquid interface energy between the solid and liquid when they are pure. Cini et al have shown that Equation (3) is satisfied when

$$(1+\frac{\sigma^{SL}-\sigma_A^{SL}}{\sigma_A^{SL}})^{\frac{3}{2}} \geq 1 \quad \text{i.e.,} \qquad \sigma^{SL}-\sigma_A^{SL} > 0 \tag{4}$$

For nucleation of the solid phase from a mixture of two liquids of compositions C_1 and C_2, the two liquids must be maintained at temperatures T_1 and T_2 such that T_1 and T_2 are close to the liquidus temperature of liquid 1and liquid 2, respectively, *i.e.*, the two liquids must be maintained at relatively low superheat. Additionally, the Gibbs free energy of the liquids prior to mixing must be less than the Gibbs free energy of the resultant liquid at its liquidus temperature, *i.e.*,

$$G_m^{MAX} \leq G_m^{final,liquidus} \tag{5}$$

In the CALPHAD method, Equation (5) takes the more detailed form shown as Equation (6)

$$G_m = X_A G_A^0 + X_B G_B^0 + RT(X_A \ln X_A + X_B \ln X_B) + X_A X_B \sum_k^n {}^K L_{A,B}^{\Phi}(X_A - X_B)^k \tag{6}$$

G_A^o and G_B^o are the molar Gibbs free energies of pure elements A and B, respectively and may be obtained from the Scientific Group Thermodata Europe (SGTE) pure elements database [12]. ${}^K L_{A,B}^{\Phi}$ is the k^{th} interaction coefficient between the A and B atoms and is given by ${}^K L_{A,B}^{\Phi} = A_k^{\Phi} + B_k^{\Phi} T + C_k^{\Phi} T \ln T$, where A_k^{Φ}, B_k^{Φ} & C_k^{Φ} may be determined experimentally. In this work, thermodynamic calculations were performed using the commercial software Pandat®[2] version 4-O-H, which uses the PanAluminum® version 2b thermodynamic database for commercial aluminum alloys, and in all calculations, comparable results were obtained from the commercial software

[2] Pandat® is marketed by CompuTherm, LLC, Madison, WI, USA.

Thermocalc®[3] using the Thermotech Aluminum database. Equation 5 and 6 represent the necessary condition for the nucleation of primary Al. In Chapter 10, it has been shown why a globular primary Al was obtained for a system with a negative heat of mixing and the absence of globular primary phase in a system with a positive heat of mixing. Once the aluminum has nucleated, the growth of primary Al into a non-dendritic structure is attributed to the convection during the process of mixing [7 - 8], and the absence of any constitutional undercooling.

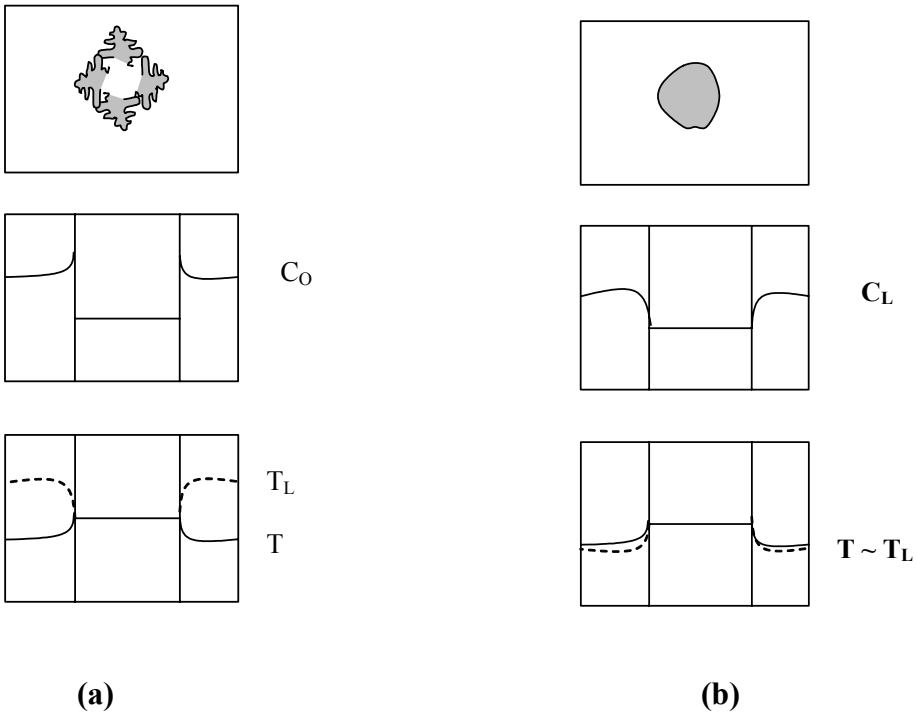

Figure 32: A) Schematic showing constitutional undercooling in a free growing dendrite in an under-cooled melt. The alloy has an initial composition of C_0, the solute is rejected across the interface, leading to a drop in the liquidus temperature (T_L) ahead of the interface. The region between the actual temperature of the liquid (T) and T_L leads to the breakdown of a planar interface into a dendritic structure. B) Schematic showing a condition when a liquid of composition C_L (say Al-33%Cu) is mixed with Pure Al. Clearly, growth of the structure follows the liquidus line, leading to minimal or no constitutional undercooling, and leading to a non-dendritic structure.

[3] Thermolcalc® is developed and marketed by the Foundation of Computational Thermodynamics, Stockholm, Sweden.

It is well established that in an alloy system, the growth of dendrite in a metallic system is by a combination of both thermal and solute diffusion. Depending on the temperature gradient, such liquid may be undercooled below its freezing temperature, even though it is hotter than liquid at the front. This is termed ***constitutional undercooling***, to emphasize that it arises from variations in liquid composition. Once constitutional undercooling occurs, the plane front becomes unstable, since a bump on the interface penetrates into undercooled liquid, where it grows more quickly. However, when liquids of different compositions are mixed, such that the colder liquid is supersaturated, a new scenario is created. In the later case, the low temperature liquid (say the Al-33% Cu) absorbs the heat from the pure Al, but because the copper atoms diffuse into the growing solid, any perturbations created leads to melting. This leads to the ripening of the primary phase to a globular structure with time.

4.2.2 Al based wrought alloys – synopsis and contribution

A casting process that is referred to as Controlled Diffusion Solidification (CDS) has been developed to circumvent problems that are typically associated with casting wrought aluminum alloys into near net shape components and to allow sound castings of these alloys with a globular microstructure that is essentially free of dendrites. The process involves mixing two alloys of pre-determined composition and temperature. The mechanism underlining this process is developed on the basis of free energy and liquid-mixing considerations and maintains that for the solid phase to nucleate and grow in a globular morphology, the two precursor alloys must be maintained at temperatures that are close to their respective liquidus temperatures and the difference between the solid/liquid interface energy when both solid and liquid are pure (σ_A^{SL}), and the solid/liquid interface energy in the alloyed state (σ^{SL}) is such that $\sigma^{SL} - \sigma_A^{SL} > 0$. Additionally, the Gibbs free energy of the precursor alloys prior to mixing must be less than the Gibbs free energy of the resultant alloy at its liquidus temperature.

While the preceding section has demonstrated the CDS method for the production of wrought aluminum-based alloys belonging to the 2xxx, 5xxx, and 7xxx series, the technique is similarly applicable to all standardized wrought alloys, as well as to the

production of non-standardized alloys. Finally, it should be mentioned that wrought alloys have been previously successfully cast with globular microstructures using semi solid metal processing techniques [13 - 15]; however, the CDS method described in this work is much simpler to implement than semi solid metal processing techniques - whether they be thixocasting or rheocasting techniques [16 - 19]. Moreover, it is well documented that the use of grain refiners can reduce the tendency of some Al-based alloys to form large dendrite clusters during solidification [20]. It is important to note that the CDS method accomplishes the same task efficiently without the additional cost of grain refiners. In summary, CDS is a viable, economical route to casting aluminum based wrought alloys into near net shaped components [**Figure 18**]. The castings produced have a microstructure akin to that of semi solid processed materials with all its associated benefits. Major attractions of the CDS process are its simplicity, and the fact that only minimum changes to conventional casting operations are needed in order to adapt an existing operation to the production of castings comprised of wrought alloys. Moreover, the CDS method is adaptable to pressure-less casting operations as well as to casting operations in permanent and sand molds with minimal pressure assistance.

Chapter 9 details the experiments performed at WPI, whilst Chapter 10 details the formation of globules from the perspective of free energy of the alloy system during mixing.

REFERENCES

1. J.M. Lommel and B. Chalmers, "*The isothermal transfer from solid to liquid in metal systems*", Transactions of the Metallurgical Society of AIME, June 1959, Vol. 215, p. 499 – 508.
2. D. Saha, S. Shankar, D. Apelian, and M.M. Makhlouf, "*Casting of Aluminum Based Wrought Alloys and Aluminum Based Cast Alloys via Controlled Diffusion Solidification (CDS)*", U.S. Patent Pending, applied for on Dec. 2, 2003.
3. D.R. Poirier and R. Speiser, "*Surface Tension of Aluminum Rich Al-Cu Liquid Alloys*", Metallurgical and Materials Transactions, 1987, Vol. 18A, p. 1156 – 1160.
4. B. Giordanengo, N. Benazzi, J. Vinckel, J.G. Gasser, and L. Roubi, "Thermal

Conductivity of Liquid Metals and Metallic Alloys", Journal of Non-Crystalline Solids, 1999, Vol. 250 – 252, p. 377 – 383.

5. J.M. Ottino, "The Kinematics of Mixing: Stretching, Chaos and Transport," ISBN 0-521-36335-7 (1989), Cambridge University Press, New York, USA.
6. E. Cini, B. Vinet and P.J. Desre, "*A Thermodynamic Approach to Homogeneous Nucleation via Fluctuations of Concentration in Binary Liquid Alloys*", Philosophical Magazine A, 2000, Vol. 80 (4), p. 955 – 966.
7. W. Shusen, W. Xueping and X. Zehui, "*A Model of Growth Morphology for Semi Solid Metals*", Acta Materialia, 2004, Vol. 52, p. 3519 – 3524.
8. A. Das, S. Ji, and Z. Fan, "*Morphological Development of Solidification Structures Under Forced Fluid Flow: a Monte-Carlo Simulation*", Acta Materialia, 2002, Vo. 50, p. 4571 – 4585.
9. P.G. Smith, T.G. M. Van De Ven and S.G. Mason, "*The transient interfacial tension between two miscible fluids*", Journal of colloidal and Interface Science, March 1981, Vol. 80, p. 1.
10. D.D. Joseph, A. Huang and H. Hu, "*Non-solenoidal velocity effects and kortewag stresses in simple in compressible liquids*", Physica D, 1996, Vol. 97, p 104 – 125.
11. D.M. Anderson and G.B. McFadden, "*Diffuse-interface methods in fluid mechanics*", Annual Review of Fluid Mechanics, 1996, Vol. 30, p. 139-165.
12. Scientific Group Thermodata Europe (www.sgte.org).
13. J. Dong, et al.*," Liquidus semi-continuous casting, reheating and thixoforming of a wrought aluminum alloy 7075",* Materials Science and Engineering A, 2003, Vol. 345 (1-2), p. 234-242.
14. A.A Kazakov., "*Alloy compositions for semisolid forming*", Advanced Materials and Processes, 2000, Vol.157 (3), p. 31-34.
15. T.M. Yue, "*Squeeze casting of high-strength aluminium wrought alloy AA7010*", Journal of Materials Processing Technology, 1997, Vol. 66 (1-3), p. 179-185.
16. C.Y. Chen et al., "*Thixoforging of aluminum alloys*", Materials Science and Engineering, 1979, Vol. 40 (2), p. 265-272.
17. M.C. Flemings, R.G. Riek, and K.P. Young, "*Rheocasting*", Materials Science and Engineering, 1976, Vol. 25, p. 103-117.

18. M.M. Rovira, B.C. Lancini, and M.H. Robert, "*Thixo-forming of Al-Cu alloys",* Journal of Materials Processing Technology, 1999, Vol. 92-93, p. 42-49.
19. M.H. Robert, and M. Adamiak, "*Preliminary studies on the suitability of rheocast Al alloys for deep drawing",* Journal of Materials Processing Technology, 2001, Vol. 109(1-2), p. 168-173.
20. Geoffery K. Sigworth, "*High strength casting alloys for automotive applications*", Proceedings of the 2002 Annual meeting: Automotive Alloys and Aluminum Sheet and Plate Rolling and Finishing Technology Symposia, Feb 18-21 2002, Seattle, WA, United States.

Chapter 5. Mixing Al-7% Si and Al-25% Si alloys

This chapter describes the first experiments performed at WPI, involving the mixing of a hypoeutectic Al-Si alloy and hypereutectic Al-25%Si alloy. The alloys were mixed by varying the temperatures to obtain a fine distribution of primary Si in the matrix. The results laid the foundation for the temperatures and composition used in Chapters 6 though 9. The paper was presented at the 7th International Conference titled *Advanced Semi-Solid Processing of Alloys and Composites*, Tsukuba, Japan, September 24-28, 2002. Published by the National Institute Of Advanced Industrial Science and Technology, Japan, 2002, pp 323-328

7th International Conference titled *Advanced Semi-Solid Processing of Alloys and Composites*, Tsukuba, Japan, September 24-28, 2002, pp 323-328

SSM PROCESSING OF HYPEREUTETCIC Al-Si ALLOY VIA DIFFUSION SOLIDIFICATION

Deepak Saha*, Diran Apelian* and Rathindra Dasgupta**

*Metal Processing Institute, WPI, MA USA (www.wpi.edu/+mpi)
** SPX Contech, Kalamazoo, MI USA(www.spxcontech.com)

Summary

Hypereutectic Al-Si alloys have gained enormous significance in the recent past due to superior properties (low coefficient of thermal expansion, high yield strength and high wear resistance). The processing of hypereutectic aluminum via semi-solid processing (SSM) route has been hampered by the growth of primary Si to an unacceptable range (> 100 microns). Various refining agents have been studied in the past to reduce the growth of primary Si; other processing variables are also important in controlling primary Si, such as cooling rate of the hypereutectic alloy to the required temperature, and isothermal hold time at that SSM temperature. In this study, the nucleation of primary Si in hypereutectic alloys was achieved by mixing two different liquids: An Al-(23-25) Si % alloy and an Al-(7- 8) Si % alloy (Sibloy^R) held in the semi-solid range. The mixing of the two liquids leads to a spontaneous heat extraction (diffusion) from the hypereutectic alloy due to imposed thermal gradients; namely, the cooler hypoeutectic extracts the heat of the hypereutectic alloy. The composition and the mass of the liquids were controlled such that the resultant composition is 17 – 18 % Si. The heat extracted was such that the final temperature of the mixed liquid was controlled to the "Slurry-on-Demand" (SoD) temperature of a typical 390 alloy. The mixed melt (having a composition of 17 – 18 % Si) was held in the two-phase range for various periods of time to study the size and distribution of primary Si. The results show that the temperature of the hypoeutectic alloy and the size of primary Al in the hypoeutectic alloy play an important role in the final microstructure. The results lay down the foundation for further research in the area of processing hypereutectic alloys via diffusion solidification.

Keywords: Hypereutectic alloys, liquid mixing, rheocasting of hypereutectic alloys, diffusion solidification, 390 alloy.

1 Introduction

Currently there are a myriad of viable methods to achieve cast components having SSM structures. The most common route used is Thixocasting, where a billet of the required alloy is reheated to the desired SSM region before casting. An alternative process is rheocasting, where the liquid metal is cooled to the required SSM range, the structure is modified (broken dendrites), or a potent nucleation event is initiated (with limited growth) and subsequently the slurry is cast. The grain (or cell) structure and other metallurgical properties are controlled

during the cooling process. Some of the methods employed to achieve the requisite microstructure involve: electromagnetic stirring, addition of grain refiners, stirring etc. It is important to note that the use of both thixocasting and rheocasting has been limited to the casting of hypereutectic alloys.

In this study, our interest is to investigate viable processing routes for SoD processing – rheocasting of hypereutectic alloys. The main issue in casting of hypereutectic Al-Si alloys is the difficulty in achieving a melt that has a homogenous distribution of primary Si in the final part. As primary Si nucleates from the liquid, it develops complex shapes depending on the cooling rate imposed on it. Nine different morphologies of primary Si have been observed and reported in the literature [1]. The morphology of the Si depends on the imposed temperature gradient, presence of impurities and the ease of nucleation. Halo of Aluminum are frequently reported around the primary Si particles. Yilmaz and Elliot [2] have attributed these halos of aluminum to growth rate and growth composition effects. Traditionally the refinement of primary Si is achieved by the addition of phosphorus to the melt. Researchers [3] have used other refining agents to refine primary Si-i.e., Germanium, Gallium, Selenium, Tellurium, Lithium, Cadmium, and Lithium Chloride. Most of the work however has been related to conventional casting of hypereutectic alloys. Studies relating to the use of these refining agents for SoD processing of hypereutectic alloys are non-existent.

Though conventional casting of hypereutectic Al - Si alloys has been successful in industry, rheocasting of these alloys for SoD processing offers significant challenges. The fundamentals of nucleation and growth of primary Si need to be studied in order to control the growth of the Si particles subsequent to their nucleation in the two-phase range. As the alloy is cooled to the SSM range, and isothermally held in the two-phase range for a period of time before casting, primary Si grows rapidly and thwarts the very purpose of utilizing hypereutectic alloys. Uneven shape and size distribution of primary Si has been reported to be detrimental to the final mechanical properties and wear characteristics [1]. Lee et al. have used mechanical stirring [4], while others have used ultrasonic treatment [5] to break down the primary Si in the two-phase range. Ideally, in SoD processing, we want to promote nucleation as the liquid approaches the liquidus temperature, minimizing growth of the Si particles. Traditional rheocasting techniques were examined, however the inherent thermal properties of the Si phase is at the core of the problem in controlling and maintaining a desirable distribution of the Si particles in the final SSM casting.

We have approached the challenge of SoD processing of hypereutectic Al-Si alloys by the mixing of two liquids, 1) hypereutectic Al-Si alloy (25 % Al-Si) and a 2) hypoeutectic alloy with 7 % Si (held in the SSM range). The hypoeutectic alloy selected is developed by Elkem (under the trademark of SiBloy^{R}), which is ideal for SSM processing of hypoeutectic Al-Si alloys because the alpha aluminum formed in the melt is independent of the hold time (no fading effects, etc.). The purpose of adding the hypereutectic alloy to the SiBloy^{R} melt is to rapidly quench the hypereutectic alloy to the SSM casting temperature. The goal of liquid-liquid mixing is to promote the diffusion of heat from the hypereutectic alloy by the dissolution of primary aluminum from the hypoeutectic alloy, while initiating nucleation of the Si phase, and minimizing its growth.

2 Experimental Procedures

Figure 1 shows the schematic of the composition and temperatures of the alloys used in the two-liquid mixing technique. Seven key experiments were performed. Two crucibles, each containing one alloy, were heated in the range of 800 – 900^{0}C for the hypereutectic alloy and 350 – 578^{0}C for Sibloy^R. Once the required temperature was obtained, the hypereutectic alloy was poured into the SiBloy^R melt and the temperature recorded. Specific processing parameters studied were: effect of varying melt temperature, holding time, and the starting SiBloy^R temperature on the resultant Si shape and size. The mixed melt was then quenched and microstructural analysis performed. Figure 2 shows the time – temperature plot for the various experiments conducted.

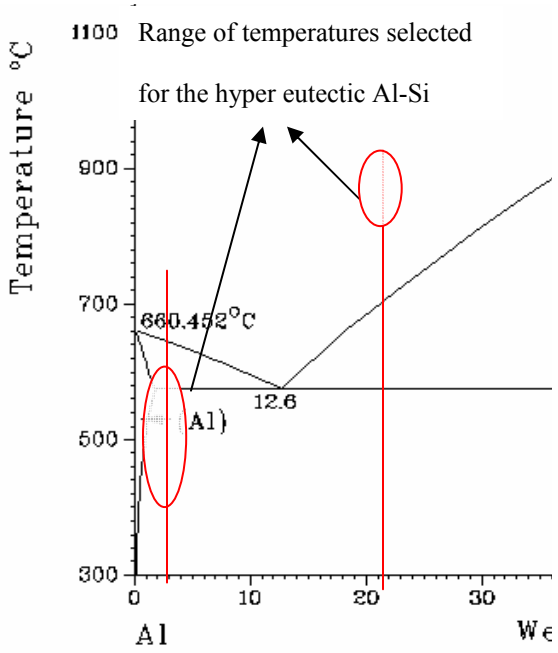

Figure 1: Range of temperatures and compositions of the alloys utilized in the mixing experiments. The hypereutectic alloy temperature was varied from 900 ^{0}C to 800 ^{0}C, and that for the Sibloy^R from 578 ^{0}Cto 350 ^{0}C

3 Results and Discussion

Figure 2 shows the temperature profiles of the key seven experiments (LM # 1 to LM # 7). Details of the experiments are listed below:

LM # 1: Sibloy^R at 578 ^{0}C and 25 % Al-Si at 900 ^{0}C (200 s hold)
LM # 2: Sibloy^R at 578 ^{0}C and 25 % Al-Si at 900 ^{0}C (300 s hold)
LM # 3: Sibloy^R at 578 ^{0}C and 25 % Al-Si at 850 ^{0}C (300 s hold)
LM # 4: Sibloy^R at 578 ^{0}C and 25 % Al-Si at 850 ^{0}C (400 s hold)
LM # 5: Sibloy^R at 350 ^{0}C and 25 % Al-Si at 850 ^{0}C (350 s hold)
LM # 6: Sibloy^R at 570 ^{0}C and 25 % Al-Si at 800 ^{0}C (350 s hold)
LM # 7: Sibloy^R at 500 ^{0}C and 25 % Al-Si at 800 ^{0}C (250 s hold)

Figures 3 through 7 show representative microstructures obtained from the mixing experiments.

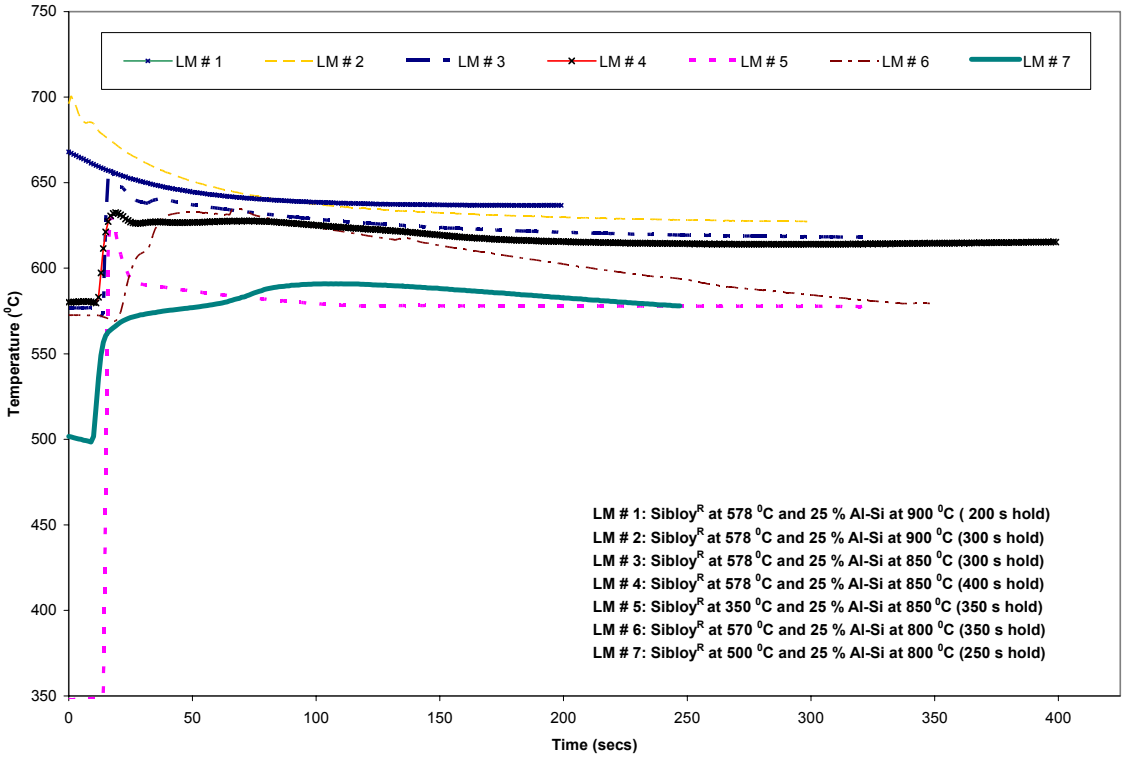

Figure 2: Various experiments and conditions of the two melts

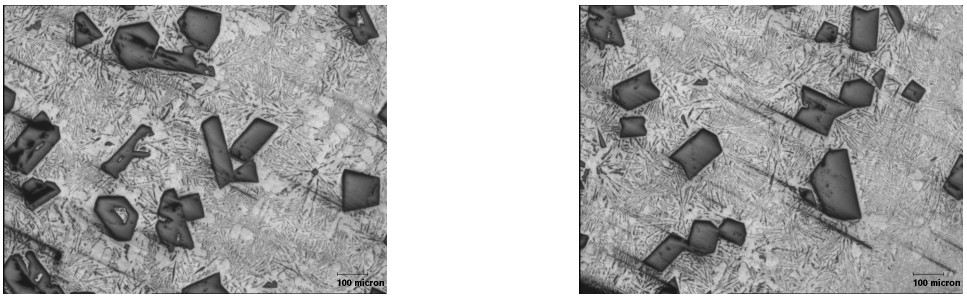

Figure 3: Typical Microstructure from experiment LM # 7(250 s hold at 587^{0}C)

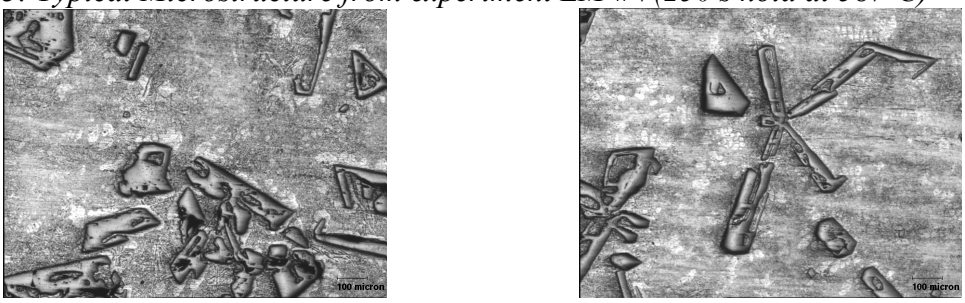

Figure 4: Typical Microstructure from experiment LM # 6 (350 s hold at 580^{0}C)

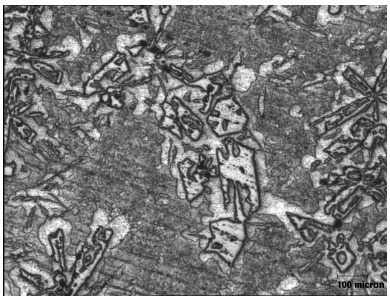

Figure 5: Typical Microstructure from experiment LM # 5 (350 s hold at 577^{0}C

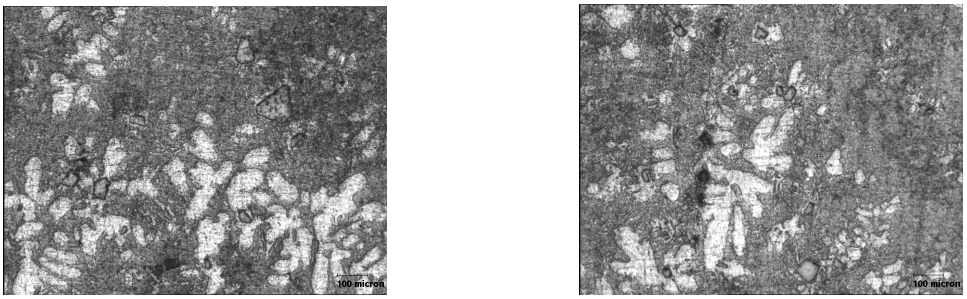

Figure 6: Typical Microstructure from experiment LM # 4 (400 s hold at 615^{0}C)

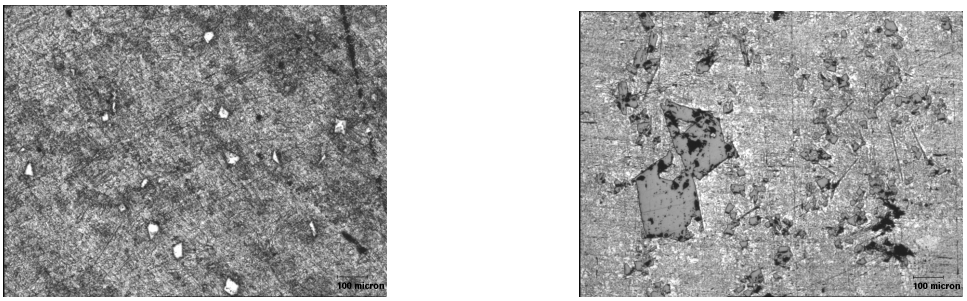

Figure 7: Typical Microstructure from experiments LM # 1, 2 & 3.

Examination of the microstructure revealed a change in the morphology and size of the primary Si depending on the imposed conditions. The primary Si size was dependent on the temperatures of the two liquids and the final temperature attained. Figure 3 shows that the primary Si range is in the order of 60 – 100 microns in diameter. Here the SiBloy^R was held at 500^{0}C and the temperature of the 25 % Al-Si was held at 800^{0}C. The final temperature of the mixed liquid before it was quenched was 580^{0}C. Figure 4 shows the altered morphology of primary Si (star shaped), and radiating from a given point. This is a typical structure of primary Si observed when the cooling rates are slow [1]. The reason for the star shaped primary Si can be attributed for the high temperature of SiBloy 570^{0}C compared to the 500^{0}C used in LM # 7. Figure 5 shows the structures obtained when SiBloy^R at 350^{0}C is mixed into the hypereutectic alloy. Due to the enormous quantities of heat required to melt the primary aluminum of SiBloy^R, the final structure displays regions of undissolved primary aluminum due to SiBloy^R. Figure 6 similarly shows undissolved primary aluminum of SiBloy^R. In this case, the final temperature was obtained to be 615 s. Small primary Si can be seen on the primary aluminum, indicating that the

heat extracted by the primary aluminum provided local undercooling and assisted in the nucleation of the primary Si. Figure 7 shows the complete dissolution of primary aluminum as the melts were held at a higher temperature (ranging from 625 – 636^{0}C). The result was an uneven distribution of primary Si size and shape. Rheocasting of hypereutectic alloys can be attained provided the requisite undercooling is achieved. The results of mixing two liquids, and attaining the desired structure via diffusion solidification are encouraging. This is a novel approach to control the nucleation and growth of primary silicon particles for SoD processing of hypereutectic alloys.

Acknowledgments

We would like to thank SPX contech, MI (www.spxcontech.com) and MPI, Worcester MA (www.wpi.edu/+mpi) for providing the technical and financial support to carry out this project.

References

1. "Hypereutectic Aluminum-Silicon Casting Alloys - A Review." Grusleski, N. Tenekedjiev, Cast Metals, 1990 Volume **3**, Number 2, pages: 96 - 105.
2. "Halo Formation in Al-Si Alloys", F.Yilmaz and R.Elliot, Metals Science, 1994, Volume 18, pages: 362 – 366
3. "Some aspects of Refinement of Hypereutectic Aluminium - Silicon Alloys" S. Ghosh and W. J. Mott, AFS Transactions, 1962, Volume 72, pages: 721 - 732.
4. "Formation of Spherical Primary Silicon Crystals During the Semi-Solid Processing of Hypereutectic Al-15.5 wt% Si Alloy", J.J.Lee, H.I. Lee and M.I. Kim, Scripta Metallurgica, 1995, Volume 32, No. 12, pp. 1945 – 1949.
5. "Hypereutectic Al-Si Based Alloy with a Thixotropic Microstructure Produced by Ultrasonic Treatment", Materials and Design, 1997, Volume 18, No 4/6, pages: 323 – 326.

Chapter 6. Industrial trials

Preface

This chapter presents the laboratory and industrials trials performed at WPI and SPX Contech, respectively. It consists of various experiments performed on both hypereutectic and hypoeutectic Al-Si alloys at SPX with the aid of M. A. Musser, Z. Brown, D. Killingsworth and Dr. Rathindra DasGupta at SPX Contech. The results clearly indicate that it is possible to achieve a fine distribution of primary Si in hypereutectic Al-Si alloys. A globular primary Al in the hypoeutectic Al-Si was also achieved. The paper was presented at the ***22ND International Die Casting Congress & Exposition, NADCA, September 15-18, 2003, Indianapolis, Indiana, pp129-134.***

22ND International Die Casting congress & Exposition, NADCA, September 15-18, 2003, Indianapolis, Indiana, pp129-134

SEMI SOLID (SSM) PROCESSING OF AL-SI ALLOYS UTILIZING THE CONCEPT OF DIFFUSION SOLIDFICATION

Deepak Saha*, Rathindra Dasgupta, and Diran Apelian***

*Metal Processing Institute, WPI, MA USA (www.wpi.edu/+mpi)

**SPX Contech, Kalamzoo, MI USA (www.spxcontech.com)

Abstract

When Rheocasting was first discovered, it was believed that one had to break up the dendritic structure during the freezing process either by mechanical stirring or via magneto-hydrodynamic forces to obtain a cellular structure. In the recent past, we have discovered that one may obtain a refined SSM structure without breaking up the dendritic structure, but rather by creating an environment where copious nucleation can occur near the liquidus temperature of the alloy, and with limited growth of the formed nuclei. Essentially, SSM structures develop by controlling the nucleation and growth processes during the early stages of freezing. During the last several years we have witnessed much SSM developmental work on Hypoeutectic Al-Si alloys. With respect to Hypereutectic Al-Si alloys, the attainment of SSM structures is more of a challenge due to the constraints of the system, and the accelerated growth of the primary Si phase (i.e., 390 alloys). In this paper we present a novel concept of utilizing diffusion solidification for achieving SSM cast parts for both Hypo as well as Hypereutectic alloys. The concept utilizes the addition of solid Al-Si chips in a controlled quantity to achieve the required SSM microstructure. The paper presents laboratory results at MPI and industrial trials performed at SPX Contech. Results indicate an alternative route for the production of SSM cast parts without the need for infrastructural changes in traditional die cast houses.

Introduction and Background

Semi Solid Processing (SSM) is a net shape manufacturing process for metals and alloys where the metal is cast in the two-phase region (Liquid + Solid). Some of the advantages of processing a metal in the two-phase range are: reduction in the heat released during the casting process, which has a direct benefit with respect to die life, reduced erosion, etc.; in addition to having a quiescent flow into the die cavity reducing entrapped gases and shrinkage voids.

The two primary routes for the production of SSM slurry are:

(i) Thixocasting - billet is reheated to the two-phase range and subsequently emplaced in the die cavity, and a cast is made, and

(ii) Rheocasting - liquid metal is processed to have a semi solid structure in the two phase range, and the slurry is fed into the die cavity (versus a reheated billet).

One can think of rheocasting as coming down in temperature while processing, whereas in thixocasting, one is reheating the billet and is going up in temperature. The rheocasting route is also coined as the Slurry-On-Demand route (SOD). The latter eliminates additional (premium) billet cost, recycling of waste generated, loss of liquid metal during reheating, and part consistency from shot to shot.

The attractive advantages of rheocasting motivated our research at MPI / SPX Contech towards the development of a "new process" wherein the advantages of the rheocasting are realized and with the caveat that the "new process" can be incorporated into existing die casting machines, without much retrofitting and infrastructural changes.

Rheocasting was the original route that was developed by the MIT team **[1]** and subsequently, the thixocasting properties of billets that did not contain the conventional cast (dendritic) structure was realized, and thus the thixocasting process was developed. Moreover, in the early days of SSM development, it was understood that one had to cool the liquid down into the two phase region, form dendrites, shear off and break the dendrites (via agitation – MHD or stirring forces), and thus produce a slurry. During the last few years, with the work that was sponsored

at ACRC – MPI by the Department of Energy **[2]**, the research team at MIT discovered that one did not need to break off dendrites to produce the semi solid structure of globules (solid phase) – or the primary alpha phase. Rather, if the temperature of the melt was such that one could produce many nuclei (copious nucleation), and if the nuclei did not grow to be very large (i.e., dendrites), nor melt off, then one could end up with a slurry having a semi solid structure with many alpha phase islands directly from the melt. This was contrary to the earlier understanding in the field, in that we thought we had to form dendrites, and then break them up, versus creating "broken dendrites' from the start. Whether technology led the development of the process, or whether science led it is certainly debatable.

In the last few years we have witnessed the development of several processes, which are derivatives of the above concept. Some of these are:

- Mechanical Stirring of the liquid metal (SSR process, or new MIT process) **[3]** where the liquid metal is stirred mechanically during the initial solidification region, leading to the nucleation of the primary phase and the dispersion of nuclei across the melt.
- CRP^{TM} (Continuous Rheocasting Process) developed by the ACRC-MPI team wherein liquid from two different reservoirs are fed into a reactor to produce a slurry. The reactor aids in the formation of the nuclei, and dispersing them throughout the bulk **[4]**
- New Rheocasting Process, (UBE Industries) **[5]** where a liquid held at relatively low superheats is poured in a cold mould, the natural convection during the pouring being utilized for the dispersion of nuclei.
- Near Liquidus Casting **[6]** which utilizes pouring at very low or near close, liquidus temperatures giving rise to semi solid structures.
- AEMP process **[7]**, which utilizes electromagnetic stirring to break up the dendrite arms to create a semi solid slurry.

All of the above mentioned processes utilize fundamentally the same concept: nucleation and dispersion of the nuclei to achieve semi solid slurry state, as the alloy is cooled below the liquidus temperature. However, semi solid processing of Hypereutectic alloys have significant

challenges (high heats of fusion and rapid growth of the primary Si phase), and the above mentioned processes may not be applicable for Hypereutectic Al-Si alloys. Accordingly, a novel approach was explored to balance the release of the high heat of fusion in Hypereutectic Al-Si alloys, and to control the growth of the primary silicon phase. Specifically, the diffusion solidification approach was investigated, and as the results point out, this novel approach has much potential for the creation of Slurry-On-Demand semi solid slurries of Hypereutectic Al-Si alloys.

Diffusion Solidification

Diffusion solidification, introduced by Apelian and Langford **[8]** is a novel approach wherein solidification is controlled by mass flow rather than heat flow. During conventional solidification processing, when an alloy is solidified, the temperature is reduced as one moves down an iso-concentration line. Partitioning takes place, and two phases are formed: primary alpha phase and enriched liquid phase. Moreover, the heat released by the liquid phase flows in the direction opposite to the motion of the liquid/solid interface, and solidification time is controlled by heat flow. In diffusion solidification, two phases – a solute enriched liquid phase and a solute poor solid phase (held at the same temperature – on an isothermal line) are brought into intimate contact, and solute diffusion from the liquid to the solid phase takes place. As the liquid loses solute, solidification proceeds via mass flow. Moreover, solidification times are independent of the size of the casting.

Originally, Apelian and Langford utilized diffusion solidification to die cast steels. In their pioneering experiments, they infiltrated a die filled with pure iron powder heated to a Temperature in the Austenite region, T_1 with cast iron liquid phase also heated to the same temperature, T_1. Carbon diffused away from the liquid into the iron powder, and since carbon diffuses interstitially, the diffusion rate is relatively high, and the liquid phase became solute (carbon) poor at T_1, and solidified. They produced a variety of cast components using diffusion solidification; commercially, the concept is utilized to make high-speed steels, and also dental amalgams.

The diffusion solidification approach has been applied to Al-Si alloys, both Hypo and Hypereutectic alloys. Specifically, we mixed solid particles (chips) with liquid metal, both

phases having the same composition prior to mixing, but not at the same temperature. The central idea behind this concept is to utilize the excess superheat from the liquid metal (latent heat of solidification), as well as the heat released during the growth of the primary Si phase in melting the chips. This approach ensured that the heat released is internally consumed in the dissolution/melting of chips, as the hotter metal solidified. The turbulence generated during pouring of the metal was used in dispersing the nuclei throughout the melt. The process is rapid, and the amount of chips added into the system determined the final temperature of the slug.

Experimental - *Results and Discussion*

Figure 1 is a schematic diagram that shows the temperature drop required in the Rheocasting of a Hypoeutectic (7% Si) and Hypereutectic (17% Si) alloys of Aluminum. The challenge is exacerbated for Hypereutectic alloys, due to the latent heat released and the rapid growth of the primary Si phase during solidification.

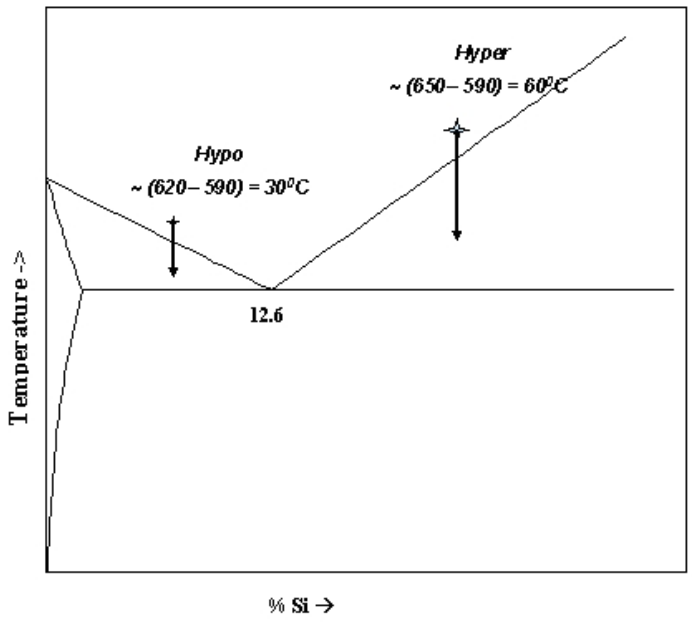

Figure 1: Schematic of the Al-Si Binary Phase diagram showing the temperature range required during typical SSM processing of a 7% and a 18 % Al-Si alloy.

Liquid metal was poured into a crucible containing a known quantity of chips (ratio of chips to liquid metal is determined by the heat release), and the temperature of the melt rapidly decreases

to the SSM processing range. The superheat was controlled so that the chips added were completely homogenized within the melt, and that the slugs did not contain any of the original chips.

Hypereutectic Alloys

Figure 2 shows the time-temperature profile, and particularly the temperature drop as 390 alloy at 760 ^{0}C is cooled rapidly to 590 ^{0}C via the addition of 390 alloy chips. Figure 3 shows representative microstructures obtained from the trials performed at WPI. The average primary Si phase is less than 40 microns, and is evenly distributed throughout the bulk (the matrix).

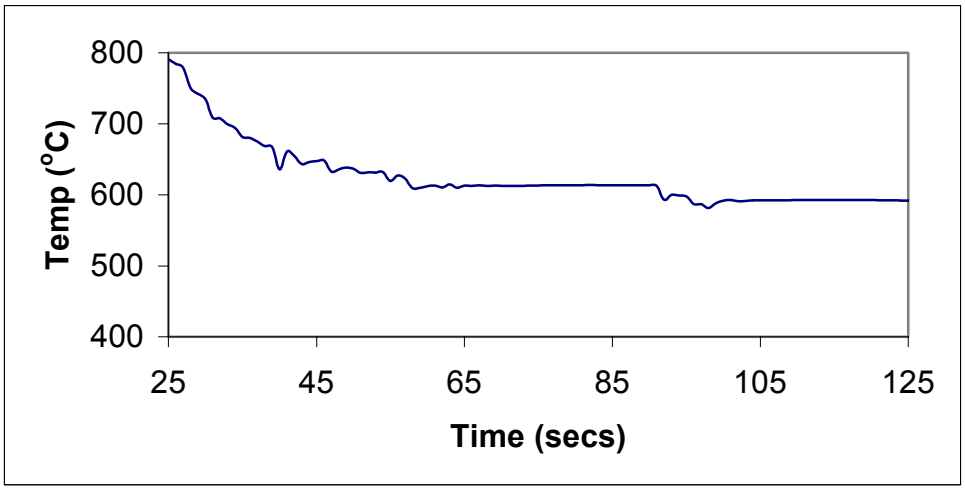

Figure 2: Time- temperature plot of Liquid 390 alloy held at 760 ^{0}C and rapidly cooled to 590 ^{0}C by the addition of 390 chips to the melt.

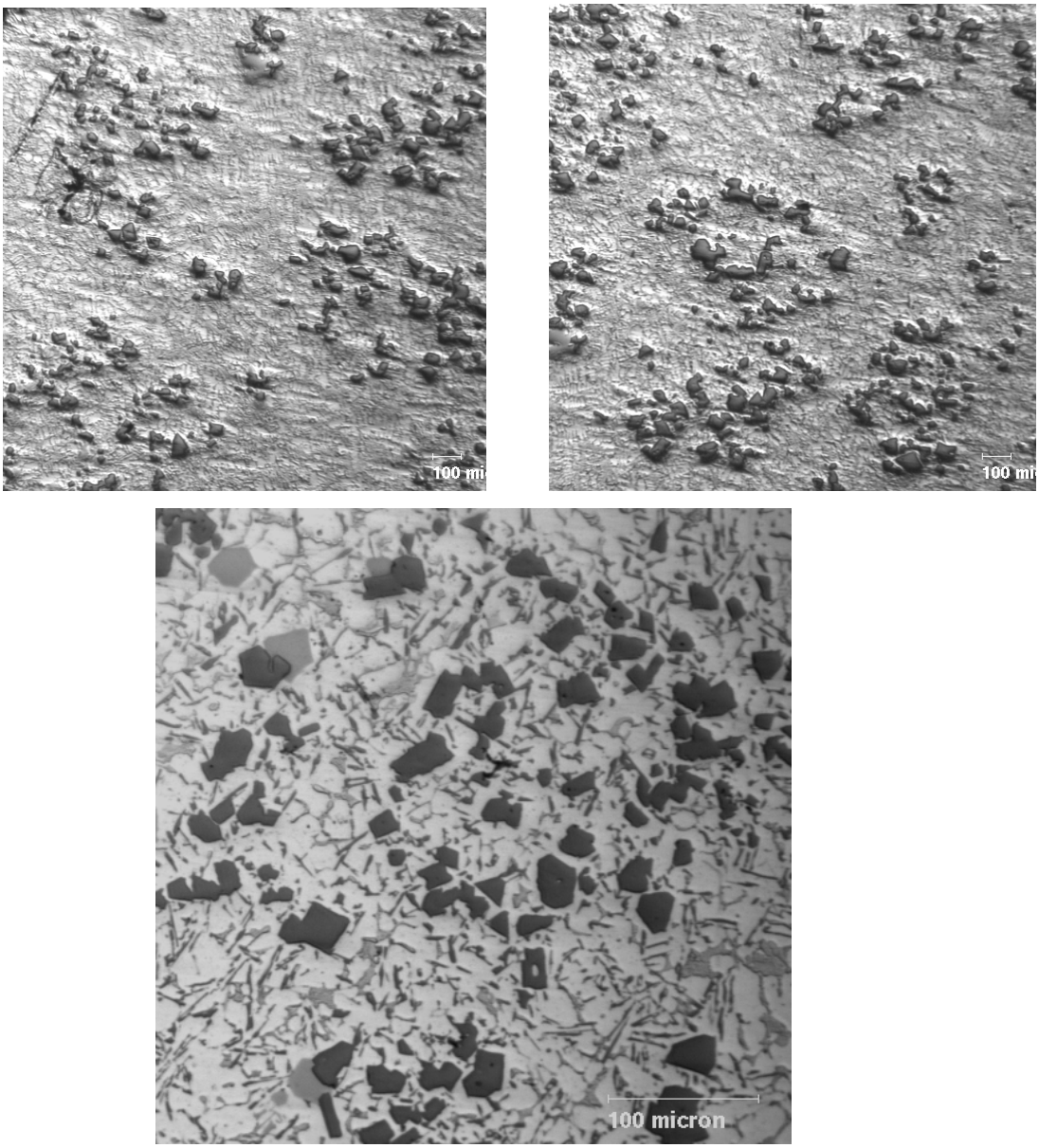

Figure 3: Representative microstructures, at various different magnifications, of 390 Alloy at 760 ^{0}C quenched to 590 ^{0}C by the addition of 390 alloy chips (initially at room temperature).

Trials were performed in a six-cavity die to investigate the effect of chip addition for the SSM processing of 390 Alloy. The shot sleeve was filled with chips constituting 10% of the total weight in the shot sleeve, and subsequently, the hot metal was poured into the shot sleeve. The parts were then examined in an X-ray machine to observe any remnants of solid chips. The cast parts were also sectioned and examined by conventional metallographic techniques. Figure 4

shows a representative microstructure of the thick walled portion of the casting. Figure 5 shows a representative microstructure of a thin walled portion of the casting.

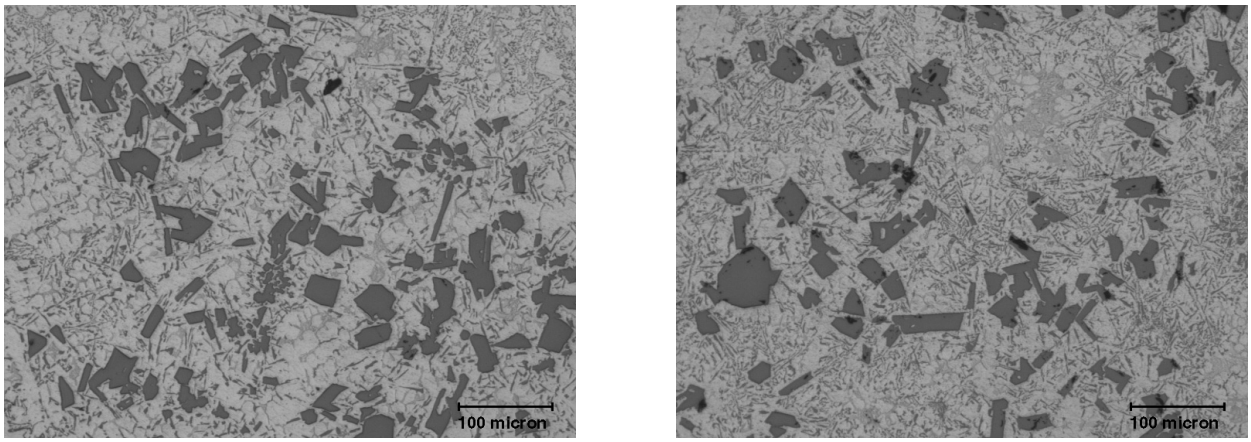

Figure 4: Representative microstructure of a thick walled section of the 390 alloy part cast by chip addition.

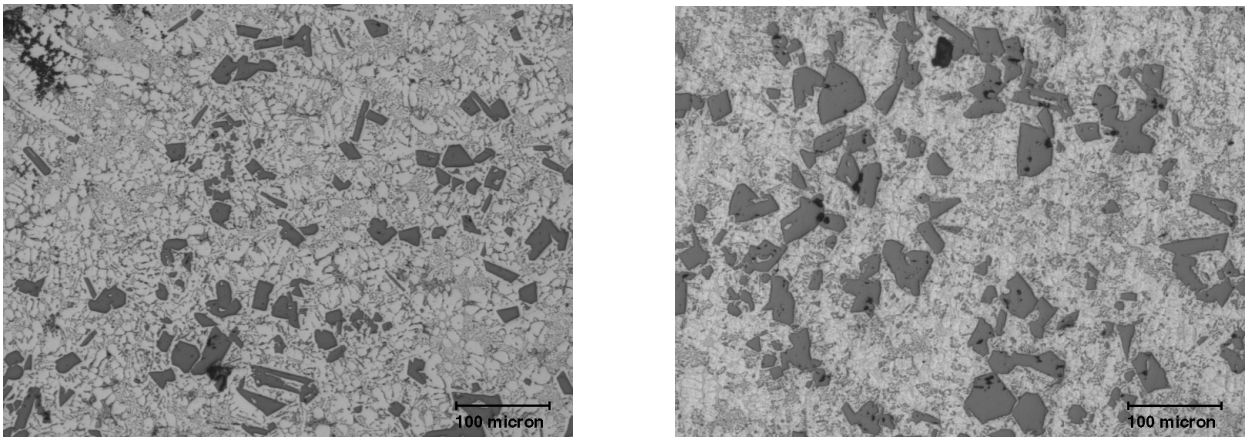

Figure 5: Representative microstructure of a thin walled section of the 390 alloy part cast by chip addition.

Hypoeutectic Alloys

Trials with Hypoeutectic Al-Si alloys were carried out at SPX Contech utilizing a commercial die casting machine. Chips of known weight were added to the shot sleeve, and subsequently, the liquid metal was poured into the shot sleeve. The semi solid slug was then quenched and the cast part was sectioned, and metallographically examined. Figure 6 shows a typical microstructure from the middle section of the slug. Figure 7 shows a representative microstructure at the edge of the slug.

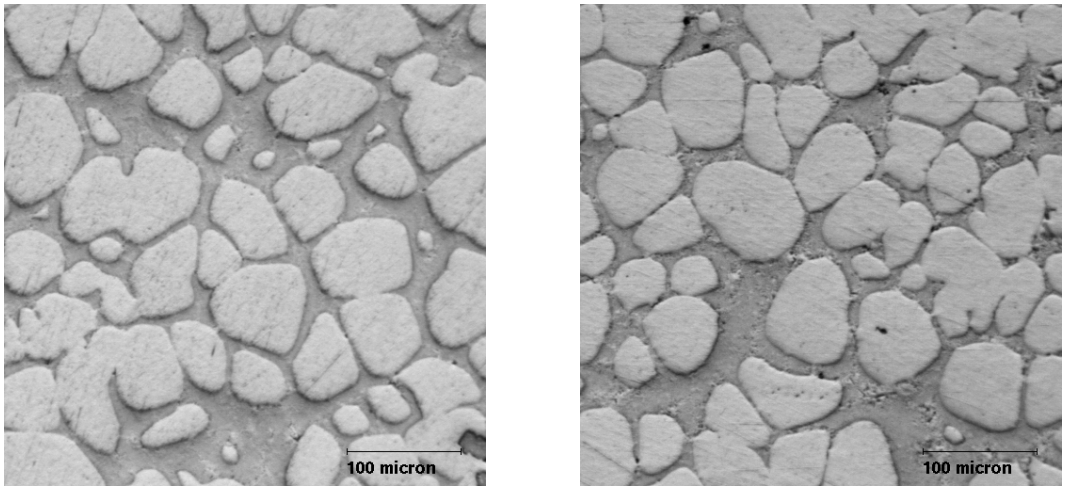

Figure 6: Typical micro-structure obtained at the center of a slug of Hypoeutectic Al-Si alloy by the addition of chips in the shot sleeve.

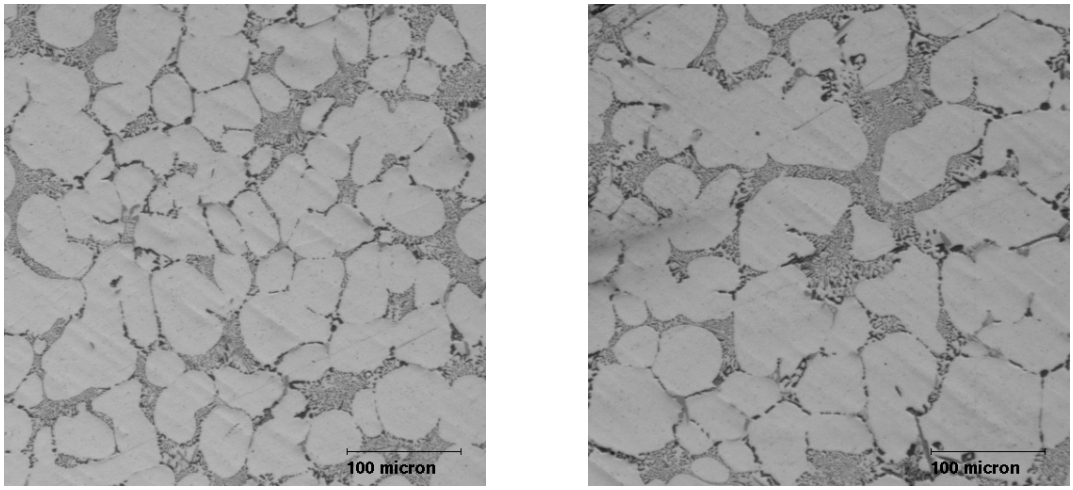

Figure 7: Typical micro-structure obtained at the edge of a slug of Hypoeutectic alloy by the addition of chips in the shot sleeve.

Discussion

A novel processing route using diffusion solidification has been utilized for the Slurry-On Demand processing of Hypo and Hypereutectic Al-Si alloys. Trials performed at SPX Contech using conventional die casting machines clearly show that SSM microstructures can be obtained by the addition of chips (controlled amount) in the shot sleeve to cool the liquid metal to the required SSM range. In the case of the Hypereutectic Al-Si alloys, the resultant size of the primary Si phase is in the order of 50 microns, with some areas of the microstructure having

primary Si size in excess of 80 microns. For the Hypoeutectic Al-Si alloy trials, the average primary Al size and their compactness is given in Table I.

Table I. Microstructural analysis for the Hypoeutectic Al-Si alloy slug made by the addition of chips

	Center of the Slug	**Edge of the Slug**
Compactness (1 = Circle)	1.6 – 1.8	2.2 – 3.0
Equivalent Cell Diameter	40 – 60 microns	40 – 60 microns

The results indicate that diffusion solidification can be a useful technique in obtaining semi solid slurry for both Hyper and Hypoeutectic Al-Si alloys. Three key events are:

- The chips at room temperature provide potent nucleation sites for the formation of the primary phase, as the chips act as a cold substrate for the liquid metal,
- The turbulence created by the poured liquid metal, provides a mechanism for the dispersion of nuclei in the solidifying melt,
- The superheat (temperature above the liquidus) and the latent heat released by the nucleation and growth of the primary phase, is absorbed internally in the dissolution of the solid chips

The combination of these three events, provide ideal conditions for the nucleation and the dispersion of the primary phase as the liquid metal cools rapidly to the SSM processing temperature. The rapid cooling of the liquid melt from the liquidus to the SSM processing range, make it potentially attractive for the rheocasting of Hypereutectic alloys. As mentioned earlier, rheocasting of Hypereutectic alloys has been stymied because of the rapid growth of primary Si as the liquid passes through the liquidus on its way to the SSM processing temperature. But the rapid heat extraction from the melt by the solid chips, provides the much elusive solution for the heat extraction and restricts growth of the Primary Si.

Conclusions

- Diffusion solidification approach can be utilized to produce Slurry-On Demand SSM material for both Hypereutectic and Hypoeutectic Al-Si alloys.
- The resultant microstructures are comparable to those obtained by most available technologies vis-à-vis primary Al size and compactness (Hypoeutectic alloys), and comparable primary Si size and distribution (Hypereutectic alloys).
- This approach is easy to incorporate into an existing casting facility. The process requires very little changes in existing die casting machinery and infrastructure.
- The waste generated in the form of runners / gates etc can be recycled as and input into the casting process in the form of solid chips, increasing the yield of the process and reduced waste generation
- The diffusion solidification approach has resulted in a reduction in cycle time from shot to shot, increasing productivity.

Acknowledgments

The authors would like to thank SPX Contech for providing the financial support for this work, use of die casting machines at the plant, and the needed man power for the successful conduction of these trials.

References

1. D.P. Spencer, R. Mehrabian, and M.C. Flemings (1972), "Rheological Behavior of Sn-15% Pb in the Crystalline Range", Metallurgical Transactions, volume 3, page 1925 – 1932.
2. DOE Report number DE-FC07-98ID13618.
3. R. Martinez, A.M. de Figueredo and J. Yurko and M.C. Flemings (2001), "Efficient Formation Structures Suitable for Semi solid Forming", Transactions of the 21st International Die Casting Congress and Exposition, Oct 29 – Nov 1, Cincinnati, Ohio, page 47 – 54.

4. A.M. de Figueredo, M. Findon, D. Apelian, and M.M. Makhlouf (2002), "Melt Mixing Approaches for the Formation of Thixotropic Semi solid Metal Structures", Proceedings of the Seventh International Conference titled Advanced Semi solid Processing of Alloys and Composites, Tsukuba, Japan, September 24-28, page 557-562.

5. European Patent EP 0 745 694 A1 (1996), By UBE Industries Ltd.

6. Science and Technology of Semi solid Metal Processing (2001), Edited by Anacleto de Figueredo, Published by the North American Die Casting Association, Rosemont, IL, page 2-12.

7. Merton Flemings (2003), "Semi solid Processing – The Rheocasting Story", Test Tube to Factory Floor: Implementing Technical Innovations, In the proceedings of the Spring Symposium May 22, 2002 published by Metal Processing Institute, Worcester Polytechnic Institute, Worcester MA 01609.

8. G. Langford and D. Apelian (1980), "Diffusion Solidification", Journal of Metals, **32**, No. 9, page. 28-34.

Chapter 7. Rheocasting of 390 alloy

Preface

This chapter presents experiments performed at WPI by mixing a semi solid slurry and a hypereutectic Al-Si alloy to achieve a 390 Alloy. Thermal analysis revealed very high undercooling, leading to very fine primary Si in the matrix. Industrial trials were performed by the addition of 390 solids into 390 liquid with varying degrees of superheat. The experiments were performed in a horizontal cold chamber die casting machine. The trials cut the die opening – closing time by 40% indicating the potential benefits of rheocasting. The average primary Si was less than 30 microns, and the distribution of primary silicon in the final part was found to be optimum at high solid fractions (10% the total weight). The author would like to thank M. A. Musser, Z. Brown, D. Killingsworth and Dr. Rathindra DasGupta for the technical and logistic help during the trials at SPX. The paper was published *as "Semi solid Processing of Hypereutectic Alloys",* ***AFS Transactions****, 2004, Vol. 112, 04-57.*

***AFS Transactions**, 2004, Vol. 112, 04-57*

Semi Solid Processing of Hypereutectic Alloys

Deepak Saha, D. Apelian

Metal Processing Institute, WPI, Worcester, MA, USA

R. DasGupta

SPX Contech, Michigan, USA

ABSTRACT

Semi solid metal (SSM) processing of hypereutectic Al-Si alloys has been limited to the thixocasting route, where a billet (MHD cast) containing extremely fine primary Si (< 15 microns) particles is re-heated to the SSM temperature, emplaced in the die cavity and then cast. Conventional casting of these high silicon alloys, have shown primary Si refinement, however the silicon size distribution in the final part is not desirable for high integrity parts. Rheocasting or Slurry-On-Demand approach offers cost advantages over thixocasting in terms of alleviating billet premiums, reheating costs, recycling, etc. Rheocasting of hypereutectic Al-Si alloys has been hampered by the growth of the primary Si phase to an unacceptable range (> 100 microns). Ironically, a large solidification range, which is believed to be ideal for SSM processing, in this instance (i.e., 390 alloys) causes accelerated growth of the primary Si phase as the alloy cools from the liquidus to the SSM processing temperature. The possibilities of refining primary Si via rheocasting are limited to: ***a)*** breaking of primary Si (using external forces), and/or ***b)*** use of growth restrictors, and/or ***c)*** rapid heat extraction within the shot sleeve, without the formation of a chill zone. In this paper we present various experiments performed at SPX Contech and MPI, wherein we utilize diffusion solidification as a means to extract heat within the slug. The novel concepts introduced in this paper are: (i) mixing of a low temperature hypoeutectic alloy with a high temperature hypereutectic alloy, and (ii) cooling of the liquid hypereutectic alloy via chips having the same/or different composition. The paper presents laboratory results carried out at MPI and industrial trials performed at SPX Contech.

INTRODUCTION

Hypereutectic Al-Si alloys have gained much attention in the recent past due to their superior properties (low coefficient of thermal expansion, high yield strength and high wear resistance). Some of the most common applications are: engine blocks, cylinder heads, cylinder sleeves, clutch input housing, clutch assembly, brake cylinders, etc. The hard primary silicon in a soft matrix of Al-Si eutectic provides the requisite wear resistance. The final properties in the cast component are dictated by the distribution and size of the primary silicon phase. Work to date (Matsuura K, 2003) has established that an increase in the volume fraction of primary silicon (or reduced size) increases the resultant mechanical properties. With commercial interests in SSM processing burgeoning in the early to mid 90's, casting 390 type alloys via thixocasting and/or rheocasting has become of great interest. Unfortunately, the work to date in SSM processing of 390 type alloys has been stymied by the growth of the primary silicon to unacceptable ranges (> 100 microns).

In this paper we will review the impedances and technical challenges that arise when hypereutectic Al-Si alloys are processed through the SSM route; review existing SSM processing routes for hypereutectic alloys, and lastly present two novel approaches for casting hypereutectic Al-Si alloys.

HYPEREUTECTIC AL-SI ALLOYS: SSM PROCESSING CHALLENGES

Processing of hypereutectic Al-Si alloys is a challenge because of the heat associated during the solidification of primary Si. Figure 1 shows the heats evolved per mole of a hypereutectic Al-Si alloy (A356) and a hypereutectic Al-Si alloy (A390). The data were obtained by PANDAT software (using non-equilibrium solidification assumptions/Scheil equation). It can be seen from Figure 1 that the heat associated during the cooling of a hypereutectic alloy is at least 2-3 times that of an equivalent solid fraction of the hypoeutectic alloy. The same heat provides the required fluidity of these alloys. In traditional castings of hypoeutectic alloys, to remove the exothermic energy released during solidification, excessive use of chills is made. The high heat released in hypereutectic Al-Si alloys is attributed to the high entropy of fusion that is released during solidification.

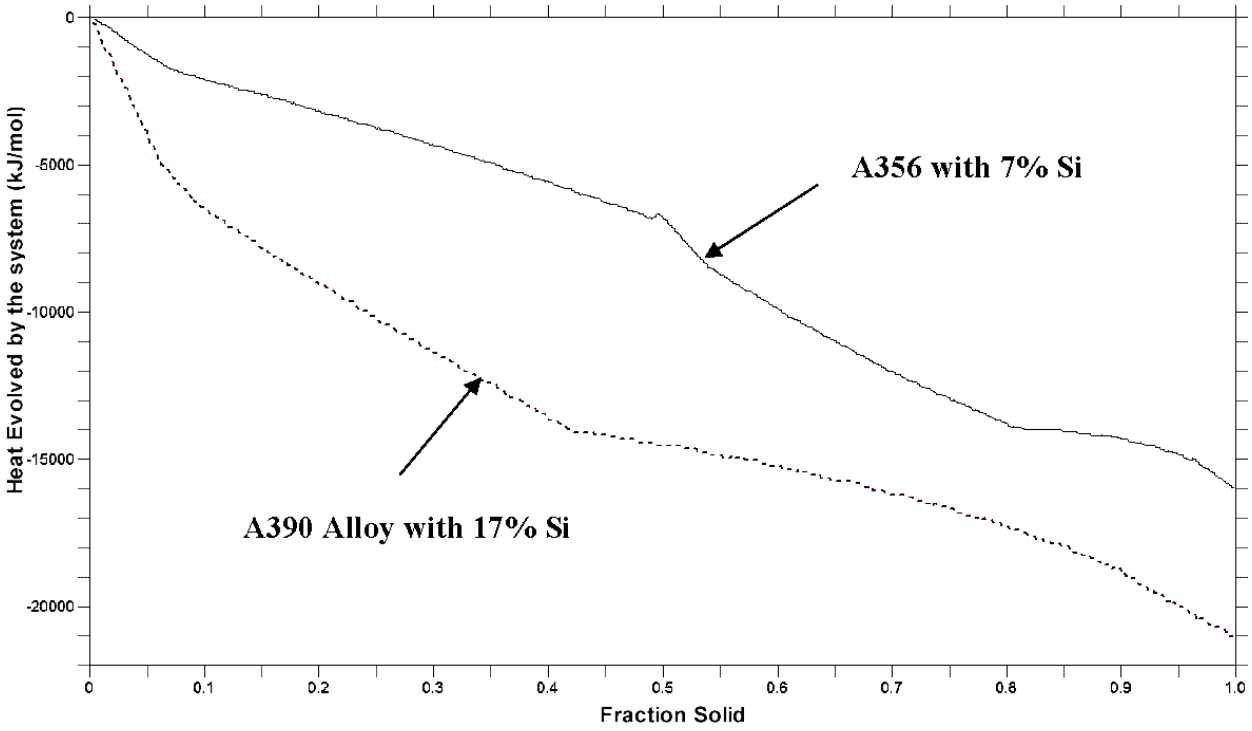

Figure 1: Heat released during the solidification of a hypereutectic Al-Si alloy (dashed) and a hypoeutectic Al-Si (continuous line) with respect to fraction solid.

The heats of fusion and the enthalpy of formation of one mole of Al (in hypoeutectic alloy) and Si (in hypereutectic alloy) are listed below:

$$\Delta S^{Si}{}_{Trans} = \frac{\Delta H_{trans}}{T_m}$$

$$\Delta S^{Si}{}_{Trans} = \frac{50{,}200}{1685} = 29.79 J/K$$

$$\Delta S^{Al}{}_{Trans} = \frac{10{,}700}{934} = 11.45 J/K$$

$$\frac{\Delta S^{Si}{}_{Trans}}{\Delta S^{Al}{}_{Trans}} = \frac{29.79}{11.45} = 2.6$$

Equation 1

Equation 1 shows that the energy released during the transformation of a mole of Si is at least 2 – 3 times that of Al. The high heat of fusion associated with Si accounts for the exothermic nature of this transformation. This can be seen by the ratio of the heats of fusion of Si with that of Al:

$$\frac{\Delta H^{Si}{}_{Trans}}{\Delta H^{Al}{}_{Trans}} = \frac{50{,}200}{10{,}700} = 4.7$$

Another problem associated with casting of hypereutectic Al-Si alloys is the role undercooling plays on the size of the primary Si. Figure 2 shows the salient results from a study performed by (Wang, 1999) on the growth mechanism of primary silicon as a function of undercooling.

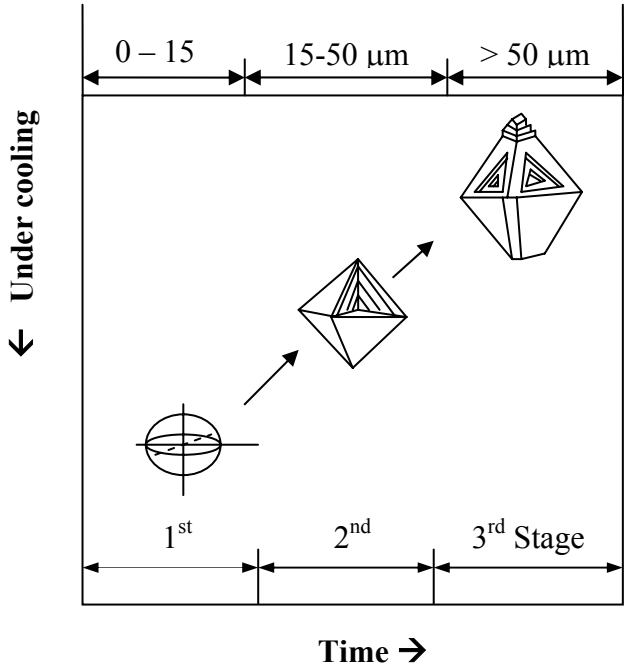

Figure 2: The three stages of growth of primary silicon as a function of undercooling (Wang, 1999).

The ideal microstructure of hypereutectic Al-Si alloys should consist of primary Si, which is small in size and evenly distributed throughout the matrix. The regions labeled as the 1st and 2nd stage give rise to the most desired primary Si microstructures. The transition from the un-faceted (1st stage) to faceted (2nd

stage) is due to the crystal structure of primary Si. Jackson (Jackson, 1958) related crystal faceting to the entropy of melting and the crystal structure. Table 1 lists the values and conclusions from his studies.

Table 1. Jackson Criterion for the Morphology of Silicon Phase (Wang, 1999).

Plane	Ns / Nv	α	Growth Mode
111	3/4	2.67	Faceted
100	2/4	1.78	Non-Faceted
110	1/4	0.89	Non-Faceted

Where: Ns = No. of atoms on the surface and Nv = No. of atoms in the cell and alpha equals the ratio (Ns/Nv) multiplied by the entropy change divided by the transformation temperature ($\Delta S/T_E$), i.e., alpha = (Ns/Nv) x ($\Delta S/T_E$). The transition from continuous to faceted growth was analyzed by Sun et al (after Wang, 1999), and is shown in Figure 3. The shaded region shows the region relevant to primary silicon. It can be seen that the driving force (which is directly proportional to the under cooling) determines the growth mode of primary silicon – i.e., faceted / un-faceted structures. Traditional castings have employed high undercooling (use of chills, etc.) to precisely prevent the coarsening of the primary silicon (regions marked 1st / 2nd stage in Figure 2). These studies lay the essential foundation for the motivation for the rheocasting of hypereutectic Al-Si alloys. Primary silicon refinement and distribution is a direct function of the under cooling achieved during the solidification of a hypereutectic alloy.

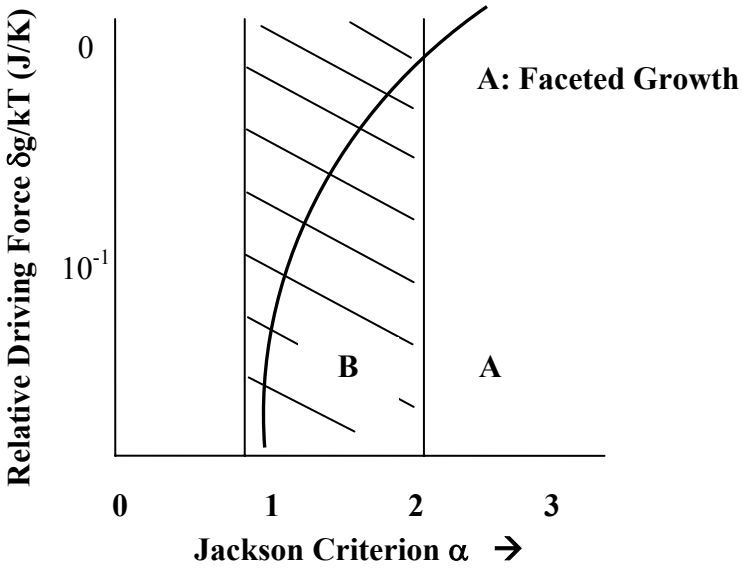

Figure 3: The variation in the driving force of transition from faceted to continuous growth. The shaded region corresponds to the values for Silicon (Wang, 1999).

SSM PROCESSING ROUTES FOR HYPEREUTECTIC Al-Si ALLOYS

In the recent past several rheocasting approaches have been developed, and have been commercially implemented. To establish context, prior to describing and reviewing the two novel approaches we have developed, existing processes will be briefly reviewed.

New Rheocasting Process, (UBE Industries) (UBE, 1996) where the liquid melt is held at relatively low superheats is poured in a cold mould, the natural convection during the pouring being utilized for the dispersion of nuclei.

A quick and initial mechanical stirring of the liquid metal in the early stages of solidification, known as SSR process, or the new MIT process (Matinez, 2001) leads to the nucleation of the primary phase and the dispersion of nuclei throughout the melt. In this process, it is important that the superheat is minimal, and controlled.

AEMP process (Flemings, 2003), which utilizes electromagnetic stirring to break up the dendrite arms to create a semi solid slurry.

Sub-Liquidus Casting (SLC/THT process) (Anacleto, 2001), which utilizes pouring at very low or near close, liquidus temperatures giving rise to semi solid structures.

CRP^{TM} (Continuous Rheocasting Process) developed by the ACRC-MPI team wherein liquid from two different reservoirs are fed into a reactor to produce a slurry. The reactor aids in the formation of the nuclei, and dispersing them throughout the bulk (DOE report).

Slurry-On-Demand and rheocasting processing routes (UBE-NRC, SSR, AEMP, SLC, CRP and etc.) for Al-Si alloys (hypoeutectic alloys) utilize the concept of nucleation and dispersion of nuclei (nucleated during the early stages of solidification) to achieve a semi solid slurry state. Applying the above processing routes to hypereutectic Al-Si alloys has significant challenges (high heats of fusion and rapid growth of the primary Si phase), and the currently available processes may not be applicable for hypereutectic Al-Si alloys. Accordingly, two novel approaches both based on diffusion solidification concepts were explored to balance the release of the high heat of fusion in hypereutectic Al-Si alloys, and to control the growth of the primary silicon phase.

DIFFUSION SOLIDIFICATION

Diffusion solidification, introduced by Apelian and Langford (Langford, 1980) is a novel approach wherein solidification is controlled by mass flow rather than heat flow. During conventional solidification processing, when an alloy is solidified, the temperature is reduced as one moves down an iso-concentration line. Partitioning takes place, and two phases are formed: primary alpha phase and enriched liquid phase. Moreover, the heat released by the liquid phase flows in the direction opposite to the motion of the liquid/solid interface, and solidification time is controlled by heat flow. In diffusion solidification, two phases – a solute enriched liquid phase and a solute poor solid phase (held at the same temperature – on an isothermal line) are brought into intimate contact, and solute diffusion from the liquid to the solid phase takes place. As the liquid loses solute, solidification proceeds via mass flow. Moreover, solidification times are independent of the size of the casting.

Originally, Apelian and Langford utilized diffusion solidification to die cast steels. In their pioneering experiments, they infiltrated a die filled with pure iron powder heated to a temperature in the Austenite region, T_1 with cast iron liquid phase also heated to the same temperature, T_1 (Figure 4). Carbon diffused

away from the liquid into the iron powder, and since carbon diffuses interstitially, the diffusion rate is relatively high, and the liquid phase became solute (carbon) poor at T_1, and solidified. They produced a variety of cast components using diffusion solidification; commercially, the concept is utilized to make high-speed steels, and also dental amalgams.

The diffusion solidification approach has been applied to Al-Si alloys, both Hypo and Hypereutectic alloys. Specifically, we mixed solid particles with liquid metal, both phases having the same composition prior to mixing, however not at the same temperature. The central idea behind this concept is to utilize the excess superheat from the liquid metal (latent heat of solidification), as well as the heat released during the growth of the primary Si phase in melting the solid particles. This approach ensured that the heat released is internally consumed in the dissolution/melting of the solid pieces, as the hotter metal solidified. The turbulence generated during pouring of the metal was used in dispersing the nuclei throughout the melt. The process is rapid, and the amount of solid particles added into the system determined the final temperature of the slug.

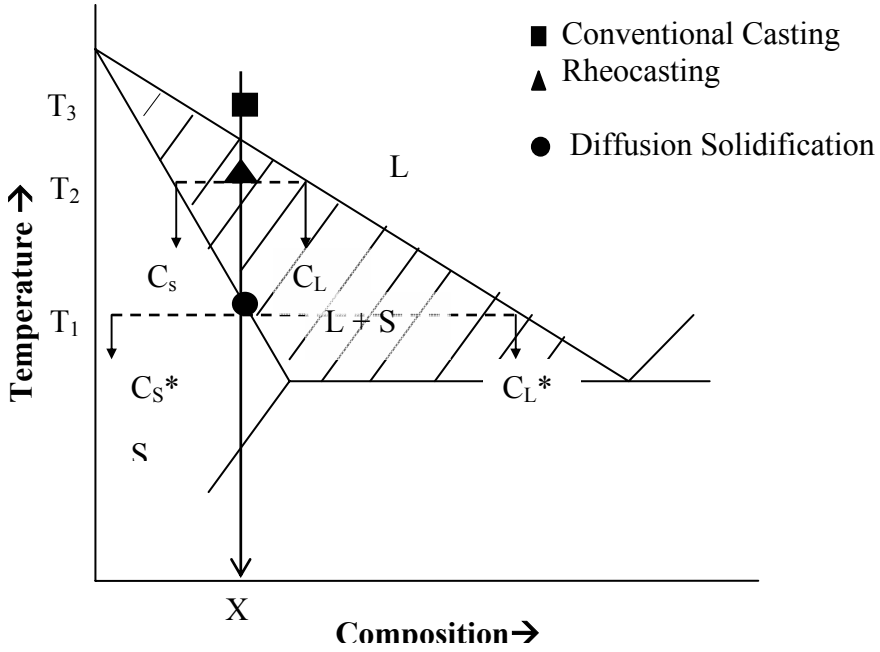

- Conventional casting at temperature T_3
- Rheocasting: alloy X is cooled to T_2 and isothermally agitated. The solid-liquid mixture consists of liquid phase of composition C_L of an amount f_L and solid phase of composition C_S and amount f_S, such that $f_S C_S + f_L C_L = X$
- Diffusion solidification: f_S amount of solid particles of composition C_S* and at temperature T_1 are infiltrated by f_L amount of liquid of Composition C_L* such that $f_S C_S^* + f_L C_L^* = X$

Figure 4: Schematic diagram illustrating the concept of diffusion solidification [9].

DIFFUSION SOLIDIFICATION: ***Mixing of TWO liquids***

We addressed the challenge of rheocasting Al-Si alloys by mixing two melts of two different compositions, each held at different temperatures. Specifically, we mixed two Al-Si alloys, one a hypoeutectic melt (6-7% Si, A356), and the other a hypereutectic alloy (25% Si). The 25% Si alloy was held above its liquidus temperature, whereas the 6-7% Si alloy was held in the semi solid range (two phase range) - see Figure 5. The purpose of adding the hypereutectic alloy to the cooler A356 alloy was to rapidly extract thermal energy from the hypereutectic melt, and to lower its temperature to the SSM casting temperature. The weight ratio of the two starting melts is 1:1, and the resultant alloy composition (based on a mass balance) is that of A390. The conceptual framework is to increase diffusion of heat from the hypereutectic alloy by the dissolution of the primary aluminum phase of the hypoeutectic alloy. The thermal imbalance leads to two advantages:

- heat from the higher Si alloy is absorbed by the cooler alloy, and concomitantly
- rapid chilling prevents the growth of primary silicon to unacceptable ranges.

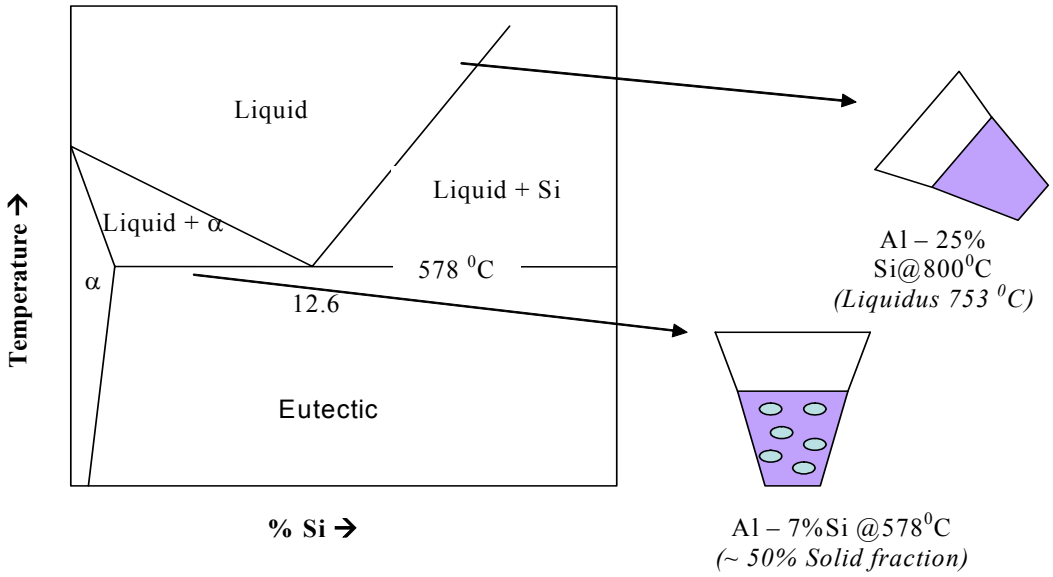

Figure 5: Diffusion Solidification concept of mixing liquid Al-Si at 800 ^{0}C, and A356 (7% Si) at 578 ^{0}C (semi solid state).

A 100 grams sample of hypoeutectic alloy (A356) was heated in a furnace and cooled slowly to 577 ^{0}C. The schematic diagram illustrating the experimental approach is shown in Figure 5.

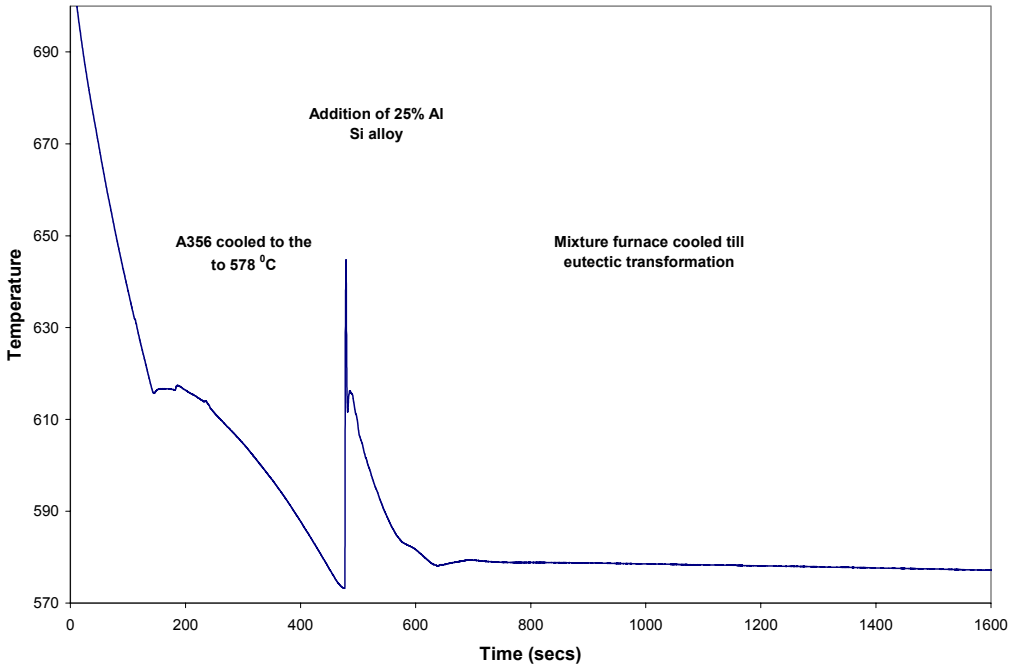

Figure 6: Time - Temperature plot at the interface during mixing of the two entities.

The temperature of the bulk was continuously measured during the duration of the experiment; Figure 6 shows the time-temperature curve obtained by the mixing of the two entities. It can be seen that the temperature at the interface rises and subsequently drops to 615 ^{0}C. Microstructures were examined at various locations from the resultant cast samples. Figure 7 summarizes the microstructures obtained at various positions in the resultant cast product. It can be seen from Figure 7, that the primary aluminum dissolves due to temperature and compositional variations. Precise experiments performed at WPI to study the thermal history of both the hypoeutectic and the hypoeutectic side is shown schematically in Figure 8.

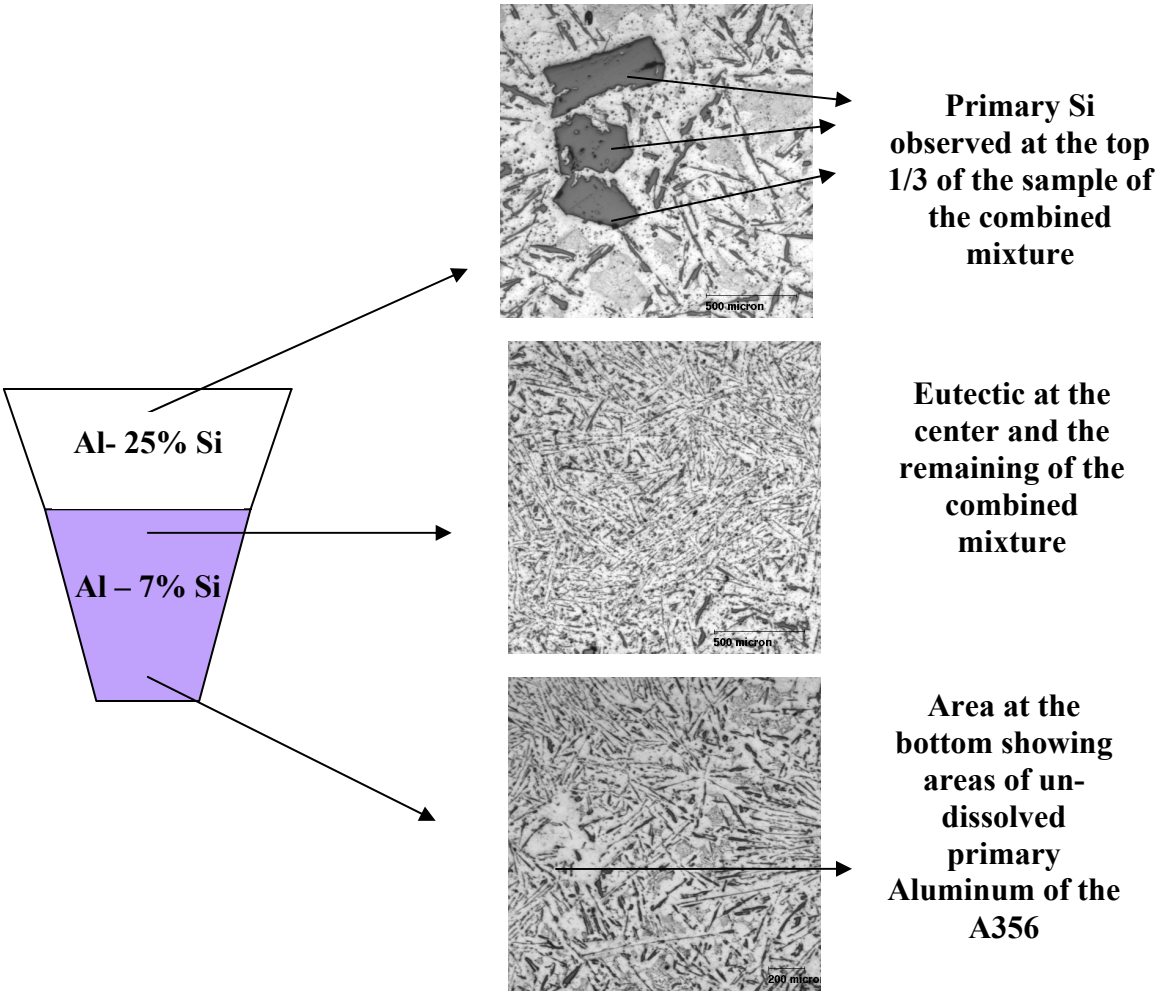

Figure 7: Microstructures of the resultant hypereutectic alloy at various positions in the mixture.

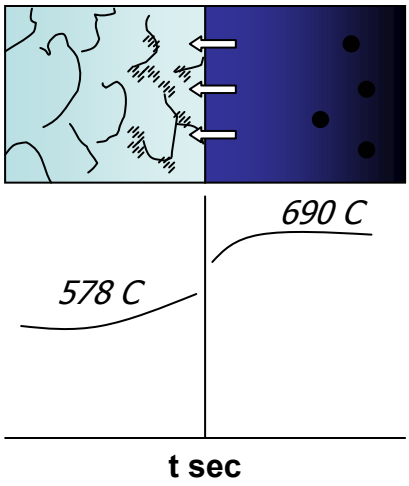

•Instantaneous precipitation of primary Si at the far end due to thermal drop to below liquidus
•Diffusion of Si / Al across the interface due to compositional imbalance/ heat imbalance

•Compositional balance between Si in the hypereutectic Al-Si alloy and the eutectic liquid of the Al- 50% Si hypoeutectic alloy

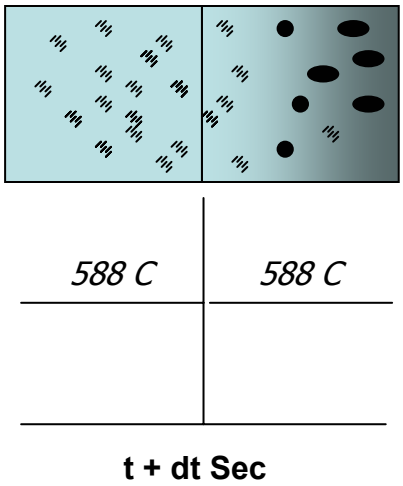

•The growth of primary Silicon at the far end is limited because of the chemical potential of Al/Si across the interface
•Conversion of 50% fraction solid to liquid of eutectic composition by diffusion solidification
•The final mixture has primary Si (due to chilling at the far end) and liquid eutectic

Figure 8: Schematic diagram of diffusion solidification between the liquid hypereutectic and the 50% hypoeutectic Al-Si alloys.

As these experiments were performed to ascertain the microstructural evolution across the interface (without the intention of controlling the primary Si size and distribution), experiments were also performed by physically mixing the liquids – i.e., the 25% Si liquid was poured into the A356 alloy. Figure 9 shows the resultant microstructure.

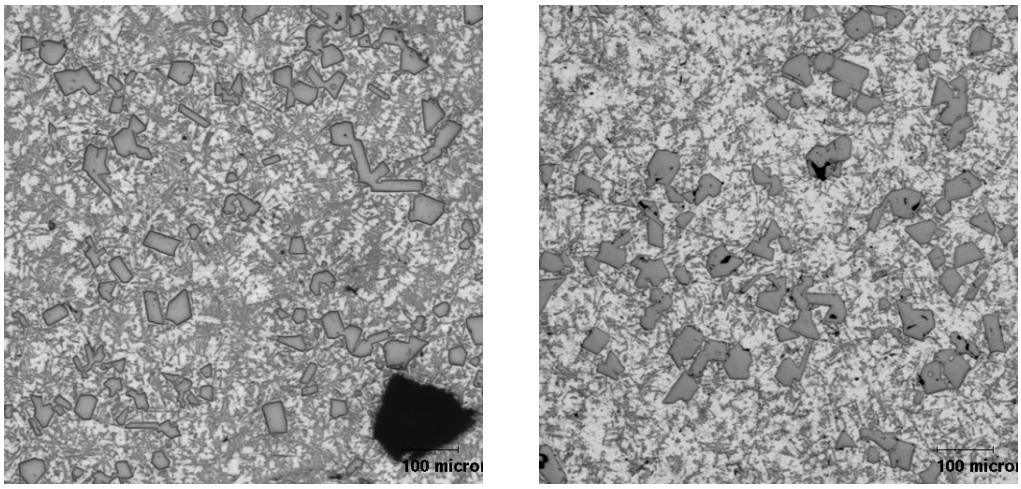

Figure 9: Microstructures obtained by stirring the mixture as the 25% Al-Si alloy was poured into the semi solid hypoeutectic A356 alloy.

The mixing of two liquids held at different compositions and temperatures shows positive results in the rheocasting of hypereutectic Al-Si alloys. Figure 9 clearly shows the dissolution of the primary aluminum of the hypoeutectic alloy (A356) that was achieved due to heat absorption and by diffusion solidification. The reactions can be broadly classified (experiment is schematically shown in Figure 8) as follows:

Liquid Hypereutectic Alloy (Al-25%Si): L → Primary Si and Eutectic

Semi solid Hypoeutectic Alloy (Al-7%Si): L + Primary Al → Eutectic

Experiments are underway at WPI to ascertain the diffusion dynamics/kinetics and the interface motion during the dissolution of primary aluminum (in the hypoeutectic alloy) to a liquid that solidifies as a eutectic alloy.

DIFFUSION SOLIDIFICATION: ***Mixing of solid PARTICLES and liquid METAL***

Another variation of the above discussed diffusion solidification approach was developed. In this process, solid particles/chunks of hypereutectic alloy were added into a liquid melt of hypereutectic Al-Si alloy (the alloy investigated being commercial 390 alloy). The addition of particles was performed to remove the heat from the liquid at a very rapid rate (to initiate nucleation of primary Si) and, to utilize the turbulence generated by the pouring liquid as a source for nuclei dispersion. Experiments were performed in two steps, schematically shown in Figures 10 and 11, respectively.

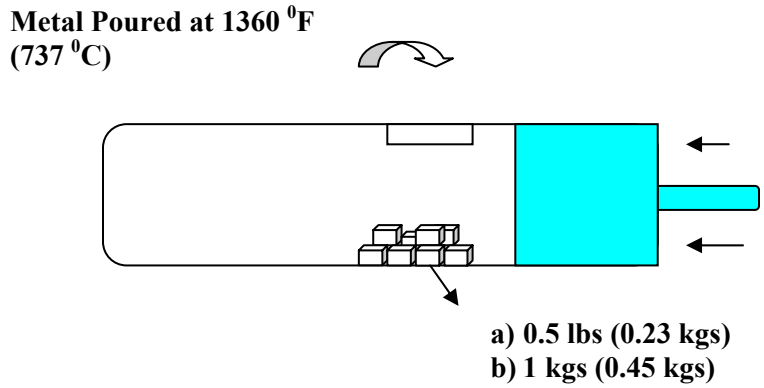

Figure 10: Schematic diagram illustrating the concept of solid particle addition into the shot sleeve.

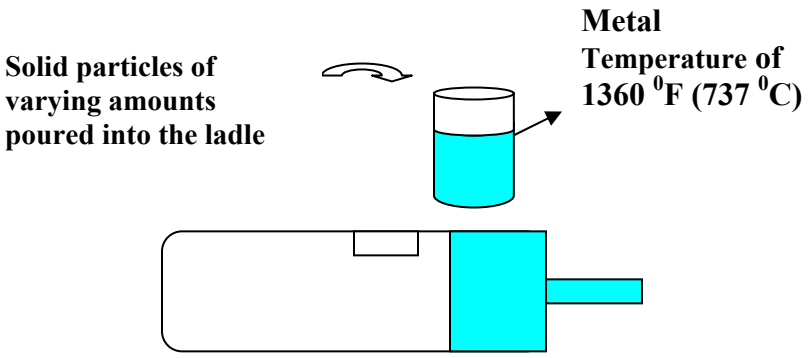

Figure 11: Schematic diagram illustrating the concept of solid particle addition into the ladle.

Table 2 lists the experiments performed in the plant trials at SPX Contech; details of the experiments are also given. The final part was cut and sections (thick and thin) were metallographically analyzed and compared to conventional die cast parts (baseline) from the same die-casting machine.

Table 2. Details of Various Experiments Performed at SPX Contech.

Experiment	**Weight of solids added**	**Metal Temperature**
Solids added into the shot sleeve		
a	0.5 lbs, 0.23 kgs (1.7% total weight)	1360 ^{0}F / 737 ^{0}C
b	1 lbs, 0.45 kgs (3.3% total weight)	
Solids added into the ladle		
c	2lbs, 0.91 kgs (6.7% total weight)	1360 ^{0}F / 737 ^{0}C
d	3lbs, 1.36 kgs (10% total weight)	

The cut samples (thick and thin) were analyzed for the primary Si size and distribution; 2-3 micrographs were taken at 100 X (to visually ascertain the special distribution of primary Si), and 4-5 micrographs (approximately 1 cm2) were taken at 200 X (to determine the size distribution of primary Si). The Dmax (shown in Figure 12) was used to estimate the silicon size. Dmax is the maximum length of primary size particle in the matrix. The primary Si are polygonal in nature, and their size distribution has a vast range; therefore the measurement of equivalent diameter is not representative, and it will be erroneous to utilize it as an index to reflect process parameter changes. The resulting microstructures are shown in Figures 13 – 16 for experiments a – d, respectively (see Table 2).

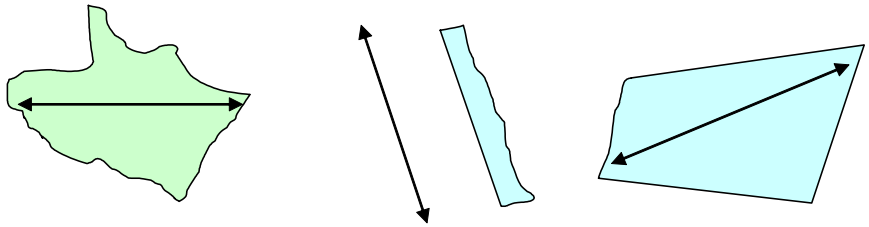

Figure 12: Schematic diagram of D_{max} for various primary Si shapes observed in the microstructure.

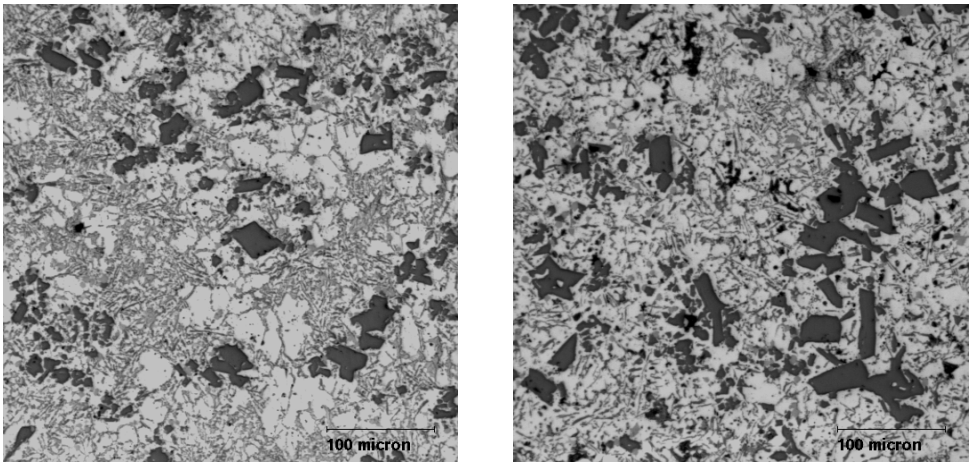

Figure 13: Representative microstructures from experiment a; thick section (left) and thin section (right).

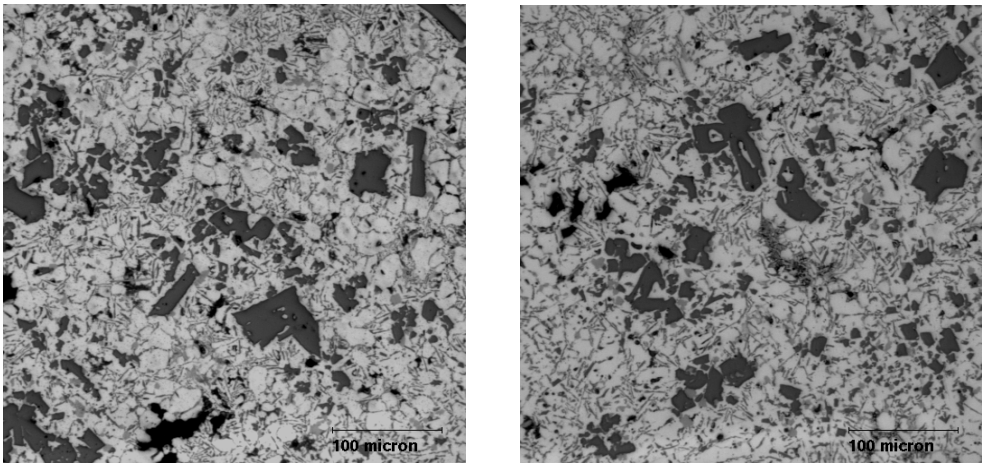

Figure 14: Representative microstructures from experiment b; thick section (left) and thin section (right).

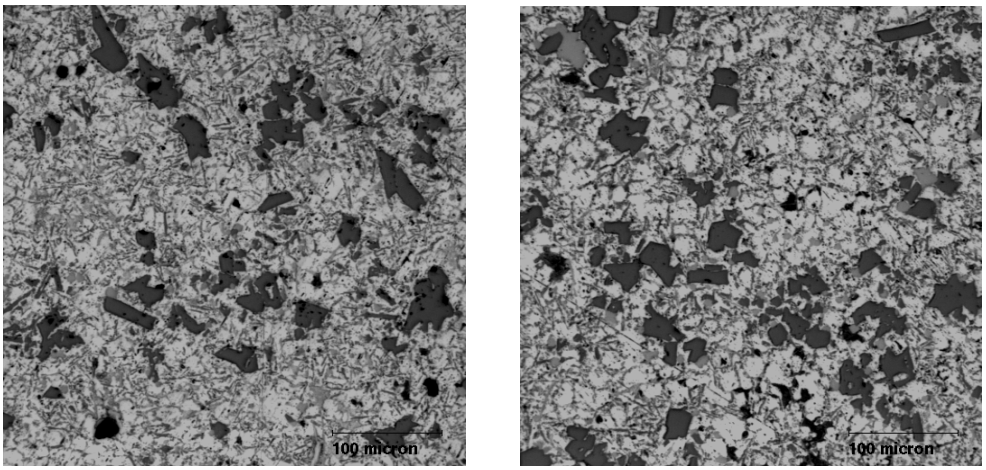

Figure15: Representative microstructures from experiment c; thick section (left) and thin section (right).

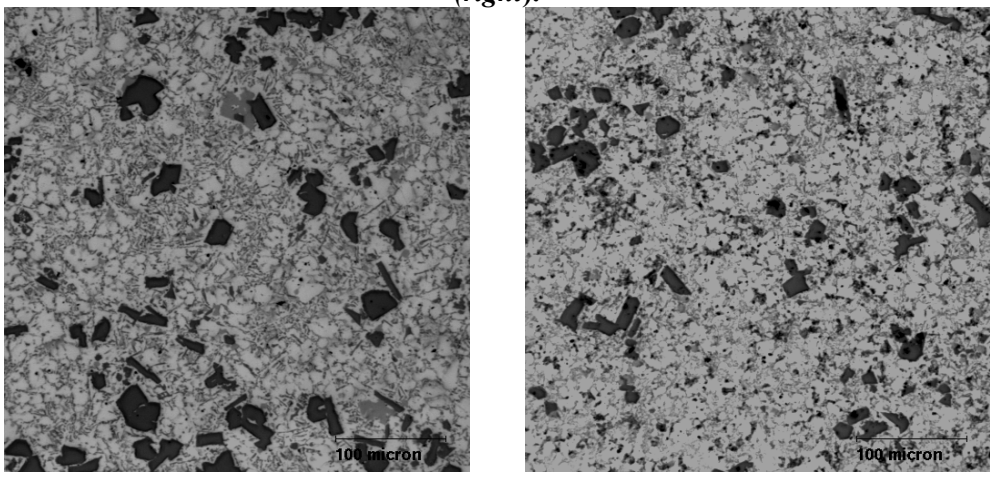

Figure16: Representative microstructures from experiment d; thick section (left) and thin section (right).

Figure 17 lists the values of Dmax obtained for the set of experiments performed (Table 2). An average value from 4-5 micrographs was calculated, and these are given in Figure 17.

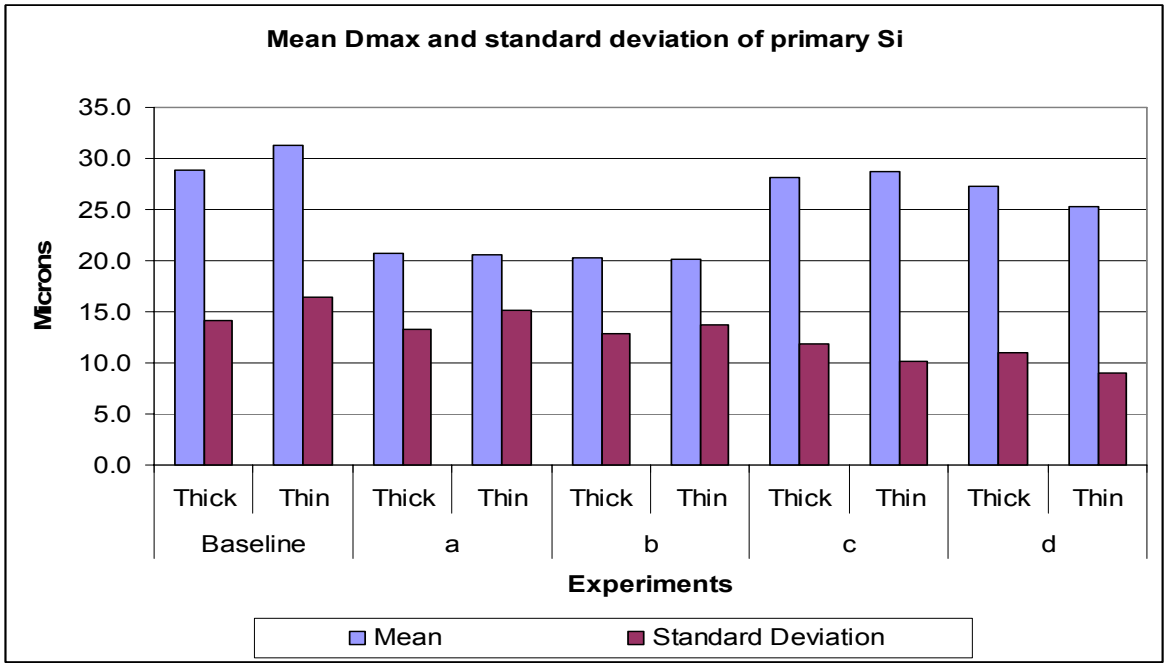

Figure 17: D_{max} and standard deviation of primary Si for the set of experiments carried out by the two novel diffusion solidification processes.

CONCLUSIONS

Hypereutectic Al-Si alloys have been a challenge to cast via semi solid processing because of the growth of the primary silicon phase, which gives rise to unacceptable morphologies, and thus unacceptable mechanical properties. In this work we have developed two novel processing methods that utilize the concept of diffusion solidification to control the growth of the primary silicon.

Diffusion solidification is controlled by mass flow rather than heat flow. During conventional solidification processing, when an alloy is solidified, the temperature is reduced as one moves down an iso-concentration line. Partitioning takes place, and two phases are formed: primary alpha phase and enriched liquid phase. Moreover, the heat released by the liquid phase flows in the direction opposite to the motion of the liquid/solid interface, and solidification time is controlled by heat flow. In diffusion solidification, two phases – a solute enriched liquid phase and a solute poor solid phase (held at the same temperature – on an isothermal line) are brought into intimate contact, and solute diffusion from the liquid to the solid phase takes place. As the liquid loses solute, solidification proceeds via mass flow.

Specifically, two novel diffusion solidification processes have been developed: one where a liquid hypereutectic alloy is mixed with a hypoeutectic alloy that is held in the semi solid state; the second process solid particles/chunks are added to the melt.

Experiments with both approaches, both at the laboratory state and in plant trials resulted in excellent microstructures of hypereutectic alloys. Results indicate that via these approaches one can control the size of the primary silicon phase in hypereutectic alloys to less than 25 microns.

ACKNOWLEDGMENTS

The authors would like to thank SPX Contech for providing the financial support for this work, use of die casting machines at the plant, and the needed man power for the successful conduction of these trials. We would also to thank Dayne Killingsworth, and Zach Brown of SPX Contech for their invaluable contributions during the trails.

REFERENCES

Anacleto Figueredo, Science and Technology of Semi solid Metal Processing, Published by the North American Die Casting Association, Rosemont, IL, page 2-12, (2001).

DOE Report number DE-FC07-98ID13618.

Flemings M.C, "Semi solid Processing – The Rheocasting Story", Test Tube to Factory Floor: Implementing Technical Innovations, In the proceedings of the Spring Symposium May 22, 2002 published by Metal Processing Institute, Worcester Polytechnic Institute, Worcester MA 01609, (2003).

Jackson K.A , Liquid Metals and Solidification, ASM, Ohio, pp 17 (1958).

Langford. G and Apelian. D, "Diffusion Solidification", Journal of Metals, 32, No.9, page. 28-34 (1980).

Martinez R. , Figueredo A.M, Yurko. and Flemings M.C, "Efficient Formation Structures Suitable for Semi solid Forming", Transactions of the 21st International Die Casting Congress and Exposition, Oct 29 – Nov 1, Cincinnati, Ohio, page 47 – 54 (2001).

Matsuura K, Kudoh M, Kinoshita H , Takahashi H, "Precipitation of Si particles in a super-rapidly solidified Al-Si alloy", Materials Chemistry and Physics, Volume 81, pp 393 – 395 (2003).

UBE Industries Ltd, European Patent No. EP 0 745 694 A1 (1996).

Wang Ru-yao, Lu Wei-hua, Logan L.M , "Growth morphology of primary Silicon in cast Al-Si alloys and the mechanism of concentric growth", Journal of Crystal Growth, Volume 207, pp 43 -54 (1999).

Chapter 8. Dissolution kinetics of α-Al in Al-Si liquid

Preface

This chapter is dedicated in understanding the fundaments of primary Al dissolution during the mixing of semi solid hypoeutectic Al-Si alloy and a hypereutectic Al-Si alloy. Experiments performed showed that the dissolution of primary Al into a supersaturated Al-SI liquid is dictated by a chemical reaction at the interface. The activation energy for the reaction was established as 30 kJ/Mol/K. The paper has been submitted to ***Metallurgical and Materials Transactions B in February 2005***.

On the dissolution of Al in Al-Si liquid during the mixing of Al-25% Si and Al-7% Si alloys

Deepak Saha and Diran Apelian
Metal Processing Institute, WPI
Worcester, MA 01609

Abstract

In the recent past, it has been discovered that one may obtain a refined SSM structure without breaking up the dendritic structure, but rather by creating an environment where copious nucleation can occur near the liquidus temperature of the alloy, and with limited growth of the formed nuclei. One such idea of copious nucleation was to utilize diffusion solidification to obtain fine primary silicon and distribution, wherein a 390 alloy (Al – 18% Si) was obtained by mixing a Al-25%Si alloy with an alloy containing 7%Si (A356). Mixing the hypereutectic Al-Si alloy (Al-25%Si) with the hypoeutectic Al-Si (Al-7%Si) led to dissolution of the primary aluminum in the lower silicon alloy (Al-7%Si), a mixture of primary Si and eutectic liquid at the end of the reaction. The α-Al in the Al-7%Si dissolves in an Al-Si liquid either by 1) interfacial reaction or 2) diffusion controlled process. The objective of this study was to identify the mechanism of dissolution of Al in a Al-Si liquid. To simulate the dissolution of α-Al from the Al-7%Si into the Al-Si liquid, rods of Al (99.99% pure) were dipped in Al-Si liquid with varying silicon concentration. The driving force for the dissolution of Al is provided by the difference in the silicon content between the rods of Al and Al-Si liquid. It was identified that the primary mode for dissolution of Al in a Al-Si liquid is via interfacial reaction at the interface and the activation energy was found to be 23-26 kcal/mol.K.

Introduction

Hypereutectic Al-Si alloys have gained much attention in the recent past due to their superior properties (low coefficient of thermal expansion, high yield strength and high wear resistance). Some of the most common applications are: engine blocks, cylinder heads, cylinder sleeves, clutch input housing, clutch assembly, brake cylinders, etc. The hard primary silicon in a soft matrix of Al-Si eutectic provides the requisite wear resistance. The final properties in the cast component are dictated by the distribution and size of the primary silicon phase. Researchers [1] had established that an increase in the volume fraction of primary silicon (or reduced size) increases the resultant mechanical properties. Some of the common problems associated with the solidification of hypereutectic alloys are:

- Heat released during the solidification of Hypereutectic Al-Si alloys is at least 2-3 times that of an equivalent solid fraction of the hypoeutectic alloy. The same heat provides the fluidity of these alloys. Use of localized chills is a very common method for extracting

heat during casting. The high heat released in hypereutectic Al-Si alloys is attributed to the high entropy of fusion that is released during solidification.

- Growth of primary Silicon into faceted structures during solidification and its direct relationship to the amount of under-cooling [2 – 3].
- The uneven distribution of primary Si during solidification. Even distribution of primary Si is ensured by enhancing the nucleation sites by the addition of phosphorus rich compounds [4 - 6]. The process of adding P rich compounds is called "refining" and has been used in the casting of hypereutectic Al-Si alloys for decades [7 – 8]. Addition of Phosphorus rich compounds has shown to increase mechanical properties by a factor of 5 – 10 [1, 5].

However, in the recent past there has been a burgeoning commercial interest in the near net shape manufacturing of aluminum alloys, especially via semi solid processing. Lee et al. have used mechanical stirring [9], while others have used ultrasonic treatment [10] to break down the primary Si in the two-phase range. Various new processes have been identified utilizing Thixocasting / forging [11 – 13]. The basic idea is however, two fold: a) increase nucleation of primary Si and b) facilitate primary Si distribution.

Rheocasting is a semi solid process, wherein the evolution of the primary phase (nucleation and growth) is controlled as metal reaches the desired two phase region. Rheocasting or Slurry-On-Demand approach offers cost advantages over thixocasting in terms of alleviating billet premiums, reheating costs, recycling, etc, which are normally associated in Thixocasting / forging. Rheocasting of hypereutectic Al-Si alloys, however, offer considerable challenges as the superimposed cooling rates in a typical rheocast process is low (promotes the growth and segregation of primary Si). Researchers have shown some success utilizing rheocasting processes [14]. An alternate process for the refining of primary silicon is by mixing two liquids [15, 16], mixing a solid and a liquid [16] to achieve a semi solid slurry. Figure 1 illustrated one such process.

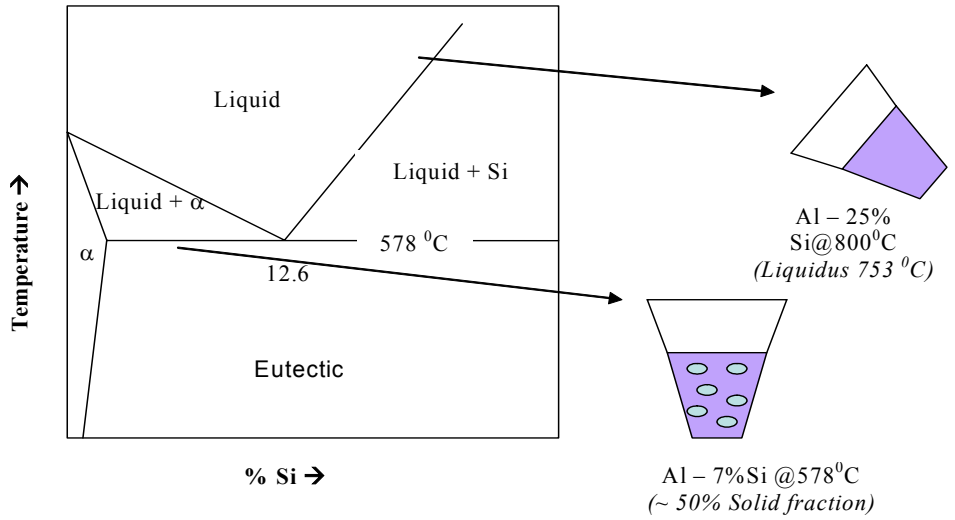

Figure 1: The process of mixing a hypereutectic Al-Si alloy with a hypoeutectic alloy to achieve fine primary silicon and distribution for net shape manufacturing [16].

Microstructures obtained by the melt mixing process (liquid and liquid / solid with liquid) provides fine primary Si and distribution, however there is a lack in the fundamental understanding of the process. The exact mode of dissolution of Al in liquid Al-Si is unknown and in this paper we identify the primary mode of dissolution of aluminum in Al-Si liquid.

Background

The mixing of a hypereutectic Al – 25% Si and Al-7%Si involves a complex process of heat and mass transfer, which can be broadly classified as follows:

4. A drop in the temperature of the Al-25% Si below the liquidus leading to the nucleation of primary Si
5. The absorption of the superheat of the Al-25% Si by the Al-7%Si
6. The gradual dissolution of the primary phase (α – Al) and the nucleation of primary Si from the Al-25%Si

To aid the understanding of the thermal history and the process in depth, we designed an experiment where a hollow cylinder was made out of a Al – 7%Si and four thermocouples were inserted as shown in Figure 2. The high temperature Al-25% liquid was poured into the hollow cylinder and the thermal profile collected. The mass ratio of the hypereutectic and the hypoeutectic alloy were equal, which ensured a final bulk composition of 16 %Si.

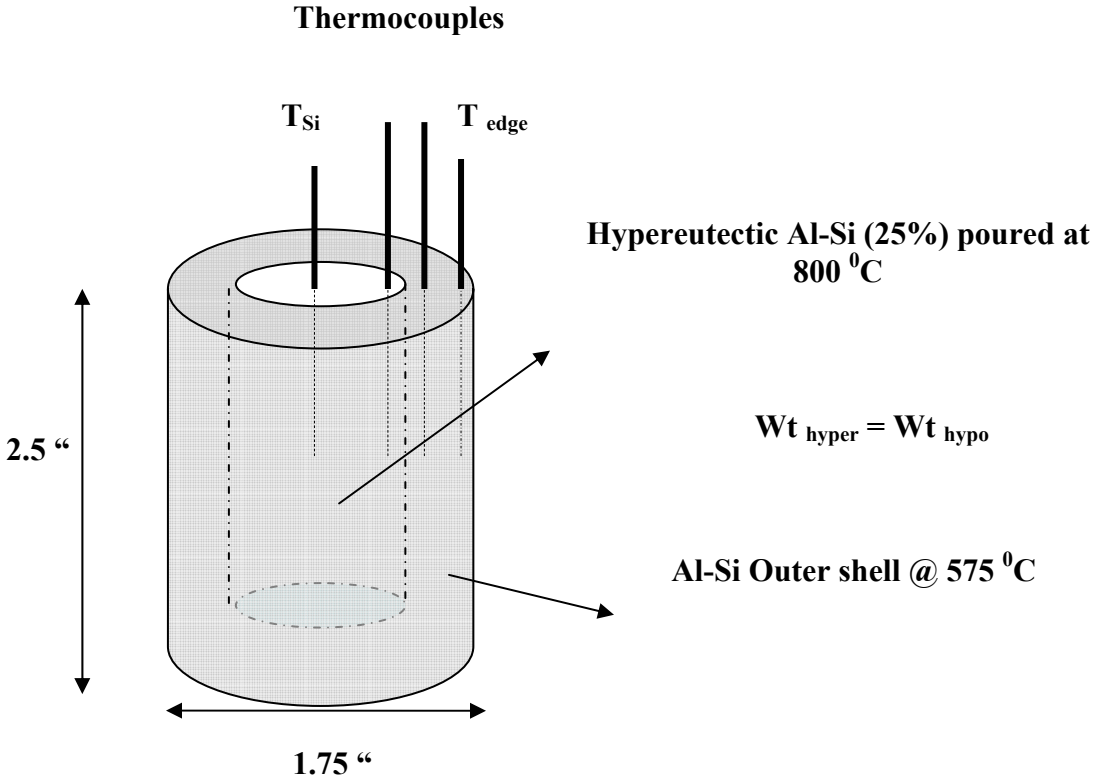

Figure 2: Schematic of the experiments performed to observe the thermal profile during the mixing of hypereutectic Al-Si alloy with a hypoeutectic Al-Si alloy.

Figure 3 shows the thermocouple data obtained as the Al-25% Si was poured into the Al-7% Si. The following information can be obtained from the thermocouple and the microstructural analysis:

1. The hypereutectic Al-Si alloy experiences a steep undercooling (T_{Si} in Figure 3), which should lead to the development of fine primary Si as shown in the microstructure observed in this region (Figure 4(a))
2. The thermocouple embedded into the Al-7% Si show a maximum temperature of 587 ^{0}C (which is a two phase region in an Al-Si binary phase diagram). However, microstructures in the vicinity of thermocouple T_{center}, show a predominantly Eutectic, as shown in Figure 4(b).
3. The thermocouple embedded at the edge of the cylinder (T_{edge}), also showing final temperature of 587 ^{0}C, but the microstructure is different as the region has a predominantly α-Al surrounded by eutectic (a typical two phase region).

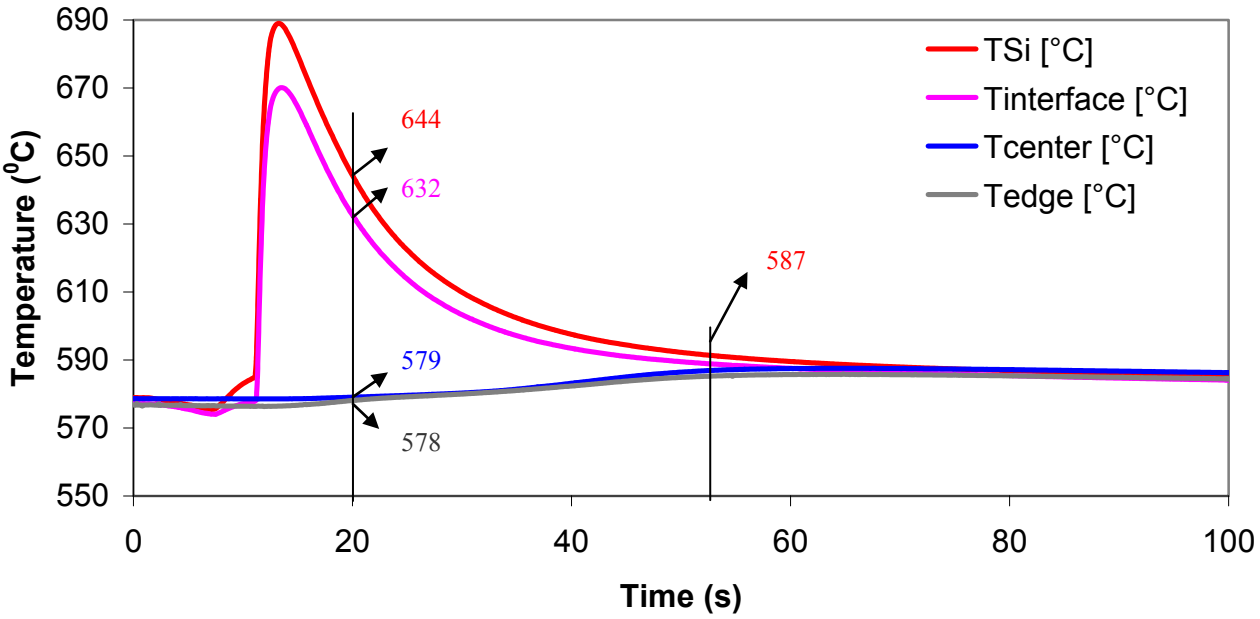

Figure 3: Thermocouple data obtained as the Al-25% Si is poured into the hollow cylinder of a Al-7% Si. The schematic and dimensions are shown in Figure 2.

(a) (b) (c)

Figure 4: Microstructures obtained at various locations in the cylinder:

a) At the center of the cylinder, which contained the Al-25%Si

b) At the center of the cylinder skin, which contained the Al-7% Si, showing a region which is predominantly Eutectic microstructure

c) At the edge of the cylinder, showing a region that is predominantly α-Al.

It can be clearly inferred from the thermal and microstructural analysis that;

- α-Al of the hypoeutectic Al-Si alloy, is in contact with an Al-Si liquid whose composition and temperature changes with time.
- α-Al of the hypoeutectic Al-Si alloy dissolves in the presence of the Al-Si liquid surrounding it to form eutectic liquid.

In this study we perform experiments to understand the dissolution kinetics of a-Al in the presence of Al-Si liquid with varying concentration of liquids. The studies are performed with the aid of thermodynamic data and microstructural analysis.

Design of experiments and results

J.M. Lommel and B. Chalmers laid the foundations for the various modes of dissolution of a solid held isothermally in a liquid. They presented and analyzed 3 different cases relating to the mass transfer across the solid liquid interface;

1. Diffusion in the liquid controls the rate of mass transfer (in stirred and unstirred liquid)
2. Surface reaction at the solid / liquid interface is rate controlling

The various equations describing the various cases are shown below:

Case 1: (Diffusion in a stirred and unstirred liquid is rate controlling)

Unstirred liquid $$z = 2\gamma\sqrt{D_L t} \qquad (1)$$

z = distance of the interface at time‘t’
D_L = diffusivity of solute in the liquid
γ = a function of C_0, C_L, and C_I. [Refer to Figure 5]

$$\sqrt{\pi}\gamma(\exp\gamma^2)[1+erf\gamma] = \frac{C_L - C_0}{C_I - C_L} \qquad (1.1)$$

Equation 2 is utilized to solve equation 1.

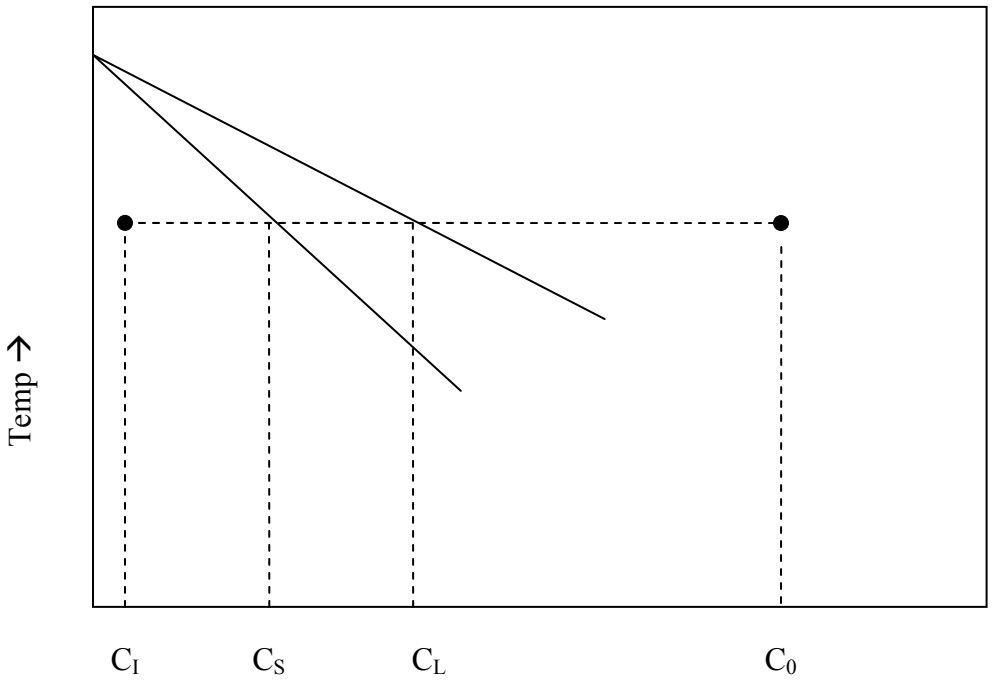

Figure 5: Schematic of the experiments performed by [17] to study the dissolution of a solid to a liquid

Stirred liquid: $$\dot{z} = \frac{D_L}{\delta}\ln[1+\frac{(C' - C_0)}{(C_I - C')}] \qquad (2)$$

Where; $\dot{z}$ = rate of interface movement
C' = concentration at the interface, between C_L & C_0, due to convection
δ = thickness of the boundary layer due to convection

Case 2: (Interfacial reaction is rate controlling)

$$\dot{z} = k[\exp(-\frac{Q_F}{RT})]*[C'-C_L] \Rightarrow \qquad \dot{z} = k(\Delta C)[\exp(-\frac{Q_F}{RT})] \qquad (3)$$

Where; $\dot{z}$ = rate of interface movement
ΔC = concentration difference at the interface
Q_F = activation energy

To study the predominant mode of dissolution of aluminum in a Al-Si liquid, the following experiments were conducted and the values of z (interface motion) were obtained as a function of time. The experiments consisted of heating Pure Al rod (99.99% Al) and a Al-Si liquid to a desired temperature. The Al-Si liquid contained 25% Si, and holding it for 3 hours at a lower temperature ensured a known final Si composition in the liquid (liquidus of the Al-Si phase diagram). The liquid was then drained into a new crucible, reheated to the desired temperature, and the rods of pure Al were dipped into the liquid. The rod was then dipped into the Al-Si liquid and held isothermally at various lengths of time to determine the rate of dissolution. Figure 6 is the schematic of the experiments performed to study the effect of Si on the dissolution kinetics of Al. The rods were then quenched in water at room temperature, and cleaned to remove traces of any sticking liquid and the interface (z) / weight loss measured. Figure 7 shows the actual photograph of the Al rods (before cleaning the surface) held at various times (pictures of Al rods dipped at 640 ^{0}C).

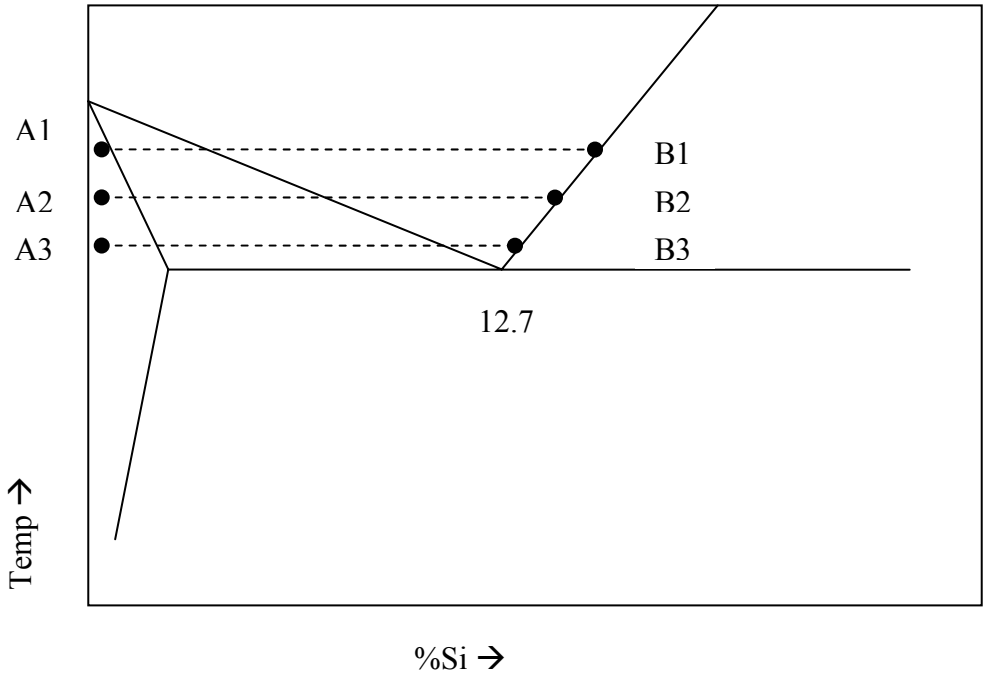

Figure 6: Schematic showing the various isothermal lines A1-B1 of Pure Al rods dipped into Al-Si liquid at various temperatures (to control the % Si in the liquid).

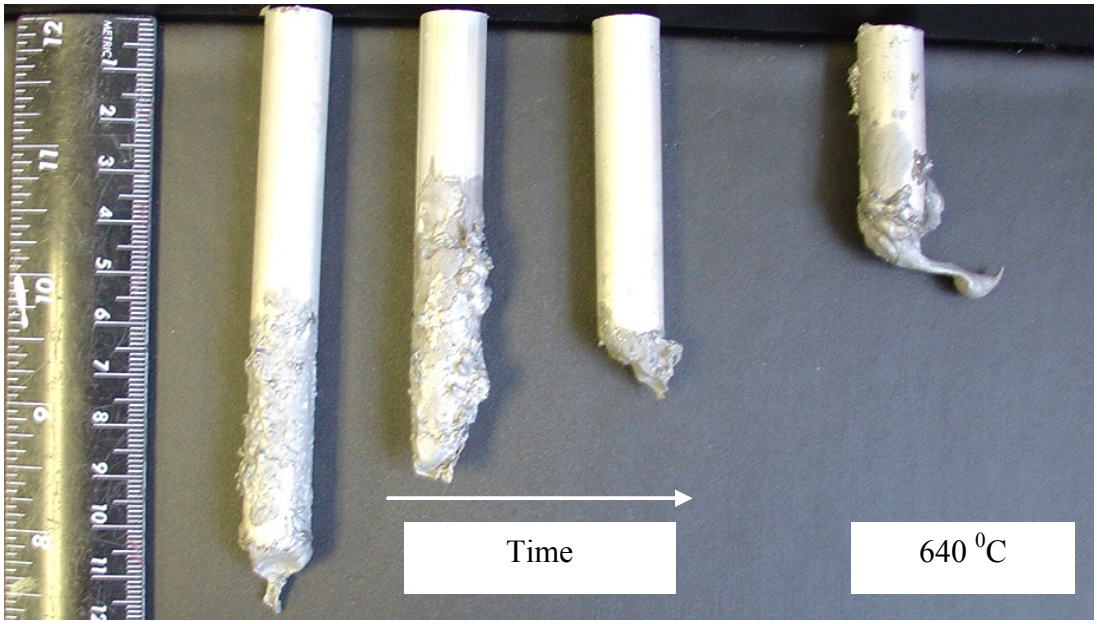

Figure 7: Photograph showing the dissolution of the rods at various times at a fixed temperature and increasing time.

It was however observed during the course of our experiments that, the Al rods corrode without a planar interface at lower temperatures. This made the calculation of z or the interface movement rather difficult. Figure 8 shows the classification of the various modes observed at lower temperatures (< 610 ^{0}C). The corrections were incorporated during the calculation of z, and by limiting the experiments to just one at 600 ^{0}C.

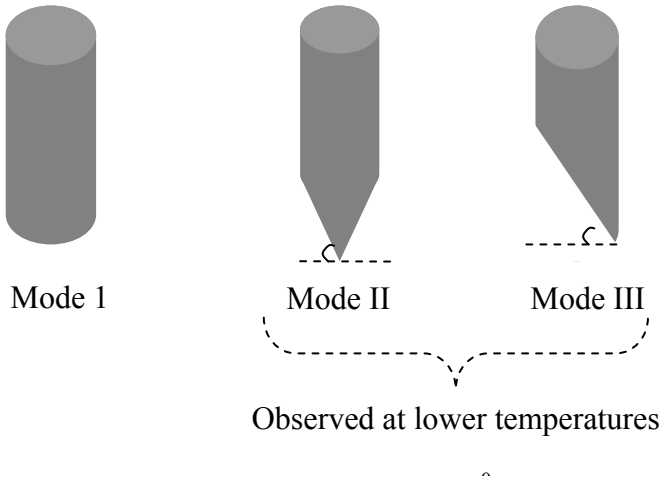

Figure 8: The predominant modes of surfaces of the cylinders observed after dissolution. The surface area was measured to calculate the flux of Al from the cylinder into the liquid.

Figure 9 shows the measured interface movement of the Al cylinder as a function of time at 640 ^{0}C. Similar data was obtained for various temperatures.

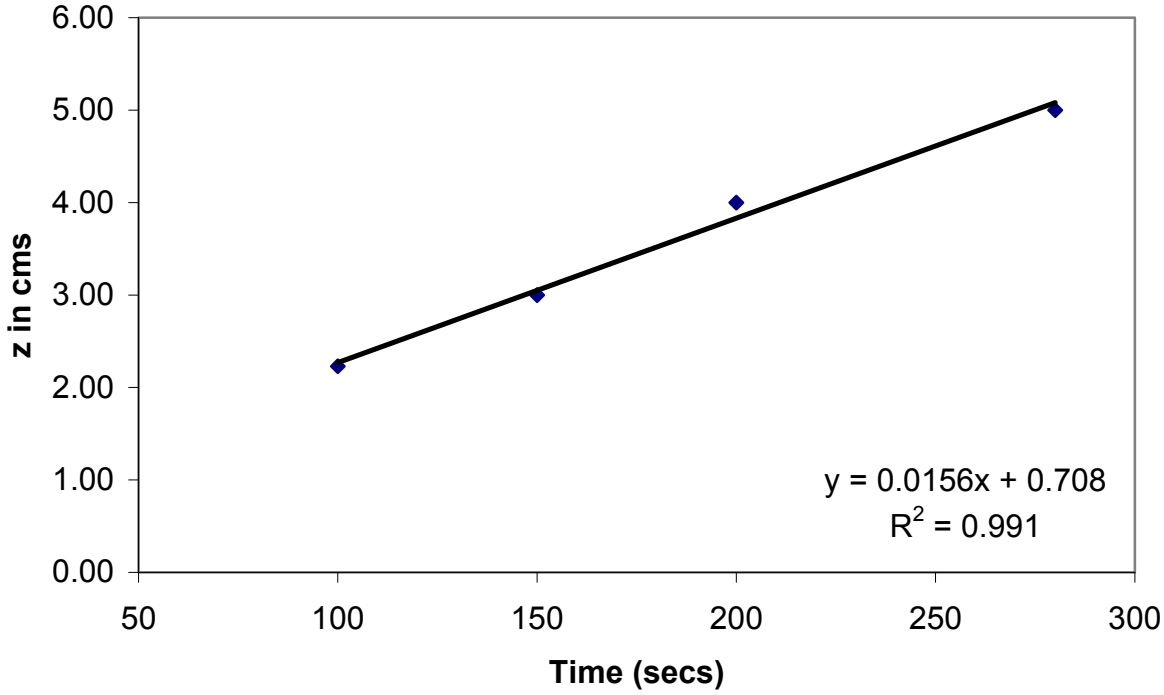

Figure 9: Interface movement as a function of time at a temperature (here 640 ^{0}C).

Diffusion or Interface reaction?

To ascertain the mode of dissolution, equation 1 was verified by calculating the theoretical data obtained from literature. Table 1 shows the values of C_L, C_0, and the calculated values of γ. A plot of z and for various values of t is shown in Figure 10 (equation 1).

Table 1: Values of various parameters utilized by equation 1.

Temperature (^{0}C)	C_0	C_L	γ by Iteration
600	14.05	9.44	0.21
620	15.34	6.51	0.43
640	16.67	3.39	0.74

The diffusion of Si in the Al-Si liquid was assumed to be in the order of 3 x 10^{-9} m^2/sec [18], and the values of z plotted as a function of time. Figure 10 shows one such plot at temperature 640 ^{0}C. Figure 10 clearly shows that there is a large difference in the observed interface movement compared to the distance the interface should have moved if it was to obey equation 1, or diffusion controlled.

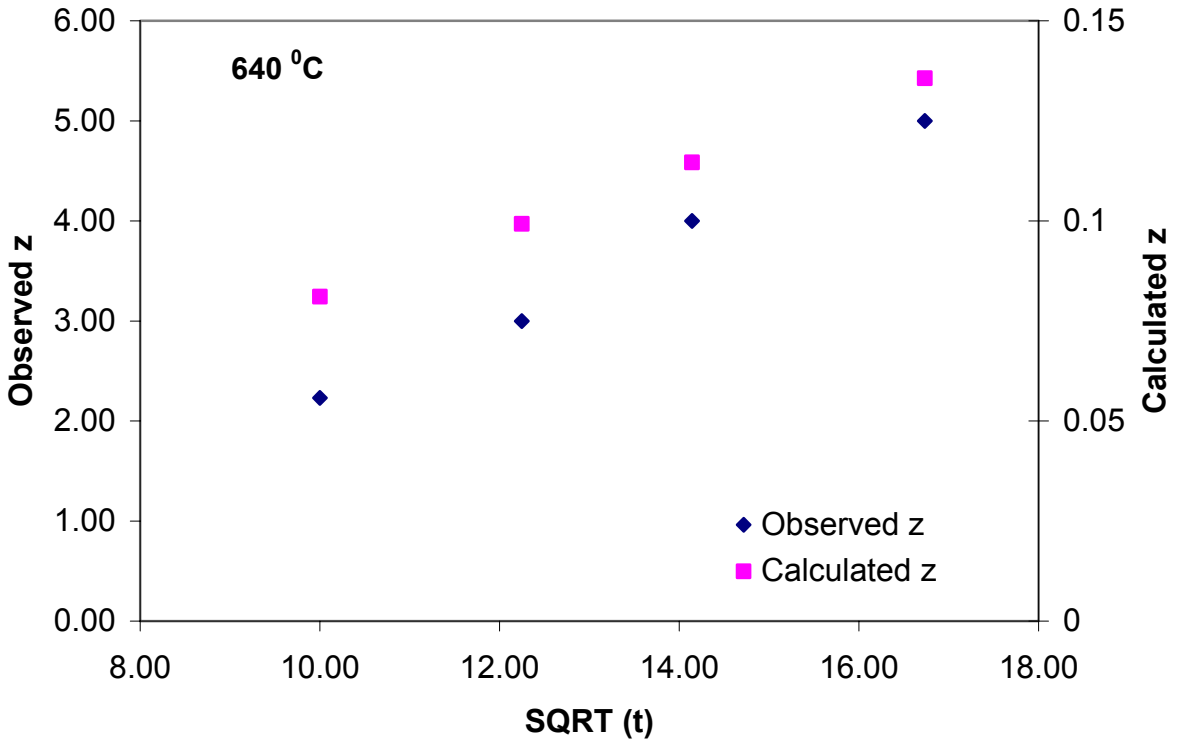

Figure 10: Figure showing the observed interface movement and the calculated interface movement if the process of dissolution was a diffusion controlled process. Clearly, the observed rate is many orders of magnitude higher than predicted by theory.

Figure 10 clearly shows that the interface motion is not diffusion controlled, and hence a plot of rate of interface motion at each different temperature ($\dot{z}$) was calculated from Figure 9 (slope or $\dot{z} = 0.0156$ for 640 ^{0}C from Figure 9). $\dot{z}$ at different temperatures were then plotted as a function of $\frac{1}{T}$. Figure 11 shows the slope, $\dot{z}$ versus $\frac{1}{T}$ for experiments performed. The data was fitted with an exponential curve to calculate the activation energy. From Equation (3) & Figure 9;

$$\dot{z} = k[\exp(-\frac{Q_F}{RT})]*[C_L - C_0] \; = \; 54367*[\exp(-\frac{13783}{T})]$$
$$\Rightarrow Q_F = 27.3 kcal/mol.K$$

A similar value of 30 kcalmol^{-1}K^{-1} was obtained by Craighead for the Al-Si alloy system [from 17]. Lommel et al [17], state that as there is an associated change in the driving force with temperature, due to the increased difference in (C_0-C_L), could lead to the process being diffusion controlled rather than a reaction controlled. The absence of chemical potential data for the Al-Si system during the late 1950's, did not permit them to examine the mass transfer in direct relationship to chemical potential difference or to make the necessary corrections to the activation energy Q_F, due to the increased difference in the (C_0-C_L) at higher temperatures.

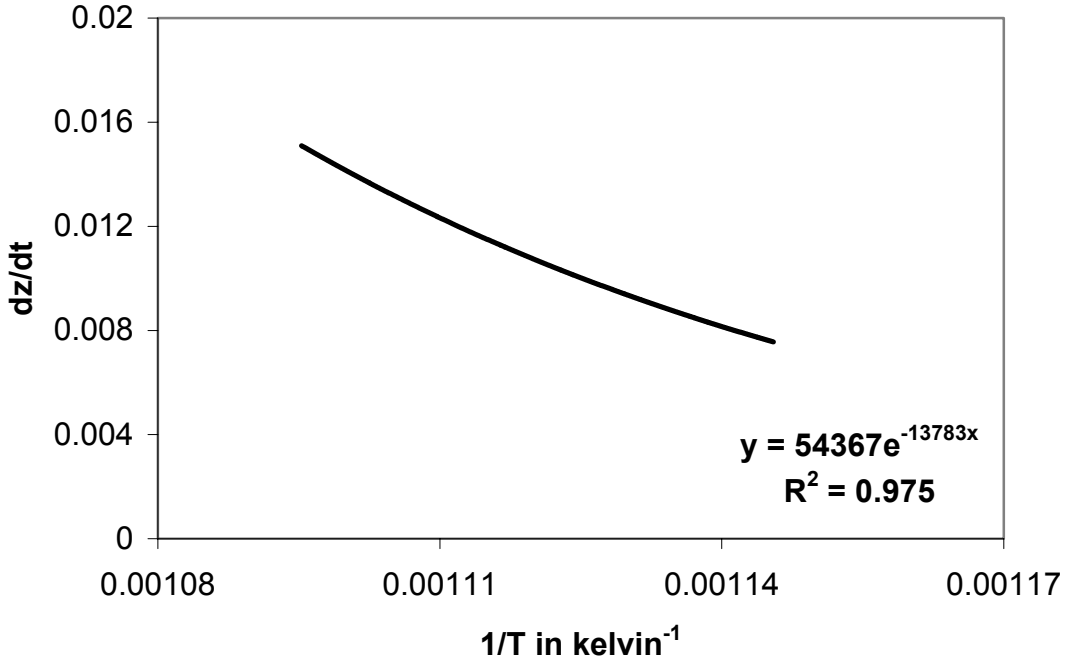

Figure 10: Rate of interface movement as a function of temperature.

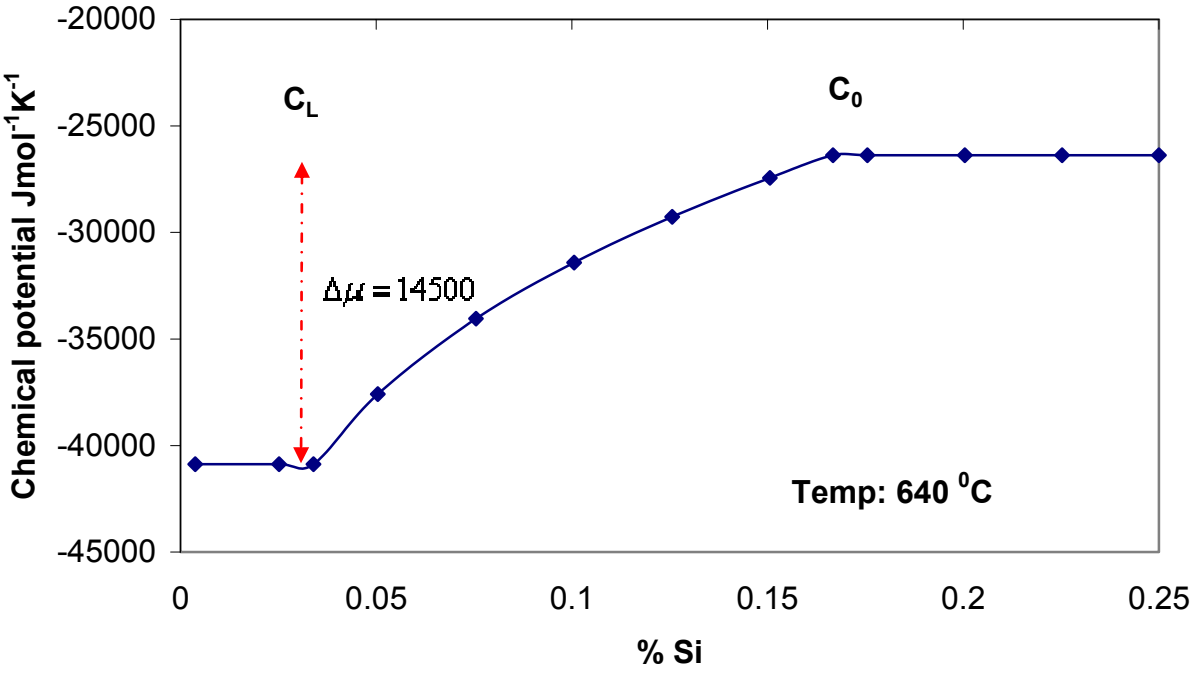

Figure 11: Chemical potential of Si with increasing Silicon percentage at 640 ^{0}C. The difference in free energy $\Delta\mu$ is the driving force for the Si atoms to transfer into the solid.

In this study we utilized PANDAT® and Thermo-calc, to calculate the chemical potential difference or the driving force for the Si atoms to transfer into the solid and lead to a reaction at the solid-liquid interface. Figure 11 shows the chemical potential of Si with varying percentages of Si at 640 ^{0}C obtained from PANDAT® / Thermo-calcData. Figure 12 shows the chemical potential difference as a function of various (C_L-C_0) (from Figure 11).

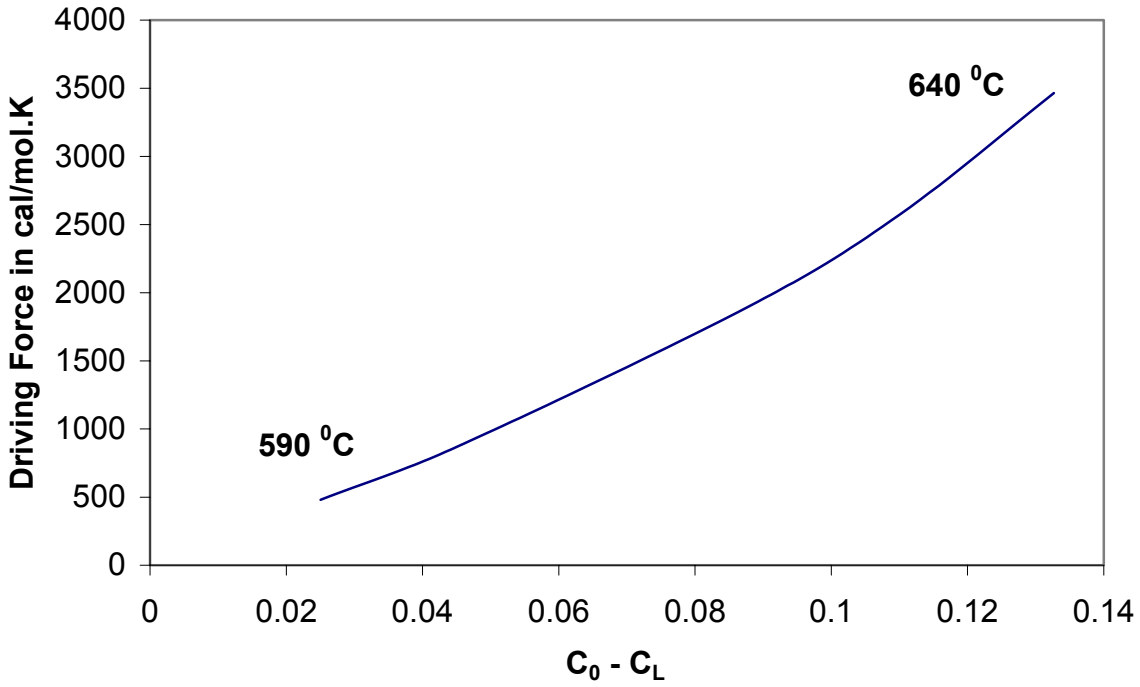

Figure 12: Chemical potential difference or driving force (from Figure 11) as a function of composition difference (C_L-C_0) between the liquidus and the composition of the interface, which is assumed to the bulk liquid.

Clearly, there is an increased driving force at increasing temperatures as predicted by Lommel et al [17], however it is only 10% of the activation energy (Q_F). A correction in the activation energy, by subtracting the driving force due to the difference in the composition leads to values ranging from 23 – 26 kcalmol^{-1}k^{-1}.

Conclusions

It has been observed that the dissolution of Al in Al-Si liquid is an interfacial reaction. Recent experiments elucidated the fact that the dissolution of the aluminum in the Al-7%Si liquid, was controlled by an *interfacial reaction* rather than by a diffusion process. The activation for the interfacial reaction is in the range of 23 – 26 kcalmol^{-1}k^{-1}.

References

1. K. Schneider "Aluminum casting alloys properties – Improvements by grain refinement", AFS transactions, 68 (1960), 176 – 181.

2. K.A Jackson, Liquid Metals and Solidification, ASM, Ohio, (1958), pp 17.

3. Wang Ru-yao, Lu Wei-hua, L.M Logan, "Growth morphology of primary Silicon in cast Al-Si alloys and the mechanism of concentric growth", Journal of Crystal Growth, Volume 207, pp 43 -54 (1999).

4. P.H. Shingu and J.I. Takamura, "Grain size refining of primary crystals in hypereutectic Al-Si and Al-Ge alloys", Metallurgical Transactions, 1 (1970), 2339 – 2340

5. N. Tenekedjiev and J.E. Gruzleski, "Hypereutectic aluminum silicon casting alloys – A review", Cast Metals, Vol. 3,(1990), 96 – 105

6. Ho, C.R. and B. Cantor, Heterogeneous nucleation of solidification of Si In Al-Si and Al-Si-P alloys. Acta Metallurgica et Materialia, 1995, 43(8): p. 3231-3246.

7. W. Thurry and H. Kessler, "An Effective Method of Grain Refining for Hypereutectic Aluminum-Silicon Alloys", Light Metals, 1956. 19(July): p. 225.

8. F.L.Arnold and J.S.Prestley., Hypereutectic Aluminum-Silicon Castings Alloys Phosphorus Refinement, AFS Transactions, 1961. 69: p. 129 - 137.

9. J.J. Lee, H.I. Lee and M.I. Kim, "Formation of Spherical Primary Silicon Crystals During the Semi solid Processing of Hypereutectic Al-15.5 wt% Si Alloy", Scripta Metallurgica, 1995, Volume 32, No. 12, pp. 1945 – 1949.

10. "Hypereutectic Al-Si Based Alloy with a Thixotropic Microstructure Produced by Ultrasonic Treatment", Materials and Design, 1997, Volume 18, No 4/6, pages: 323 – 326.

11. C. M. Chen, C. C. Yang and C. G. Chao "Thixocasting of hypereutectic Al–25Si–2.5Cu–1Mg–0.5Mn alloys using densified powder compacts", Materials Science and Engineering A, Volume 366, Issue 1, 5 February 2004, Pages 183-194.

12. P. Kapranos et al., "Thixoforming of an automotive part in A390 hypereutectic Al–Si alloy", Journal of Materials Processing Technology, Volume 135, Issues 2-3, 20 April 2003, Pages 271-277.

13. P. J. Ward et al., "Semi solid processing of novel MMC's based on hypereutectic aluminum-silicon alloys", Acta Materialia, Volume 44, Issue 5, May 1996, Pages 1717-1727.

14. J.A. Yurko, R.A. Martinez and M.C. Flemings, "SSR^{TM}: The spheroidal growth route to semi solid forming", Paper # 2-1in the Proceedings of the Eighth International Conference on Semi solid Processing of Metals and Alloys, Limassol, Cyprus, September 2004; published by NADCA, Wheeling, Illinois.

15. Tatsuya Ohmi et al, "Formation of fine primary silicon crystals by mixing of semi solid slurry of hypoeutectic Al-Si alloy and phosphorus-added hypereutectic Al-Si alloy melt", Journal of the Japan Institute of Metals, v 58, n 3, Mar, 1994, p 324-329.

16. Deepak Saha, R. DasGupta and D. Apelian, "Semi solid Processing of Hypereutectic Alloys", AFS Transactions, 2004, Vol. 112, 04-57.

17. J.M. Lommel and B. Chalmers, "The isothermal transfer from solid to liquid in metal systems", Transactions of the metallurgical society of AIME, June 1959, Vol. 215, pp. 499 – 508.

18. Young Du et al, "Diffusion coefficients of some solutes in fcc and liquid Al: Critical evaluation and correlations", Material Science and Engineering A, 2003, A363, pp. 140-151.

Appendix I

Consider a system shown in **Figure 33** which shows a system held isothermally at some temperature T, wherein a solid of composition C_{sol} is dipped into a liquid of composition C_{Liq}. Appendix I shows the mathematical reasoning adapted in Chapter 5.

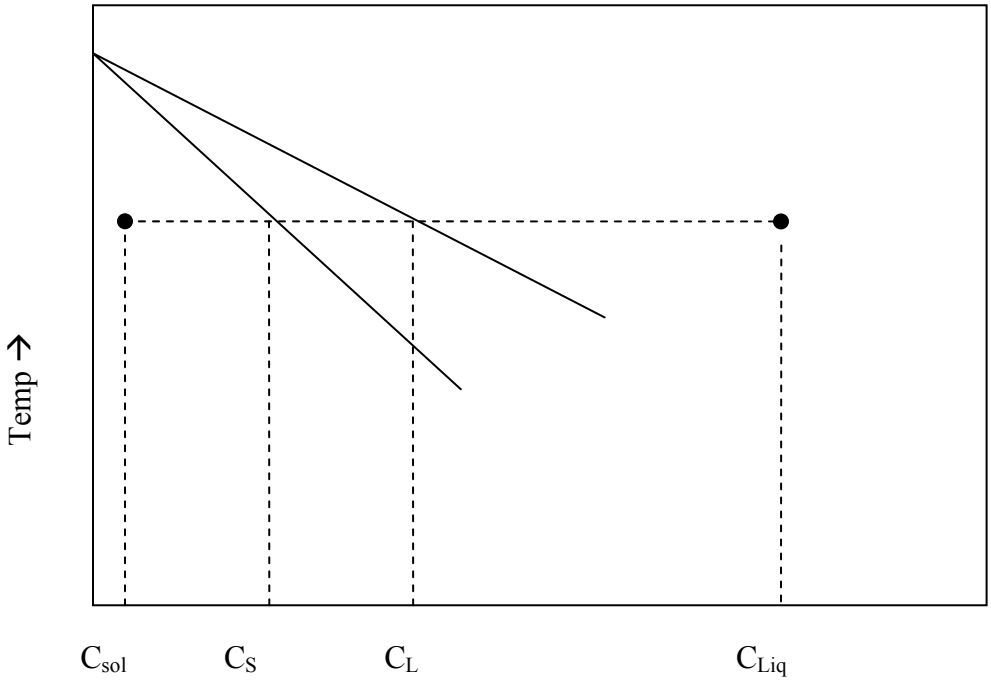

Figure 33: Schematic showing the various composition of solids and liquids when a solid of composition C_{Sol} is dipped in a liquid of composition C_{Liq}.

The dissolution of the solid in a supersaturated liquid of composition of C_{Liq} can occur in various processes. **Figure 34** is a schematic showing the various processes.

Dissolution in a liquid with no stirring

The set of equation defining the mass flow of the solute from the solid into the liquid is provided by Fick's as shown below;

In the liquid, the solute is removed by diffusion

$$D_L \frac{\partial^2 C_1}{\partial x^2} = \frac{\partial C_1}{\partial t} \qquad x < z \qquad (1)$$

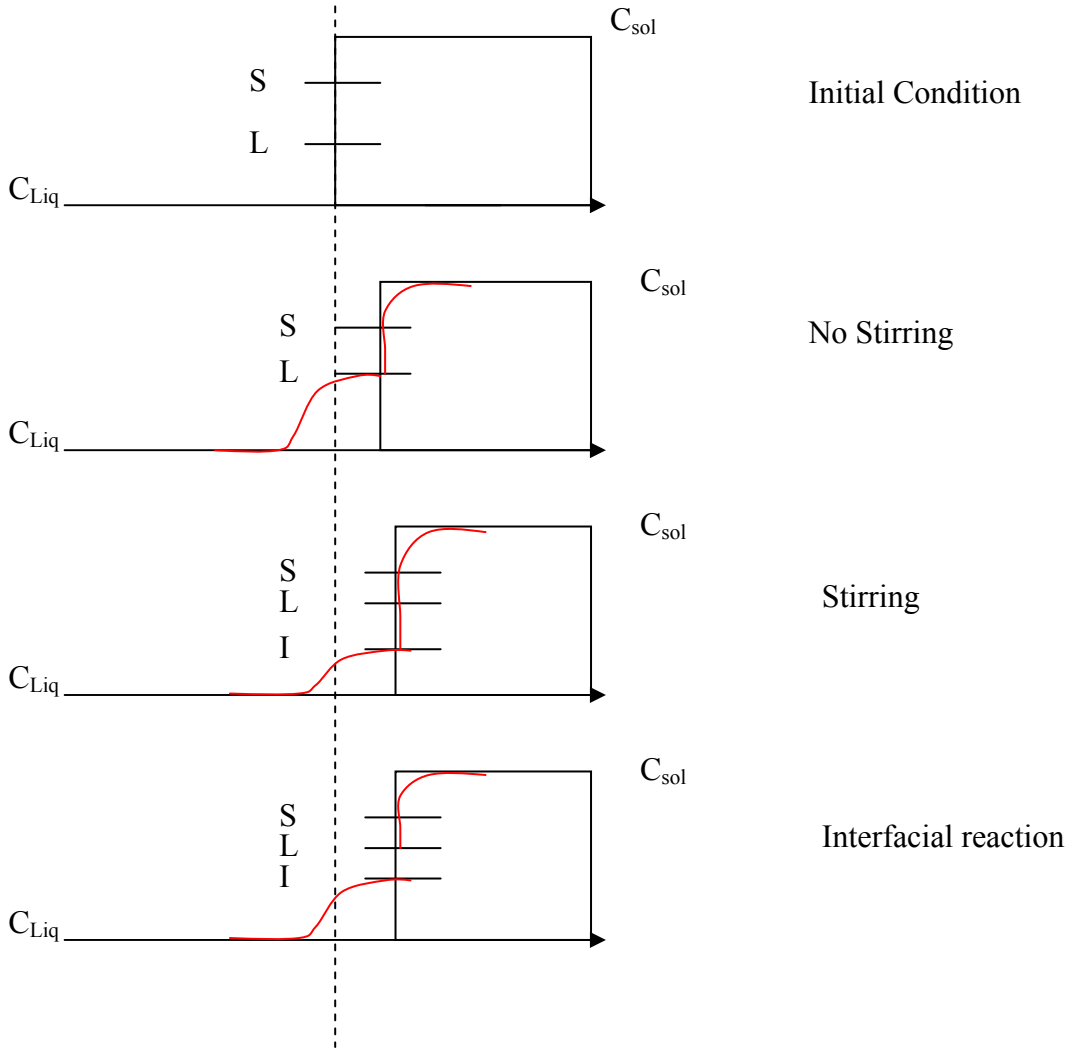

Figure 34: Various paths for the dissolution of the solid phase in the supersaturated liquid

In the solid, the solute is removed by diffusion and should satisfy the boundary condition

$$D_S \frac{\partial^2 C_2}{\partial x^2} = \frac{\partial C_2}{\partial t} \qquad x > z \qquad (2)$$

Boundary conditions

At the interface (x=z) $C_1 = C_L$ & $C_2 = kC_L$ (3a)

From Phase diagram $C_S = kC_L$ and K is the partition coefficient

At $x = 0$; $C_1 = C_{Liq}$ (3c)

At $x = \infty$; $C_2 = C_{sol}$ (3d)

Solution to equations 1 and 2 are given by standard solutions using separation of variables as shown below

Liquid
$$C_1 = C_{Liq} + A\left[1 + erf\frac{x}{2\sqrt{D_L t}}\right] \quad (4)$$

Solid
$$C_2 = C_{Sol} + B\left[1 - erf\frac{x}{2\sqrt{D_S t}}\right] \quad (5)$$

Solving for A at interface, using condition 3a at x=z;

Liquid
$$A\left[1 + erf\frac{z}{2\sqrt{D_L t}}\right] = C_L - C_{Liq} \quad (6)$$

Solid
$$B\left[1 - erf\frac{z}{2\sqrt{D_S t}}\right] = C_{Sol} - kC_L \quad (7)$$

For the equation to have a solution, z has to be a function of t and the authors [1] have assumed the following form to eliminate A and B. Also because the diffusion of solutes in liquids are in general many orders of magnitude (10^{-3} - 10^{-5}) higher than a solute in a solid (10^{-8} – 10^{-10}), it is convenient to take z as a function of D_L. Hence,

$$z = 2\gamma\sqrt{D_L t} \quad (8)$$

From equation 6 and 7:
$$\frac{A[1 + erf\gamma]}{B\left[1 - erf\gamma\sqrt{\frac{D_L}{D_S}}\right]} = \frac{C_L - C_{Liq}}{C_{Sol} - kC_L} = \Gamma(\gamma)$$

Where $\Gamma(\gamma)$ is some function of γ to calculate γ.

A simplified function of $\Gamma(\gamma)$ has been used to solve for γ as a function of known quantities. This function is

$$\Gamma(\gamma) = \sqrt{\Pi}\gamma(\exp\gamma^2)[1 + erf\gamma] = \frac{C_L - C_{Liq}}{C_{Sol} - kC_L} \quad (9)$$

The value of γ is calculated from equation 9, the rate of dissolution can be calculated utilizing equation 8 for known values of the composition.

Dissolution in a liquid with stirring

In the case of stirring, the equation 1 changes as now the solute has to diffuse across a boundary layer of thickness δ, this changes as a function of turbulence across the interface. The net result is the change in the composition of the liquid at the interface, (Stirring in **Figure 34**). The composition of the liquid is now C^I compared to C_I in the case without stirring. The steady-state solution to this problem is given by [1]; for a moving boundary; x=x' - vt, and partial differentiation and equation 1 and 2 give

$$\partial x = \partial x' \qquad \frac{\partial x}{\partial t} = -v$$

Liquid
$$D_L \frac{\partial^2 C}{\partial x'^2} + \dot{z} \frac{\partial C}{\partial x'} = \frac{\partial C}{\partial t} \qquad x' < 0 \qquad (10)$$

Solid
$$D_S \frac{\partial^2 C}{\partial x'^2} + \dot{z} \frac{\partial C}{\partial x'} = \frac{\partial C}{\partial t} \qquad x' > 0 \qquad (11)$$

Boundary conditions are

Liquid Side	C (δ, t)	=	C_{Liq}	&	C (0,t)	=	C^I
Solid Side	C(∞, t)	=	C_{Sol}	&	C(0,t)	=	C_S

The general solutions equations 10 & 11 with the above boundary conditions are [1].

$$C = C^I + \left(C_{Liq} - C^I\right)\frac{\left[1 - \exp(-\frac{\dot{z}x'}{D_L})\right]}{\left[1 - \exp(\dot{z}\frac{\delta}{D_L})\right]} \qquad x' < 0 \qquad (12)$$

$$C = C_{Sol} + \left(C_S - C_{Sol}\right)\exp(-\frac{\dot{z}x'}{D_S}) \qquad x > 0 \qquad (13)$$

Mass conversation $(\text{Mass out - Mass in})_{Solid}$ = (Diffusion in liquid),

$$\dot{z}(C^I - C_{Sol}) = D_L\left(\frac{\partial C}{dx'}\right) \qquad (14)$$

Substituting equation 12 into equation 14 gives;

$$\dot{z} = \frac{D_L}{\delta}\ln[1 + \frac{(C' - C_0)}{(C_I - C')}] \qquad (15)$$

Dissolution by surface reaction

In the kinetic theory of freezing, the net rate of motion of a solid-liquid interface is given by the difference between the rate of freezing and the rate of atoms leaving (rate melting) from the surface. It can be represented by a simple equation;

$$\dot{z} = R^A_{Melting} - R^A_{Freezing} \tag{16}$$

Where;

$$R^A_{Melting} = V_o N_S C v_S A^A_M G^A_M \exp(-\frac{Q^A_M}{RT}) \tag{17}$$

$$R^A_{Freezing} = V_o N_L C v_L A^A_F G^A_F \exp(-\frac{Q^A_F}{RT}) \tag{18}$$

V_o = Atomic Volume of atom A
N = Number of atoms per unit surface at the interface
C = Composition at the interface
v = Atomic vibration
A = Accommodation factor
G = Geometric Factor
Q = Activation energy

Combining equations 11 – 13;

$$\dot{Z} = V_o N_L C v_L A^A_F G^A_F \exp(-\frac{Q^A_F}{RT})\left[C_I(\frac{C_L}{C_S}) - C^I \right] \tag{19}$$

Equations 9, 15 and 19 are the final required equations used in Chapter 4 and Chapter 7.

References

1. J.M. Lommel and B. Chalmers, "*The isothermal transfer from solid to liquid in metal systems*", Transactions of the metallurgical society of AIME, June 1959, Vol. 215, p. 499 – 508.

Chapter 9. Globular primary phase in wrought alloys

Preface

Chapter 8 presents the experiments performed at WPI showing the formation of globular primary Al phase during the mixing of two liquids. The precursor liquids were held at different temperatures and having different compositions. The temperature was controlled and the mixing ratio of the liquids determined the final composition of the alloy. The results paved a new method for the formation of globular primary phase in Al based alloys. The results would have been impossible without the input, help and enthusiasm of Dr. Sumanth Shankar[*]. The results were published and is given in this chapter - "*Casting of Aluminum Based Wrought Alloys using Controlled Diffusion Solidification", **Metallurgical and Materials Transactions,** July 2004, Vol. 35A, No. 7, Pages 2174 – 2180.*

[*] Associate Professor at McMaster University, Canada, previously research associate MPI, WPI.

Metallurgical and Materials Transactions, *July 2004, Vol. 35A, No. 7, Pages 2174 – 2180*

Casting of Aluminum Based Wrought Alloys Using Controlled Diffusion Solidification

Deepak Saha, Sumanth Shankar, Diran Apelian, and Makhlouf M. Makhlouf

Metal Processing Institute
Worcester Polytechnic Institute
Worcester MA 01609

Aluminum based alloys containing elements such as silicon, copper, magnesium, and manganese are widely used in domestic, automotive and aerospace applications. These alloys are broadly classified into two groups: casting alloys and wrought alloys; the latter group of alloys cannot be used in the as cast condition because they develop hot tears during solidification and are shaped by rolling, drawing, or forging, etc. Of the two groups of aluminum-based alloys, the wrought alloys are the most widely used in aerospace applications because of their superior properties, particularly their high strength to weight ratio and their resistance to corrosive environments. In many instances, however, it would be economically advantageous to cast wrought alloys directly into near-net-shape components. Hot tears initiate during various stages of solidification, as detailed by Eskin et al [1]. Quantitative details regarding hot tears, particularly analytical models that incorporate the details of hot tear formation are only now beginning to emerge. Nevertheless, it is generally accepted that hot tears originate due to the inadequate permeability of the dendritic network for the flow of the interdendritic liquid to take place, as well as the strength of the dendritic network as solidification proceeds, and shrinkage forces come into play. Consequently, alloys with large solidification ranges, higher eutectic liquid contents, and large as-cast grain sizes are more prone to hot tearing than others, and adjustments to alloy constitution and/or casting procedures that favorably change the effects of these characteristics may minimize the tendency of the alloy towards hot tearing during casting.

A novel and easy to employ method has been devised to allow casting of wrought alloys. The method is based on the concept of diffusion solidification that was introduced by Apelian and Langford in 1980[2] and later employed by Saha, Apelian and DasGupta in the processing of Al-Si semi solid alloys [3]. The difference between conventional solidification and diffusion solidification can best be explained with the aid of Figure 1[4]. During conventional solidification, as the alloy solidifies and its temperature drops, its composition changes down the iso-concentration line. Partitioning occurs, and two phases form, namely a solute-depleted solid phase and a solute enriched liquid phase. In this case, solidification time depends on the rate of

[4] Although a binary alloy is considered in this illustration, the concept extends to multi-component alloys.

heat extraction from the liquid. In contrast, during diffusion solidification, two phases, namely a solute-rich liquid phase and a solute-depleted solid phase, both held at the same temperature (i.e., both on an isothermal line in the phase diagram), are brought into contact with one another so that solute diffuses down the solute concentration gradient from the liquid phase to the solid phase. Solidification proceeds as the liquid loses solute and therefore depends on the rate of diffusion of the solute atoms. Consequently, in diffusion solidification, solidification time is independent of the size of the casting.

Controlled Diffusion Solidification (CDS) relies on mixing two precursor liquid alloys of *precisely controlled chemistry and temperature* in order to produce a predetermined alloy composition. The final temperature of the resultant alloy is aimed at a temperature that is a few degrees below its liquidus temperature, and therefore contains some fraction solid that allows fast, copious nucleation of the solid phase from the liquid. Consequently, the resultant alloy solidifies over a short temperature range and has a non-dendritic microstructure that minimizes its tendency towards hot tearing and makes it more amenable to casting operations, rather than the predominantly dendritic microstructure that is typical of casting alloys. Because the resultant alloy solidifies over a short temperature range, the CDS process is most suited to die casting operations where the residence time of the alloy in the shot sleeve[5] is less than 5 seconds. The average cooling rate in the shot sleeve of a typical cold chamber die casting machine is 2.5-3°C/s, and since most wrought alloys have a coherency temperature that is 7-10°C below the liquidus temperature, the alloy begins to stiffen after 2-3 seconds in the shot sleeve. Given the high pressures involved in die-casting operations, a melt under these conditions should easily flow and fill the die cavity. It should be noted however that the CDS method is not restricted to die casting operations. Making use of the thermal insulating characteristics of sand and foam together with strategically located heaters in the molds will allow wide operation windows for these casting processes.

The following paragraphs demonstrate the CDS method in the production of various wrought aluminum-based alloys.

Casting of 2014 alloy

The CDS method was used to cast 2014 alloy having the following nominal composition:

Cu (wt.%)	Minor elements[6]	Al
4.4	2.0	Remainder

Table I shows the chemical analyses, weight fractions, and temperatures of the precursor liquid alloys. Precursor liquid alloy #1 and precursor liquid alloy #2 were poured in a crucible and allowed to mix naturally while they air-cooled. The chemistry of the resultant solidified alloy was measured using spark emission spectroscopy and the microstructure of polished

[5] The shot sleeve of a die casting machine is where a "shot" of alloy is poured before it is pushed under high pressure into the die cavity.

[6] Predominantly Mg, Si, and Mn.

metallographic samples taken from the solidified alloy was examined using optical and scanning electron microscopy. These characteristics of the alloy were compared to the corresponding characteristics of standard 2014 alloy that was air-cooled but at a superheat.

Figure 2 shows the microstructure of the alloy produced *via* CDS; the concept of CDS is shown in Figure 2(c). In contrast, Figure 3 shows the microstructure of 2014 alloy cast in a ceramic crucible with a superheat of 50°C. Notice that the morphology of the α-Al grains in the casting produced *via* CDS is predominantly globular and that very few, if any, dendrites were observed throughout the microstructure. It should also be noted that the inter-dendritic liquid in the alloy produced *via* CDS is dispersed throughout the microstructure and envelopes the globular α-Al grains. Figure 4 compares the microstructure of 2014 alloy castings produced *via* CDS to the microstructure of 2014 alloy castings made in a steel mold using conventional casting methods solidified at different cooling rates and having different initial superheats. In contrast to the castings made using the conventional casting method, which contain numerous α-Al dendrites, α-Al dendrites are absent in the castings produced *via* CDS for all three cooling rates. Figure 5 compares cross sectional views of the microstructure for castings produced *via* CDS to those of 2014 alloy castings poured in a steel mold using conventional casting methods. The extent of "*piping*" as indicated by the depression at the top surface of the castings should be noted. The improved liquid feeding characteristics in the casting produced *via* CDS can clearly be seen (Figure 5), and one can note the reduced shrinkage, better feeding and improved yield.

Table I: Precursor Liquid Alloys' Chemistry, Weight Fraction, and Temperature for Casting 2014 Alloy using CDS.

Chemical analysis:	Precursor Liquid Alloy #1	Precursor Liquid Alloy #2*
Cu	33 wt.%	
Al	67 wt.%	~ 98 wt.%
Liquidus temperature (°C)	548	660
Weight fraction	~ 0.14	~ 0.86
Temperature (°C)	550	665
Liquidus temperature of 2014 alloy (°C)	648	
Maximum temperature of resultant alloy (°C)	646	

* Precursor Liquid Alloy #2 is commercially pure aluminum. It contains the following impurities: 0.5 – 0.8 wt% Fe, 0.1 - 0.5 wt% Mn, and 0.5 - 0.8 wt% Si.

The measured chemistry of the alloy produced *via* CDS was as follows:

Cu (wt.%)	Minor elements[7]	Al
4.57	1.5	Remainder

[7] Predominantly Si, Mg, and Mn from commercially pure aluminum.

Casting of 5056 alloy

Similarly, the CDS method was used to cast 5056 alloy, which has the following nominal composition:

Mg (wt.%)	Mn (wt.%)	Cr (wt.%)	Al
5.0	0.12	0.12	Remainder

Table II shows the chemical analyses, weight fractions, and temperatures of the precursor liquid alloys.

Table II: Precursor Liquid Alloys' Chemical Analyses, Weight Fractions, and Temperatures for Casting 5056 Alloy *via* CDS.

Chemical analysis:	Precursor Liquid Alloy #1	Precursor Liquid Alloy #2
Mg	35 wt.%	
Al	65 wt.%	~ 98 wt.%
Liquidus temperature (°C)	451	660.7
Weight fraction	~ 0.14	~0.86
Temperature (°C)	445	665
Liquidus temperature of 5056 alloy (°C)	636.8	
Maximum temperature of resultant alloy (°C)	638	

The measured chemistry of the alloy produced *via* CDS is as follows:

Mg (wt.%)	Mn (wt.%)	Cr (wt.%)	Al
4.8	0.15	0.02	Remainder

Figure 6(a) shows the microstructure of the casting produced *via* CDS, and Figure 6(b) shows the microstructure of 5056 alloy using conventional casting methods. Notice that, similar to the 2014 casting produced *via* CDS, the morphology of the α-Al grains in the CDS cast 5056 alloy is predominantly globular. It should also be noted that, similar to the 2014 CDS alloy, the inter-dendritic liquid in the 5056 CDS alloy is dispersed throughout the microstructure and envelopes the globular α-Al grains. The CDS microstructure, compared to the 5056 alloy cast in a ceramic crucible with a 15°C superheat shows a predominantly non-dendritic microstructure.

Casting of 7050 alloy

Again, similar to the 2014 and 5056 alloys, the CDS method was used to cast 7050 alloy, which has the following nominal composition:

Zn (wt.%)	Mg (wt.%)	Cu (wt.%)	Al
6.2	2.2	2.3	Remainder

Compared to 2014 and 5056 alloys, 7050 is an alloy with several alloying elements, and thus there are many possibilities for the precursor alloy liquids that can yield the resultant 7050 alloy chemistry. Table III shows one possible set of chemical analyses, weight fractions, and temperatures for the precursor liquid alloys.

Table III: Precursor Liquid Alloys' Chemical Analyses, Weight Fractions, and Temperatures for Casting 7050 Alloy *via* CDS.

Chemical Analysis	Precursor Liquid Alloy #1	Precursor Liquid Alloy #2
Cu	~ 24 wt.%	-
Mg	-	~ 2.65 wt.%
Zn	-	~ 7 wt.%
Al	76 wt.%	Balance
Liquidus temperature (°C)	589	634
Weight fraction	~ 0.10	~ 0.89
Temperature (°C)	592	640
Liquidus temperature of 7050 (°C)	630	
Maximum temperature of resultant alloy (°C)	628	

The measured chemistry of the alloy produced *via* CDS is as follows:

Zn (wt.%)	Mg (wt.%)	Cu (wt.%)	Al
6.7	2.2	2.5	Remainder

Figure 7(a) shows the microstructure of the alloy produced *via* CDS, and in contrast, Figure 7(b) shows the microstructure of 7050 alloy conventionally cast in a ceramic crucible with a superheat of 15°C. It should be pointed out that similar to 2014 and 5056 alloys produced *via* CDS, the morphology of the α-Al grains in the 7050 CDS alloy is predominantly globular and few dendrites are observed in the microstructure. Similar to the 2014 and 5056 castings produced *via* CDS, the inter-dendritic liquid in the 7050 CDS alloy is dispersed throughout the microstructure and envelopes the globular grains.

While the preceding examples demonstrate the Controlled Diffusion Solidification method for the production of wrought aluminum-based alloys belonging to the 2xxx, 5xxx, and 7xxx series, the technique is similarly applicable to all standardized wrought alloys, as well as to the production of non-standardized alloys. Finally, it should be mentioned that wrought alloys have been previously successfully cast with globular microstructures using semi solid metal processing techniques [4-6]; however, the Controlled Diffusion Solidification method described in this communication is much simpler to implement than semi solid metal processing techniques - whether they be thixocasting or rheocasting techniques [7-10]. Moreover, it is well documented that the use of grain refiners can reduce the tendency of some Al-based alloys to

form large dendrite clusters during solidification [], it is important to note that the CDS method accomplishes the same task efficiently without the additional cost of grain refiners. In summary, Controlled Diffusion Solidification (CDS) is a viable, economical route to casting aluminum based wrought alloys into near net shaped components. In addition to the enhanced mechanical properties commensurate with the chemistry of these alloys, the castings produced have a microstructure akin to that of semi solid processed materials with all its associated benefits. Major attractions of the CDS process are its simplicity, and the fact that only minimum changes to conventional casting operations are needed in order to adapt an existing operation to the production of castings comprised of wrought alloys. Equally attractive are the significant energy savings attained from the application of this technology. Moreover, the CDS method is adaptable to pressure-less casting operations as well as to casting operations in permanent and sand molds with minimal pressure assistance.

References

1. Eskin, D.G., Suyinto, and L. Katgerman, "*Mechincal Properties in the Semi solid State and Hot Tearing of Aluminum Alloy,".* Progress in Material Science, In Press, Corrected Proof, available on-line at http://www.sciencedirect.com/science/article/B6TX1-4991N9T-3/2/2e261c3483550d8bdbb9c1fdd23441b8.
3. G. Langford and D. Apelian, "*Diffusion Solidification,"* Journal of Metals, 1980, Vol. 32**,** Issue 9, page 28-34.
2. D. Saha, D. Apelian, and R. DasGupta, "*SSM Processing of Al-Si Alloys Utilizing the Concept of Diffusion Solidification*," *Proceedings of 22nd. International Die Casting Congress,* 2003. Indianapolis.
4. J. Dong, et al., *Liquidus semi-continuous casting, reheating and thixoforming of a wrought aluminum alloy 7075.* Materials Science and Engineering A, 2003, Vol. 345, Issue 1-2, page 234-242.
5. Kazakov, A.A., *Alloy compositions for semisolid forming.* Advanced Materials and Processes, 2000, Vol.157, Issue 3, page 31-34.
6. Yue, T.M., *Squeeze casting of high-strength aluminium wrought alloy AA7010.* Journal of Materials Processing Technology, 1997, Vol. 66, Issue 1-3, page 179-185.
7. Chen, C.Y., et al., *Thixoforging of aluminum alloys.* Materials Science and Engineering, 1979, Vol. 40, Issue 2, page 265-272.
8. Flemings, M.C., R.G. Riek, and K.P. Young, *Rheocasting.* Materials Science and Engineering, 1976, Vol. 25, page 103-117.
9. Rovira, M.M., B.C. Lancini, and M.H. Robert, *Thixo-forming of Al-Cu alloys.* Journal of Materials Processing Technology, 1999, Vol. 92-93, page 42-49.
10. Robert, M.H. and M. Adamiak, *Preliminary studies on the suitability of rheocast Al alloys for deep drawing.* Journal of Materials Processing Technology, 2001, Vol. 109, Issue 1-2, page168-173.

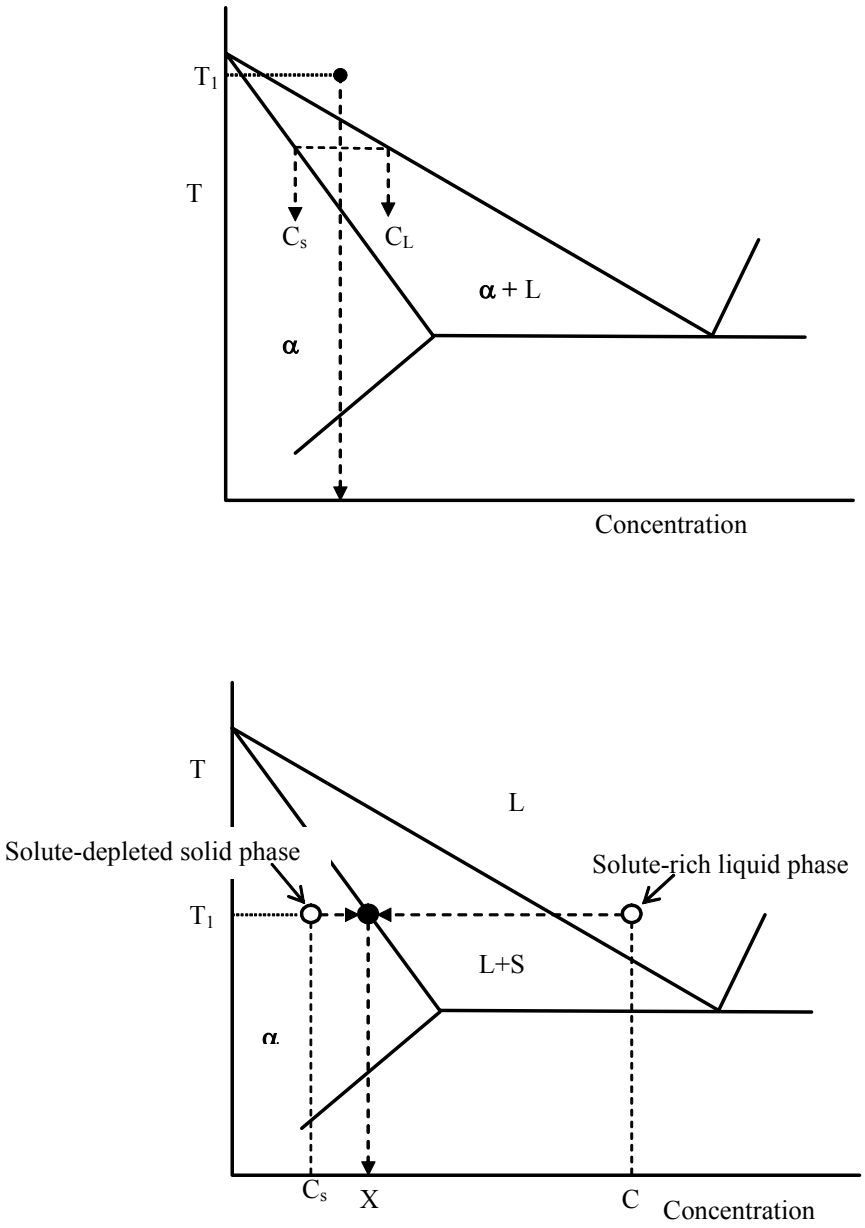

Figure 1: Schematic phase diagram of a binary alloy illustration (a) conventional solidification and (b) diffusion solidification. In (a), liquid alloy of composition X solidifies from temperature T_1; partitioning occurs during solidification leading to segregation of the solute, note that the solid phase has the average composition X. In (b), an amount f_s of the solute alloy of composition C_s at temperature T_1 is mixed with an amount f_L of a liquid alloy of composition C_L also held at T_1 such that $f_sC_s + f_LC_L = X$.

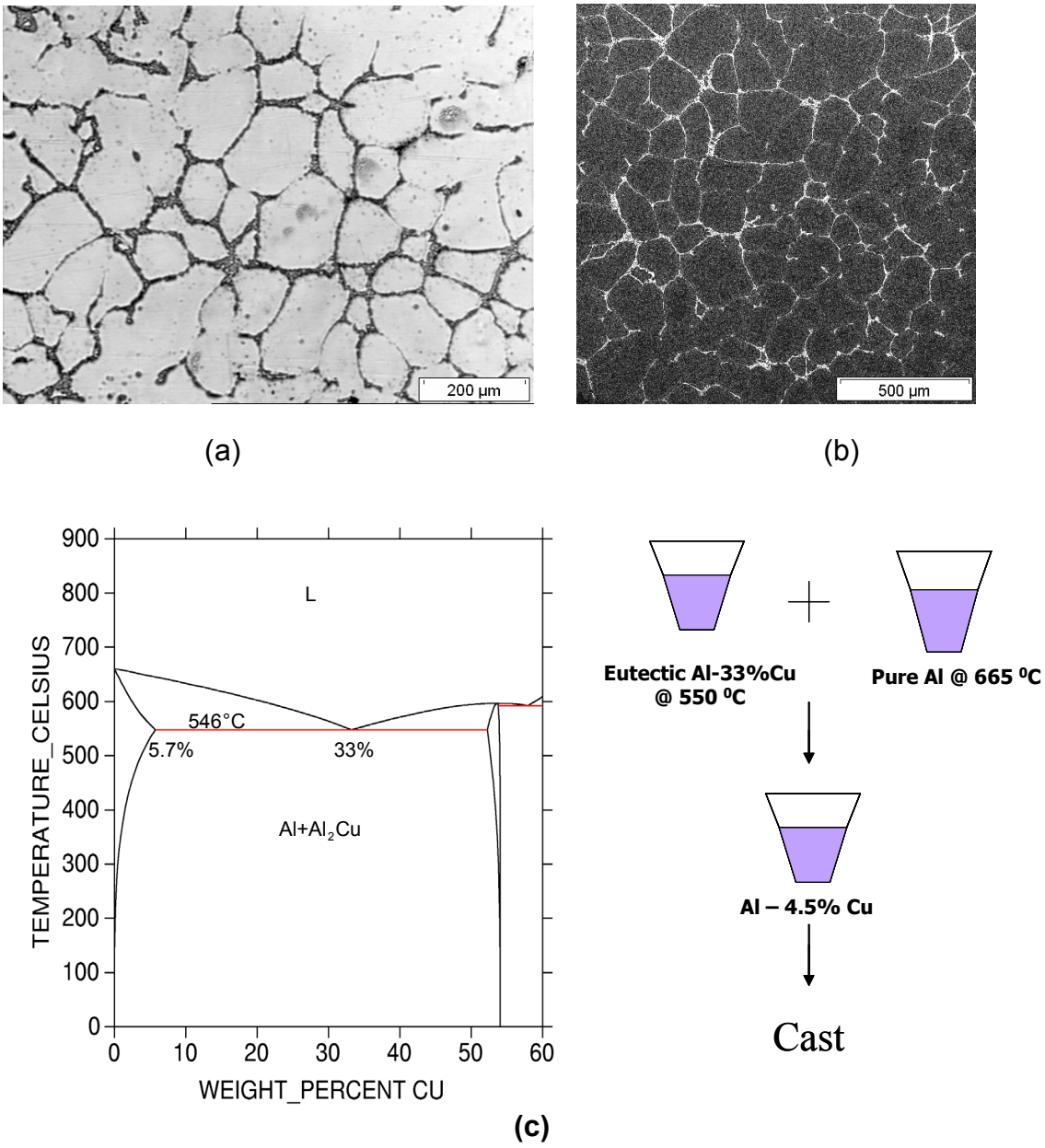

Figure 2: Micrographs of 2014 alloy cast using the CDS method;
(a) optical image of the final solidified structure,
(b) back scattered SEM image of the final solidified structure,
(c) schematic illustrating the concept of the CDS method.

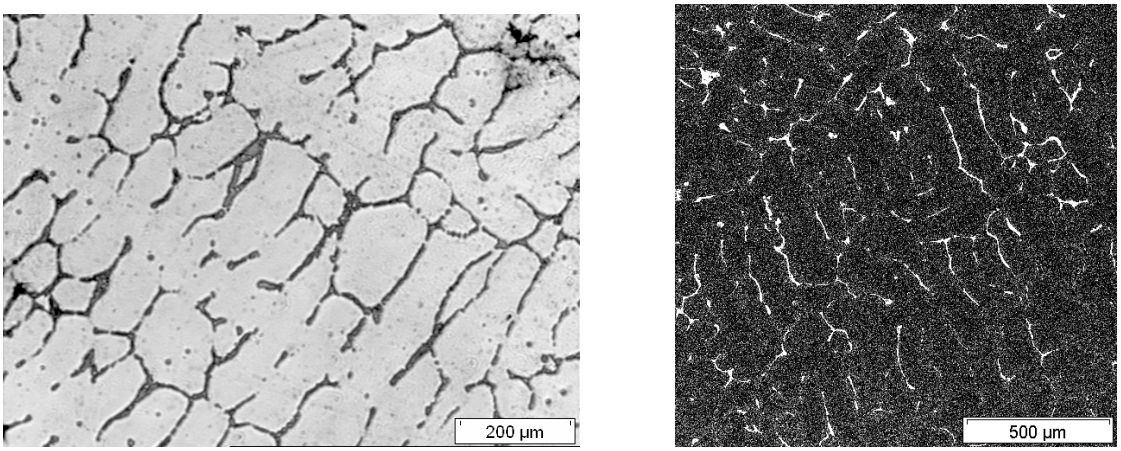

(a) (b)

Figure 3: Micrographs of 2014 wrought alloy in the as-cast condition, samples cast with 50°C superheat; (a) optical image of the final solidified structure,
(b) back scattered SEM image of the final solidified structure.

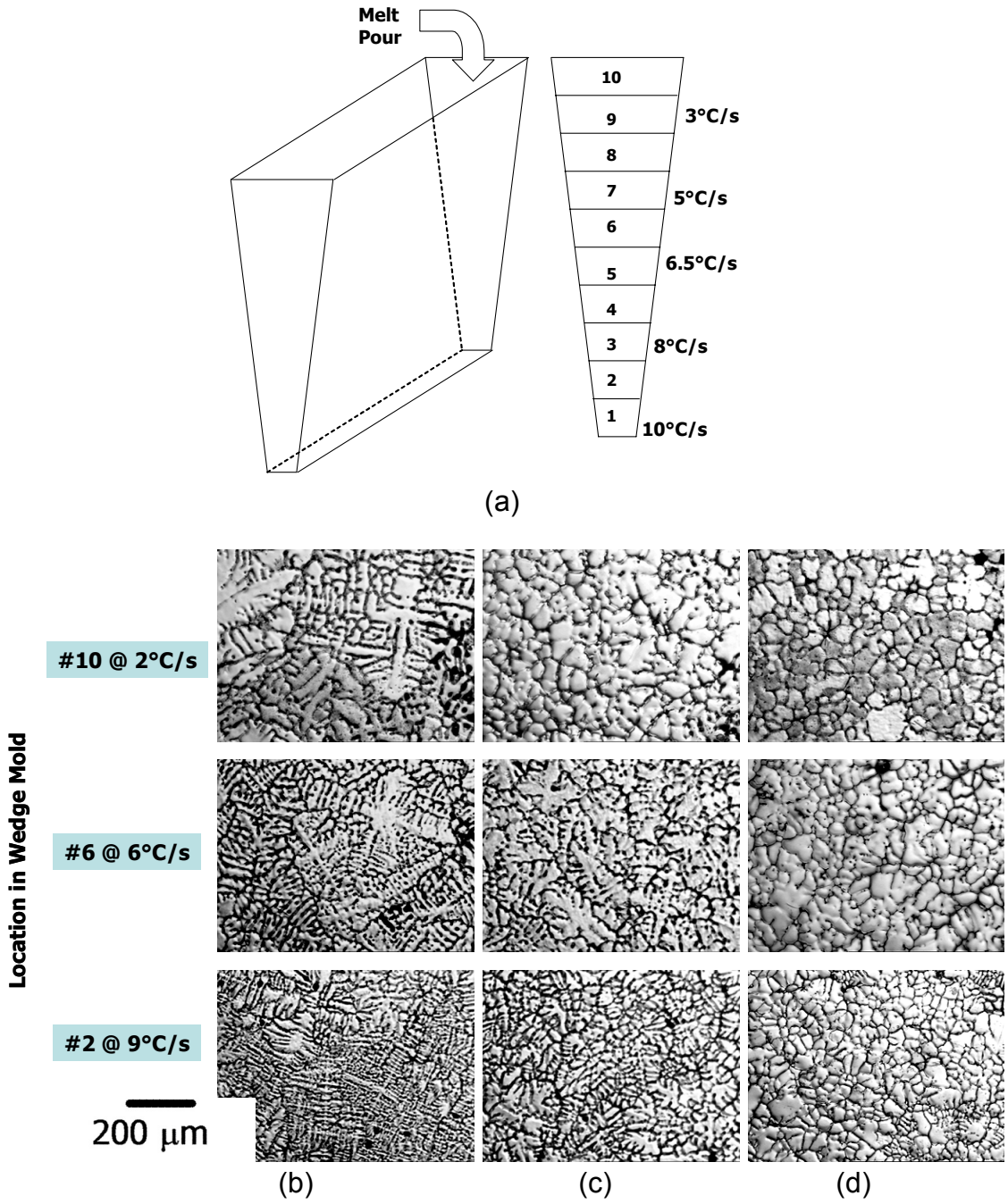

Figure 4: Representative microstructures at various positions in the wedge mould for 2014 alloy in the as-cast condition with varying degrees of superheat, and CDS approach;

(a) Schematic of the wedge mould and cooling rates obtained at different depths
(b) 2014 alloy poured with 50°C superheat,
(c) 2014 alloy poured with 5°C superheat,
(d) 2014 alloy produced using the CDS method.

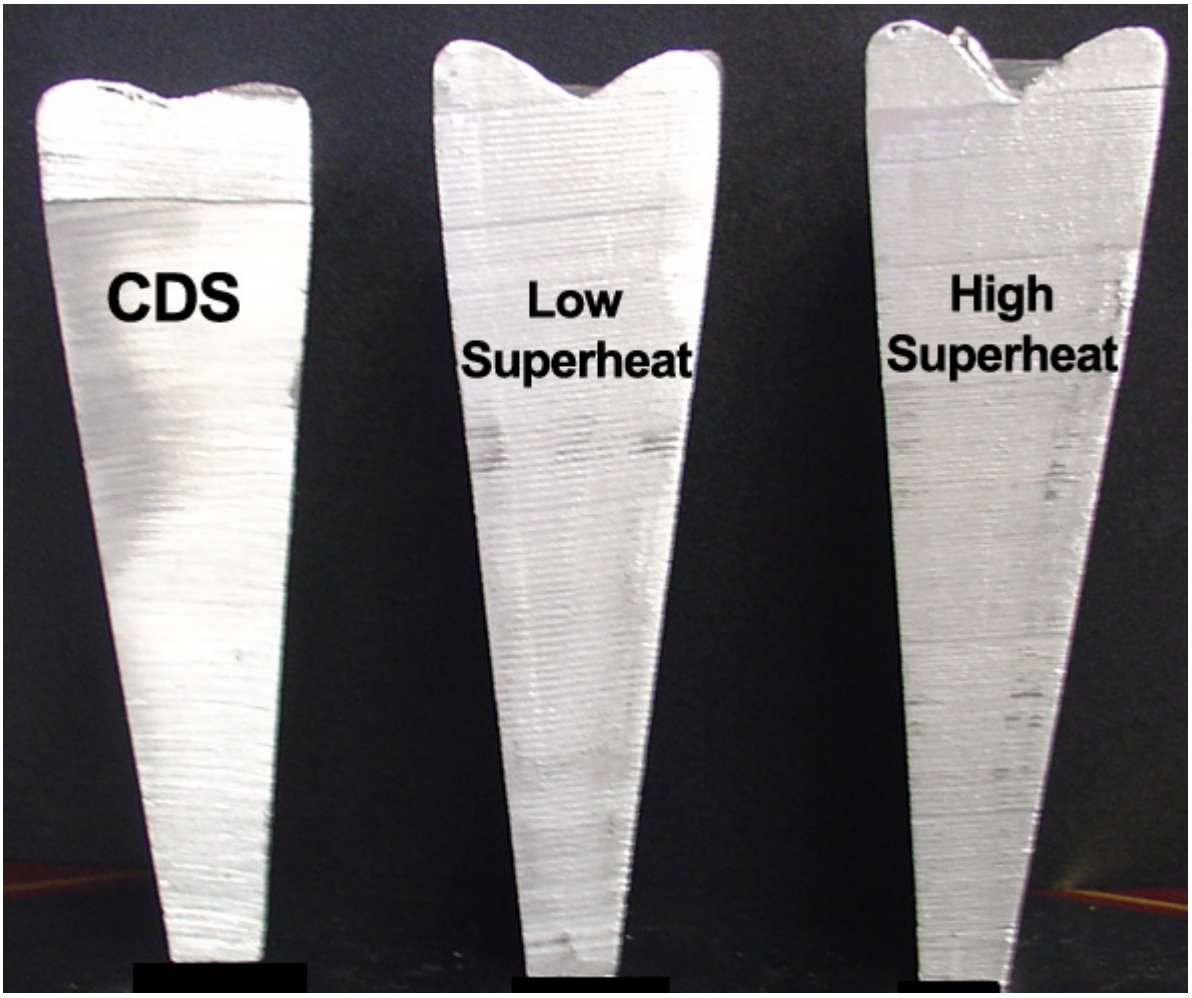

Figure 5: Formation of pipe in castings poured in the wedge mold shown in Figure 4
(a) 2014 alloy cast using the CDS method,
(b) 2014 alloy melted and cast with 5°C,
(c) 2014 alloy melted and cast with 50°C.

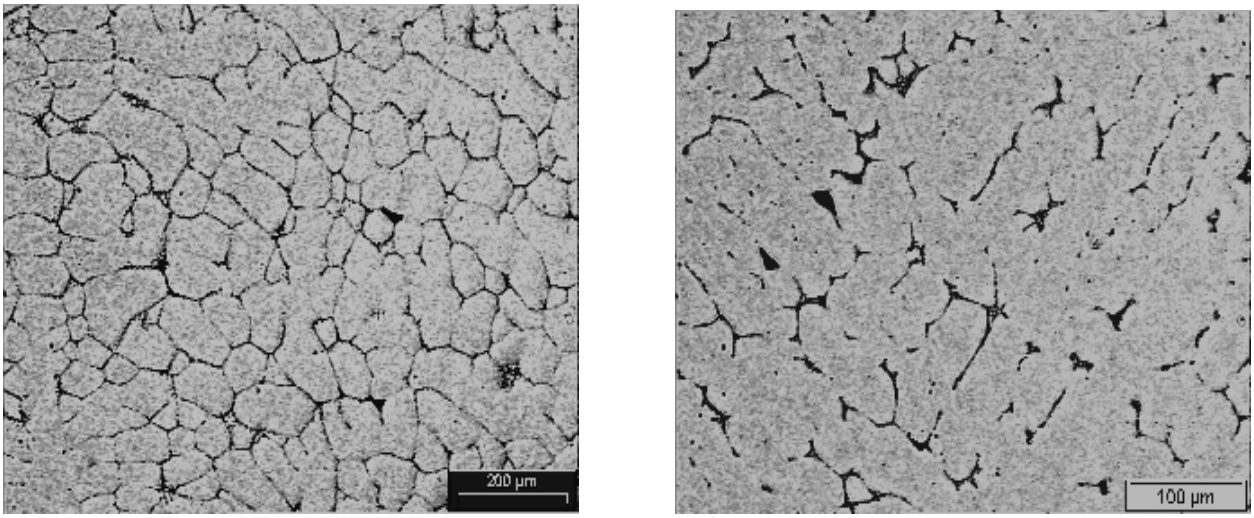

(a) (b)

Figure 6: Cast microstructures of 5056 alloy;
(a) CDS and air cooled in crucible,
(b) cast with 15°C superheat and air cooled in crucible.

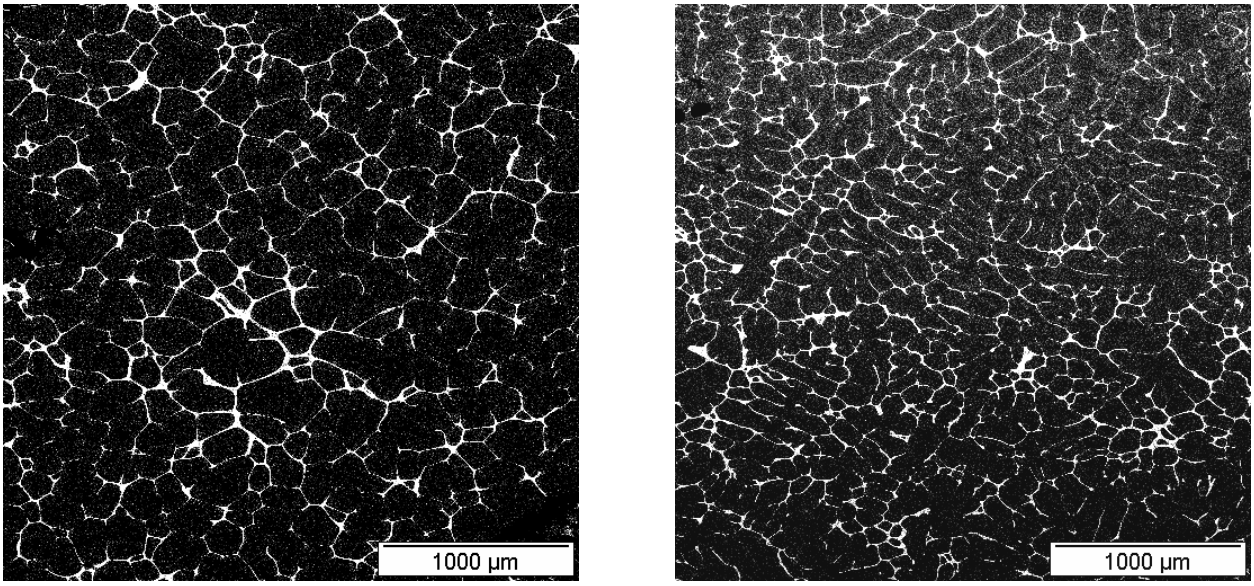

(a) (b)

Figure 7: Cast microstructures of 7050 alloy;
(a) CDS and air cooled in crucible,
(b) cast with 15°C superheat and air cooled in crucible.

Chapter 10. Mechanism of globular primary phase

Preface

This chapter details the thermodynamic and energy consideration for the formation of globular primary phase in Al based wrought alloys by the mixing of two liquids. The mechanism underlining this process is developed on the basis of free energy and liquid-mixing considerations. For the solid phase to nucleate and grow in a globular morphology, two criteria must be met:

- The two precursor alloys must be maintained at temperatures that are close to their respective liquidus temperatures,
- The difference between the solid / liquid interface energy when alloyed versus unalloyed must be $\sigma^{SL} - \sigma_A^{SL} > 0$, where σ^{SL} is the solid liquid interface energy in alloyed state and σ_A^{SL} is the solid liquid interface energy in pure state.

Additionally, the Gibbs free energy of the precursor alloys prior to mixing must be less than the Gibbs free energy of the resultant alloy at its liquidus temperature. Successful casting of wrought alloys *via* the Controlled Diffusion Solidification method is commensurate with the choice of precursor alloys that satisfy these conditions and is demonstrated by the results from controlled experiments. The manuscript given in this chapter has been submitted to Acta Materialia in Feb 2005.

Submitted to Acta Materialia in Feb 2005

Casting of Aluminum Wrought Alloys with a Globular Primary Phase using Controlled Diffusion Solidification

Deepak Saha, Sumanth Shankar, Makhlouf M. Makhlouf and Diran Apelian

Worcester Polytechnic Institute, Worcester MA 01609

Abstract

Aluminum-based wrought alloys are used extensively in the aerospace and automotive industries due to their high tensile strength and good ductility. Unfortunately, near net shape manufacturing of these alloys into usable components by means of conventional casting processes is not commonly practiced due to problems that are often encountered in casting these alloys, including excessive hot tearing during solidification and incomplete filling of mold cavities. A process has been developed to circumvent these problems and to allow sound castings of these alloys with a globular microstructure that is essentially free of dendrites. The process involves mixing two liquids of pre-determined composition and temperature, which are selected such that their combined free energy is lower than the free energy of the resultant alloy at its liquidus temperature. A mechanism based on free energy and liquid-mixing analyses is presented and the evolution of the globular microstructure in castings made *via* the new process is discussed and supported by results of controlled experiments.

Introduction

Aluminum-based wrought alloys, for example alloys that belong to the 2xxx series, the 3xxx series, the 4xxx series, the 5xxx series, the 6xxx series, and the 7xxx series are used extensively in the aerospace industry and the automotive industry due to their high strength to weight ratio, good ductility, and corrosion resistance. Unfortunately, it is not possible to cast these alloys directly into near net shape components because of problems that often occur during their solidification, including excessive hot tearing and incomplete filling of mold cavities resulting from the alloys' relatively high coherency temperature [1, 2]. Table I presents estimated coherency point for some of these alloys [3]. Note that in each case, the coherency temperature is very close to the liquidus temperature of the alloy. The high coherency temperature coupled with the large solidification range renders these alloys prone to hot tearing.

Table I. Coherency point of some aluminum-based alloys.

Alloy	Coherency point		Liquidus (°C)	$\Delta T = T_{Liquidus} - T_{Coherency}$
	Temperature (°C)	Solid Fraction (wt %)		
2014	642 – 643	25	648 - 650	~ 6 - 8
5056	630 – 631	25	635 – 637	~ 5 - 7
7050	622 – 624	25	630 – 631	~ 7 - 9

Hot tears are brittle interdendritic fractures that initiate during solidification of metallic castings. Alloys with larger solidification ranges, and alloys that solidify into structures where the primary phase is predominantly dendritic, as well as alloys that solidify with large as-cast grain size are more prone to hot tearing than others. Accordingly, many aluminum-based alloys that belong to these systems are termed *wrought alloys*. Wrought alloys are worked, i.e., they are extruded, forged, etc., and subsequently shaped. In contrast to *casting alloys*, which must contain specific elements that improve their casting characteristics, wrought alloys do not suffer from this constraint and are designed primarily for enhanced properties. A major gain for the casting industry could be had by providing a method that allows easy and direct casting of aluminum-based wrought alloys into components that have microstructures that do not result in hot tears and that have desirable mechanical properties.

It is generally accepted that hot tears occur because of insufficient permeability of the dendritic network for flow of the interdendritic liquid to occur during the later stages of solidification [2]. Consequently, alloys such as 2014, which exhibit a large solidification range, higher eutectic liquid content, and large as-cast grain size are more prone to hot tearing than others. Adjustments to alloy constitution and/or casting procedures that favorably change the effects of these characteristics on the permeability of the dendritic network may minimize the tendency of the alloy to hot tear during solidification. A method based on the concept of diffusion solidification introduced by Langford and Apelian [4] in the 1970's has been developed. The method, which has been dubbed *Controlled Diffusion Solidification* (CDS), minimizes hot tearing tendencies of the alloy by changing the morphology of the primary α-Al from a dendritic morphology to a predominantly globular morphology. This change in the morphology of the primary α-Al phase results in an increase in the channels that are available for feeding the casting with liquid during the later stages of solidification.

Controlled Diffusion Solidification

In the CDS process, which is depicted schematically in Figure 1, predetermined quantities of two molten alloys of different composition and temperature are brought together and then cast into a near-net shape component. The composition and amount of the two precursor alloys is chosen so that the resultant alloy has a pre-determined composition. The temperature of each of the precursor molten alloys is also chosen such that the temperature of the resultant alloy is at, or just below, its liquidus temperature. Consequently, the resultant alloy contains some fraction solid that allows instantaneous copious nucleation of the primary solid phase from the liquid.

Accordingly, the resultant alloy solidifies over a short temperature range with a non-dendritic microstructure that minimizes its tendency towards hot tearing and makes it more amenable to casting operations.

In this publication, the mechanism underlying the evolution of the globular microstructure during Controlled Diffusion Solidification of aluminum-based wrought alloys is developed based on thermodynamic considerations and the concept of free energy, together with considerations of liquid mixing. In addition, the use of CDS to cast 2014 and 7050 wrought alloys is demonstrated and in each case the microstructure of the resultant casting is characterized using optical and scanning electron microscopy (SEM) and compared to the conventionally cast microstructure.

Thermodynamic Considerations

The condition for spontaneity for a reaction is that the total Gibbs free energy of the system is lowered by the reaction. This criterion is used to elucidate the mechanism underlying the evolution of the globular microstructure during controlled diffusion solidification of aluminum-based alloys.

The incremental change in Gibbs free energy of a regular binary solution (ΔG^M) caused by the mixing of its components A and B to form one mole of a regular binary solution is given by Equation (1),

$$\Delta G^M = \Delta G^{M,id} + G^{XS} \qquad (1)$$

In Equation (1), $\Delta G^{M,id}$ is the incremental change in Gibbs free energy of the binary solution caused by the mixing of its components A and B to form one mole of a regular binary solution, and G^{XS} is the excess Gibbs free energy of the binary solution due to its deviation from ideal behavior. $\Delta G^{M,id}$ and G^{XS} are given by Equations (2) and (3), respectively.

$$\Delta G^{M,id} = RT(X_A \ln X_A + X_B \ln X_B) \qquad (2)$$

$$G^{XS} = \alpha RTX_A X_B \qquad (3)$$

where X_A and X_B are the mole fractions of A and B atoms, respectively.

Substitution of Equations (2) and (3) into Equation (1) gives the incremental change in Gibbs free energy of mixing of a regular binary solution

$$\Delta G^M = RT(X_A \ln X_A + X_B \ln X_B) + \alpha RTX_A X_B \qquad (4)$$

Since the Gibbs free energy per mole of the unmixed components of the solution is $\left(X_A G_A^o + X_B G_B^o\right)$, then the total Gibbs free energy per mole of a regular binary solution (G_m) may be given by Equation (5).

$$G_m = RT(X_A \ln X_A + X_B \ln X_B) + \alpha RTX_A X_B + \left(X_A G_A^o + X_B G_B^o\right) \qquad (5)$$

In Equation (5), G_A^0 and G_B^0 are the molar Gibbs free energies of pure elements A and B in the binary solution, respectively. Equation (5) shows that the behavior of a solute A in a regular binary A-B solution is determined by the nature and magnitude of the interactions between the A and B atoms. When a second solute, C, is added, three types of atomic interactions occur, namely A with B, A with C, and B with C, and the thermodynamic behavior of the system is determined by the relative magnitudes of these three interactions. Expanding on this thought, the degree of difficulty in quantifying the Gibbs free energy of a multi-component alloy system becomes apparent. Having access to all the data needed to describe the many interactions in a consistent form is virtually impossible without the use of computational thermochemistry. The CALPHAD method, which was developed by Larry Kaufman in 1970 [5], allows calculating all the necessary data from a unique set of thermodynamic model parameters of the alloy system. CALPHAD which is an acronym for Computer **CAL**culation of **PHA**se **D**iagrams, uses thermodynamic models that are based on experimental information from phase diagrams, such as solubility limits, invariant temperatures, etc., and measured thermochemical data, such as enthalpies, chemical potentials, etc., together with theoretical calculations and empirical rules that describe the Gibbs free energy of each phase in a given system to supply quantitative data that can guide the development of new alloys and the optimization of materials processing methods. The CALPHAD method enables the tracking of individual alloys during solidification by calculating the phase distribution and phase compositions. Obviously, for the successful application of the CALPHAD method, a reliable database that provides thermodynamic parameters for each phase in the alloy, in addition to reliable software that performs the necessary calculations using these thermodynamic parameters must be available. In this work, thermodynamic calculations were performed using the commercial software Pandat®[8] version 4-O-H, which uses the PanAluminum® version 2b thermodynamic database for commercial aluminum alloys, and in all calculations, comparable results were obtained from the commercial software Thermocalc®[9] using the Thermotech Aluminum database.

In the CALPHAD method, Equation (5) takes the more detailed form shown as Equation (6)

$$G_m = X_A G_A^0 + X_B G_B^0 + RT(X_A \ln X_A + X_B \ln X_B) + X_A X_B \sum_k^n {}^K L_{A,B}^{\Phi} (X_A - X_B)^k \qquad (6)$$

In Equation (6), G_A^o and G_B^o are the molar Gibbs free energies of pure elements A and B, respectively and may be obtained from the Scientific Group Thermodata Europe (SGTE) pure elements database [6]. ${}^K L_{A,B}^{\Phi}$ is the k^{th} interaction coefficient between the A and B atoms and is given by ${}^K L_{A,B}^{\Phi} = A_k^{\Phi} + B_k^{\Phi} T + C_k^{\Phi} T \ln T$, where A_k^{Φ}, B_k^{Φ} & C_k^{Φ} may be determined experimentally.

---

[8] Pandat® is marketed by CompuTherm, LLC, Madison, WI, USA.

[9] Thermolcalc® is developed and marketed by the Foundation of Computational Thermodynamics, Stockholm, Sweden.

Consider two liquids of compositions C_1 and C_2 maintained at temperatures T_1 and T_2, respectively. Using Equation (6), the Gibbs free energy of liquid 1 may be written as

$$G_m^1 = X_A^1 G_A^0 + X_B^1 G_B^0 + RT_1(X_A^1 \ln X_A^1 + X_B^1 \ln X_B^1) + X_A^1 X_B^1 \sum_k^n {}^K L_{A,B}^{\Phi}(X_A^1 - X_B^1)^k \quad (7)$$

Similarly, using Equation (6), the Gibbs free energy of liquid 2 may be written as

$$G_m^2 = X_A^2 G_A^0 + X_B^2 G_B^0 + RT_2(X_A^2 \ln X_A^2 + X_B^2 \ln X_B^2) + X_A^2 X_B^2 \sum_k^n {}^K L_{A,B}^{\Phi}(X_A^2 - X_B^2)^k \quad (8)$$

The available Gibbs free energy of the two liquids is a weighted average of their individual Gibbs free energies, *e.g.*, if the weights of the two liquids are in the ratio a:b to one another, then their available Gibbs free energy is

$$G_m^{MAX} = \frac{a.G_m^1 + b.G_m^2}{(a+b)} = f^1 G_m^1 + f^2 G_m^2 \quad (9)$$

If the two liquids are brought together so that their atoms are allowed to intermix, then the resultant liquid will have x_A^f mole fraction A atoms and X_B^f mole fraction B atoms where X_A^f and X_B^f are given by Equations (10) and (11) respectively

$$X_A^f = \frac{aX_A^1 + bX_A^2}{(a+b)} \quad (10)$$

$$X_B^f = \frac{aX_B^1 + bX_B^2}{(a+b)} \quad (11)$$

and the equilibrium Gibbs free energy per mole of the resultant liquid is

$$G_m^{final} = X_A^f G_A^0 + X_B^f G_B^0 + RT_3(X_A^f \ln x_A^f + X_B^f \ln X_B^f) + X_A^f X_B^f \sum_k^n {}^K L_{A,B}^{\Phi}(X_A^f - X_B^f)^k \quad (12)$$

Liquid Mixing Considerations

When two liquids are brought together and their atoms are allowed to intermix, either one of the three processes depicted schematically in Figure 2 occurs [7]. Moreover, competition between thermal diffusion and mass diffusion occurs in the resultant liquid due to the difference in solute concentration and temperature between the two liquids. Thermal equilibration of the resultant liquid occurs by the transport of heat *via* electronic conduction from the hotter to the relatively colder regions of the liquid (if the liquids are metallic) [8], and equilibration of solute concentration occurs by diffusion of solute atoms across the diffuse interface that forms between the two liquids [9]. The formation of a diffuse interface between liquids has been observed experimentally and its decay rate has been mathematically modeled and shown to be proportional to $1/\sqrt{t}$ [9-11]. Typically, when two metallic liquids are brought together their temperatures tend to equilibrate faster than their composition as shown schematically in Figure 3. The result of this difference between thermal and concentration equilibration leads to the formation of pockets in the resultant liquid that are under-cooled relative to their local

composition. These pockets of under-cooled liquid may act as nucleation sites for the solid phase, provided that their surface energy favors the formation of the solid phase. Cini et al [12] have shown that "suitable concentration fluctuations can provide favored sites for nucleation". According to Cini et al [12], the energy barrier for nucleation due to a concentration gradient is lower than the classical energy barrier for nucleation if

$$\frac{a}{a+b} < (1+\frac{\sigma^{SL}-\sigma_{Al}^{SL}}{\sigma_{Al}^{SL}})^{\frac{3}{2}} \tag{13}$$

In Equation (13), $a = \mu_A^{(s)} - \mu_A^l(c_0)$ is the chemical potential difference of component A between its solid phase and its liquid phase that has composition C_0, *i.e.*, X_A^f and X_B^f. Similarly, $b = \mu_A^{(1)} - \mu_A^l(c=1)$ is the chemical potential difference of component B between its solid phase and its liquid phase if the solid phase has formed from pure liquid, *i.e.*, if C=1. σ^{Sl} is the solid-liquid interface energy between the solid and liquid of composition C_0, σ_A^{SL} is the solid-liquid interface energy between the solid and liquid when they are pure. Cini et al [12] have shown that Equation (13) is satisfied when

$$(1+\frac{\sigma^{SL}-\sigma_A^{SL}}{\sigma_A^{SL}})^{\frac{3}{2}} \geq 1 \quad \text{i.e.,} \qquad \sigma^{SL}-\sigma_A^{SL} > 0 \tag{14}$$

From the preceding it should be clear that for nucleation of the solid phase from a mixture of two liquids of compositions C_1 and C_2, the two liquids must be maintained at temperatures T_1 and T_2 such that T_1 and T_2 are close to the liquidus temperature of liquid 1and liquid 2, respectively, *i.e.*, the two liquids must be maintained at relatively low superheat. Additionally, the Gibbs free energy of the liquids prior to mixing must be less than the Gibbs free energy of the resultant liquid at its liquidus temperature, *i.e.*,

$$G_m^{MAX} \leq G_m^{final,liquidus} \tag{15}$$

A liquid that satisfies both conditions given by Equations (14) and (15) will contain pockets of under cooled liquid with surface energy that thermodynamically favors formation of the solid phase.

Solidification Considerations

Das [13] has shown that fluid flow significantly affects the morphology of the primary solid phase that forms during solidification of metal alloys. Das submits that particle rotation in a streamlined fluid flow leads to the formation of a rosette-like primary solid phase that becomes more compact and tends towards a spherical morphology as the extent of turbulence in the flow field increases. Shushen [14] supports Das's ideas and submits that turbulence is inevitable during liquid mixing and therefore once the solid phase has nucleated in a liquid alloy, the newly formed nuclei are inevitably exposed to turbulence and therefore will tend to grow with a globular morphology. Consequently, satisfaction of the conditions set forth by Equations (14) and (15) is the only requisite for formation of a globular microstructure in the CDS process.

Materials and Procedures

Two sets of experiments were performed in order to illustrate the preceding principles for formation of a solid phase with a globular microstructure by mixing two liquids. The materials used in the experiments are commercially pure aluminum, Al-33% Cu, and Al-12.8%Si (constituted from the commercially pure aluminum (99.9% Purity) and pure Si (99.99%). The chemical composition of the starting materials as well as the Al-32.3%Cu and Al-12.8%Si alloys were determined using spark emission spectrometry[10,11], and are presented in Table II.

Table II. Chemical composition of materials used.

	Si	Cu	Fe	Mg	Mn
Commercially pure Al	0.5-0.8		0.5-0.8	0.2 max.	0.2 max.
Al-32.3 %Cu master alloy	0.07	33	0.11		
Al-12.8%Si	12.5	<0.05	0.05	< 0.05	<0.05

In the first set of experiments, 350 grams of commercially pure aluminum at 665°C (*i.e*., at 5°C superheat) was poured into a crucible that contained 50 grams ofAl-32.3%Cu at 550°C (*i.e*., at 5°C superheat) and allowed to mix naturally while cooling in room temperature air. A type K thermocouple was inserted near the center of the crucible and connected to a data acquisition system[12] in order to record the thermal history of the liquid as it cooled. In similar experiments, the resultant alloy was quenched in water when its temperature reached 646°C, 641°C, and 635°C in order to track the evolution of microstructure as the alloy cooled. After every experiment, the composition of the resultant solid ingot was measured using spark emission spectroscopy and the ingot was sectioned into two halves. One half was used to produce specimens for microstructure characterization, while the second half was re-melted at 700°C (*i.e.,* at 50°C superheat), conventionally cast in a second crucible, and allowed to cool in room temperature air, then sectioned to produce specimens for microstructure characterization.

In the second set of experiments, 200 grams of commercially pure aluminum at 665°C (*i.e*., at 5°C superheat) was poured into a crucible that contained 300 grams ofAl-12.8%Si at 580°C (*i.e*., at 2-5°C superheat) and allowed to mix naturally while cooling in room temperature air. A type K thermocouple was inserted near the center of the crucible and connected to a data acquisition system in order to record the thermal history of the liquid as it cooled. Upon solidification, the composition of the resultant ingot was measured using spark emission spectroscopy and the ingot was sectioned into two halves. One half was used to produce specimens for microstructure characterization, while the second half was re-melted at 700°C (*i.e.,* at ~50°C superheat), conventionally cast in a second crucible, and allowed to cool in room temperature air, then sectioned to produce specimens for microstructure characterization.

---

[10] Model Spectro Lab-Max LMXM3, Spectro Analytical Instruments, Fitchburg, MA, USA.

[11] Accuracy of the spark transmission spectrometer is Si ±0.3, Fe ±0.0003 when Fe<0.01, and ±0.0022 when Fe>0.1. Other relevant elements show negligible measurement errors.

[12] Dasylab Version 5.6

In addition, the following procedures were performed in order to demonstrate the applicability of the CDS method to casting alloys from the 2xxx, 4xxx, 5xxx, and 7xxx systems.

Casting of 2014 alloy using CDS

In order to demonstrate the applicability of the CDS method to casting wrought alloys that belong to the 2xxx system, the CDS method was used to cast 2014 alloy having the following nominal composition,

Cu (wt.%)	Minor elements[13]	Al
4.4	2.0	Remainder

Table III shows the chemical analyses, weight fraction, and temperature of the precursor alloys.

Table III. Chemical Analyses, Weight Fraction, and Temperature of the Precursor Alloys Used in Casting 2014 Alloy *via* CDS.

Chemical analysis:	Precursor Alloy #1	Precursor Alloy #2
Cu (wt.%)	33	-
Al (wt.%)	67	~ 98
Liquidus temperature (°C)	548	660
Weight fraction	~ 0.14	~ 0.86
Temperature (°C)	550	665
Liquidus temperature of 2014 alloy (°C)	648	
Maximum temperature of resultant alloy (°C)	646	

Precursor alloy #1 and precursor alloy #2 were poured in a crucible and allowed to mix naturally while they air-cooled. The measured chemistry of the resultant alloy was as follows:

Cu (wt.%)	Minor elements[14]	Al
4.57	1.5	Balance

Casting of 4145 alloy using CDS

In order to demonstrate the applicability of the CDS method to casting wrought alloys that belong to the 4xxx system, the CDS method was used to cast 4145 alloy having the following nominal composition:

Si (wt.%)	Cu (%)	Al
10	4	Remainder

[13] Predominantly Si, Mg, and Mn.
[14] Predominantly Si, Mg, and Mn from commercially pure aluminum.

Table IV shows the chemical analyses, weight fraction, and temperature of the precursor alloys.

Table IV. Precursor Alloys' Chemical Analyses, Weight Fractions, and Temperatures for Casting of 4145 Si alloy

Chemical Analysis	Precursor Alloy #1	Precursor Alloy #2
Cu	~ 33 wt.%	-
Si	-	~ 12.7 wt.%
Al	67 wt.%	Balance
Liquidus temperature (°C)	548	578
Weight fraction	~ 0.14	~ 0.86
Temperature (°C)	550	585
Liquidus temperature of 4145 alloy (°C)	580	
Maximum temp. of resultant alloy on mixing(°C)	578	

The measured chemistry of the alloy produced *via* CDS was as follows:

Si(wt.%)	Cu(wt.%)	Al
10.37	4.72	Remainder

Casting of 5056 alloy using CDS

In order to demonstrate the applicability of the CDS method to casting wrought alloys that belong to the 5xxx system, the CDS method was used to cast 5056 alloy, which has the following nominal composition:

Mg (wt.%)	Mn (wt.%)	Cr (wt.%)	Al
5.0	0.12	0.12	Balance

Table V shows the chemical analyses, weight fraction, and temperature of the precursor alloys.

Table V. Chemical Analyses, Weight Fraction, and Temperature of the Precursor Alloys Used in Casting 5056 Alloy *via* CDS.

Chemical analysis:	Precursor Alloy #1	Precursor Alloy #2
Mg (wt.%)	35	-
Al (wt.%)	65	~ 98
Liquidus temperature (°C)	451	660.7
Weight fraction	~ 0.14	~ 0.86
Temperature (°C)	445	665
Liquidus temperature of 5056 alloy (°C)	636.8	
Maximum temperature of resultant alloy (°C)	638	

The measured chemistry of the alloy produced *via* CDS was as follows:

Mg (wt.%)	Mn (wt.%)	Cr (wt.%)	Al
4.8	0.15	0.02	Balance

Casting of 7050 alloy using CDS

In order to demonstrate the applicability of the CDS method to casting wrought alloys that belong to the 7xxx system, the CDS method was used to cast 7050 alloy, which has the following nominal composition:

Zn (wt.%)	Mg (wt.%)	Cu (wt.%)	Al
6.2	2.2	2.3	Balance

Compared to 2014, and 5056, 7050 is a complex alloy with several alloying elements, and thus there are many possibilities for precursor alloys that can yield 7050 alloy. Table VI shows one possible set of chemical analysis, weight fraction, and temperature of precursor alloys.

Table VI. Chemical Analysis, Weight Fraction, and Temperature of the Precursor Alloys Used in Casting 7050 Alloy *via* CDS.

Chemical Analysis	Precursor Alloy #1	Precursor Alloy #2
Cu (wt.%)	~ 24	-
Mg (wt.%)	-	~ 2.65
Zn (wt.%)	-	~ 7
Al	76	Balance
Liquidus temperature (°C)	589	634
Weight fraction	~ 0.10	~ 0.89
Temperature (°C)	592	640
Liquidus temperature of 7050 (°C)	630	
Maximum temperature of resultant alloy (°C)	628	

The measured chemistry of the resultant alloy was as follows:

Zn (wt.%)	Mg (wt.%)	Cu (wt.%)	Al
6.7	2.2	2.5	Balance

In all procedures specimens for microstructure characterization were mounted in Bakelite, polished using standard metallographic techniques. The specimens were observed using optical[15] and scanning electron microscopy (SEM)[16].

[15] Nikon Epiphot
[16] Jeol 840

Results and Discussion

The Al-Cu System – An alloy system with a negative heat of mixing

Equation (16) gives the variation of surface tension, σ, of binary Al-Cu alloys as a function of weight % Cu, C_L [15];

$$\sigma = 868 + 0.721 C_L + 0.012 C_L^2 \qquad (16)$$

For pure Cu, $C_L = 0$ and Equation (16) gives σ = 868 dynes/cm. Similarly, for the eutectic composition, $C_L = 32.2$ and Equation (16) gives σ = 903.65 dynes/cm so that the difference in surface tension between the two alloys is $\Delta\sigma \cong 36$ dynes/cm. Therefore, according to Equation (14), mixing pure Al with eutectic Al-Cu leads to the formation of a diffuse interface between the two liquids [7 - 11], which satisfies the interface requirement set forth in Equation (14).

Figure 5 shows the Gibbs free energy of the Al-Cu binary system as calculated using Equation (6). Figure 5 was obtained by means of the commercial software Pandat® version 4-O-H, and comparable results were obtained from the commercial software Thermocalc®. Figure 6 shows a similar plot to the plot in Figure 5. In Figure 6, the Gibbs free energies per mole of the individual liquids are C_1 and C_2, respectively, and if the two liquids are brought together in the ratio 6 (Al):1 (Al+32.2%Cu) in order to produce an alloy with the composition Al-4.7%Cu, then the Gibbs free energy per mole of the resultant alloy is G_m^{MAX}, where G_m^{MAX} is the weighted arithmetic mean of the Gibbs free energies per mole of Al and Al-32.2% Cu. Point C_3 in Figure 6 is the Gibbs free energy per mole of mixing of the resultant alloy ($G_m^{4.6Cu,\ Liquidus}$). Note that for this alloy

$$G_m^{Max} \le G_m^{4.6Cu,Liquidus}$$

Which satisfies the Gibbs free energy requirement set forth in Equation (15).

Since both the thermodynamic and liquid mixing requirements for formation of a solid phase with a globular morphology by mixing two liquids are satisfied by the Al-Cu system, castings made from this alloy system *via* the CDS method should solidify with a predominantly globular microstructure. Figure 7(a) shows the thermal history of the alloy as it cooled in room temperature air. Notice that there is an initial rise in temperature to about 647°C, which corresponds to the introduction of the liquid Al into the crucible followed by a change in the slope of the cooling curve from about -0.25°C/sec to about -0.08°C/sec. For better visualization, Figure 7(b) is a "zoom-in" on the relevant section of Figure 7(a).

Figures 8(a) and 8(b) show the microstructure of the solid alloy obtained by mixing liquid commercial purity Al and liquid Al-32.2%Cu. Notice that the morphology of the α-Al grains in this casting is predominantly globular and that the microstructure is essentially free of dendrites. For comparison, Figures 8(c) and 8(d) show the microstructure of the re-melted and conventionally cast ingot. Notice that in this case the morphology of the α-Al grains is predominantly dendritic.

Figure 9 depicts the evolution of microstructure during mixing of the precursor alloys and the subsequent growth of the primary phase in the alloy of Figure 8. Figures 9(a) – 9(c) were obtained by quenching the melt in cold water that was maintained at 15°C when the melt's temperature reached 646°C, 641°C, and 635°C, respectively. Figure 9(d) is a magnified image of Figure 9(a) and shows the quenched liquid (solidified as dendrites) and the already nucleated primary phase (solidified as globules). Clearly, nucleation of the primary phases starts immediately after bringing the two precursor alloys together, and once nucleated, the primary phase grows as shown in Figures 9(b) and 9(c).

The Al-Si System – An alloy system with a positive heat of mixing

Figure 10 shows the Gibbs free energy per mole of the Al-Si binary system at three different temperatures, namely the liquidus temperature (the curve marked G_L in Figure 10), the liquidus temperature + 5°C superheat (the curve marked (G_L + 5) in Figure 10), and the liquidus temperature + 15°C superheat (the curve marked (G_L+15) in Figure 10). Similar to Figure 5, Figure 10 was obtained by means of the commercial software Pandat® version 4-O-H, and comparable results were obtained from the commercial software Thermocalc®. Consider the curve marked (G_L + 5) in Figure 10, *i.e.*, the two liquids (Al and Al-12.8%Si) are at 5°C above their respective liquidus temperatures. The Gibbs free energies per mole of the individual liquids are C_1 and C_2, respectively, and if the two liquids are mixed in the ratio **2** (Al): **3** (Al+12.8%Si) in order to produce a liquid alloy with the composition Al-7%Si, then the Gibbs free energy of the resultant liquid alloy is G_m^{MAX}, where G_m^{MAX} is the weighted arithmetic mean of the Gibbs free energies of Al and Al-12.8% Si. Point C_3 in Figure 10 is the Gibbs free energy per mole of mixing of the resultant liquid alloy ($G_m^{7.8Si,Liquidus}$). Note that for this alloy

$$G_m^{Max} > G_m^{Al-Si}$$

Which does not satisfy the Gibbs free energy requirement set forth in Equation (15). Accordingly, castings made from this alloy system *via* CDS should solidify with a predominantly dendritic microstructure. Figure 11 shows the microstructure of the solid alloy obtained by mixing liquid commercial purity Al and liquid Al-12.8%Si. Notice that the morphology of the α-Al in this micrograph is predominantly dendritic.

Application of the CDS Method to Casting Wrought Alloys

The CDS method can be successfully applied to casting any wrought or casting alloy provided that the energy and liquid mixing requirements set forth in the preceding discussion are satisfied. In that vein, and as a demonstration, the CDS method was used to cast 4145, 5056, and 7050 alloys (Tables IV – VI).

Casting 2014 alloy using CDS

Figure 8 shows the successful casting of Al-Cu alloy and the subsequent microstructures obtained.

Casting 4145 alloy using CDS

Figure 12(a) shows the microstructure of 4145 alloy produced *via* CDS. In contrast, Figure 12(b) shows the microstructure of 4145 alloy conventionally cast in a ceramic crucible with a superheat of 70°C. Notice that the morphology of the α-Al grains in the casting produced *via* CDS is predominantly globular and that very few, if any, dendrites are observed throughout the microstructure. Also notice that the inter-dendritic liquid in the alloy produced *via* CDS is dispersed throughout the microstructure and envelopes the globular α-Al grains.

Casting 5056 alloy using CDS

Figure 13(a) shows the microstructure of 5056 alloy produced *via* CDS. In contrast, Figure 13(b) shows the microstructure of 5056 alloy conventionally cast in a ceramic crucible with a superheat of 15°C. Notice that the morphology of the α-Al grains in the casting produced *via* CDS is predominantly globular and that very few, if any, dendrites are observed throughout the microstructure. Also notice that the inter-dendritic liquid in the alloy produced *via* CDS is dispersed throughout the microstructure and envelopes the globular α-Al grains.

Casting of 7050 alloy using CDS

Figure 14(a) shows the microstructure of 7050 alloy produced *via* CDS. In contrast, Figure 14(b) shows the microstructure of 7050 alloy conventionally cast in a ceramic crucible with a superheat of 15°C. Similar to 2014, 4145, and 5056 alloys produced *via* CDS, the morphology of the α-Al grains in the 7050 alloy cast *via* CDS is predominantly globular and few dendrites are observed in the microstructure. Similar to the 2014 castings produced *via* CDS, the inter-dendritic liquid in the 7050 alloy cast *via* CDS is dispersed throughout the microstructure and envelopes the globular grains.

Conclusions

A casting process that is referred to as Controlled Diffusion Solidification (CDS) has been developed to circumvent problems that are typically associated with casting wrought aluminum alloys into near net shape components and to allow sound castings of these alloys with a globular microstructure that is essentially free of dendrites. The process involves mixing two alloys of pre-determined composition and temperature. The mechanism underlining this process is developed on the basis of free energy and liquid-mixing considerations and maintains that for the solid phase to nucleate and grow in a globular morphology, the two precursor alloys must be maintained at temperatures that are close to their respective liquidus temperatures and the difference between the solid/liquid interface energy when both solid and liquid are pure (σ_A^{SL}), and the solid/liquid interface energy in the alloyed state (σ^{SL}) is such that $\sigma^{SL} - \sigma_A^{SL} > 0$. Additionally, the Gibbs free energy of the precursor alloys prior to mixing must be less than the Gibbs free energy of the resultant alloy at its liquidus temperature. Successful casting of wrought alloys *via* the CDS method is commensurate with the choice of precursor alloys that satisfy these conditions and is demonstrated by the results of controlled experiments.

References

1. Van Haaften, W.M., W.H. Kool, and L. Katgerman. Journal of Materials Engineering and Performance 2002; 11(5): 537.
2. D.G. Eskin, Suyinto, and L. Katgerman. Progress in Materials Science 2004; 49(5): 629.
3. L. Arnberg, G. Chai, and L. Backerud. Materials Science and Engineering A 1993; 173(1-2): 101.
4. G. Langford and D. Apelian. Journal of Metals 1980; 32(9): 28.
5. L. Kaufman and H. Bernstein, *Computer Calculation of Phase Diagram* Academic Press, New York. 1970; pp 16-28.
6. Scientific Group Thermodata Europe (www.sgte.org)
7. J.M. Ottino, The kinematics of mixing: Stretching, Chaos and Transport, ISBN 0-521-36335-7, Published by Cambridge University Press, New York, USA
8. B. Giordanengo, N. Benazzi, J. Vinckel, J.G. Gasser and L. Roubi. Journal of non-crystalline solids 1999; 250 – 252: 377.
9. P.G. Smith, T.G. M. Van De Ven and S.G. Mason. Journal of colloidal and Interface Science 1981; 80: 1.
10. D.D. Joseph, A. Huang and H. Hu. Physica D 1996; 97: 104.
11. D.M. Anderson and G.B. McFadden, Annual Review of Fluid Mechanics 1996; 30:139
12. E. Cini, B. Vinet and P.J. Desre. Philosophical Magazine A 2000; 80(4): 955.
13. Das, S. Ji, and Z. Fan. Acta Materialia 2002; 50: 4571.
14. W. Shusen, W. Xueping and X. Zehui. 2004; 52: 3519.
15. D.R. Poirier and R. Speiser. Metallurgical and Materials Transactions 1987; 18A:1156.
16. M. Gunduz and J.D. Hunt. Acta Metallurgica 1985; 33(9): 1651.

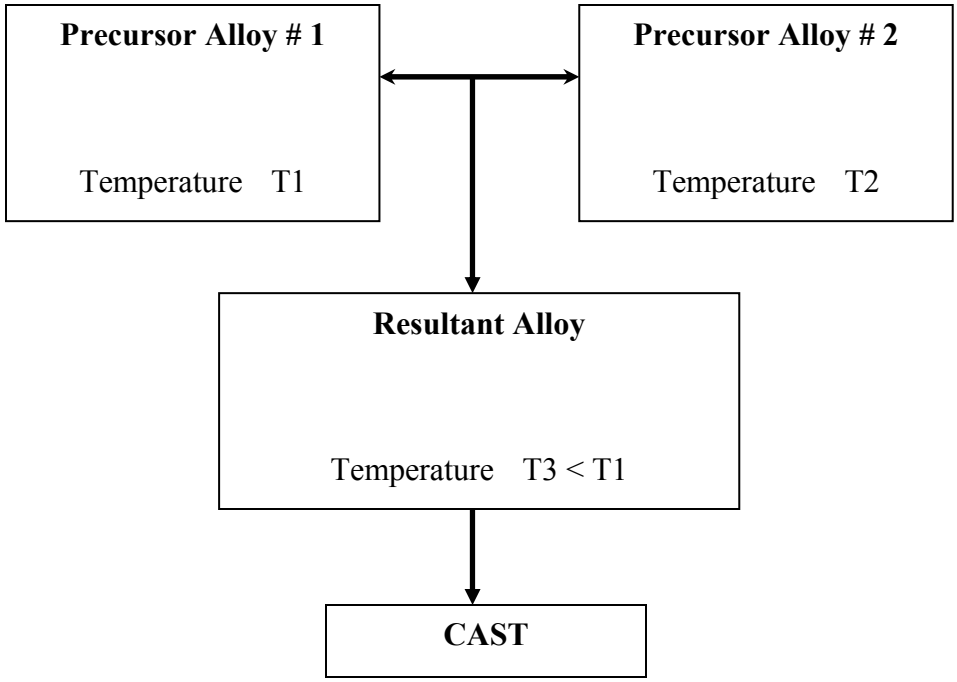

Figure 1: Schematic of the CDS process showing the mixing of two liquids at different temperatures and composition, which are mixed at a predetermined ratio to achieve a third alloy.

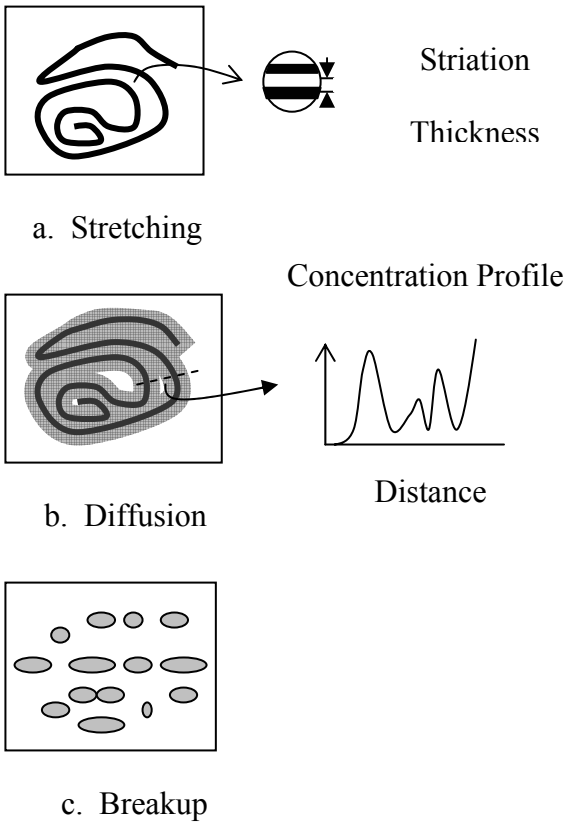

Figure 2: Basic processes occurring during the mixing of fluids: a) with no surface tension difference and interdiffusion b) diffuse boundary c) interfacial tension dominating.

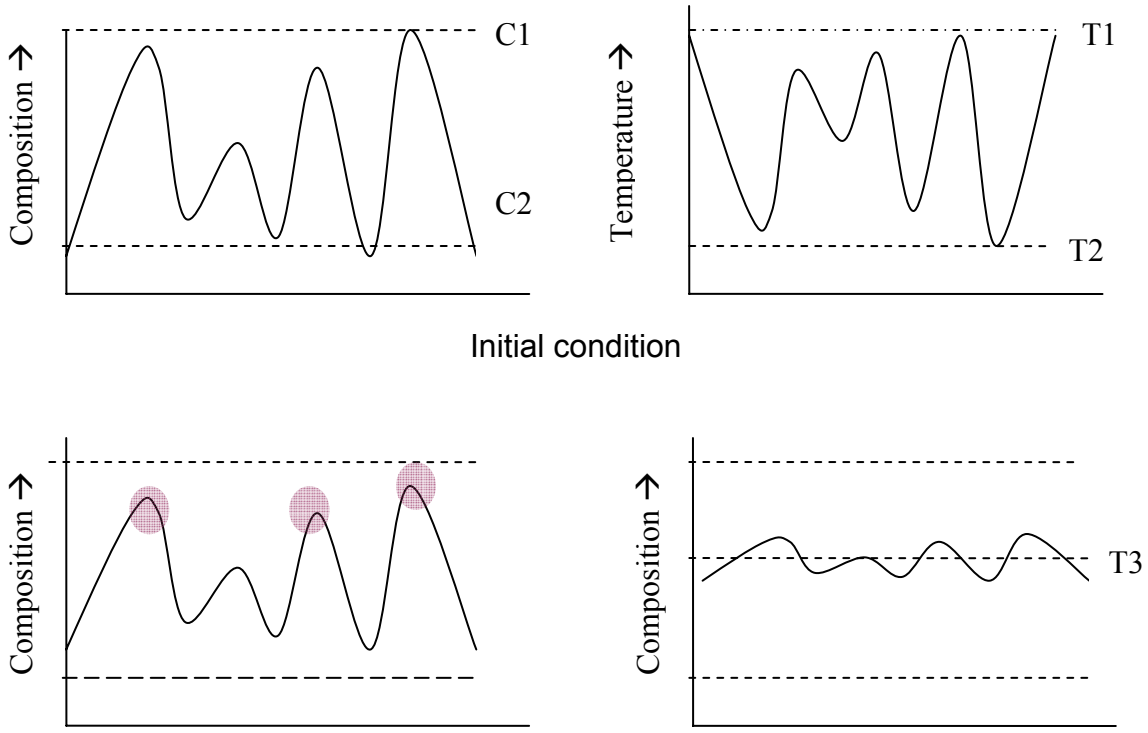

The difference between the thermal and mass diffusivities will lead to a unique condition where the higher temperature alloy is thermally under cooled. The thermally under cooled liquid is shown as the colored spots on the composition line. The closer T1 is to the liquidus of C1, the higher the degree of under cooling

Figure 3: Schematic showing how higher thermal diffusivities can lead to pockets of local under cooling in the liquid.

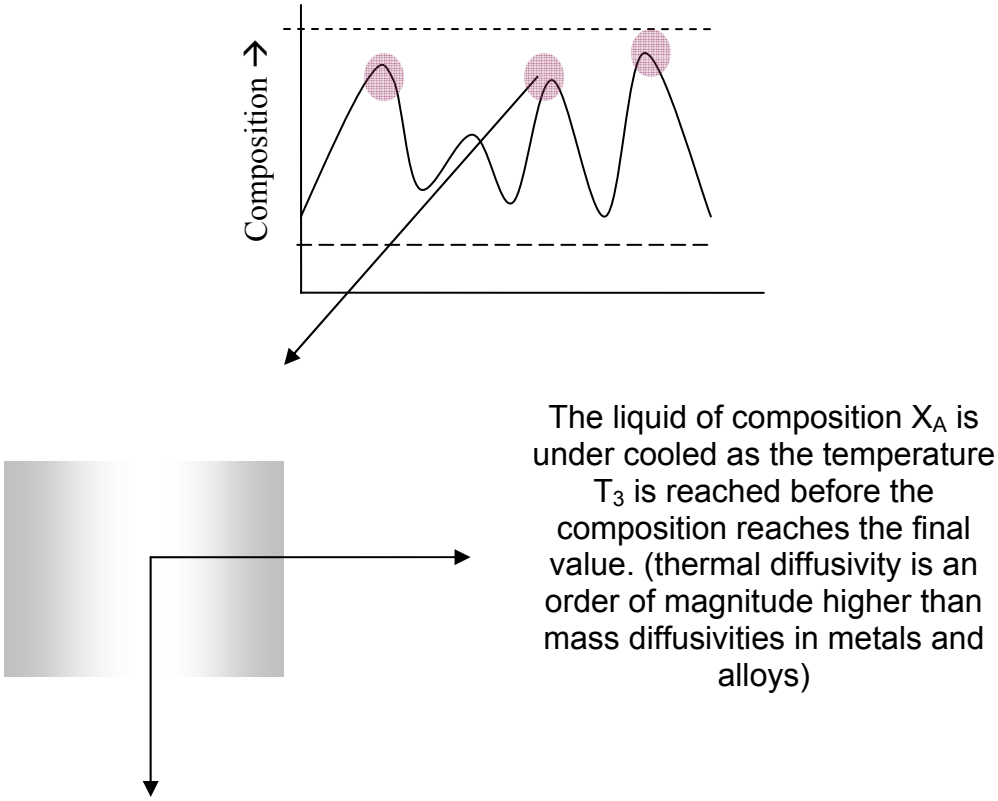

Figure 4: Schematic showing the necessary condition for the nucleation of a primary phase due to concentration gradient and an under cooling.

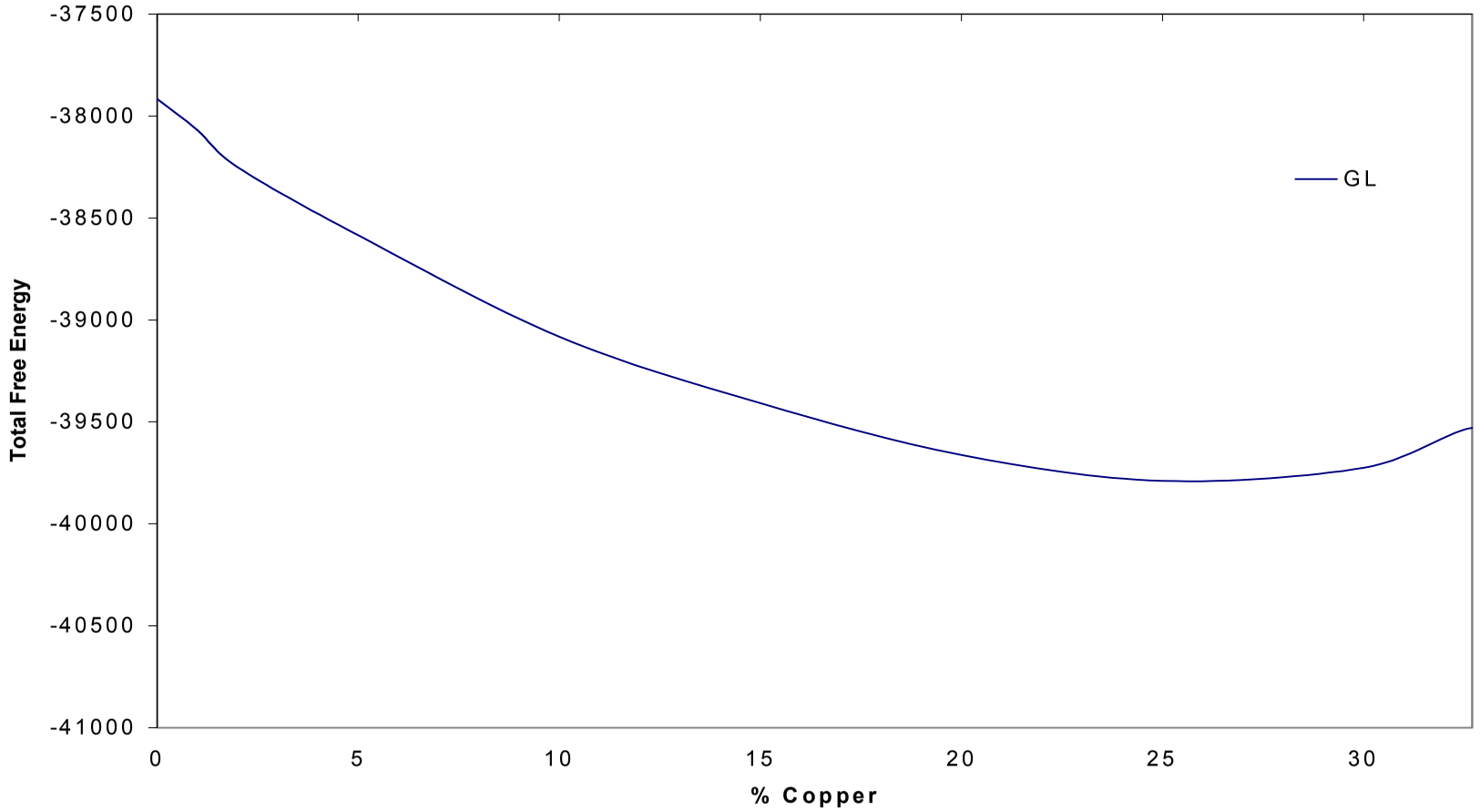

Figure 5: Free energy of mixing of an Al-Cu system near the liquidus (data obtained from Thermo-calc© and verified by Pandat®). Al-Cu system has a negative heat of mixing.

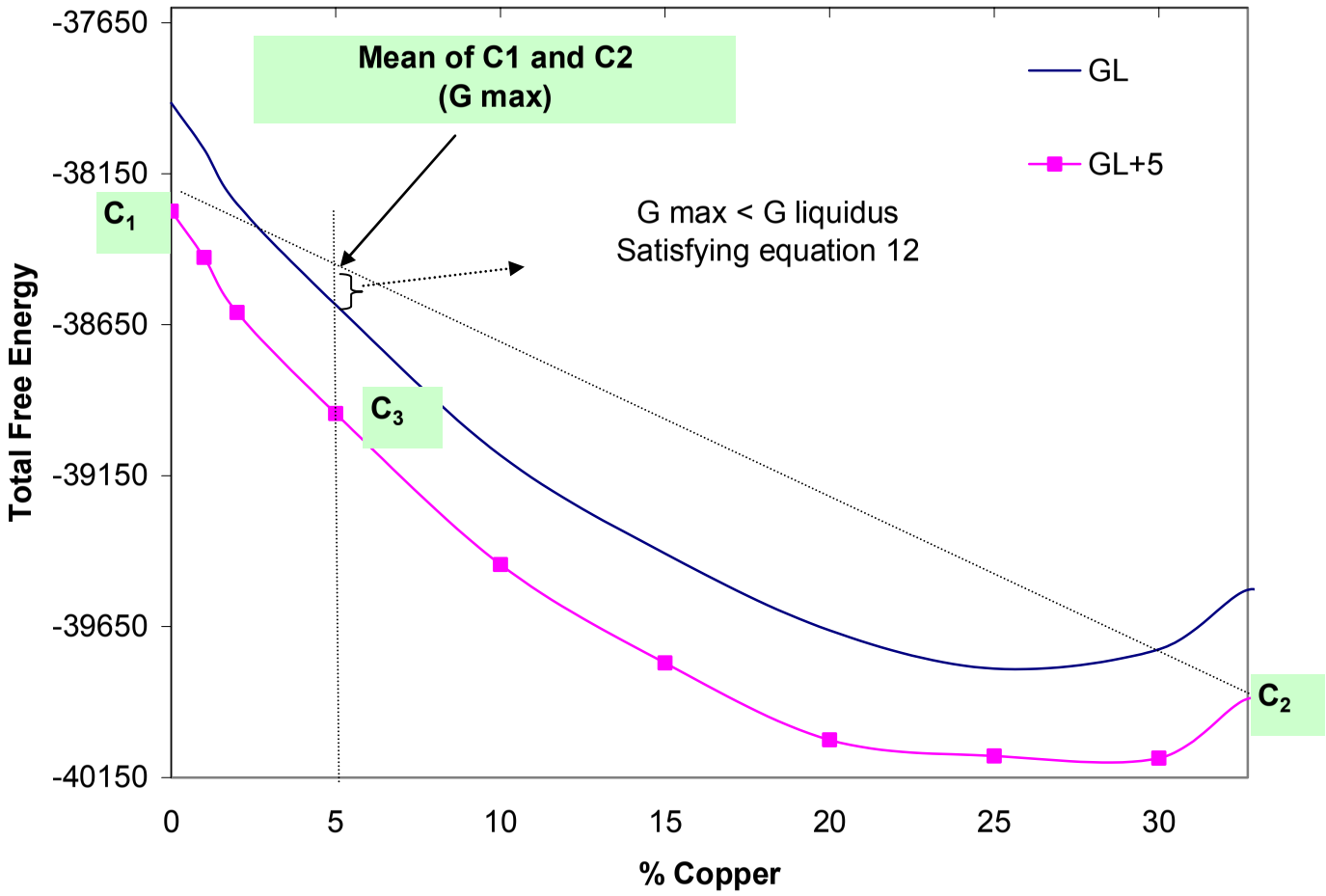

Figure 6: Free energy of Al-Cu at different temperatures (at liquidus, at 5^0 from superheat and at 15^0 degree from superheat). Point C_1 is the free energy of pure Al at a 5 degree superheat, C_2 is the free energy of eutectic Al-Cu at a 5 degree superheat, C_3 is the free energy of the liquidus of a Al-4.6% Cu alloy.

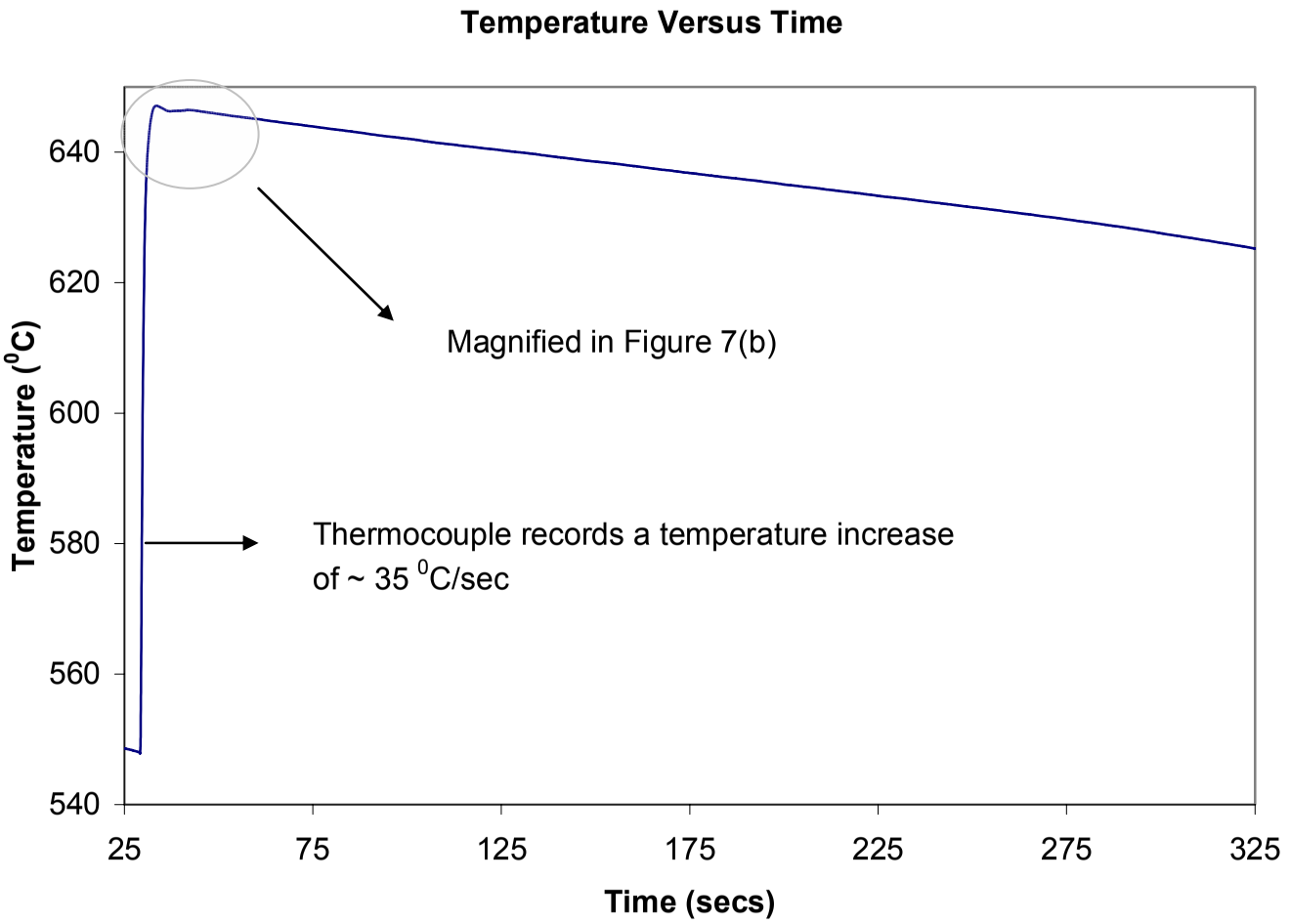

Figure 7(a): Thermocouple data obtained during the process of mixing of Pure Al and Al-Cu eutectic liquid. The thermocouple was in the Al-Cu eutectic liquid.

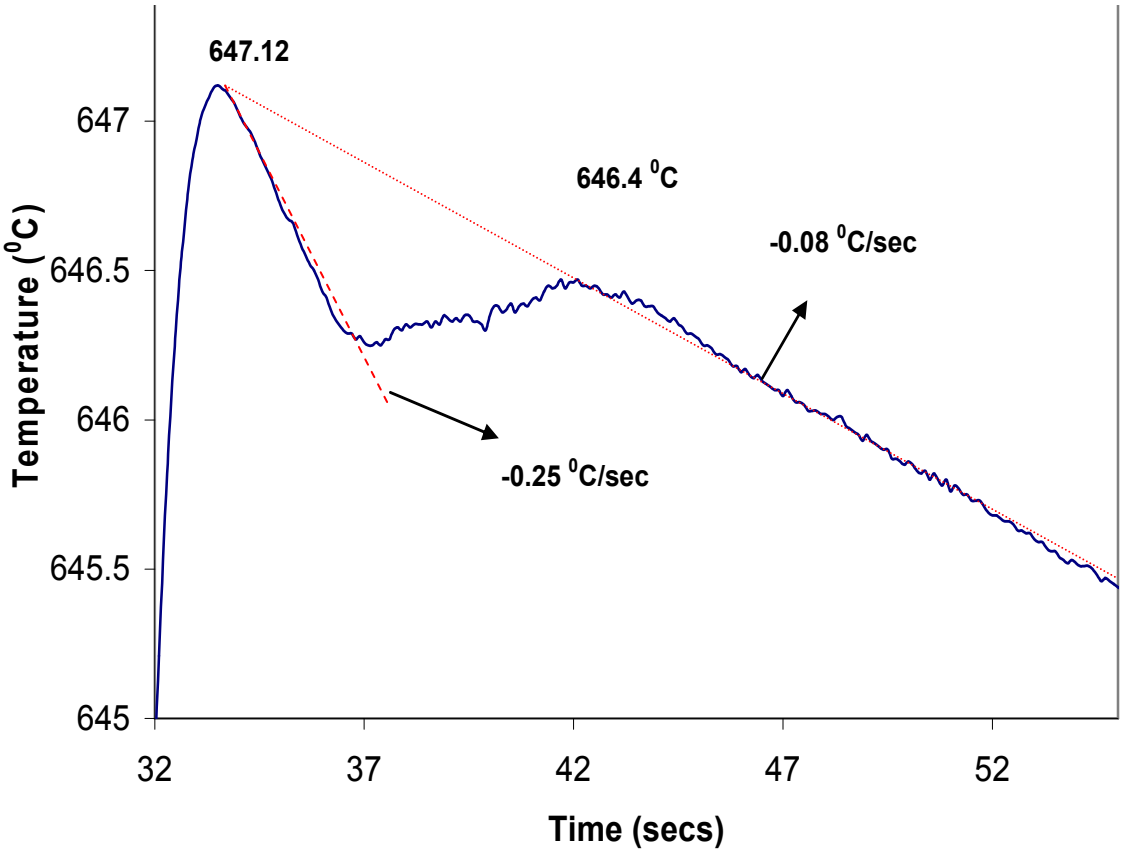

Figure 7(b): Thermal data magnified to showing the nucleation / growth of the primary phase during the mixing of pure Al and Al-33% Cu eutectic liquid. Similar curve was observed in the examples listed in Table IV to VI.

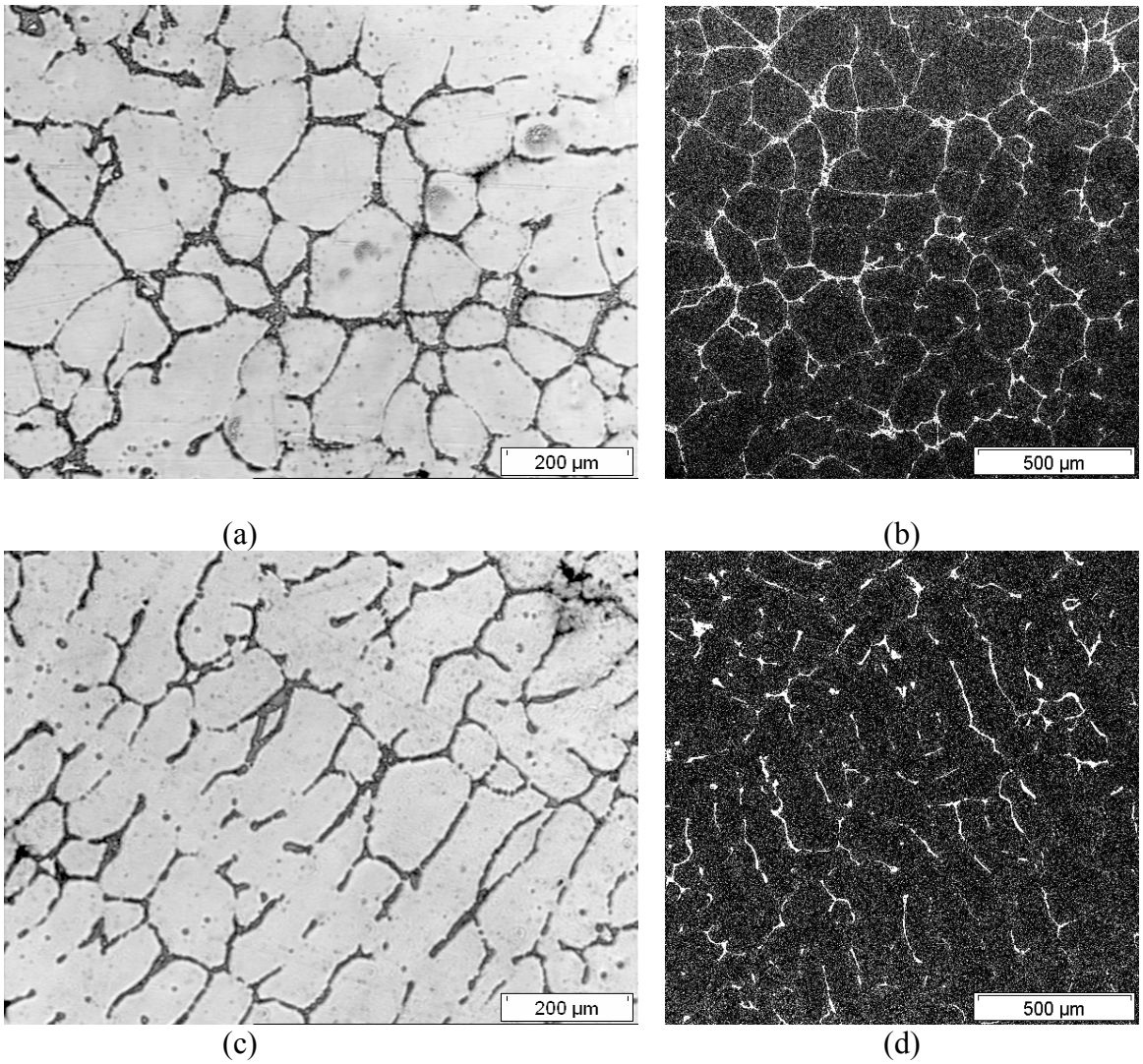

Figure 8: Micrographs of a Al-Cu alloy cast by mixing Pure Al and Al-33%Cu; (a) optical image of the final solidified structure, (b) back scattered SEM image of the final solidified structure, (c) Optical image of the same alloy remelt at 50 degree superheat and cast (d) SEM back scattered image of the reheated sample. Notice the dendritic microstructure in the re-melt sample.

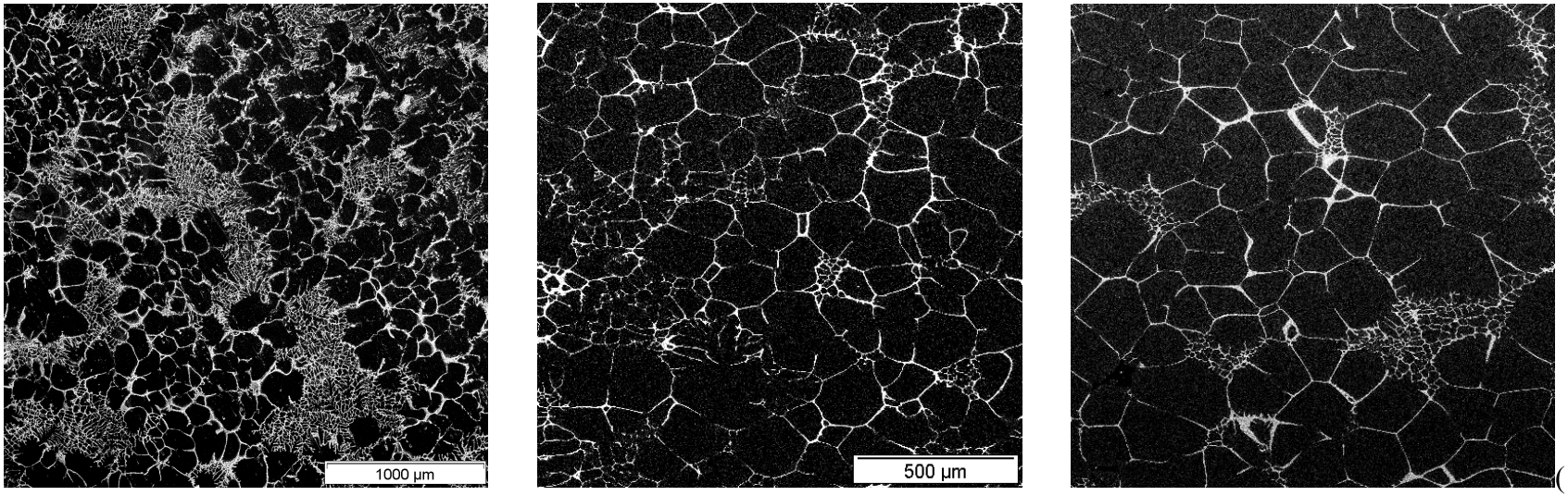

Figure 9: Back scattered images showing the evolution of the semi solid microstructure during the process of liquid mixing (The liquidus of the final alloy was 648 ^{0}C);
(a) quenched immediately on mixing Pure Al and Al-33%Cu liquid, the temperature was 646 ^{0}C
(b) quenched after the alloy has reached a temperature of 641 ^{0}C
(c) quenched after the alloy was at temperature of 636 ^{0}C.

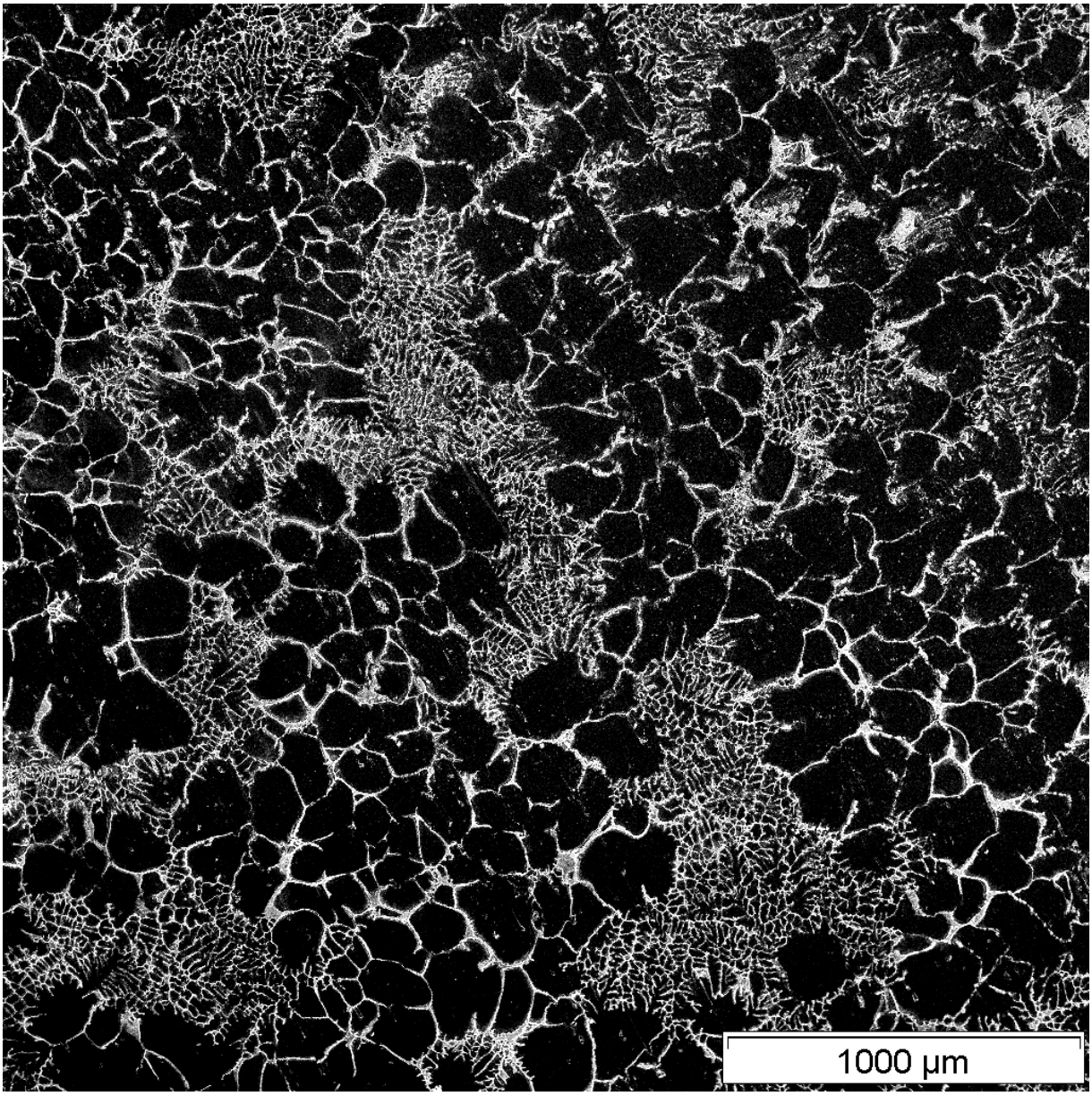

Figure 9 (d): Magnified image of Figure 9(a), showing the co-existence of globular and dendritic microstructure (quenched).

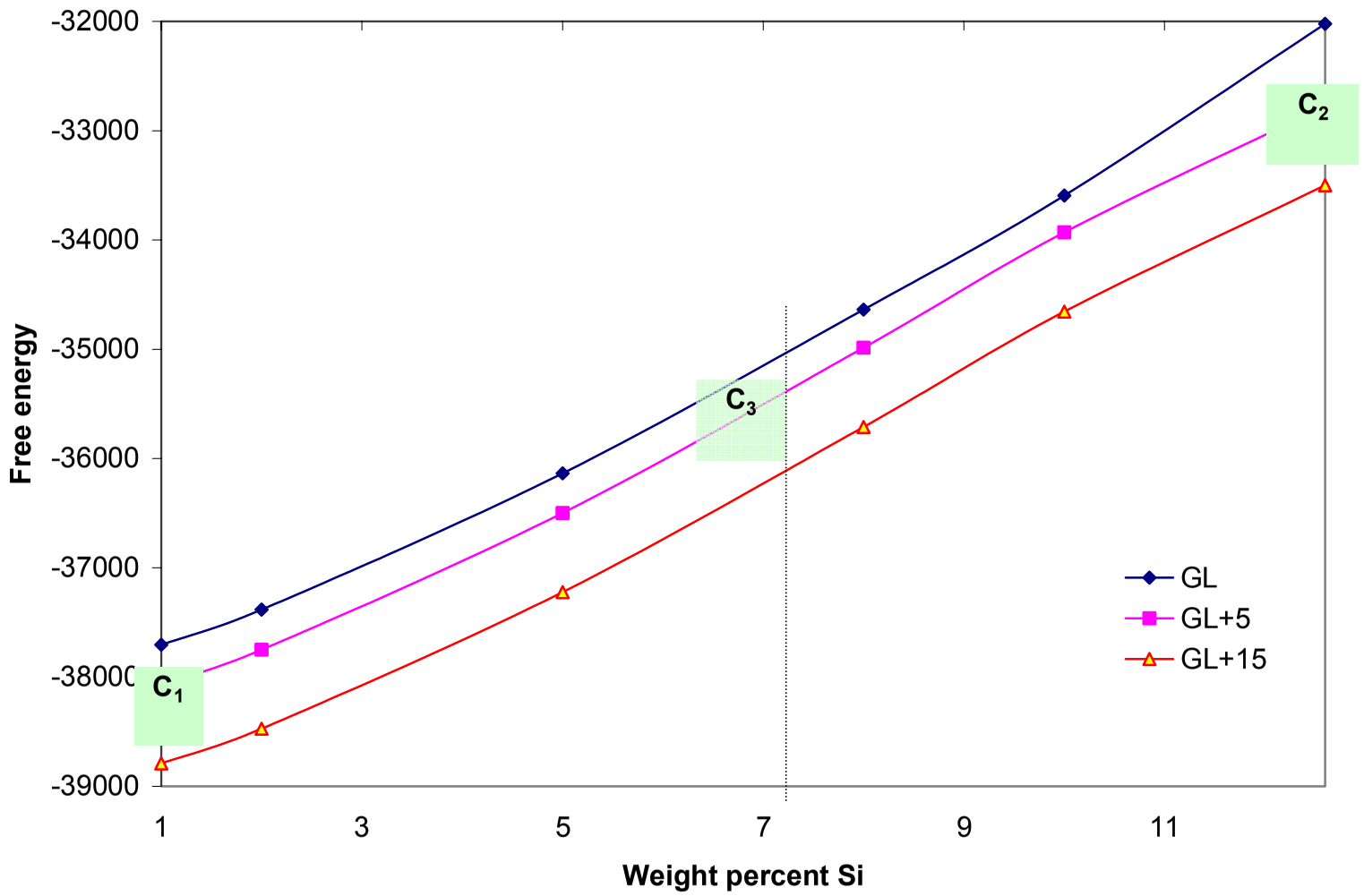

Figure 10: Total Free energy of Al-Si at different temperatures (at liquidus, at 5 degree above superheat and at 15 degree above superheat). Point C_1 is the free energy of pure Al at a 5 degree superheat, C_2 is the free energy of eutectic Al-Si at a 5 degree superheat. C3 is the final composition on mixing C1 and C2 in a ratio of 2:3.

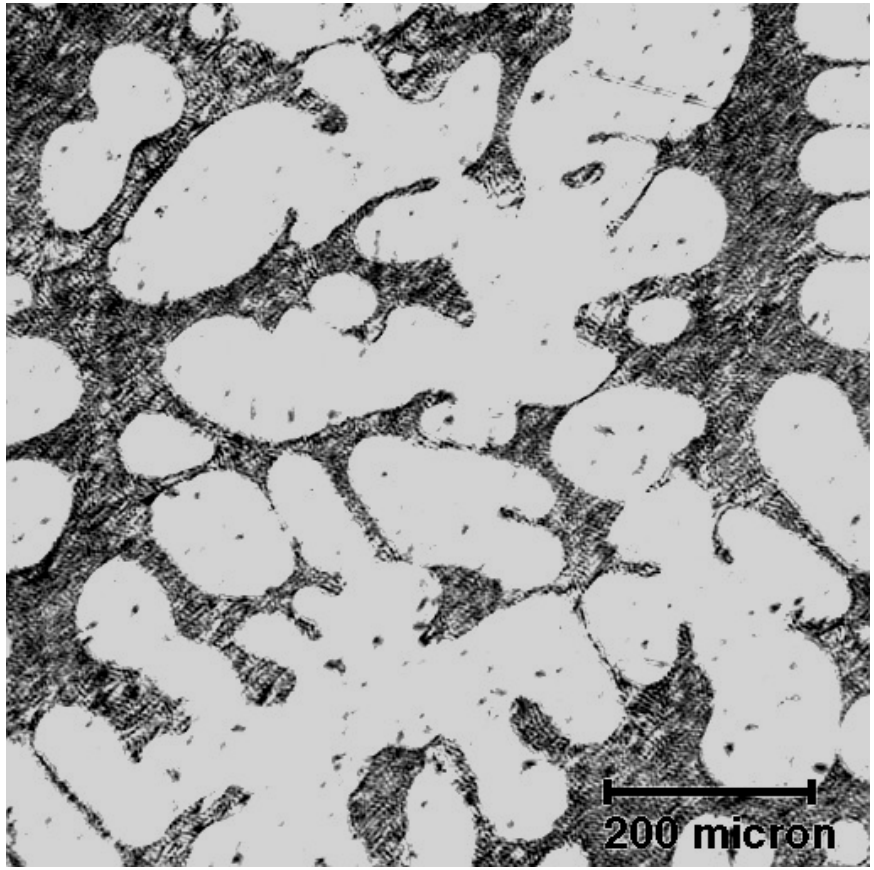

Figure 11: Microstructures obtained by mixing pure Al and eutectic Al-Si to form 4343 Al-Si wrought alloy. Observe the dendritic / regular low super heated cast microstructure. The primary phase is not globular.

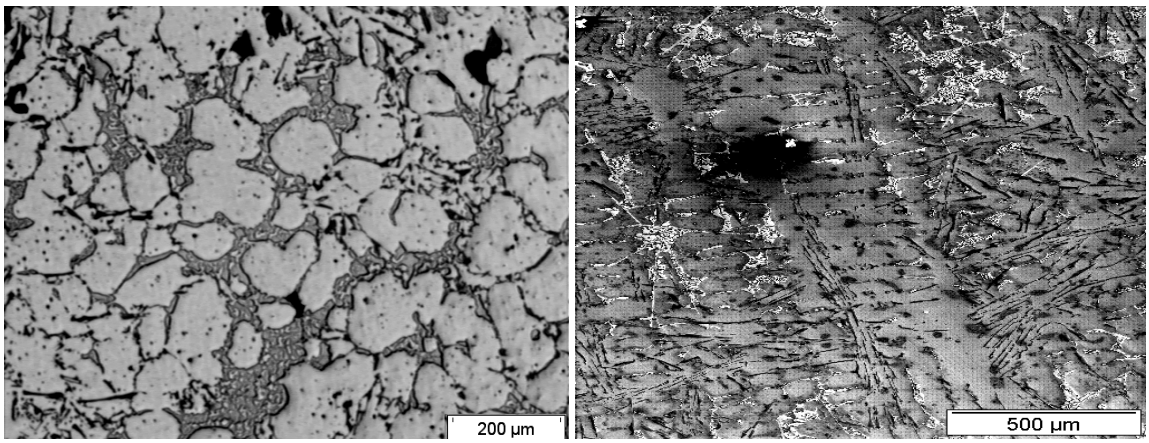

Figure 12: (a) Microstructures obtained by mixing eutectic Al-Cu and eutectic Al-Si (Table IV) to produce a 4145 Al-Si-Cu wrought alloy. (b) Same sample reheated to 650 ^{0}C (~ superheat of 70^{0}C) and cast.

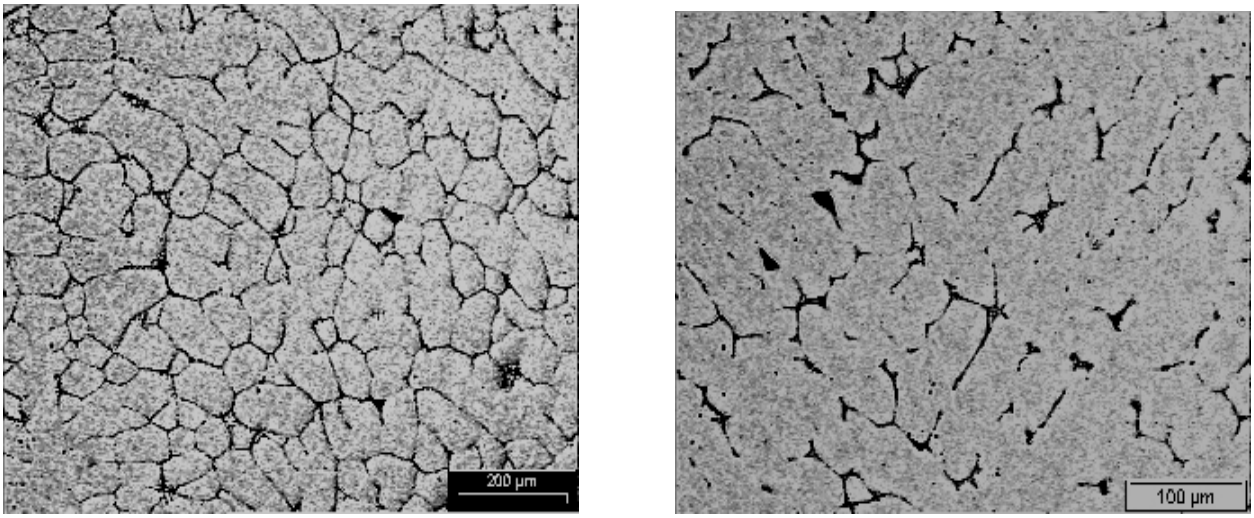

(a) (b)

Figure 13: (a) Microstructures obtained by mixing Al- 35% Mg and Pure Al (Table V) and air cooled in crucible, (b) the same crucible reheated with a 15°C superheat and air cooled in crucible. Notice the presence of dendrites in regular casting.

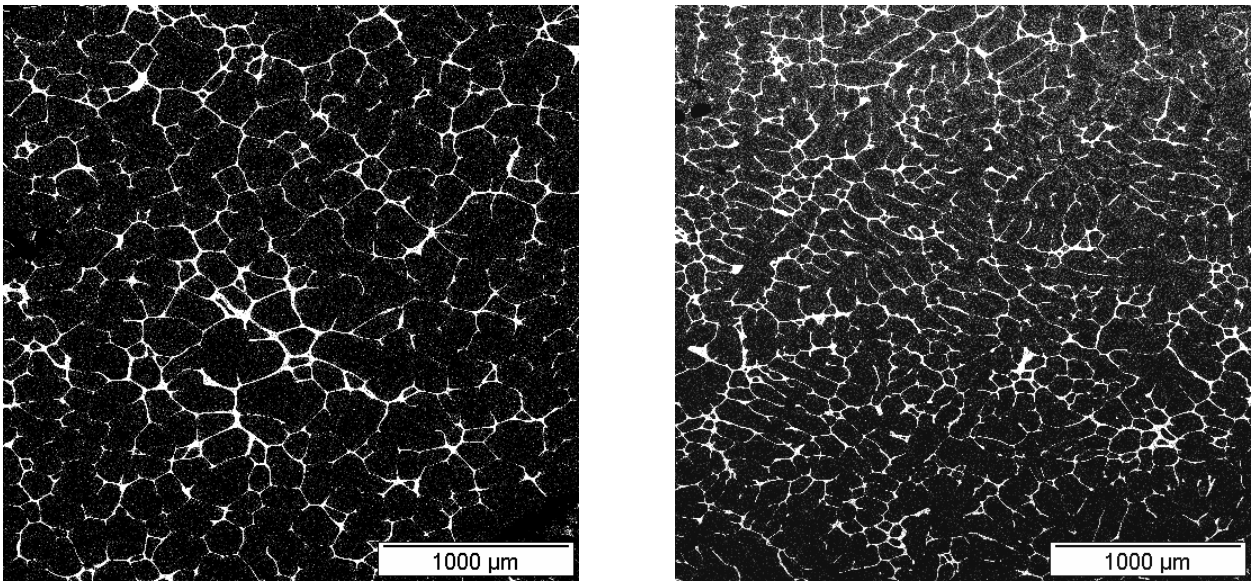

(a) (b)

Figure 14: (a) Microstructures obtained by mixing Al-Mg-Zn and Al-Cu liquids (Table VI) via and air cooled in crucible, (b) the same crucible reheated with a 15°C superheat and air cooled in crucible. Notice the presence of dendrites in regular casting.

Chapter 11. Nucleation study

Chapter 10 is an attempt in refining primary Si in the 390 alloy by the addition of inoculants. The various inoculants studied were selenium, nickel selenide, suphides of iron and copper. Thermal analysis and microstructural analysis showed that selenium and iron sulphide refined both primary and eutectic Si. This paper was presented at the 8th International Conference on Semi solid Processing of Metals and Alloys, Limassol, Cyprus, September 2004; published by NADCA, Wheeling, Illinois.

Inoculants for the Control of Primary Silicon Size and Distribution in Hypereutectic Alloys

Deepak Saha*, Diran Apelian* and Rathindra DasGupta**

*Metal Processing Institute, WPI, MA USA (www.wpi.edu/+mpi)

** SPX Contech, Kalamazoo, MI USA (www.spxcontech.com)

Keywords: Hypereutectic Al-Si Alloys, Inoculation, Primary silicon

Abstract

In this study, our interest was to investigate possible inoculants for the rheocasting of hypereutectic Al-Si alloys. The main issue in casting of hypereutectic Al-Si alloys is the homogenous distribution of primary Si in the final part. As primary Si nucleates from the liquid, it develops complex shapes depending on the cooling rate imposed on it. Nine different morphologies of primary Si have been observed and reported in the literature[1]. Traditionally the refinement of primary Si is achieved by the addition of phosphorus to the melt; over the years, researchers have studied many refining agents to refine primary Si. A mixed success of refining has been reported by the use of Germanium, Gallium, Selenium, Tellurium, Lithium, Cadmium, and Lithium Chloride. However, most of the work has been related to conventional casting of hypereutectic alloys. Due to different mechanisms operating during rheocasting, traditional nucleants (like phosphorus) do not work as effectively as they during conventional casting. In this study we address the size and distribution issues of hypereutectic Al-Si alloys by the use of some refining agents in conjunction with growth restrictors.

Introduction

Hypereutectic alloys posses outstanding wear properties coupled with high strength due to the presence of a hard phase (primary silicon) in a soft matrix. The presence of silicon increases the fluidity of these alloys[2] providing these alloys with excellent casting characteristics. However, there is a limit beyond which increasing the amount of silicon in the alloy affects the fluidity. Arnold[2] et al have shown that fluidity of these alloys reaches a maximum at 16 – 18 % silicon and that an increase in silicon percentages beyond 20% leads to the blocky primary silicon, which deters fluidity. The increased fluidity and excellent casting characteristics of hypereutectic Al-Si alloys (16-18% Si) have led to the widespread use of 390 alloy. The typical composition of 390 alloy is shown in Table 1.

Table I. Typical composition of 390 Al-Si hypereutectic alloy

Si	Fe	Cu	Mg	Mn	Zn	Ti	P
16-18	1.0 max	4.0-5.0	0.5-0.65	0.1 max	0.2 max	Traces	0.1 max

However, casting of these alloys posed a challenge because of the growth of primary silicon to sizes, which were unacceptable and led to deterioration of part quality. The ideal microstructure in these hypereutectic alloys would consist of fine primary silicon distributed evenly throughout the soft aluminum matrix. These requirements gave rise to the use of phosphorus to refine primary silicon in these alloys. Presence of phosphorus leads to the reduction of the size of primary silicon by a factor of 5-10[1]. In tandem, refinement of primary silicon causes an increase in mechanical properties as reported by Schneider[3]. The accepted theory for the refinement of primary silicon is that AlP aids nucleation of primary silicon. Researchers[4] have identified a phosphorus rich compound at the center of primary silicon. Phosphorus refinement in hypereutectic Al-Si alloys is an accepted norm throughout the casting industry.

Another aspect of primary silicon refinement is the amount of undercooling or amount of heat extracted during the cooling of hypereutectic Al-Si alloys[5]. Most die casting operations can achieve fine primary silicon in the absence of any phosphorus because of the high cooling rates experienced during solidification, which aids the attainment of fine primary silicon. In the early 90's, as semi solid processing was applied to hypereutectic alloys certain advantages were realized such as longer die life, lower operating temperatures, non-turbulent flow, and superior primary silicon distribution over conventional high pressure die casting. Thixocast hypereutectic Al-Si alloys (reheating of billets to semi solid range) were shown to have better silicon distribution and size compared to conventional high pressure die cast parts[6]. Quality advantages of Thixocasting were, however, marred, with increasing cost of billets and reheating costs associated with this net shape manufacturing process. Rheocasting of hypereutectic alloys is preferred over thixocasting for economic reasons as well as scrap recycling issues, which also has an economical impact. Rheocasting of hypereutectic Al-Si alloys is a challenge in that controlling the nucleation and growth of the primary silicon phase is a difficult task. In rheocasting, the liquid is cooled to the semi solid state; primary silicon nucleates and grows as the liquid is cooled at a slow rate, leading to coarse primary silicon (> 120 μm) and the occurrence of segregation of primary silicon. The problems are compounded by the fact that, each mole of silicon that nucleates releases 4.5 more heat during solidification compared to a mole of aluminum[1]. The additional heat of fusion during the growth of primary silicon renders currently used equipment- (insulated molds, etc. for SSM processing of hypoeutectic alloys) useless. In this study, we investigate the micro-structural changes in a hypereutectic Al-Si alloy by the addition of various compounds that - aid the nucleation and also prevent the growth of the primary silicon as it cools below the liquidus. The experiments in this study were carried at slow rates (air cooled) to identify the effect of these inoculants in an attempt to mask the role of thermal gradients.

Experimental Plan and Design

In this investigation, we have explored the effects of the addition of the following compounds:

1. Nickel Selenide
2. Selenium
3. Copper Sulphide
4. Iron Sulphide
5. Iron Copper Sulphide

The procedure involves the preparation of a pure Al-Si alloy; 80 grams of 99.99 % purity aluminum and 20 grams of 99.99% purity silicon were melted in a crucible and held at 750^0C. It is important to note that no modifiers/grain refiners were added to the melt. The following elements were wrapped in aluminum foil and dropped into the melt and stirred. The melt was then reheated to 750^0C and subsequently air cooled. Melt temperature was recorded as the melt cooled. The crucible was sectioned and two samples were obtained for analysis. A sample was observed under the scanning electron microscope (SEM) at a high magnification to observe the size and distribution of primary silicon, and the other sample was electro-etched in a Glycol-Percholic acid solution and was observed via SEM.

Results and Discussion

Figure 1 shows the microstructure obtained during the solidification of a pure Al-Si alloy. Figures 2 – 5 show the microstructures obtained by the addition of the NiSe, Se, FeS, Cu_2S and $CuFeS_2$, respectively. Each figure consists of 2 sets of micrographs, one at a lower magnification and –the other reveals the nature of the morphology of the eutectic structure at a higher magnification.

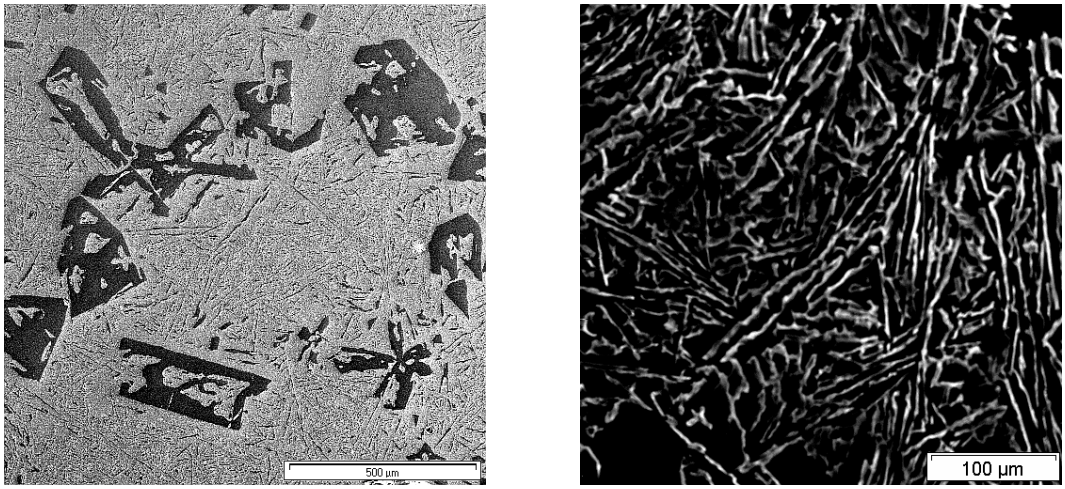

a) **b)**

Figure 1: Microstructure obtained during the solidification of pure Al-Si a) low magnification showing star shaped primary silicon and b) higher magnification sample showing the eutectic (Electro-etched).

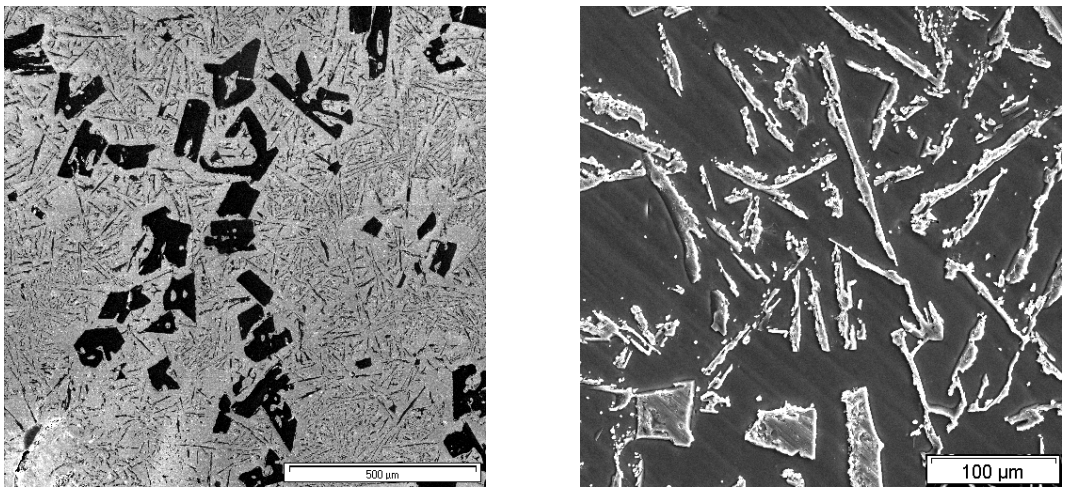

a) **b)**

Figure 2: Microstructure obtained during the solidification of pure Al-Si with nickel selenide a) low magnification showing refined primary silicon b) higher magnification sample showing a modified eutectic structure (Electro-etched).

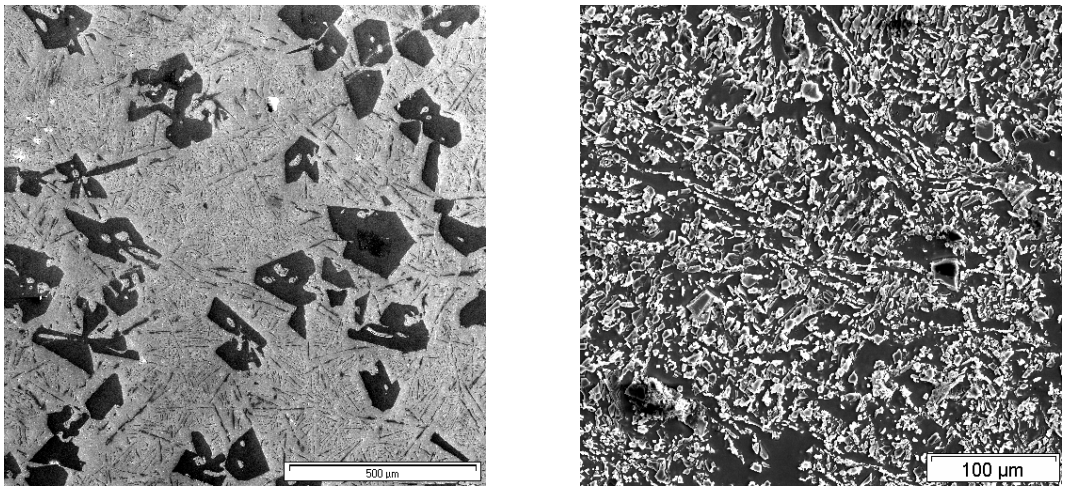

Figure 3: Microstructure obtained during the solidification of pure Al-Si with selenium a) low magnification showing refined primary silicon b) higher magnification sample showing a modified eutectic structure (Electro-etched).

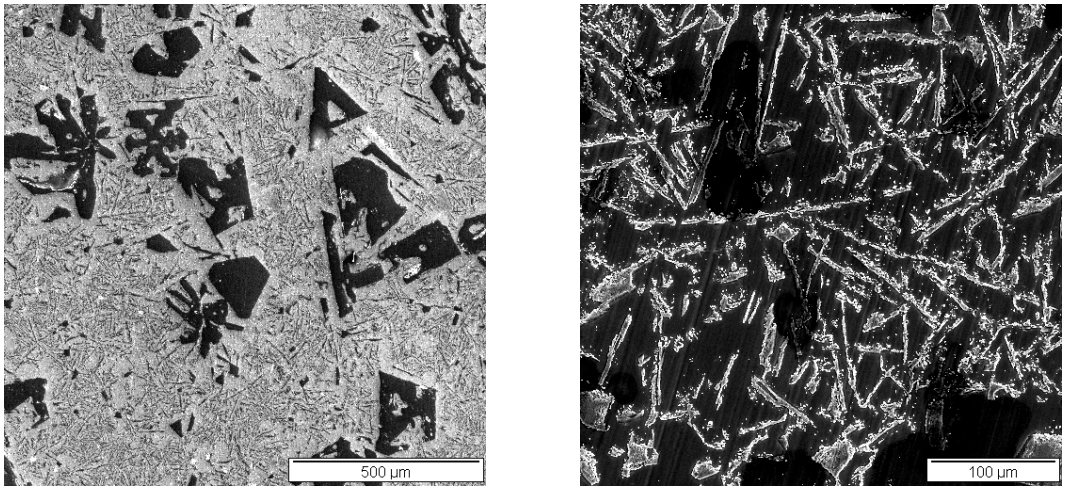

Figure 4: Microstructure obtained during the solidification of pure Al-Si with copper (1) sulphide (Cu_2S) a) low magnification showing refined primary silicon b) higher magnification sample showing the unmodified eutectic structure (Electro-etched).

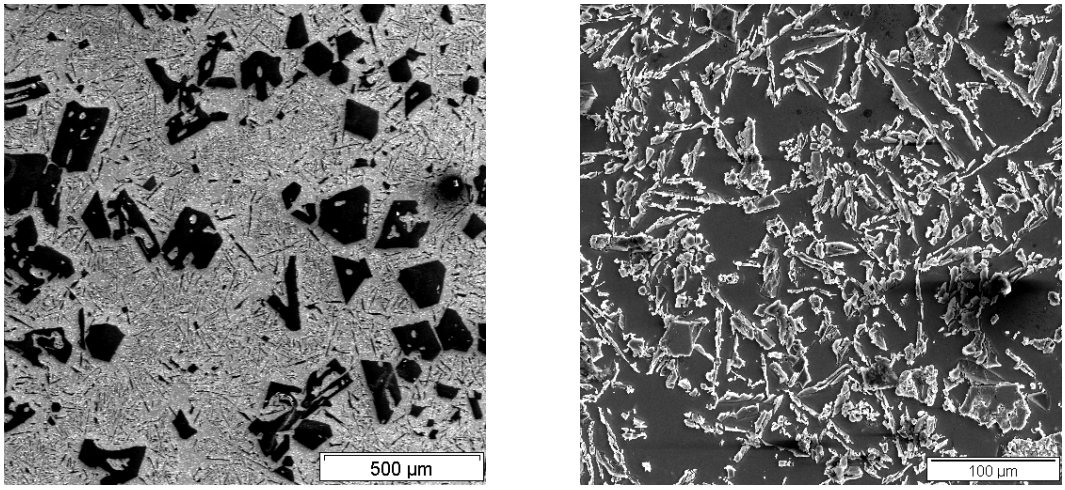

Figure 5: Microstructure obtained during the solidification of pure Al-Si with iron sulphide (FeS) a) low magnification showing refined primary silicon b) higher magnification sample showing a modified eutectic structure (Electro-etched).

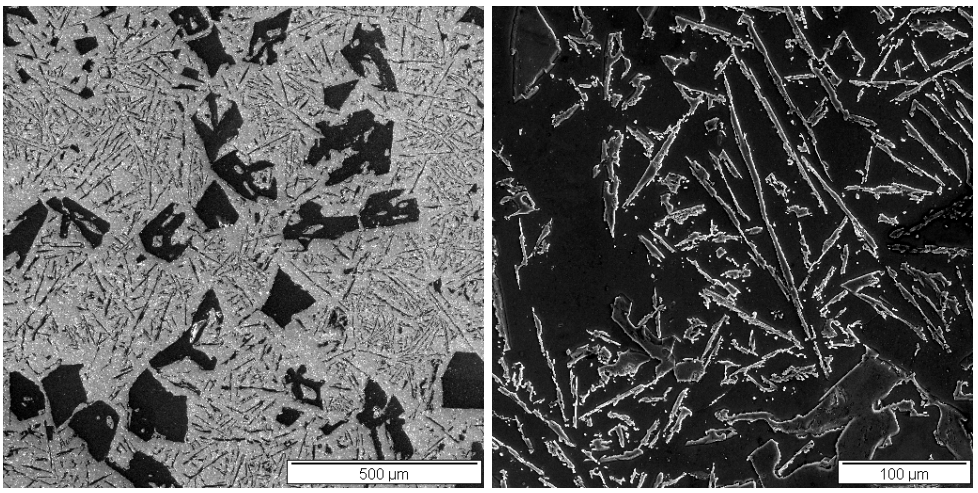

a) **b)**

Figure 6: Microstructure obtained during the solidification of pure Al-Si with chalcopyrite ($CuFeS_2$) a) low magnification showing refined primary silicon b) higher magnification sample showing a modified eutectic structure (Electro-etched).

Figures 2 – 6 clearly show the effect of the inoculants on the final shape and distribution of primary silicon. The presence of selenium (either in the pure form or as nickel selenide) refined primary silicon and modified the eutectic silicon even at relatively low cooling rates. However, working with selenium compounds is unsafe for the environment and is detrimental to the health of the end user. So the use of selenium in the industry can be ruled out, although even a small quantity of selenium refines primary and eutectic silicon. The use of sulphides in the form of iron and copper sulphides was motivated because 390 alloy contains copper in the range of 3 – 4 % by weight and can accommodate iron upto 1% by weight. Copper and iron sulphide when added independently to the pure Al-Si melt, refine primary silicon and eutectic silicon, but added in the form of chalcopyrite (commonly used ore of copper), refine primary silicon and leaves the eutectic silicon unmodified.

Figures 7 -8 show the thermal profile obtained from the experiments mentioned above. Figure 7 shows the cooling curves obtained when the alloys cooled. Figure 8 shows the first derivative of the cooling curve ($\frac{dT}{dt}$) thermal curves provide temperature – time signatures of critical events during solidification such as: start of nucleation, formation of precipitates, phase change, etc. Most metallurgical events such as nucleation and phase transformation involve thermal fluctuations, which appear as spikes in the ($\frac{dT}{dt}$) curve. Figure 8 clearly shows the difference in the thermal curve due to the addition of various inoculants.

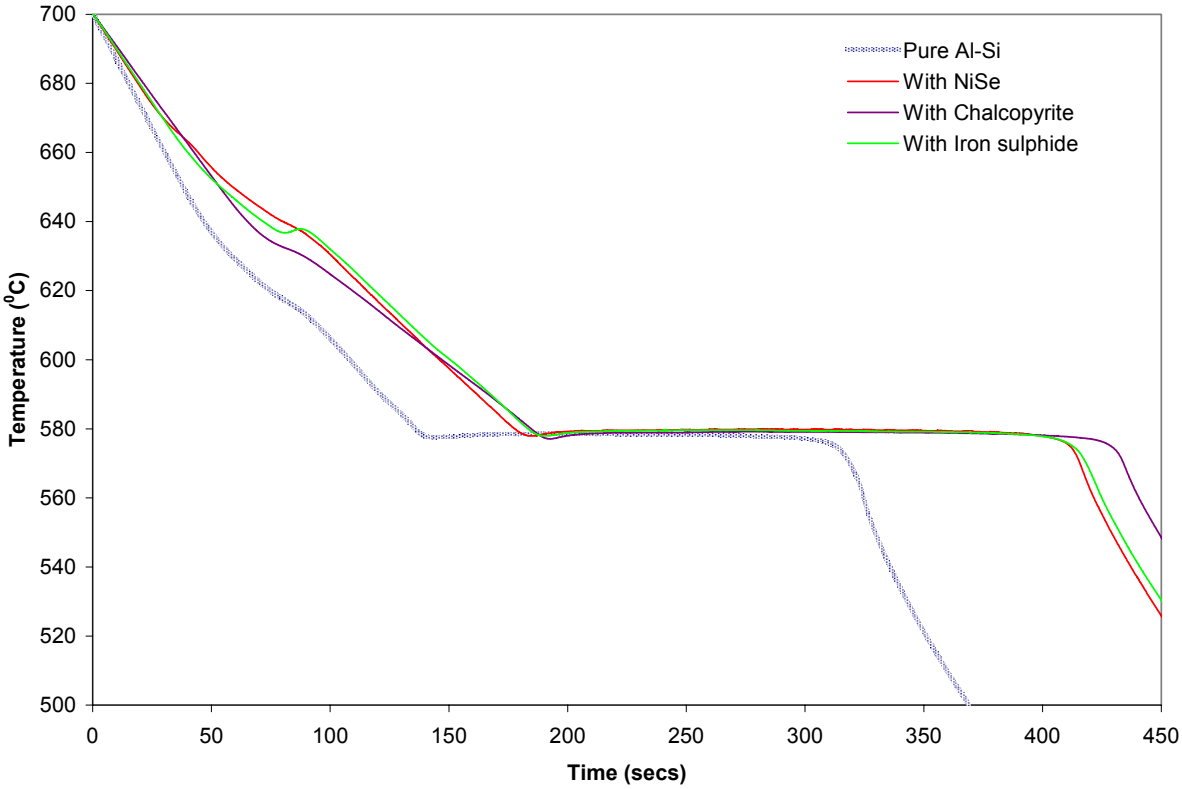

Figure 7: Time-Temperature plots during the cooling of the Al-Si alloy with the addition of various inoculants.

Figure 8, shows the important thermal signatures during the cooling of the Al-Si alloy with the inoculants. It can be clearly observed (when compared to pure Al-Si alloy), that there are certain reactions occurring either before the nucleation of primary silicon or before the nucleation of eutectic Al-Si. Addition of NiSe and FeS show a peak prior to the nucleation of primary silicon. The refinement of primary silicon is higher in these two experiments (refer to Figures 2 and 5 for the primary silicon structure). Similar curves where obtained by the addition of selenium and copper sulphide (not shown in Figure 8 due to data cluttering). Surely, addition of the above mentioned compounds show primary silicon refinement at slow cooling rates. Table II shows the crystal lattice parameters of the above mentioned compounds and their respective space groups. All the above mentioned compounds were selected for similar crystal group and lattice parameters. Selenium was added because many selenium compounds (zinc, copper, silicon, manganese, etc.) exist in the space group with similar lattice parameter to primary silicon. However, the ability of these compounds to "wet" primary silicon is the most important parameter, and very little data exists in the literature in this regard. Experiments and micro-structural analysis is underway at WPI to ascertain the nucleating phase during these experiments.

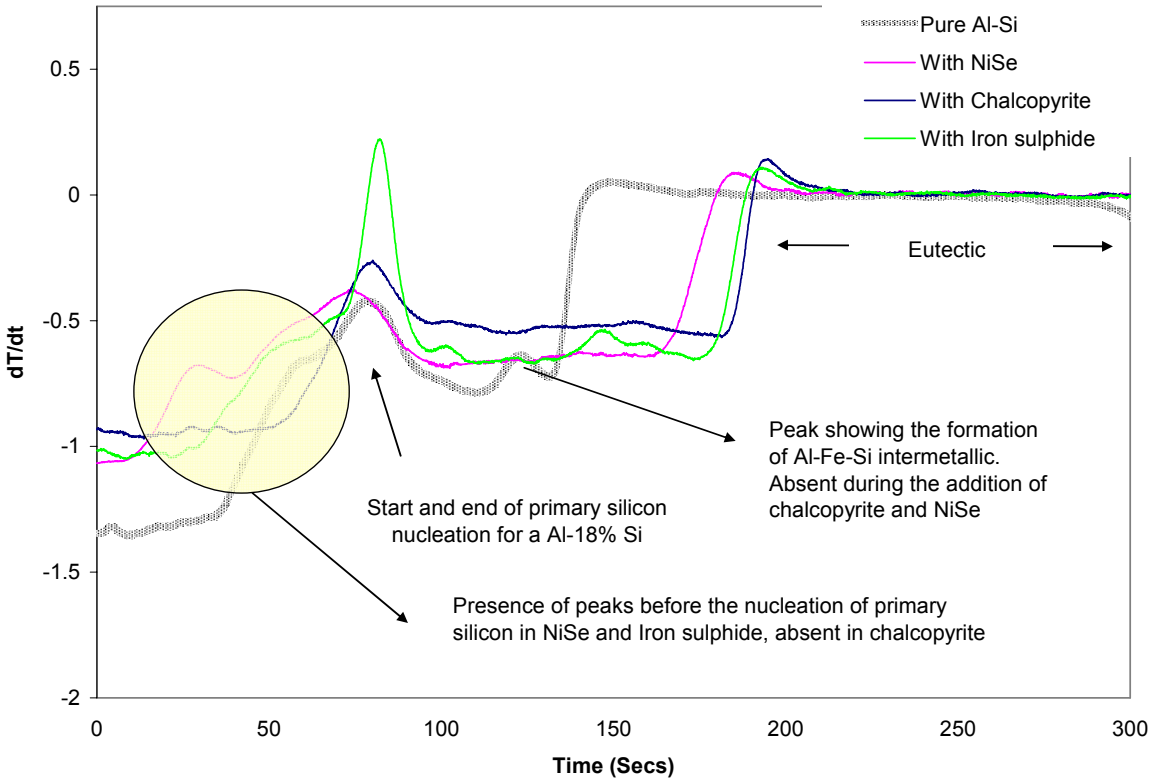

Figure 8: ($\frac{dT}{dt}$) and time plot showing the thermal signatures during the cooling of an Al-Si alloy with the addition of various inoculants.

Table II: Lattice parameters and crystal structure of the inoculants

	Silicon	Nickel Selenide	Copper Sulphide	Chalcopyrite	Iron Sulphide
Space Group	$F\bar{4}3m$	$F\bar{4}3m$	$F\bar{4}3m$	$F\bar{4}3m$	$F\bar{4}3m$
Lattice Parameter(a)	5.392	5.423	5.707	5.294	5.419
Crystal Structure	Fcc	Fcc	Fcc	Fcc	Fcc

Conclusions

Our study identifies selenium and selenium compounds as potent primary silicon refiners, but use of selenium is toxic and is not recommended for industrial use. Sulphides of iron and copper have shown potential in refining primary silicon and modifying eutectic silicon simultaneously. Further studies are underway at WPI to identify and ascertain the nucleation mechanism and the phases formed, leading to nucleation of primary silicon.

The authors would like to thank SPX Corporation for supporting the work.

References

1. N. Tenekedjiev and J.E. Gruzleski, "Hypereutectic aluminum silicon casting alloys – A review", *Cast Metals*, 3 (2)(1990), 96 – 105.
2. F.L. Arnold, J.L. Jorstad and G.E. Stein, "Fluidity characteristics of some alloys in the aluminum-silicon system", *Current Engineering Practice*, 6 (June)(1963), 10 – 15.
3. K. Schneider "Aluminum casting alloys properties – Improvements by grain refinement", *AFS transactions*, 68 (1960), 176 – 181.
4. P.H. Shingu and J.I. Takamura, "Grain size refining of primary crystals in hypereutectic Al-Si and Al-Ge Alloys", *Metallurgical Transactions*, 1 (1970), 2339 – 2340.
5. Wang Ru-yao, Lu Wei-hua and Logan L.M. , "Growth morphology of primary Silicon in cast Al-Si alloys and the mechanism of concentric growth", *Journal of Crystal Growth*, 207 (1999), 43 -54.
6. *Science and Technology of Semi solid Metal Processing*, Edited by Anacleto de Figueredo (Rosemount IL USA, North American Die Casting Association), 4-13.

Chapter 12. Conclusions

This thesis can be broadly classified into two distinct parts. The first part [Chapters 5 – 7] deals with the identification of novel processes for the microstructural control of primary silicon in hypereutectic Al-Si alloys. The second part [Chapters 8 – 9] deal with the identification of a novel process for the casting of Al based wrought alloys by the mixing of two liquids. The main conclusions for each of these parts are given below:

Hypereutectic Al-Si alloys

- Two novel diffusion solidification processes have been developed: one where a liquid hypereutectic alloy is mixed with a hypoeutectic alloy that is held in the semi solid state; whereas, in the second process solid particles/chunks are added to the melt.
- Experiments with both of the above approaches, was conducted at the laboratory and in plant trials; the results show that excellent microstructures of hypereutectic alloys were achieved. It was demonstrated that size of the primary silicon phase in hypereutectic alloys to less than 25 microns can be obtained by these processes.
- It was concluded that the dissolution of Al in Al-Si liquid is via interfacial reaction. The reaction follows the classical Arrhenius equation with an activation energy of 23 – 26 $kcalmol^{-1}k^{-1}$, depending of the amount of silicon in the liquid Al-Si.
- The study on the identification of potent nucleants for primary silicon from a hypereutectic Al-Si alloy, confirmed that selenium and selenium compounds are

potential primary silicon refiners. Iron sulphide aids in the refinement of primary silicon and eutectic Si.

Al based wrought alloys

- The diffusion solidification approach of mixing two liquids was utilized to obtain a non-dendritic primary phase during the solidification of Al based wrought alloys. The precursor alloys are selected such that they are close to the liquidus and have a combined free energy which is less than the liquidus of the final alloy upon mixing.
- It was concluded that alloys which has a tendency to form X-X bonds in the liquid state (positive heats of energy) are difficult to cast with a globular primary phase even if the energy conditions are met.
- Non-dendritic structures were demonstrated via experiments in Al based 2000 series (Al-Cu system), 7000 series (Al-Zn system) and 5000 series (Al-Mg system). Non-dendritic structures were also obtained for some cast Al alloys such as 222 (Al-Cu system), 356 (Al-Si system)

Chapter 13. Future Work

It has been demonstrated in this work, that one can control the microstructure of Al based alloys not through heat controlled solidification, but rather through a combination of heat and mass diffusion. Formation of globular primary phase in wrought alloys and the prevention of primary Si growth are a testimony of that fact. This is the first time in the history of wrought Al alloys (more than 50 years of existence), that a non-dendritic primary phase has been obtained directly from the liquid. The following need to be studied in detail to commercialize the technologies:

- Study the response of currently available heat treatments to wrought alloys with a non-dendritic microstructure.
- Optimize the heat treatment cycles of Al base wrought alloys and Al-Si alloys with a non-dendritic microstructures to utilize the benefits mechanical strength and near net shape manufacturing.
- Study the effect of non-dendritic primary phase on the hot tearing tendency.
- Effect of grain refiners like Ti into the pure Al liquid to obtain the finer globular primary, as finer phase improves the mechanical strength.